

Library Copy

EPA-450/3-77-022a

October 1977

**RELATION
OF OXIDANT LEVELS
TO PRECURSOR EMISSIONS
AND METEOROLOGICAL
FEATURES -**

**VOLUME I: ANALYSIS
AND FINDINGS**



**U.S. ENVIRONMENTAL PROTECTION AGENCY
Office of Air and Waste Management
Office of Air Quality Planning and Standards
Research Triangle Park, North Carolina 27711**

EPA-450/3-77-022a

Final Report

October 1977

THE RELATION OF OXIDANT LEVELS TO PRECURSOR EMISSIONS AND METEOROLOGICAL FEATURES

Volume I: Analysis and Findings

By: F. L. LUDWIG
SRI International
E. REITER
Colorado State University
E. SHELAR and W. B. JOHNSON
SRI International

Prepared for:

ENVIRONMENTAL PROTECTION AGENCY
OFFICE OF AIR QUALITY PLANNING AND STANDARDS
RESEARCH TRIANGLE PARK, NORTH CAROLINA 27711
Attention: MR. PHILLIP L. YOUNGBLOOD

CONTRACT 68-02-2084

SRI Project 4432

Approved by:

R.T.H. COLLIS, *Director*
Atmospheric Sciences Laboratory

RAY L. LEADABRAND, *Executive Director*
Electronics and Radio Sciences Division



SRI International
Menlo Park, California 94025 • U.S.A.

ABSTRACT

Published ozonesonde data, radioactive fallout measurements and alpine ozone observations have been used to estimate the stratospheric contribution to observed ozone concentrations at ground level. Long term average effects from the stratosphere over the U.S. are on the order of 10 ppb, with a springtime maximum around 20 to 25 ppb. Short term stratospheric intrusion events resulting in one-hour-average concentrations of stratospheric ozone in excess of 80 ppb in the lower troposphere have a frequency of only about 0.2 percent. Still fewer (but some) of these events lead to ground-level impacts of such a magnitude.

Tropospheric causes of high ozone concentrations away from cities have been investigated by statistical analysis of meteorological conditions and the precursor emissions occurring along air trajectories and by comparisons of weather maps and large-scale O₃ distributions. Meteorological factors are statistically more strongly correlated with ozone concentration than are emissions, with air temperature being the most highly correlated. At sites well removed from cities, the upwind emissions of oxides of nitrogen are more strongly related to ozone concentrations than are the emissions of hydrocarbons. Widespread violations of the federal oxidant standard are most likely to be found in association with a stagnant high-pressure system or in the warm southwesterly flow in the western portion of a high pressure area, often ahead of an approaching cold front.

The results of this and other studies suggest that not all violations of the federal oxidant standard are controllable and this fact must be considered in the design of control strategies. Also, for areas within about 125 km of large cities, control might be achieved through the reduction of HC emissions. In more remote areas, control strategies involving NO_x control throughout large regions must be considered.

TABLE OF CONTENTS

ABSTRACT	iii
LIST OF ILLUSTRATIONS	vii
LIST OF TABLES	xiii
ACKNOWLEDGEMENTS	xv
CONCLUSIONS	1
1. INTRODUCTION	5
1.1. Motivation and Objectives	5
1.2. Lines of Investigation	6
1.3. Brief Description of Methods	7
1.3.1. General	7
1.3.2. Stratospheric Intrusion Analyses	8
1.3.3. Studies of Tropospheric Transport Processes	8
1.3.4. Synoptic Scale Ozone Distributions and Weather Patterns	11
2. ANALYSIS AND RESULTS	13
2.1. Stratospheric Sources	13
2.1.1. Ozonesonde Case Studies	13
2.1.2. Evidence of Ozone Transport from the Stratosphere as Deduced from Studies of Radioactive Debris	46
2.1.3. Ozone Observations at Zugspitze	59
2.2. Tropospheric Sources	63
2.2.1. Trajectory Analyses	63
2.2.2. Studies of Synoptic-Scale Ozone Distributions and Weather Patterns	101
2.2.3. Combining the Trajectory Approach with Synoptic Scale Comparison	124
3. DISCUSSION	139
3.1. How Much Does Stratospheric Ozone Contribute to Ground-Level Ozone Concentrations?	139
3.1.1. General	139
3.1.2. Long-term Average Stratospheric Contribution	140
3.1.3. Short-term Stratospheric Contributions	140
3.2. What Are the Tropospheric Causes of High Ozone Values in Areas Removed from Emissions?	141
3.2.1. Meteorological Factors	141
3.2.2. Emissions Factors	142
3.3. Implications for Control Strategies	143
3.3.1. Interactions between Ozone of Stratospheric and Tropospheric Origins	143
3.3.2. Strategies for Control of Ozone of Tropospheric Origin	144
3.4. Recommendations for Future Research	146
REFERENCES	149

LIST OF ILLUSTRATIONS

Figure		Page
1:	Candidate and Selected Sites for Detailed Analyses of Air Histories	9
2:	Ozone Sounding at Goose Bay, Canada, 2 May 1963	17
3:	Radiosonde Ascent at Goose Bay, Canada, 2 May 1963, 0000 GMT.	18
4:	North American Surface and 500 mb Charts, 28 April to 3 May 1963	20
5:	Montgomery Stream Function Analyses, 30 April - 2 May 1963	23
6:	Composite 6-hour Trajectory Segments from 29 April, 1963, 1800 GMT, 2 May 1963, 1200 GMT	24
7:	Radiosonde Ascent at Baker Lake, Canada, 1 May 1963, 1200 GMT	25
8:	Ozone Sounding at Thule, Greenland, 1 May 1963	26
9:	North American Weather Maps, 24-25 June 1963	28
10:	Ozone Sounding at Bedford, Massachusetts, 26 June 1963	29
11:	North American Weather Maps 10 August to 15 August 1963	30
12:	Ozone and Dewpoint Sounding at Tallahassee, Florida, 14 August 1963	32
13:	Temperature and Dewpoint Soundings at Tallahassee, Florida, 14 August 1963	33
14:	Montgomery Stream Function Analyses, 12 August to 14 August 1963	34
15:	Sounding at Montgomery, Alabama, 14 August 1963, 1200 GMT	35
16:	Soundings for Omaha, Nebraska and Columbia, Missouri, 13 August 1963, 0000 GMT	37
17:	Soundings for The Pas (11 August 1963) and Resolute (12 August 1963), Canada, 0000 GMT	38
18:	Composite 6-hour Trajectory Segments from 11 August, 1963, 1800 GMT to 14 August 1963, 1200 GMT	39

LIST OF ILLUSTRATIONS (Continued)

Figure	Page
19: Ozone Sounding at Seattle, Washington, for 8 April 1964.	40
20: North American Weather Maps, 6-7 April 1964	41
21: Ozone Sounding at Seattle, Washington, 15 April 1964.	42
22: Ozone Sounding at Seattle, Washington, 17 April 1964.	43
23: North American Surface and 500 mb Charts, 13 April to 17 April 1964.	44
24: Mean Meridional Distribution of Ozone	48
25: Monthly Mean Total Ozone Amounts at Arosa, Switzerland.	49
26: Mean Ozone Distribution for March-April 1963 and Strontium 90 Distribution for May-August 1963	50
27: Stratospheric Inventory of Sr90 in the Northern Hemisphere	51
28: Atmospheric Ozone and Sr90 Distributions, Fall 1964 and Spring 1965.	52
29: Sr90/O3 Ratios as a Function of Time.	53
30: Mean Fallout in 1963.	56
31: Seasonal, Maximum and Daily Fallout Frequency Maps for 1963.	57
32: Maximum 24-hour Fallout in 1964	58
33: Joint Frequency Diagram of Peak-Hour Versus 24-Hour Average Ozone Concentrations at Zugspitze	59
34: Ozone Concentrations at Zugspitze 8-9 January 1975.	61
35: McHenry Trajectories--Ozone Concentrations in Top 20 Percentile.	64
36: McHenry Trajectories--Ozone Concentrations not in Top 20 Percentile.	65

LIST OF ILLUSTRATIONS (Continued)

Figure	Page
37: Queeny Trajectories--Ozone concentrations in top 20 percentile.	66
38: Queeny Trajectories--Ozone Concentrations not in top 20 percentile.	67
39: Wooster Trajectories--Ozone concentrations in top 20 percentile.	68
40: Wooster Trajectories--Ozone concentrations not in top 20 percentile.	69
41: Yellowstone Lake Trajectories--Ozone concentrations in top 20 percentile.	70
42: Yellowstone Lake Trajectories--Ozone concentrations not in top 20 percentile.	71
43: Scatter Diagram of Ozone Concentration Versus Precipitation Index During Last 12 hours of Trajectory-Combined Data. . . .	76
44: 95% Confidence Limits for Coefficients in the Regression Equations Using Weighted Emissions Indices.	83
45: 95% Confidence Limits for Coefficients in the Regression Equations Using Emissions for Last 12 Hours	84
46: Scatter Diagram of Observed Ozone Concentrations versus Those Estimated from a Regression Equation Using Indices of Emissions and Temperature During the Last 12 Hours	86
47: Scatter Diagram of Observed Ozone Concentrations Versus Those Estimated from a Regression Equation Using Temperature and Weighted Emissions Indices.	87
48: Scatter Diagram of Observed Ozone Concentrations Versus Those Estimated from a Regression Equation Using Temperature and NOx Emissions	89
49: Scatter Diagrams of Estimated Versus Observed Ozone Concentrations for Two Piecewise Linear Regression Expressions	91

LIST OF ILLUSTRATIONS (Continued)

Figure		Page
50:	Scattergram of Estimated Versus Observed Ozone Concentrations for Piecewise Linear Regression Using Temperature and Insolation.	93
51:	Scatter Diagram of Ozone Concentration Versus the Distance to the Air Parcel Position 12-hours before Measurement . . .	95
52:	Scatter Diagram of Ozone Concentration Versus the Distances to the Air Parcel Position 36 Hours Before Measurement. . . .	96
53:	Frequency Distributions of 12 and 36 Hour Travel Distances	98
54:	Scatter Diagram of Ozone Concentration Versus the Direction to the Air Parcel Position 12 Hours Before Measurement.	99
55:	Scatter Diagram of Ozone Concentration Versus the Direction to the Air Parcel Position 36 Hours Before Measurement.	100
56:	Frequency Distributions of "High" and "Not High" Ozone Travel Directions.	101
57:	Locations of SAROAD Sites in the Eastern United States Measuring Ozone During 1974	102
58:	Example of High Ozone Concentrations Southeast of Lakes Erie and Ontario and in the St. Louis-Ohio River Valley . . .	106
59:	Example of High Ozone Concentrations in Western Kansas and the New York-New England Area	107
60:	Example of High Ozone Concentrations South of Lake Michigan and in the New England area.	108
61:	Example of High Ozone Concentrations Southeast of Lakes Erie and Ontario and Along the Texas-Louisiana Gulf Coast . .	109

LIST OF ILLUSTRATIONS (Continued)

Figure	Page
62: Example of High Ozone Concentrations in Western Kansas, The Florida Peninsula and the Washington-Philadelphia Corridor.	110
63: Counties with Average Annual NO _x Emissions Greater than 75 t mi ⁻² yr ⁻¹	111
64: Prototype Pressure Pattern and the Ozone Pattern for the Same Day.	116
65: Prototype Ozone Pattern and the Weather Map for the Same Day	117
66: Locations of Grid Points Used for Classifying Ozone and Pressure Patterns and for Pressure-Ozone Correlations	119
67: Weather Map and Ozone Distribution for Sunday, 21 July 1974 .	121
68: Weather Map and Ozone Distribution for Sunday, 28 April 1974.	122
69: Weather Map and Ozone Distribution for Friday, 20 September 1974	123
70: Ozone-Pressure Relationships at McRae, Montana.	125
71: Weather Map, Ozone Distribution and Trajectories for 7 July 1974	126
72: Weather Map, Ozone Distribution and Trajectories for 8 July 1974	127
73: Weather Map, Ozone Distribution and Trajectories for 10 July 1974.	129
74: Weather Map, Ozone Distribution and Trajectories for 11 July 1974.	130
75: Weather Map, Ozone Distribution and Trajectories for 12 July 1974.	131
76: Weather Map, Ozone Distribution and Trajectories for 13 July 1974.	132

LIST OF ILLUSTRATIONS (Continued)

Figure		Page
77:	Weather Map, Ozone Distribution and Trajectories for 14 July 1974.	133
78:	Weather Map, Ozone Distribution and Trajectories for 18 July 1974.	134
79:	Weather Map, Ozone Distribution and Trajectories for 21 July 1974.	136
80:	Weather Map, Ozone Distribution and Trajectories for 22 July 1974.	137
81:	Weather Map, Ozone Distribution and Trajectories for 26 July 1974.	138
82:	Areas Appropriate for Hydrocarbon Emissions Control According to Meyer.	147

LIST OF TABLES

Table	Page
1: Frequency Distribution of Maximum Ozone Concentrations in the Lower Troposphere as Measured by Ozonesondes	15
2: Ozone Concentrations in the Lower Troposphere that Exceeded 80 ppb	16
3: Correlation Coefficients Between Observed Ozone Concentrations and Various Meteorological and Chemical Indices	72
4: Spearman Rank Correlations between Ozone and Meteorological and Chemical Indices for the Combined Data for all sites.	78
5: Correlation between Pairs of Meteorological Indices	80
6: Correlation Between Hydrocarbon and NOx Emissions	81
7: Regression Constants Relating Ozone Concentrations to Weighted Indices of NOx and Hydrocarbon Emissions, and to Temperature During the Last 12 Hours.	82
8: Regression Constants Relating Ozone Concentrations to Temperature and Emissions Indices for the Last 12 Hours of the Trajectory	85
9: Standard Error of Estimate of the Regression Equations.	85
10: Frequency of Occurrence of Days when the Federal Oxidant Standards were Violated in the Eastern United States	104
11: Number of Cases for each Month with Daily Maximum O3 > 80 ppb in Specified Regions of the Eastern United States	112
12: Winds Reported on Morning Weather Map in Areas Where Peak-Hour Ozone Exceeded 80 ppb During the Day.	113
13: Meteorological Features Associated with High Ozone Concentrations.	115
14: Dates Classified as Having Pressure and Ozone Patterns Similar to the Prototypes	118
15: Frequency of Correlation Values Between Pressure and Ozone at 20 Points in the Eastern United States	120

ACKNOWLEDGEMENTS

We are indebted to Mssrs. E. L. Meyer, E. L. Martinez, W. P. Freas and H. R. Richter of EPA's Air Management Technology Branch for their valuable comments. D. H. Barrett and J. A. Tikvart of the Source Receptor Analysis Branch have also provided many valuable suggestions.

We are especially indebted to the Project Officer, Mr. Philip L. Youngblood, for his many useful suggestions during the course of the project and for his valuable comments concerning the final report.

At SRI the following people assisted in the analyses of data and the preparation of the reports: J.H.S. Kealoha, A.H. Smith, L.J. Salas, R. Trudeau, L. Jones, W. Ligon, R. Troche, and S. Gillen. Mr. Dale Coventry of EPA and Mr. R. Haws of Research Triangle Institute provided many useful data, as have the staff of the National Climatic Center.

CONCLUSIONS

General

The analyses presented here, when combined with other evidence from the literature, provide a reasonably clear picture of the importance of stratospheric and tropospheric processes in determining ground level ozone concentrations. The findings can be grouped into the following five categories.

1. The importance of stratospheric ozone sources
2. The importance of anthropogenic emissions to ozone concentrations in rural areas
3. The identification of geographical and meteorological factors conducive to the occurrence of high ozone concentrations in rural areas
4. The likelihood of tropospheric/stratospheric interactions to produce high ozone concentrations
5. The feasibility of oxidant control strategies that can be applied over extended geographical areas.

A discussion follows the conclusions under each of these categories:

The Importance of Stratospheric Ozone

There is strong evidence for the following conclusions:

- Stratospheric contributions are greatest during late winter and spring
- During these seasons, the long term average stratospheric contribution to the tropospheric ozone burden amounts to about 20 to 25 ppb
- The greatest contributions occur near the mean positions of the polar and arctic jet streams and perhaps in the lee of the Rockies
- Ozone concentrations from stratospheric intrusions exceed the federal standard only about 0.2 percent of the time in the lower troposphere, and even less frequently at ground level.
- Ground level hour-average ozone concentrations in excess of 150 ppb can be caused by stratospheric intrusions that have been observed under special circumstances.

The studies described here have identified at least some of the special circumstances that can lead to very strong stratospheric influences at ground level. Subsidence in the stratosphere, coupled with tropopause folding can introduce large amounts of ozone into the troposphere which can be brought to the ground with minimal dilution by strong convection in the lower troposphere. This is an uncommon combination of events. It is uncertain whether other combinations of events also transfer ozone at high concentration from the stratosphere to ground level. It is almost certain that such transfers are quite rare and probably of limited duration (a few hours) and spatial extent (several tens of kilometers).

The Importance of Anthropogenic Emissions

Meyer's (1977) analysis indicates that anthropogenic emissions, especially hydrocarbons, are important determinants of ozone concentrations for distances of up to 125 km from very large cities and to shorter distances from smaller cities. This is quite consistent with observations of urban "plumes" at similar ranges. The importance of hydrocarbons is consistent with smog chamber results that show ozone concentrations to be a function of hydrocarbon concentrations when hydrocarbon/NO_x ratios are low, such as they usually are in and around cities.

The results of the present study suggest that ozone concentrations in rural areas are more dependent on NO_x emissions than on hydrocarbon emissions. This too is consistent with smog chamber studies that show ozone dependence on NO_x very high at hydrocarbon/NO_x ratios such as are common in nonurban areas. The findings also agree with similar results obtained by Meyer et al (1976) and by Singh, Ludwig and Johnson (1977).

Meteorological and Geographical Factors Associated with High Ozone Concentrations in Rural Areas

The one factor most highly correlated with the maximum daily, hour-average ozone concentrations in rural areas is the air temperature during the last 12 hours before the observation. It should be noted that air temperature is closely related to other factors that are also likely to be instrumental in the photochemical formation of ozone. Solar radiation is probably the most important of these other factors.

High ozone concentrations are often, but not always, associated with light winds and recent trajectories that are characterized by a clockwise curvature. Both of these conditions are conducive to increased buildup of precursor concentrations. Light winds encourage this buildup because less air is available to dilute the emissions. Clockwise, or anticyclonic, motion is generally associated with subsidence and a resulting atmospheric stratification which inhibits vertical mixing and dilution. Subsidence also tends to suppress cloudiness, thereby allowing for more solar radiation to drive the photochemical processes. If temperatures are high, ozone formation is even further enhanced.

This combination of conditions is frequently found near and to the west of high pressure centers in the summertime.

Light winds and strong atmospheric stability are not essential to the accumulation of precursors and photochemical production of ozone. Extended travel over large emissions areas can also lead to substantial concentrations of ozone if the air is warm and there is sufficient sunshine. Several extended areas of high emissions are oriented generally southwest-northeast in the eastern United States. This configuration undoubtedly contributes to the fact that a large portion of the violations of federal ozone standards are accompanied by southwest winds. Air movement from the southwest in these elongated regions would allow the accumulation of precursors necessary for ozone formation. It happens that southwest-toward-northeast is the generally prevailing air movement over the eastern United States during the summer months and it also happens that the occurrence of the meteorological conditions identified as being conducive to ozone formation often accompany such air motions.

Stratospheric/Tropospheric Interactions

It is important to understand that significant stratospheric intrusions are unlikely to occur concurrently with large tropospheric buildups of anthropogenic ozone. Stratospheric intrusion is most likely in the late winter or spring when the sunshine necessary for photochemical processes in the troposphere is relative weak. Stratospheric intrusions are most likely to occur behind cold fronts where rain, cool temperatures, high winds, and strong convection are likely to work against the buildup of anthropogenic ozone from photochemical activity. Thus it does not appear that these two sources of ozone (i.e., stratospheric intrusion, and photochemical formation from anthropogenic precursor emissions) interact to the extent that control strategies for anthropogenic ozone cannot be formulated.

Implications for Control Strategies

Although the frequency of violations of the federal ozone standard caused by stratospheric intrusion appears to be small, the reality of such events cannot be ignored. It is important that such uncontrollable incidents be recognized so that the strategies will focus on those incidents that are the result of controllable processes.

In addition to the unusual instances, the design of control strategies should also recognize that there exists an uncontrollable reservoir of "background" ozone arising in large part from an ongoing interchange between the stratosphere and the troposphere. In the spring this reservoir may have concentrations of about one-half the federal standard (Singh, Ludwig and Johnson, 1977).

It appears that control strategies uniformly applied within restricted areas are feasible for meeting the federal oxidant standard. As Meyer (1977) shows, the major effects of urban areas are most often

realized within some reasonable distance of the city. That distance is generally less than 125 km. Meyer's (1977) approach of defining hydrocarbon control regions by a circle centered on the city might be refined by introducing asymmetry. For instance, if certain wind directions are disproportionately associated with ozone incidents, the boundaries for control might be extended in those directions. Nevertheless, the concept of a radius of influence seems useful in the design of generalized control strategies.

At greater distances from cities the control of ozone appears to require the control of NO_x emissions. It also appears that high ozone concentrations in rural areas are influenced by emissions at greater distances and over greater periods of time than is usually the case with the high concentrations found near cities. Thus, the control of ozone in rural areas poses much more of a problem than that in or near urban areas. The regions to be considered are apt to be quite large so that the definition of source-receptor relationships is likely to be quite difficult. It may not be possible to identify the area where controls should be applied in order to lower the ozone concentrations at a specified rural area. Furthermore, the strategies for controlling rural ozone are apt to involve a large-scale curtailment of NO_x emissions. This could be a difficult feat. Finally, there is the distinct possibility that the control of NO_x emissions to reduce ozone concentrations in rural areas could lead to a worsening of the ozone problem in and near urban areas.

1. INTRODUCTION

1.1. Motivation and Objectives

The United States has established ambient air quality standards (AAQS) for several toxic pollutants, including photochemical oxidant. * The rationale underlying these standards is that they should be met in order to protect public health. The concept of the AAQS has been extended to include the formulation of plans for the control of emissions so that the standards are met. These plans usually involve the curtailment or rearrangement of some human activities, tacitly assuming that human activities are responsible for the observed violations of the AAQS. This thesis is hard to dispute for most pollutants in urban areas, but there are frequent occasions when the oxidant standard of 80 ppb (measured as ozone) is violated in rural areas well removed from urban centers. Questions arise concerning the importance of natural processes, such as the intrusion of ozone-rich stratospheric air to ground level, and the importance of long-range transport.

The answer to the question of long-range transport directly affects the formulation of strategies to prevent the violation of the oxidant standard. If emissions affect oxidant formation over a wide area, then the control strategies may well have to involve more than the immediate surroundings where the violations occur. It becomes important, therefore, to define the appropriate domain for the application of oxidant control plans. In an effort to resolve these dilemmas, the research described here seeks to answer the following specific questions:

- What causes the high oxidant values that are frequently observed in areas well removed from major sources of anthropogenic precursor emissions?
- How much does ozone of stratospheric origin contribute to ground-level oxidant concentrations?
- Over what distances is oxidant traceable to upwind precursor emissions?
- What are the effects of synoptic and smaller-scale meteorological variables on ground-level oxidant formation and transport?
- Is it possible, on the basis of relationships among oxidant concentrations, emission patterns, and synoptic-scale meteorological conditions, to identify geographic regions for uniform oxidant control strategies? If so, how?

The objective of the whole program is then to use the answers to these questions to formulate emission control strategies that are consistent with the physical processes governing the observed ozone concen-

* Throughout this report the terms "oxidant" and "ozone" are used interchangeably except where the context of the discussion dictates otherwise.

trations. Specifically, EPA hopes to determine if it is feasible to define geographic areas in which precursor control strategies can be applied to lower oxidant concentrations to acceptable levels.

1.2. Lines of Investigation

The approach to the problems outlined above was essentially descriptive. Two possible mechanisms that may lead to high oxidant concentration areas were examined:

- Intrusion of ozone from the ozone-rich stratosphere to ground level
- The formation and transport of oxidant in the lower atmosphere under meteorologically favorable conditions.

The intrusion of ozone is difficult to verify because it is not possible to distinguish stratospheric ozone from anthropogenic ozone unless other trace constituents of either stratospheric or tropospheric origin are examined at the same time. Such concurrent observations, however, are rare. Therefore, it was necessary to examine the behavior of a surrogate for stratospheric ozone. To this end the behavior of radioactive debris injected into the stratosphere during nuclear weapons testing was studied. The transfer of this debris from the stratosphere to the troposphere, and downward to ground level, was used to trace the transfer processes that would move stratospheric ozone over the same route. Another approach was to identify a few selected cases of high ozone concentrations at low altitudes having conditions of dryness and thermal stratification that suggested possible stratospheric origins for the air. These cases were then carefully analyzed to determine whether the observed ozone concentrations had actually come from the stratosphere.

The importance of photochemical and transport processes in the lower atmosphere was first investigated through a detailed examination of the history of the air arriving at several different locations. Where the air had been during the preceding days, what meteorological conditions prevailed, and what anthropogenic pollutants had been introduced were determined and used as a basis for interpreting the observed ozone concentration at the end of the period studied. This "Lagrangian" approach of examining the effects of events along the trajectory on the resulting ozone concentrations provides focus on processes and influences affecting ozone which may be generally applicable in all geographical areas. Thus, more than one location can be compared on a common basis. In addition to providing a means of identifying the factors that are important to ozone production, this approach also helps to identify what might be called the "historical span of influence", within which it is hypothesized that an existing ozone concentration is influenced appreciably by the past emissions and meteorological history of the air. Events in the more distant past are probably less influential than similar events that occurred more recently. The concept of historical span of influence can be translated into one of spatial span of influence by

examining the distances associated with the time intervals over which the processes are effective.

A second approach to the question of tropospheric photochemistry and transport was to study the relation between ozone patterns and synoptic scale weather patterns. The trajectory and meteorological history of the air are the direct products of synoptic scale meteorological patterns. So it was natural to examine weather and ozone patterns in concert. This is largely the Eulerian equivalent of the trajectory analyses. Although the two facets of investigation were conducted sequentially, they are closely related. In presenting the results there is, of necessity, some separation between the discussion of these two facets of the tropospheric work. Nevertheless, it should be remembered that the trajectory analysis and the synoptic map comparisons are simply Lagrangian and Eulerian attempts to answer the same general questions concerning the process of ozone formation and transport in the troposphere.

1.3. Brief Description of Methods

1.3.1. General

The details of the methods used in the data analysis are given in the appendices to this report, included in Volume III. These detailed descriptions should be consulted by readers who would provide their own interpretations to the results, or who might wish to apply the methods to other data sets. However, proper understanding of the results requires at least a brief description of the methods. This section is intended to provide that understanding.

As noted above, the research was divided into three parts:

- (1) Stratospheric intrusion analyses
- (2) Tropospheric transport studies
- (3) Studies of synoptic-scale ozone distributions and weather patterns.

The purpose of the stratospheric intrusion analyses was to evaluate the degree to which the stratosphere affects ground-level ozone concentrations. The objective of the tropospheric transport studies was to examine relationships between ozone concentrations and the emissions and meteorological conditions to which the air had been subjected. The synoptic analyses identified patterns of ozone distribution in the eastern United States that could be related to the emissions and meteorological features in the same area. Each part of the research had its own requirements. These are described briefly in the following subsections.

1.3.2. Stratospheric Intrusion Analyses

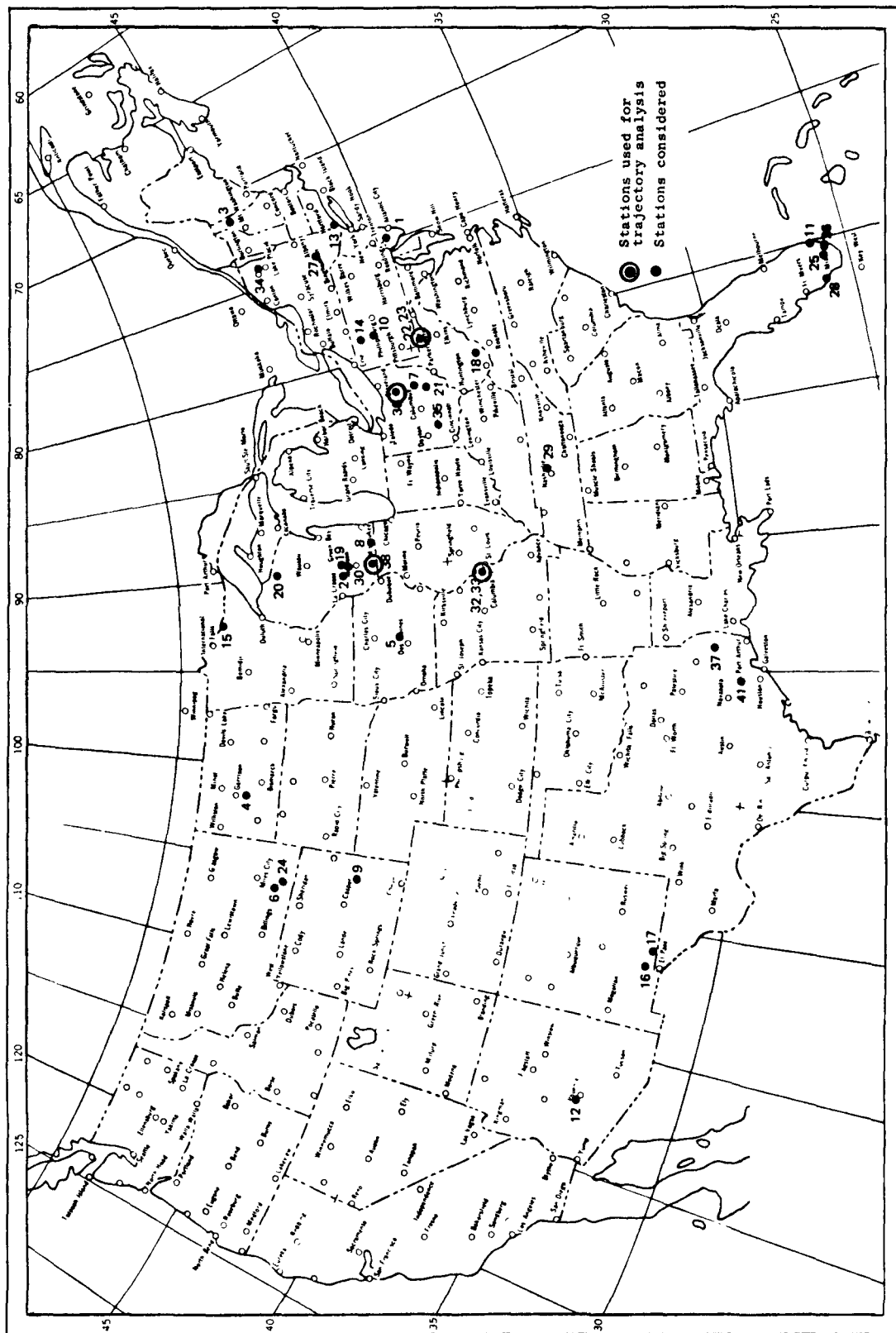
The determination of the magnitude of ozone intrusion from the stratosphere was based largely on the study of other identifiable stratospheric constituents, especially radioactive debris from nuclear tests or cosmic radiation processes. These serve as tracers of stratospheric air, and hence of stratospheric ozone. The use of the radioactive debris data as a surrogate for stratospheric ozone allows a tracing of the processes that transfer ozone from the stratosphere to ground level. Case studies of specific ozone observations were also undertaken to estimate the frequency with which stratospheric ozone might be brought to the lower troposphere at high concentration as a result of the intense meteorological processes that have been proposed in the literature (e.g. Danielsen and Mohnen, 1976).

1.3.3. Studies of Tropospheric Transport Processes

In studying the importance of tropospheric formation and transport of ozone, the meteorological and emissions history of ozone-containing air was examined in detail by means of trajectory analysis. This part of the research was undertaken in six steps:

- Selection of suitable sites for study
- Selection of suitable cases for study at each site
- Construction of the trajectory for each case
- Specification of meteorological conditions prevailing along each trajectory
- Specification of the amounts of ozone precursors introduced into the air along each trajectory
- Statistical analysis of relationships between the ozone concentration and the preceding meteorological and emissions conditions.

Four sites were selected for study after the review of data sources described in Volume II of this report. The review identified 38 candidate sites, but many were unsuitable for reasons such as insufficient data or proximity to urban areas. Figure 1 shows the locations of the 38 sites originally considered and the four finally selected. Those selected were McHenry, Maryland; Queeny, Missouri; Wooster, Ohio; and Yellowstone Lake, Wisconsin. These sites are circled on Figure 1. They provide widespread geographical coverage of the northeastern quarter of the United States, a fact that influenced their selection.



SA-4432-10

FIGURE 1 CANDIDATE AND SELECTED SITES FOR DETAILED ANALYSES OF AIR HISTORIES

Thirty cases from each location were chosen in such a way that a broad spectrum of ozone concentrations would be represented, but with an emphasis on the higher concentrations. Half the cases represent days on which the peak one-hour concentrations are in the top 20 percent of all days in the period considered (June - October, 1974). The remainder are among the lowest 20 percent or are days with peak-hour ozone concentrations near the median (between the 40th and 60th percentiles). Within these constraints the cases were selected to represent a variety of synoptic meteorological conditions, hours of the day when the maximum ozone concentration occurred, and days of the week. The selection of the cases is described in detail in Appendix A (Volume III).

The next step in the research was to construct air trajectories for the 60 hours preceding each of the 120 selected ozone observations. This was done using a version of Heffter and Taylor's (1975) trajectory model. The trajectory determinations were based on observed winds in the layer between 300 m and the average height (generally, 1500-2000 m) of the summer afternoon mixing layer near the selected sites (as reported by Holzworth, 1972). The model determined the location of the air at 3-hour intervals.

Once the trajectories had been calculated, the meteorological conditions prevailing during each 3-hour segment were determined from concurrent National Weather Service weather maps. Specifically, the following parameters were obtained from the weather maps:

- Temperature
- Dew point
- Cloud cover
- Current and recent precipitation (rain, snow, etc.)
- Cloud types
- Wind

Some of these parameters were used to derive indices of conditions that are more directly relatable to ozone formation and dilution processes than are the primary data. Specifically, cloud conditions were used in combination with solar elevation to provide a measure of incoming solar radiation (insolation). This insolation index was also used, along with surface wind speed, to determine atmospheric stability. Temperature and dewpoint were used to calculate relative humidity.

Hydrocarbons (HC) and oxides of nitrogen (NO_x) are known to be important to the formation of ozone. Therefore, emissions of these two pollutants were determined for the trajectory segments. Estimates of annual-average countywide emission rates of HC and NO_x were obtained for each U.S. county from the National Emissions Data System (NEDS). These data, corrected for diurnal and seasonal changes, were used to determine the HC and NO_x emitted into each trajectory segment.

In summary, indices of those emissions and surface meteorological parameters thought to affect the eventual ozone concentration were determined for each 3-hour segment of each of the 120 trajectories that were examined. The indices represented the following variables:

- NOx emissions
- HC emissions
- Insolation
- Temperature
- Dew point
- Relative humidity
- Precipitation
- Atmospheric stability

To reduce the number of indices that had to be treated in subsequent statistical analyses, the 3-hour values for the indices were averaged over 12-hour periods. Thus, there were five indices for each of the above variables for each of the 60-hour trajectories.

The statistical analyses are described in more detail in subsequent sections. In general, this study was limited to standard techniques involving single and multiple linear regression and correlations. Simple factor analysis was also employed.

1.3.4. Synoptic Scale Ozone Distributions and Weather Patterns

The influence of meteorological factors on ozone formation was studied from still one more point of view. Over the eastern two-thirds of the U.S. the large scale patterns of ozone were examined to determine what relation they bore to concurrent synoptic weather patterns. The weather patterns for the study were taken directly from the National Weather Service analyses published in the "Daily Weather Map" series. The basic data for the ozone analyses came from the SAROAD (Storage and Retrieval of Aerometric Data) files of EPA. The highest hourly average ozone concentration was determined for each station for each day on which reasonably complete data were available. Isopleth maps of maximum hour-average ozone were then constructed for each day. The method for drawing the isopleths is explained in detail in Appendix D (Volume III).

This part of the study treated those states east of, or traversed by, 100 degrees W. Meridian. Ozone observing sites are distributed reasonably well so that the large scale patterns could be derived. It is also an area where meteorological systems are more clearly definable than they are in the more mountainous western states. The ozone patterns were used to identify those parts of the eastern United States where ozone concentrations most frequently exceeded the federal standard

during the study year 1974. The various weather patterns most conducive to ozone formation were also identified. Pattern classification methods were applied for those days when ozone concentrations exceeded the federal standard over an appreciable area in the eastern U.S.

2. ANALYSIS AND RESULTS

2.1. Stratospheric Sources

Two approaches have been used to examine the contributions of stratospheric ozone to the concentrations observed at the surface. The two approaches reflect the two different time scales of the stratospheric contribution: 1) the average, long-term contributions to the ground-level ozone burden, and 2) the short-term impact of individual intrusions of stratospheric ozone to ground level.

As discussed in Volume II of this report, the following mechanisms are known to be important in the exchange of mass between the stratosphere and the troposphere:

- Seasonal adjustment of tropopause level
- Mean meridional circulation
- Stratospheric exchange between hemispheres
- Small-scale eddies.
- Large-scale eddies

The first four of the above transport processes proceed rather slowly and allow enough time for turbulent dilution of ozone in the troposphere. Thus, these four mechanisms relate to the average, long-term contribution. On the other hand, the large-scale eddy phenomenon is a mechanism of potentially high, short-term impact of stratospheric ozone on ground-level concentration.

The transport of radioactive debris from the stratosphere to the troposphere was studied in detail during the years of atmospheric nuclear testing and for some time after the test-ban treaty went into effect in 1963 (for summaries of research findings see Reiter, 1972; 1976a). These studies have provided a valuable basis for understanding the processes affecting both the short-term and the long term interchange of air between the stratosphere and the troposphere. Also, extensive ozonesonde measurements were made over North America during the early 1960's. These data were analyzed to estimate the impact of stratospheric intrusion on short-term ozone concentrations. These two approaches have proved quite useful in estimating the impacts of stratospheric ozone. The results are discussed in the following sections.

2.1.1. Ozonesonde Case Studies

2.1.1.1. General

Studies were made of ozonesonde observations which had been taken at 13 stations on the North American continent for the period between December 1962 and December 1965 (Hering, 1964; Hering and Borden, 1964; 1965a; 1965b; and 1967). Hering (1964) has alluded to possible inconsistency in the data due to problems with instrument sensitivity, cali-

bration, and stability. However, the data were assumed to be correct for purposes of this analysis. From a total of 1477 soundings the maximum ozone mixing ratios encountered below the 800-mb surface (below the 750-mb surface for the stations at Albuquerque, New Mexico and Fort Collins, Colorado) were determined (800 mb corresponds roughly to 7000 feet above mean sea level, 750 mb to 8500 feet). Table 1 presents a frequency distribution of these maximum mixing ratios.

As shown in Table 1, concentrations of 80 ppb (federal oxidant standard for one-hour average) were exceeded in this data sample 25 times; i.e., in less than 2% of all sounding ascents. Table 2 summarizes the dates and places of these occurrences. In most of these cases, the high ozone concentrations were associated with high relative humidities--a clear indication that the air masses in which these ozone concentrations were observed came from the troposphere rather than from the dry stratosphere. Also, subsidence of stratospheric air into the troposphere results in a temperature inversion in that air. Thus, stratospheric intrusions will be characterized by dry, stable layers. Numerous cases analyzed by Reiter and other authors (for references see Reiter, 1972) show that stable layers of air of stratospheric origin embedded in the lower troposphere are so dry that the radiosonde humidity sensor does not respond.

Using low relative humidities and the presence of a stable layer as criteria for the possible involvement of air masses of stratospheric origin, all but the following soundings were excluded:

Goose Bay, Canada	2 May, 1963
Bedford, Massachusetts	26 June, 1963
Tallahassee, Florida	14 August, 1963
Seattle, Washington	8 April, 1964
Seattle, Washington	15 April, 1964

Many of the soundings that did not meet the selection criteria were characterized by major ozone maxima very close to the ground. Such vertical gradients of ozone are characteristic of a ground-based, rather than a stratospheric, ozone source. The ground-based source is most likely anthropogenic. A discussion follows of the five cases which were selected.

2.1.1.2. Goose Bay, Canada, 2 May 1963

Figure 2 shows the ozone partial pressures and mixing ratios as measured by the ozonesonde ascent at Goose Bay on May 2 (1117 GMT). The Weather Bureau radiosonde ascent, plotted on a tephigram, is reproduced in Figure 3. A comparison of the two figures reveals that the highest ozone concentration in the lower troposphere appears to be centered near

Table 1

FREQUENCY DISTRIBUTION (Number of Cases) OF MAXIMUM OZONE CONCENTRATIONS
IN THE LOWER TROPOSPHERE AS MEASURED BY OZONESONDES

Concentration ppb	0.6	12	18	24	30	36	42	48	54	60	66	72	78	84	90	96	102	108	114	120	126	132	138	144	150	Total Number of Observations
Station																										
Thule, Greenland	6	23	15	18	10	4	3	3																		82
Fairbanks, Alaska	1	10	15	9	7	4	2	4	3	2																57
Churchill, Canada	1	10	13	13	12	16	15	8	4	2	4	2														100
Goose Bay, Canada	3	17	34	25	20	13	8	4	1	2	1				2											135
Seattle, Washington	25	28	22	23	11	15	9	4	3	1	2				2	1	1	1	1							148
Green Bay, Canada	9	15	12	15	4	8	3	6	6	1	2															81
Bedford, Massachusetts	21	45	32	33	28	15	17	13	8	3	3	1			1	1	3	2								225
Ft. Collins, Colorado	26	35	27	25	18	9	9	12	2	1																165
Pt. Mugu, California	1	3	3			1	2			1			1	2				1					2	1		18
Albuquerque, New Mexico	2	35	36	29	28	21	18	18	7	3	3	1														242
Tallahassee, Florida	8	21	13	11	19	20	13	10	7	4	1	3			1	2	1	1								135
Grand Turk Isl., Bahamas	1	13	11	10	7	2	5	1																		50
Balboa, Canal Zone	3	24	21	13	7	1	3	1	4	2	1	1														81
Total Cases	10	196	295	229	208	150	125	90	68	37	22	16	6	3	5	3	5	1	4	1				2	1	1477
Percentage	1	13	20	16	14	10	8	6	5	3	1	1	(-----2-----)												100

Table 2
OZONE CONCENTRATIONS IN THE LOWER TROPOSPHERE
THAT EXCEEDED 80 ppb

<u>Date</u>	<u>Maximum Ozone Concentration (ppb)</u>	<u>Station</u>
5-2-63	90	Goose Bay
6-26-63	114	Bedford
7-3-63	102	Bedford
8-7-63	90	Bedford
8-14-63	114	Tallahassee
9-11-63	102	Tallahassee
9-11-63	102	Seattle
9-18-63	90	Tallahassee
1-20-64	102	Bedford
4-8-64	108	Seattle
4-15-64	96	Seattle
4-17-64	120	Seattle
4-20-64	120	Seattle
7-15-64	102	Bedford
7-15-64	90	Goose Bay
8-26-64	114	Bedford
1-22-65	90	Tallahassee
7-14-65	96	Bedford
10-6-65	114	Pt. Mugu
10-7-65	144	Pt. Mugu
10-8-65	144	Pt. Mugu
11-3-65	84	Pt. Mugu
11-10-65	150	Pt. Mugu
12-1-65	84	Pt. Mugu
12-1-65	84	Tallahassee

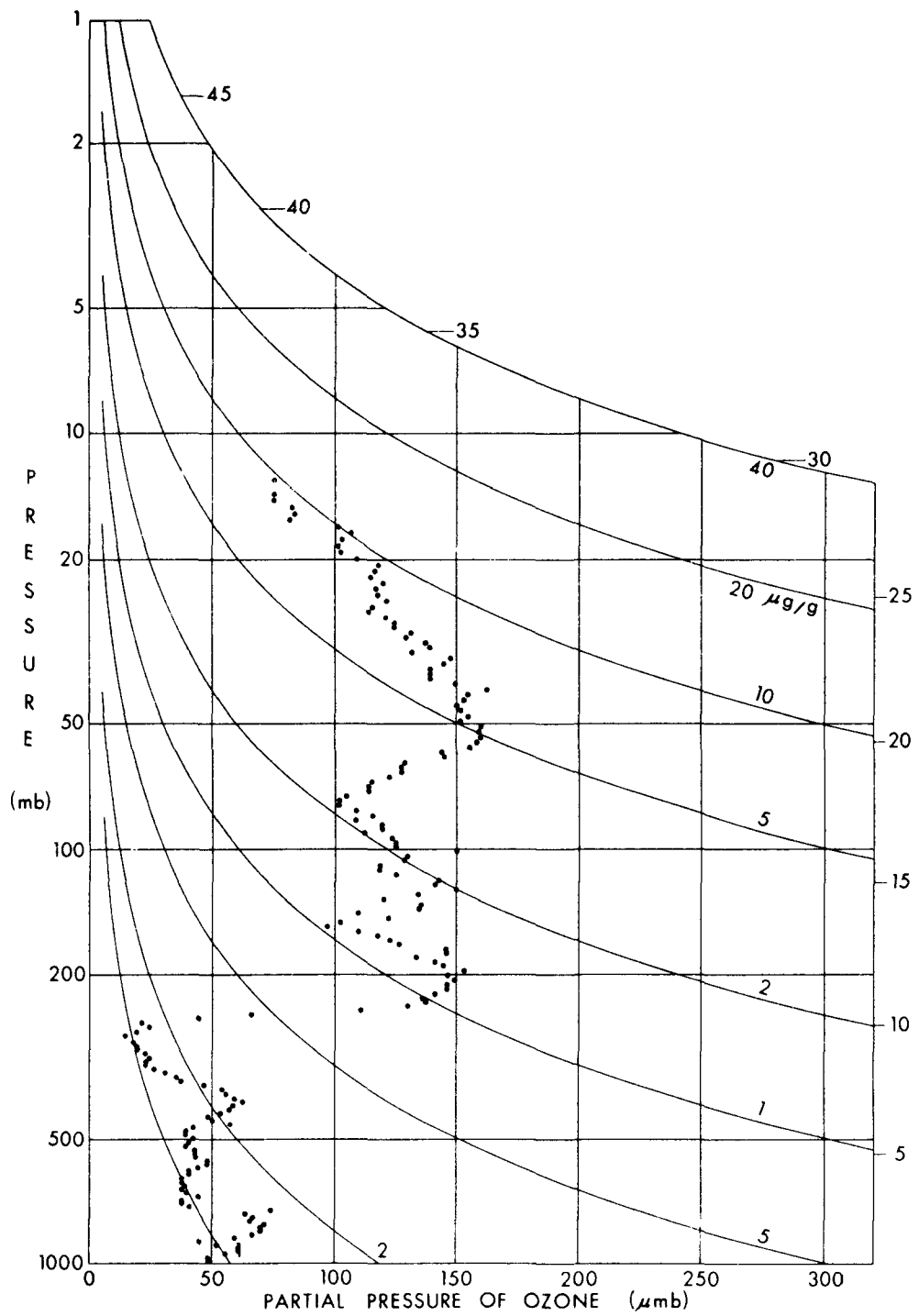


FIGURE 2 OZONE SOUNDING AT GOOSE BAY, CANADA, 2 MAY 1963

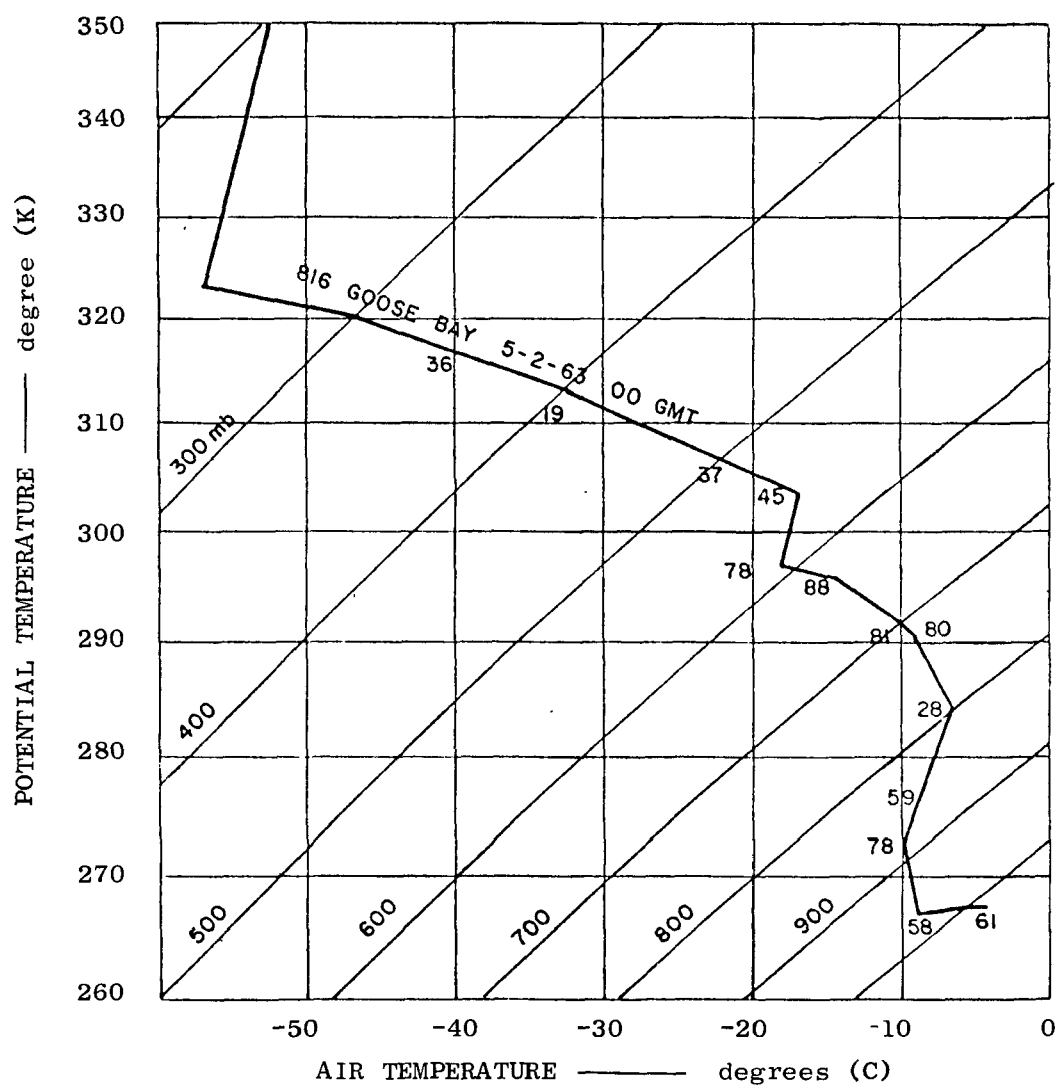


FIGURE 3 RADIOSONDE ASCENT AT GOOSE BAY, CANADA, 2 MAY 1963, 0000 GMT
(Numbers along the sounding curve indicate relative humidities at significant points)

the 282°K isentropic surface * within a stable layer with a low relative humidity of 28%.

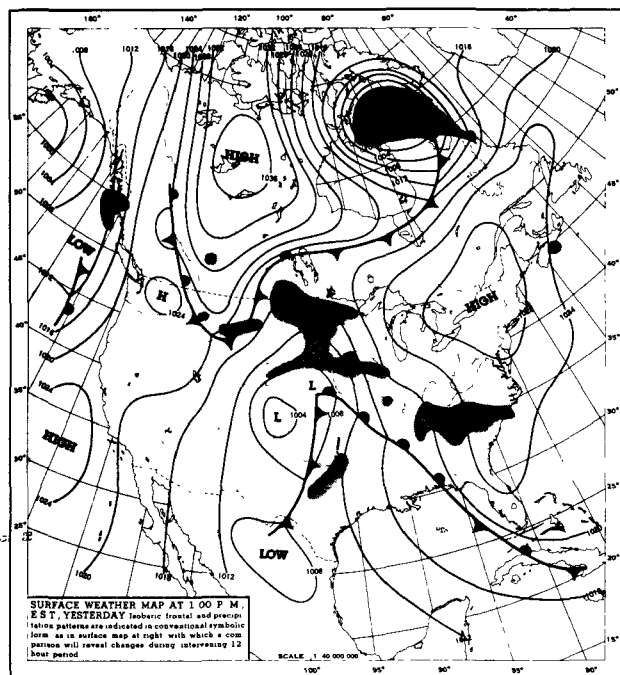
The sequence of surface weather maps and 500 mb (about 18,000 feet above sea level) charts in Figure 4 reveals the formation of an intensive outbreak of arctic air over Hudson Bay on 28, 29, and 30 April. The outbreak is associated with a deep low pressure center over Baffin Island. The leading edge of this cold-air is marked by the trough axis on the 500-mb surfaces for those dates (Figure 4). The frontal system delineating the cold outbreak had slowed down considerably by 1 May. The ozone sounding taken at Goose Bay on 2 May was launched directly into this frontal zone.

To assess the possibility that stratospheric air was responsible for the relatively high ozone concentrations, isentropic trajectories were constructed on the 282°K surface, starting over Goose Bay on 2 May at 1200 GMT, and running backward in time. (The procedure used in computing isentropic stream functions is outlined in Appendix C (Volume III)). The Montgomery stream function analyses between 30 April, 0000 GMT, and 2 May, 1200 GMT surface are shown in Figure 5. The temperature of the isentropic surface used for the analysis was changed with time to reflect the radiational cooling of the descending air mass. For air undergoing rapid descent from the tropopause, such cooling is usually about 1°C/day. The stream function diagrams in Figure 5 show 12-hour trajectory segments that are centered on the time indicated. The composite trajectory is reproduced in Figure 6.

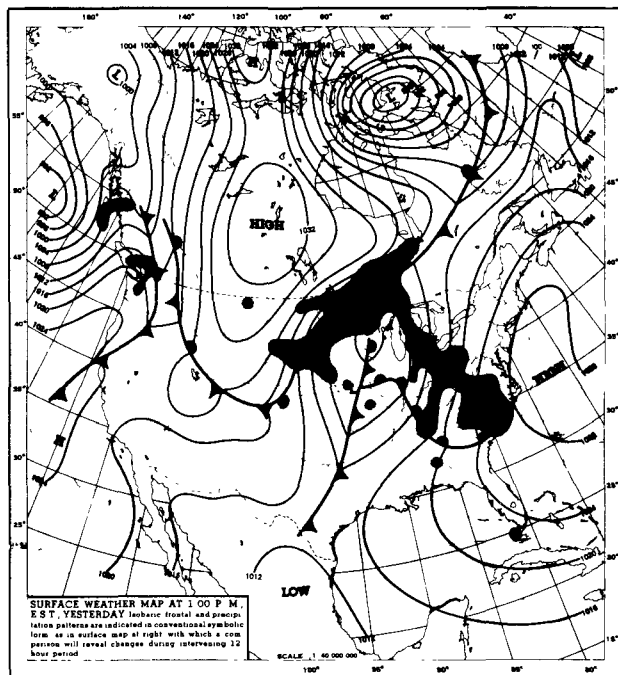
In the course of 2-1/2 days the air mass containing high ozone concentrations had moved from Baffin Island across Hudson Bay to Goose Bay, descending from the 600-mb to the 820-mb level. The sparsity of upper-air synoptic observations made it impractical to trace the air trajectory further back in time. It should be noted, however, that tropopause heights inside the deep cyclone over Baffin Island were very low. As shown by the 1 May sounding for Baker Lake (reproduced in Figure 7), the tropopause was near 560-mb at a potential temperature of 281°K. Thule, Greenland, also reported high ozone concentrations below the 500-mb surface on 1 May at 1117 GMT. Thule was also influenced by the Baffin Island low. The high ozone concentrations observed there, and shown in Figure 8, can be taken as characteristic of the lower stratosphere in polar latitudes.

Thus, even though the trajectory construction could not be completed for lack of upper air data, all evidence indicates that the high ozone concentrations observed in the planetary boundary layer over Goose Bay on 2 May 1963 were of stratospheric origin.

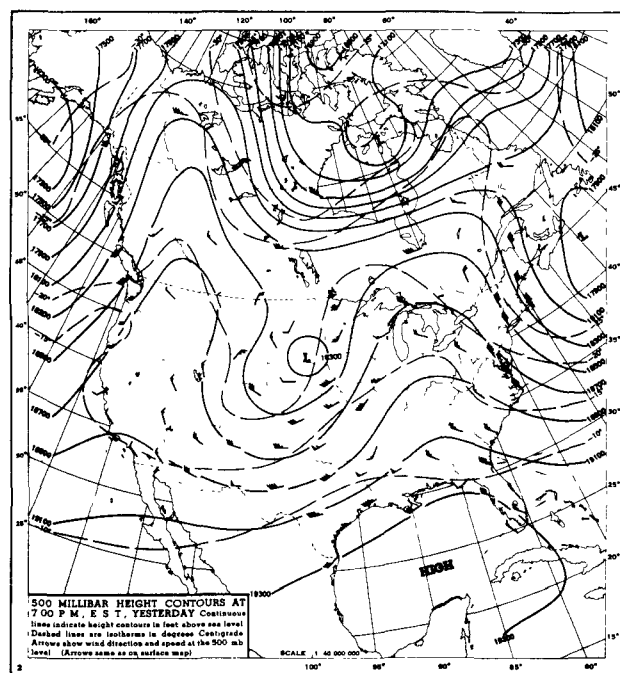
* An isentropic surface is one of constant potential temperature. Air will move along such surfaces in the absence of diabatic processes. Since most processes occurring in subsiding air are nearly adiabatic, tracing air along these surfaces provides a reliable method for determining 3-dimensional motions.



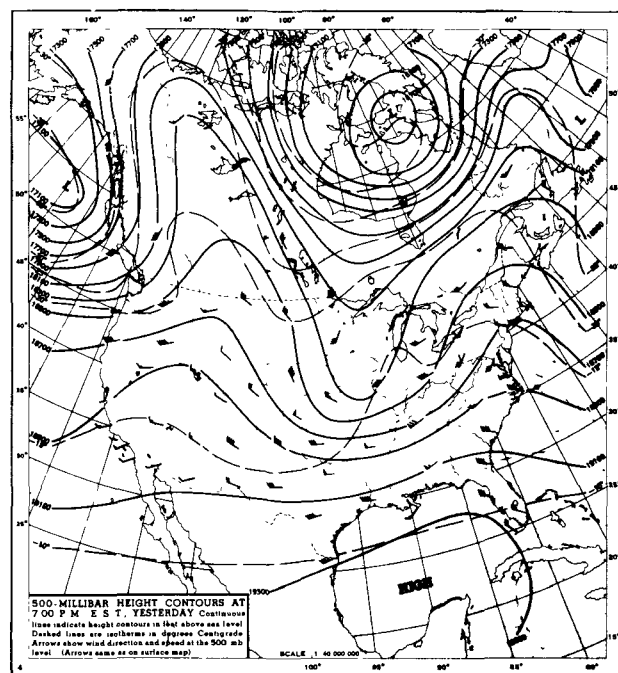
SURFACE MAP, 28 APRIL 1963, 1800 GMT



SURFACE MAP, 29 APRIL 1963, 1800 GMT

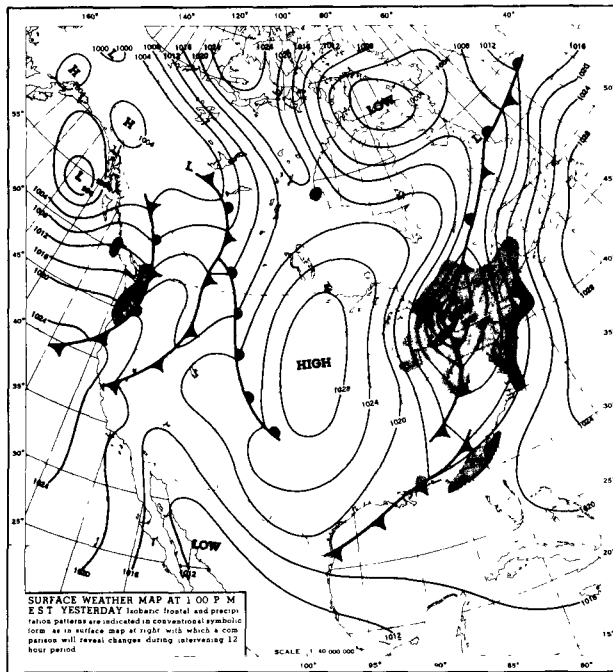


500 MB MAP, 29 APRIL 1963, 0000 GMT

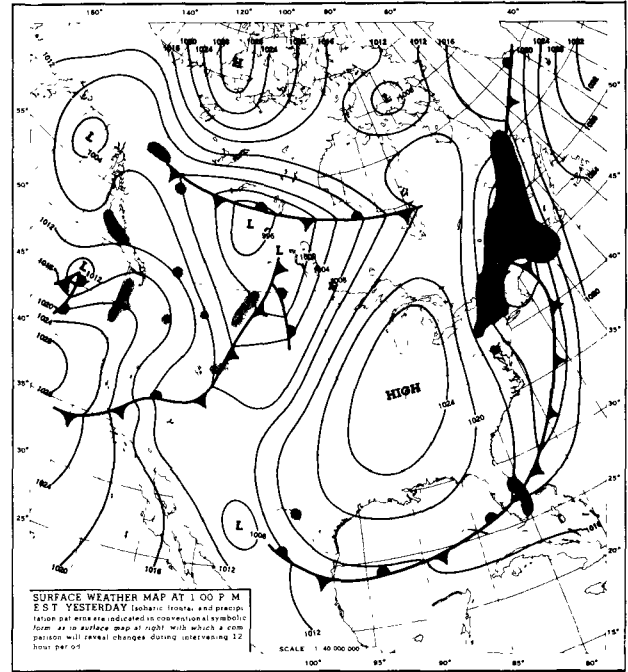


500 MB MAP, 30 APRIL 1963, 0000 GMT

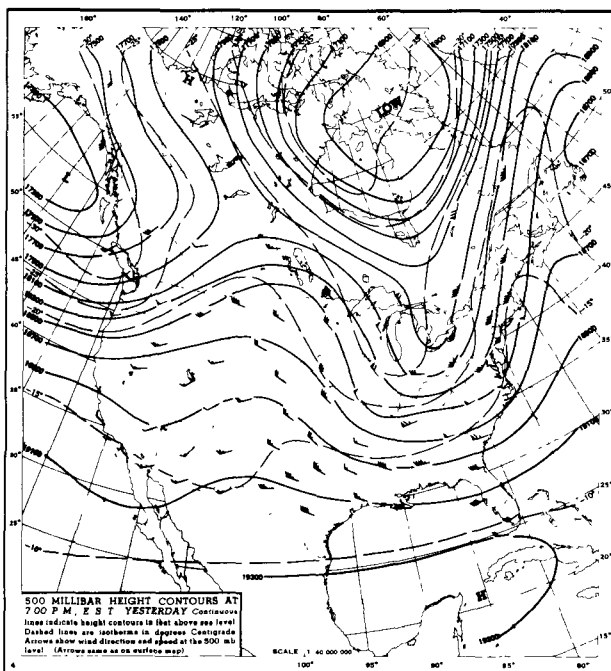
FIGURE 4 NORTH AMERICAN SURFACE AND 500MB CHARTS, 28 APRIL TO 3 MAY 1963



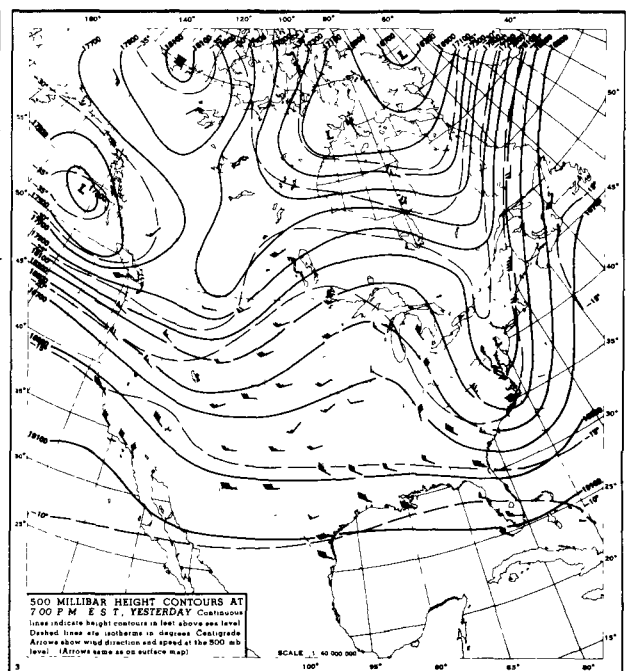
SURFACE MAP, 30 APRIL 1963, 1800 GMT



SURFACE MAP, 1 MAY 1963, 1800 GMT



500 MB MAP, 1 MAY 1963, 0000 GMT



500 MB MAP, 2 MAY 1963, 0000 GMT

FIGURE 4 NORTH AMERICAN SURFACE AND 500MB CHARTS, 28 APRIL TO 3 MAY 1963 (Continued)

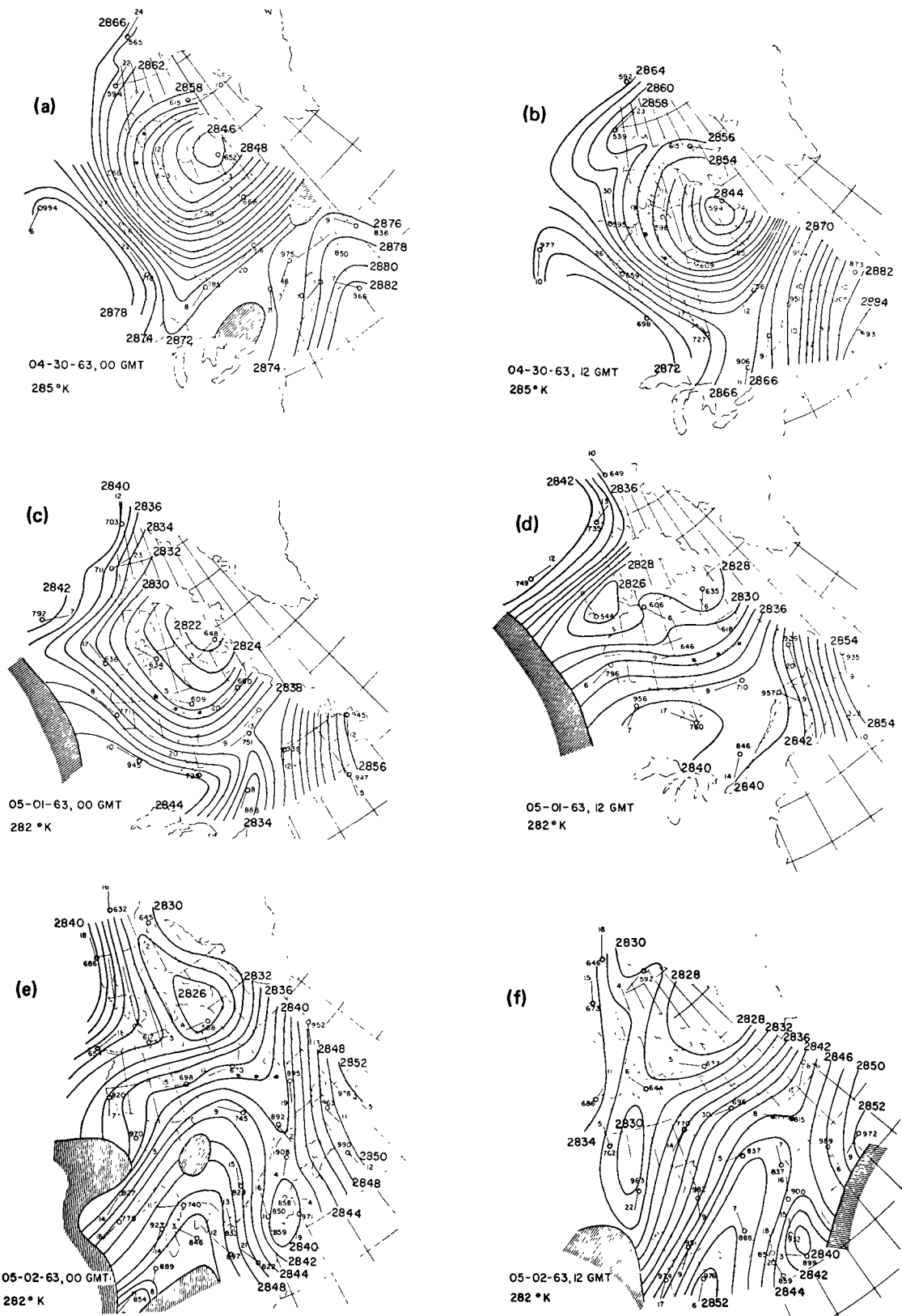


FIGURE 5 MONTGOMERY STREAM FUNCTION ANALYSES ($10^6 \text{ cm}^2 \text{ s}^{-2}$) 30 APRIL-2 MAY 1963

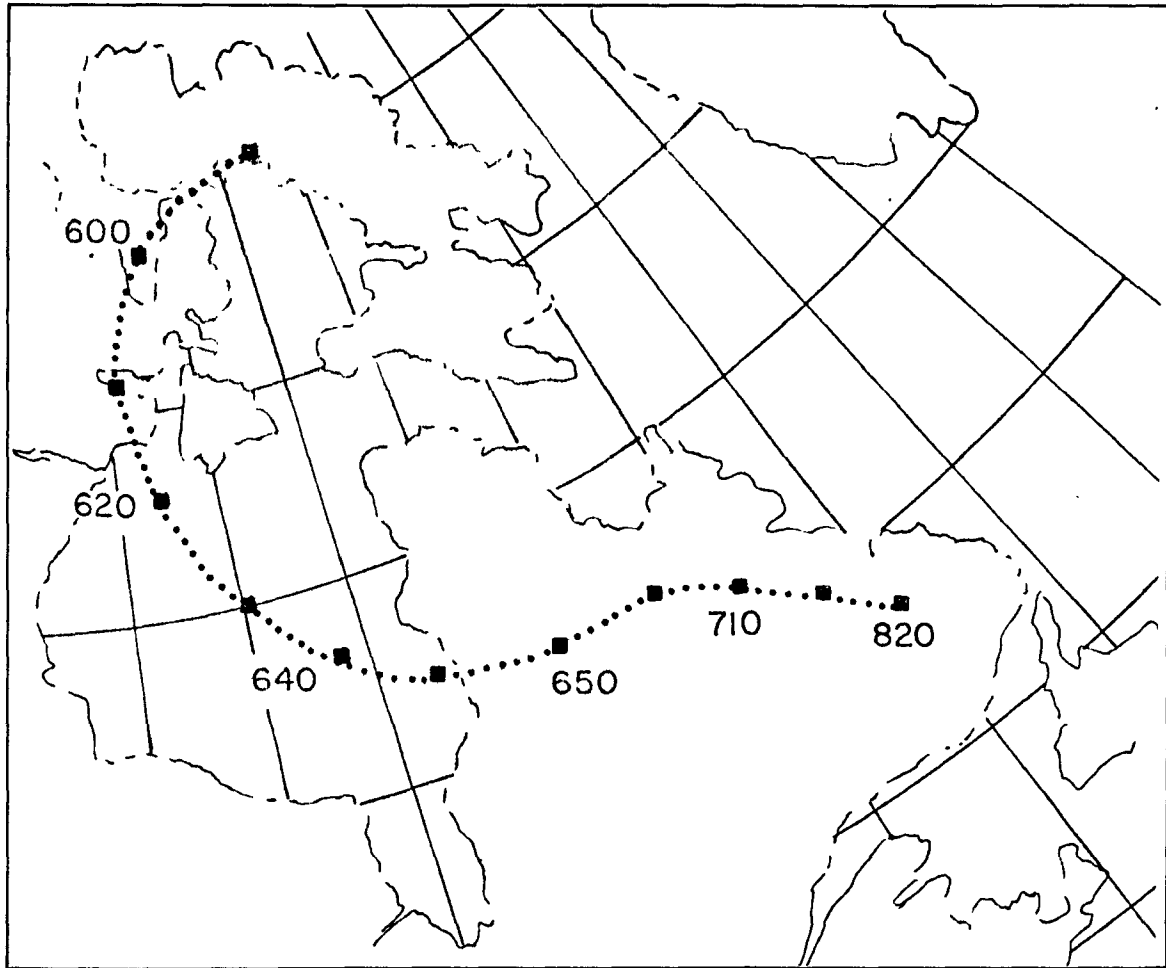


FIGURE 6. COMPOSITE 6-HOUR TRAJECTORY SEGMENTS FROM 29 APRIL 1963, 1800 GMT, TO 2 MAY 1963, 1200 GMT (Pressures in millibars are indicated next to dots corresponding to synoptic observation times.)

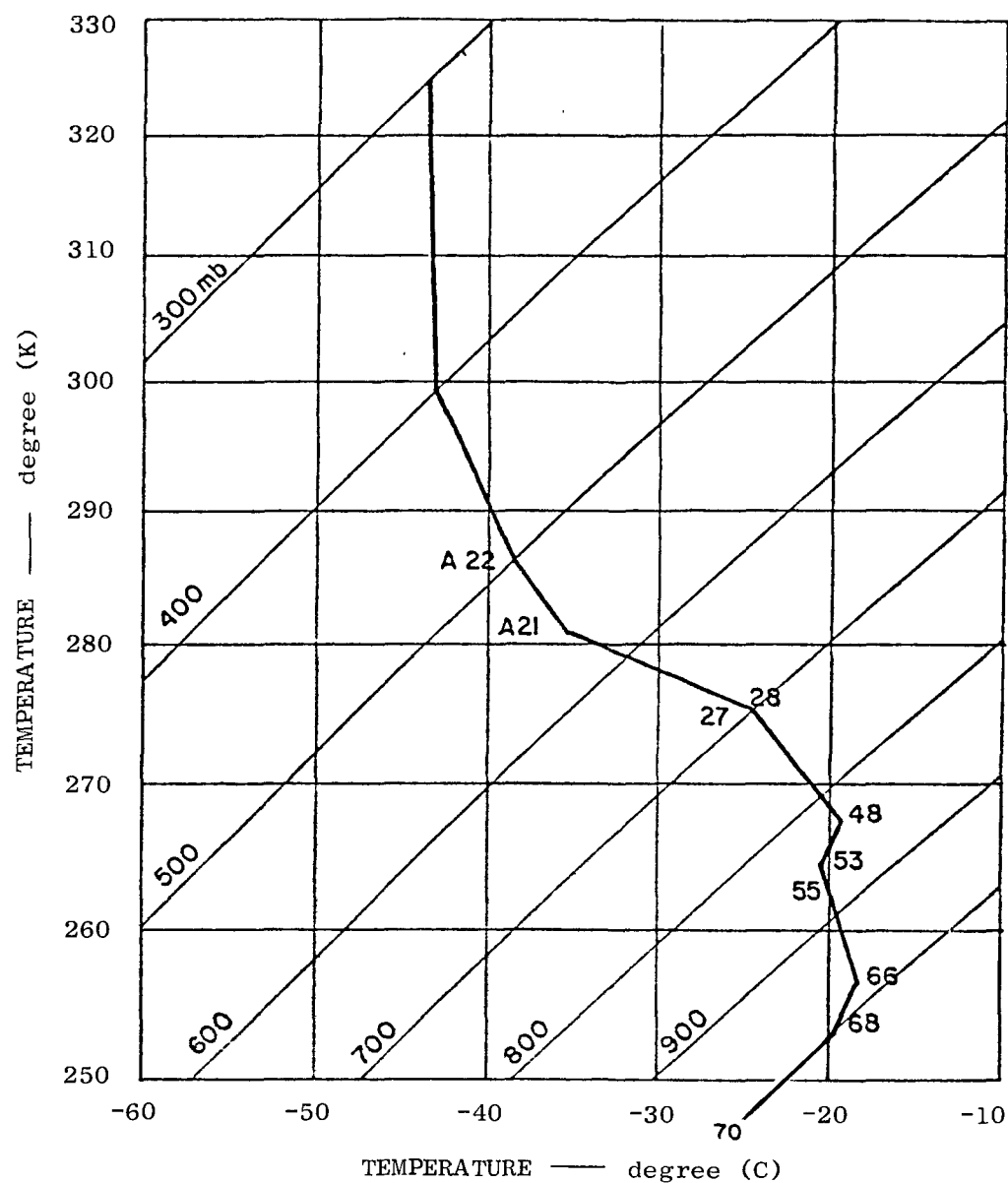


FIGURE 7 RADIOSONDE ASCENT AT BAKER LAKE, CANADA, 1 MAY 1963, 1200 GMT
 (Numbers along the sounding curve indicate relative humidities at significant points.
 'A' signifies that ambient humidity less than the value shown rendered the sensor
 inoperative.)

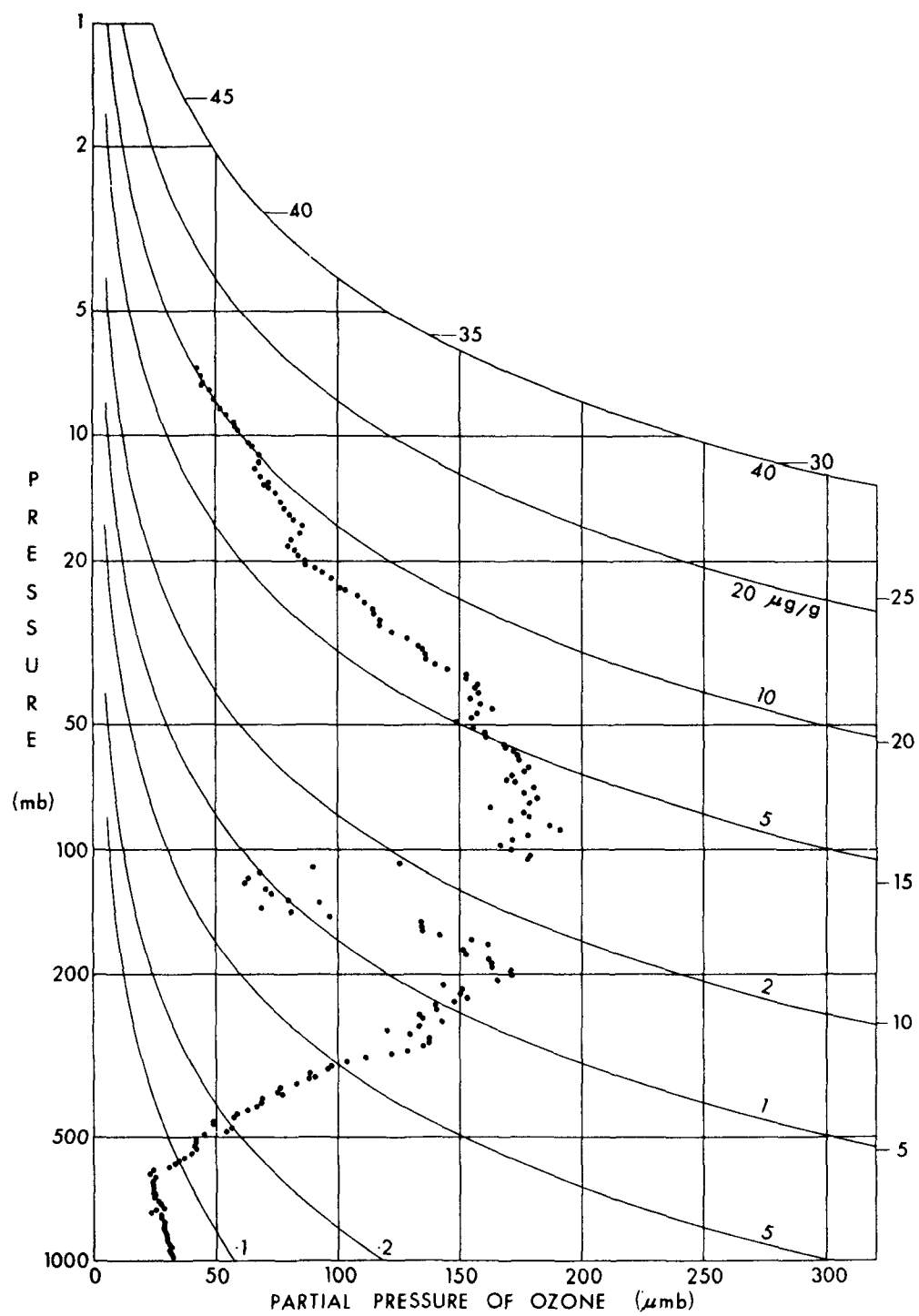


FIGURE 8 OZONE SOUNDING AT THULE, GREENLAND, 1 MAY 1963

2.1.1.3. Bedford, Massachusetts, 26 June 1963

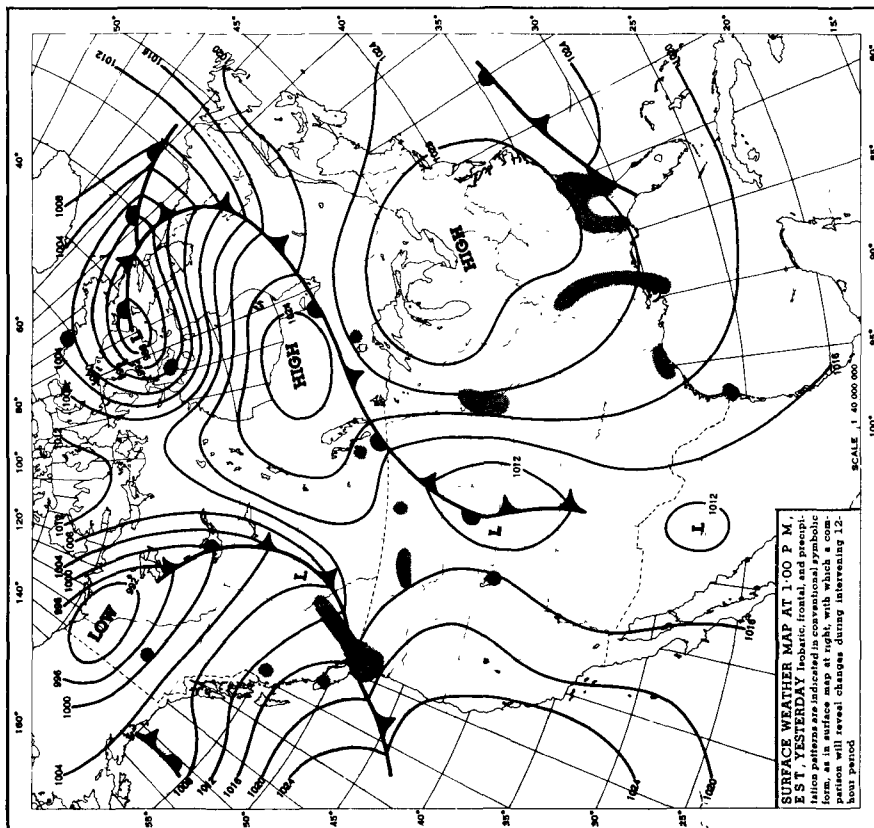
The weather conditions prevailing in this area are shown in Figure 9. The anticyclonic conditions and absence of frontal activity over the northeastern United States are inconsistent with ozone transport from the stratosphere. The confinement of the high ozone concentrations to the lowest level, as shown in Figure 10, also suggests low tropospheric origins. The low humidities that caused this case to be included among those when ozone from the stratosphere was suspected are probably the product of offshore winds and diurnal warming. Thus, stratospheric intrusion was ruled out in this case.

2.1.1.4. Tallahassee, Florida, 14 August 1963.

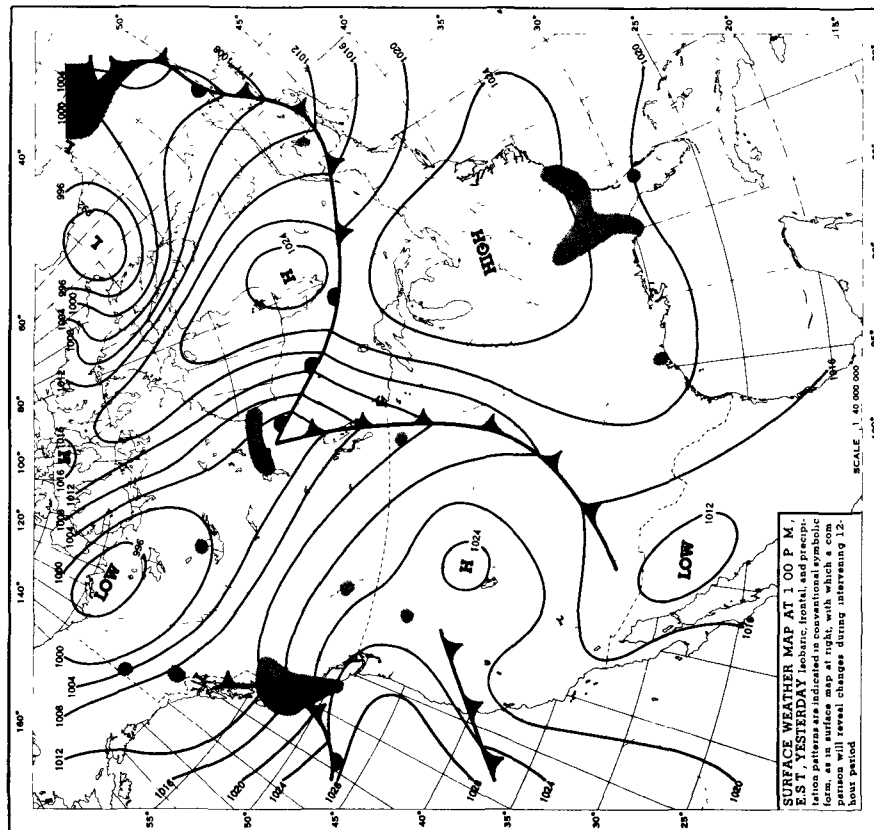
As can be seen in Figure 11, a cold front passed Tallahassee shortly after 0600 GMT on 15 August 1963. The Tallahassee ozone sounding shown in Figure 12 measured exceptionally high ozone concentrations in the lower troposphere around 1212 GMT on 14 August. The temperature sounding in Figure 13 shows stable layer that corresponds with the high ozone concentrations. Very low relative humidities observed between about 700 and 850-mb suggest the presence of pronounced subsidence. The surface weather map of 14 August at 0000 GMT (not depicted here) showed a squall line northwest of Tallahassee with thunderstorm and cumulonimbus development. Subsidence ahead of this squall line could conceivably have carried air from the stratosphere toward the ground. To test this possibility, the isentropic trajectories shown in Figure 14 were constructed backward in time, starting with 14 August at 1200 GMT, on the 304°K isentropic surface over Tallahassee. This surface was chosen because the nearest upwind sounding (Montgomery, Alabama), for that time revealed a frontal inversion at 304°K potential temperature (Figure 15).

It is important to remember that active cyclogenesis had been associated with the front in question a few days earlier (11 August). Mahlman and Reiter (for references see Reiter, 1972) have identified periods of strong cyclogenesis as prerequisites for the transport of stratospheric air into the troposphere and toward the ground. Usually such stratospheric air is found in stable layers above the planetary boundary layer, especially in the anticyclonic area developing behind an advancing cold front. In the present case it appears likely that the squall-line development ahead of the front disrupted the normal course of events, allowing some of the stratospheric air to intrude ahead of the cold front. It is somewhat analogous the occasional transport of stratospheric ozone to the ground by the action of strong waves in the lee of the Rocky Mountains (Reiter, 1975).

It is reasonable to assume that the major transport of stratospheric air was associated with the frontal inversion centered on the 304°K isentropic surface on 12 August, at 1200 GMT. The Montgomery stream function and trajectory analyses presented in Figure 14 show that the trajectory ending at Tallahassee on 14 August at 1200 GMT had come from the northwest and was subjected to strong subsidence during its course.



SURFACE MAP, 24 JUNE 1963, 1800 GMT



SURFACE MAP, 25 JUNE 1963, 1800 GMT

FIGURE 9 NORTH AMERICAN WEATHER MAPS, 24-25 JUNE 1963

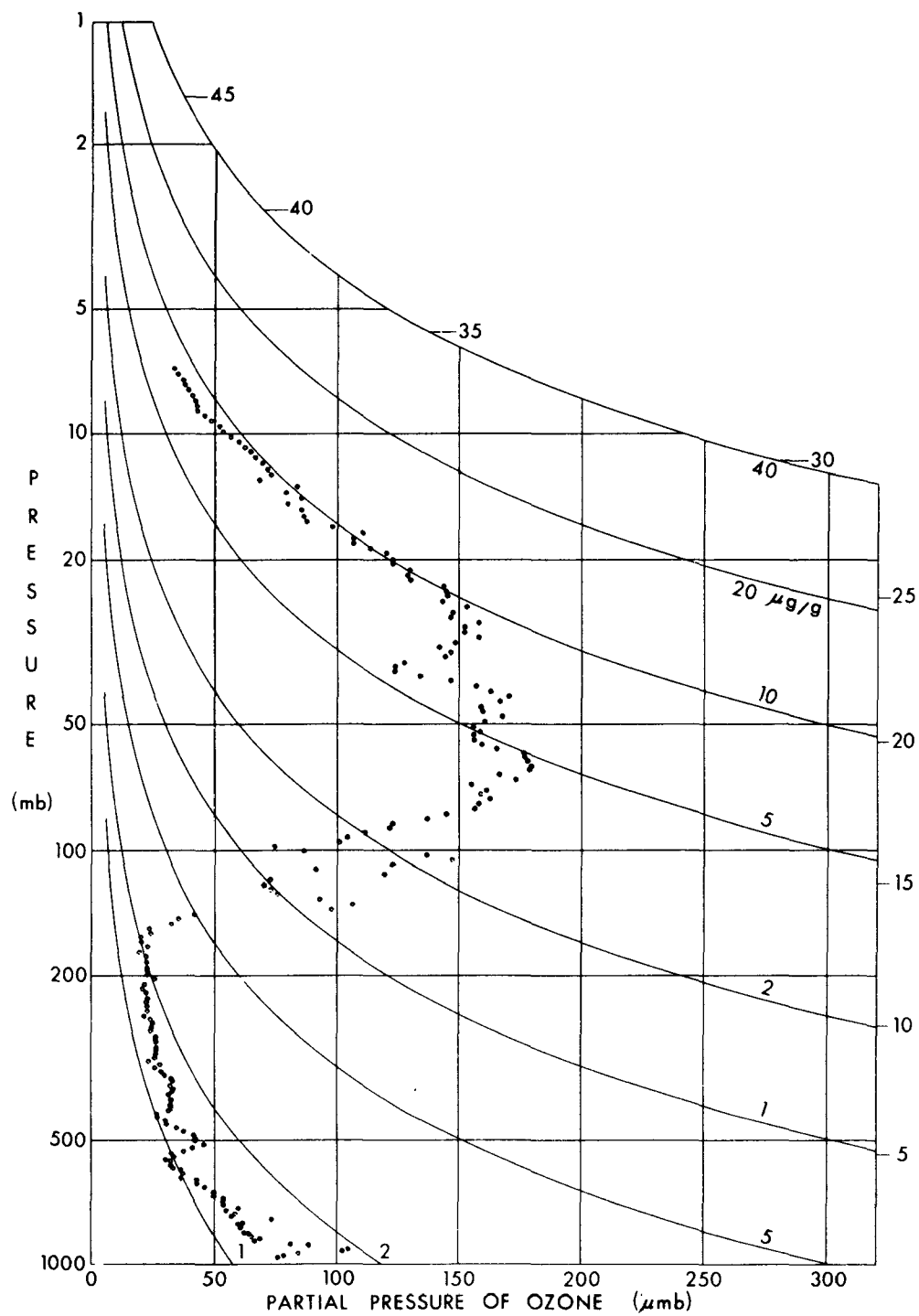
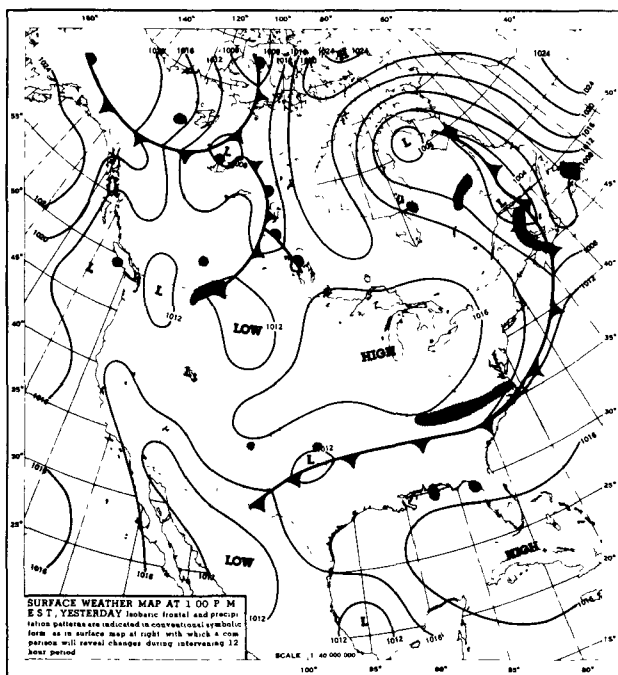
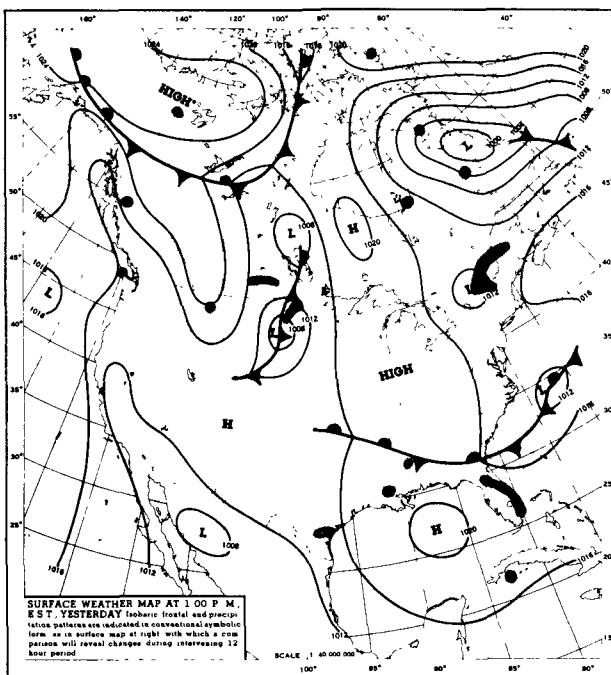


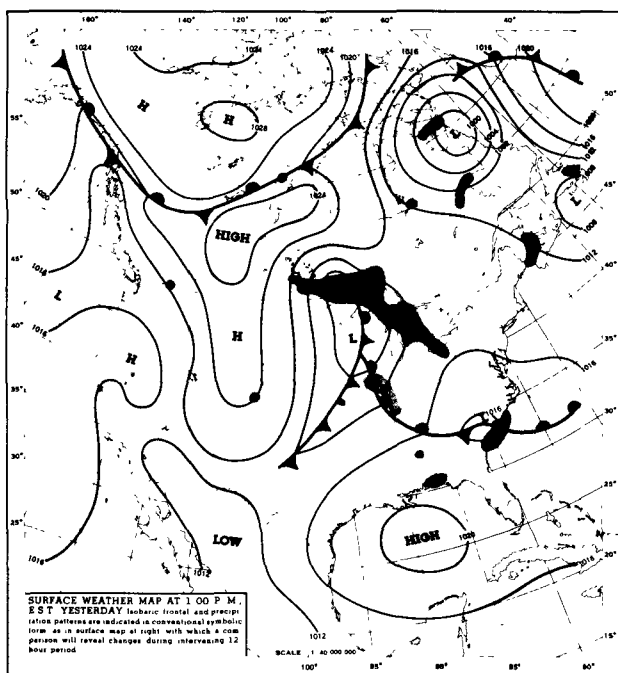
FIGURE 10 OZONE SOUNDING AT BEDFORD, MASSACHUSETTS, 26 JUNE 1963



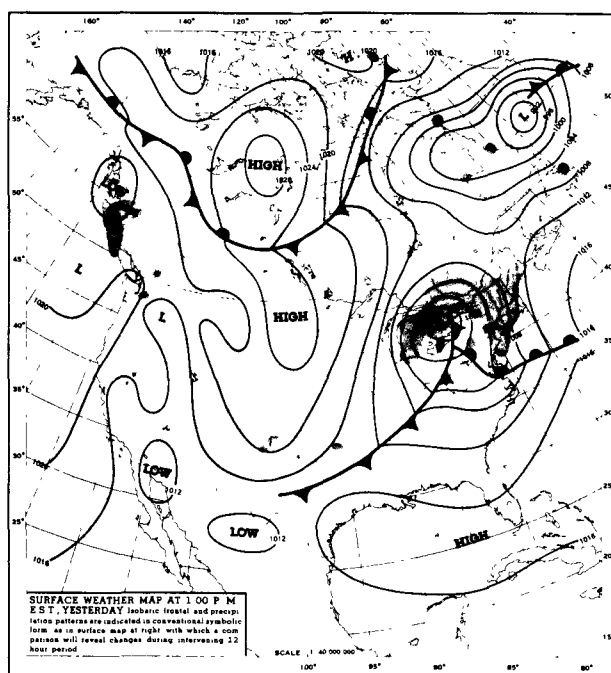
SURFACE MAP, 10 AUGUST 1963, 1800 GMT



SURFACE MAP, 11 AUGUST 1963, 1800 GMT

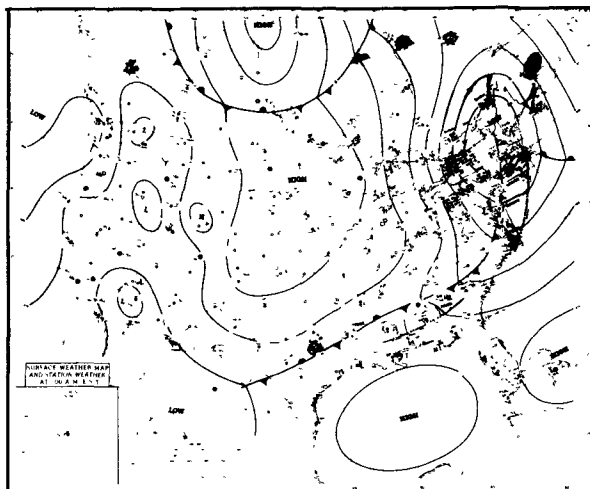


SURFACE MAP, 12 AUGUST 1963, 1800 GMT

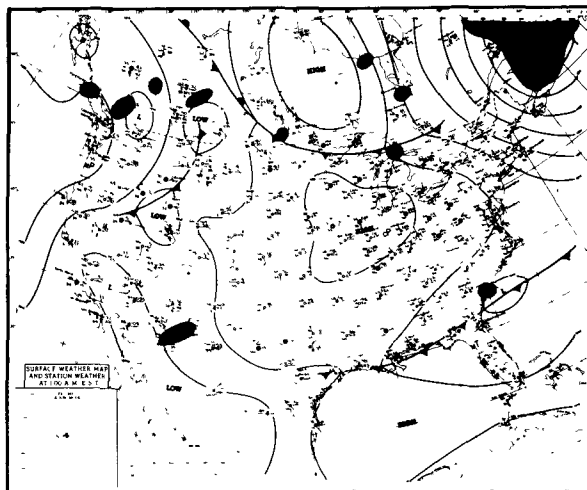


SURFACE MAP, 13 AUGUST 1963, 1800 GMT

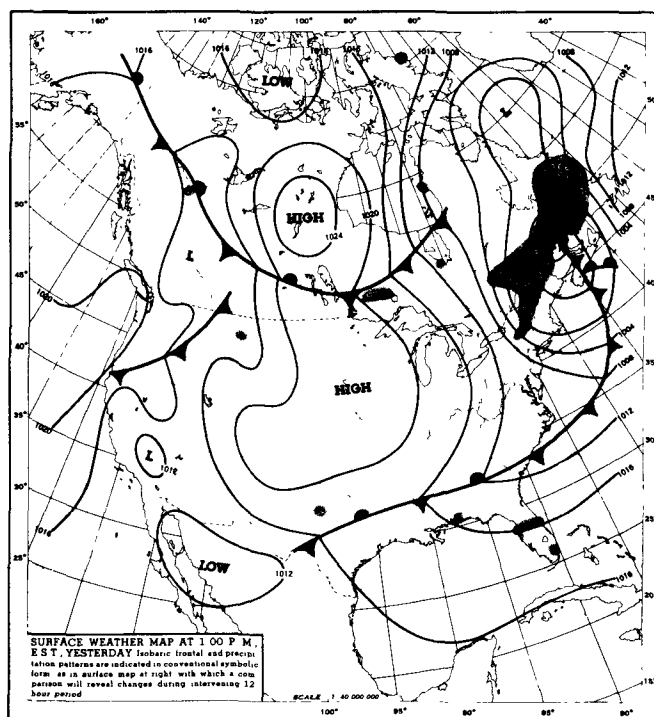
FIGURE 11 NORTH AMERICAN WEATHER MAPS, 10 AUGUST TO 15 AUGUST 1963



SURFACE MAP, 14 AUGUST 1963, 0600 GMT



SURFACE MAP, 15 AUGUST 1963, 0600 GMT



SURFACE MAP, 14 AUGUST 1963, 1800 GMT

FIGURE 11 NORTH AMERICAN WEATHER MAPS, 10 AUGUST TO 15 AUGUST 1963 (Concluded)

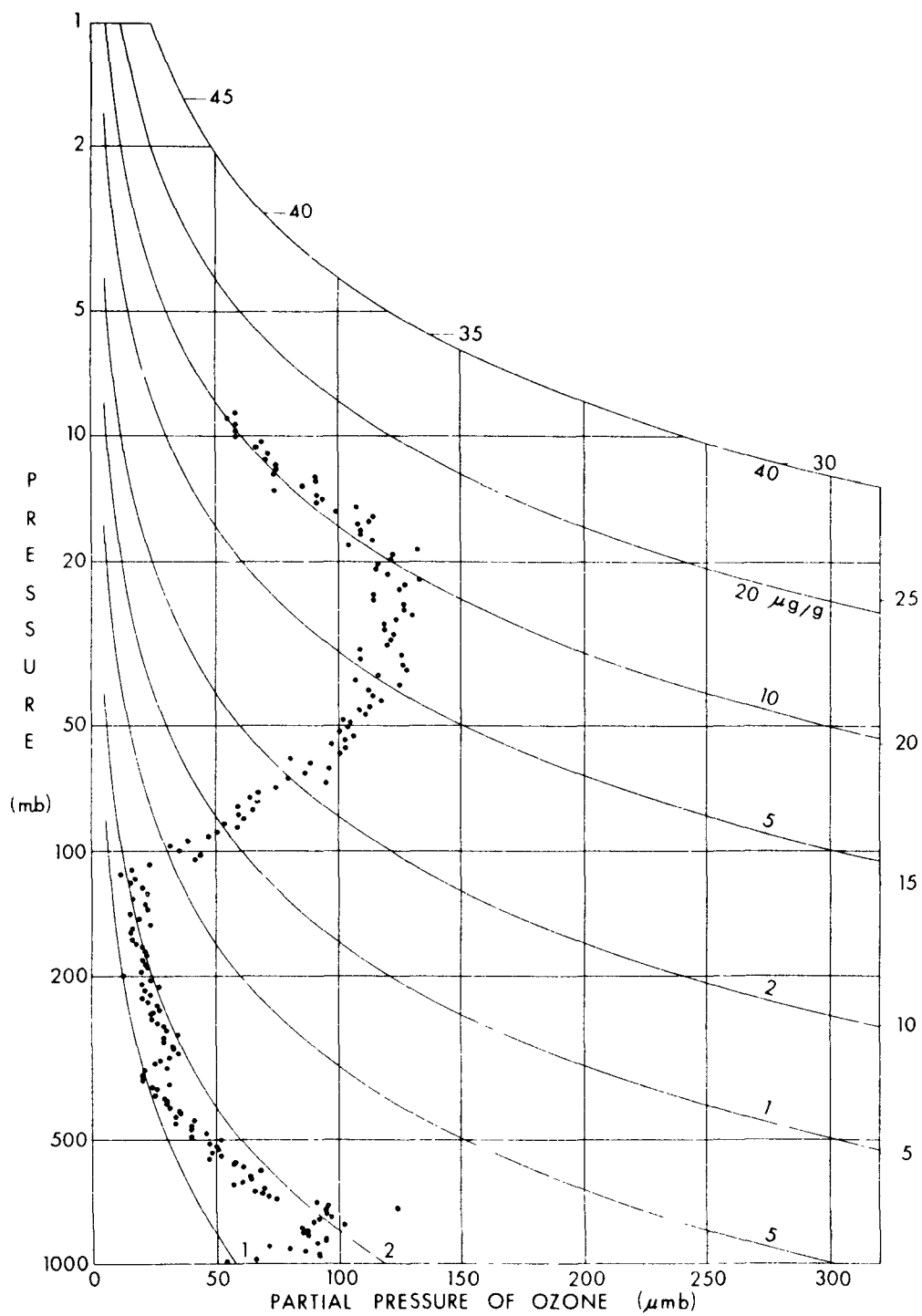


FIGURE 12 OZONE SOUNDING AT TALLAHASSEE,
FLORIDA, 14 AUGUST 1963

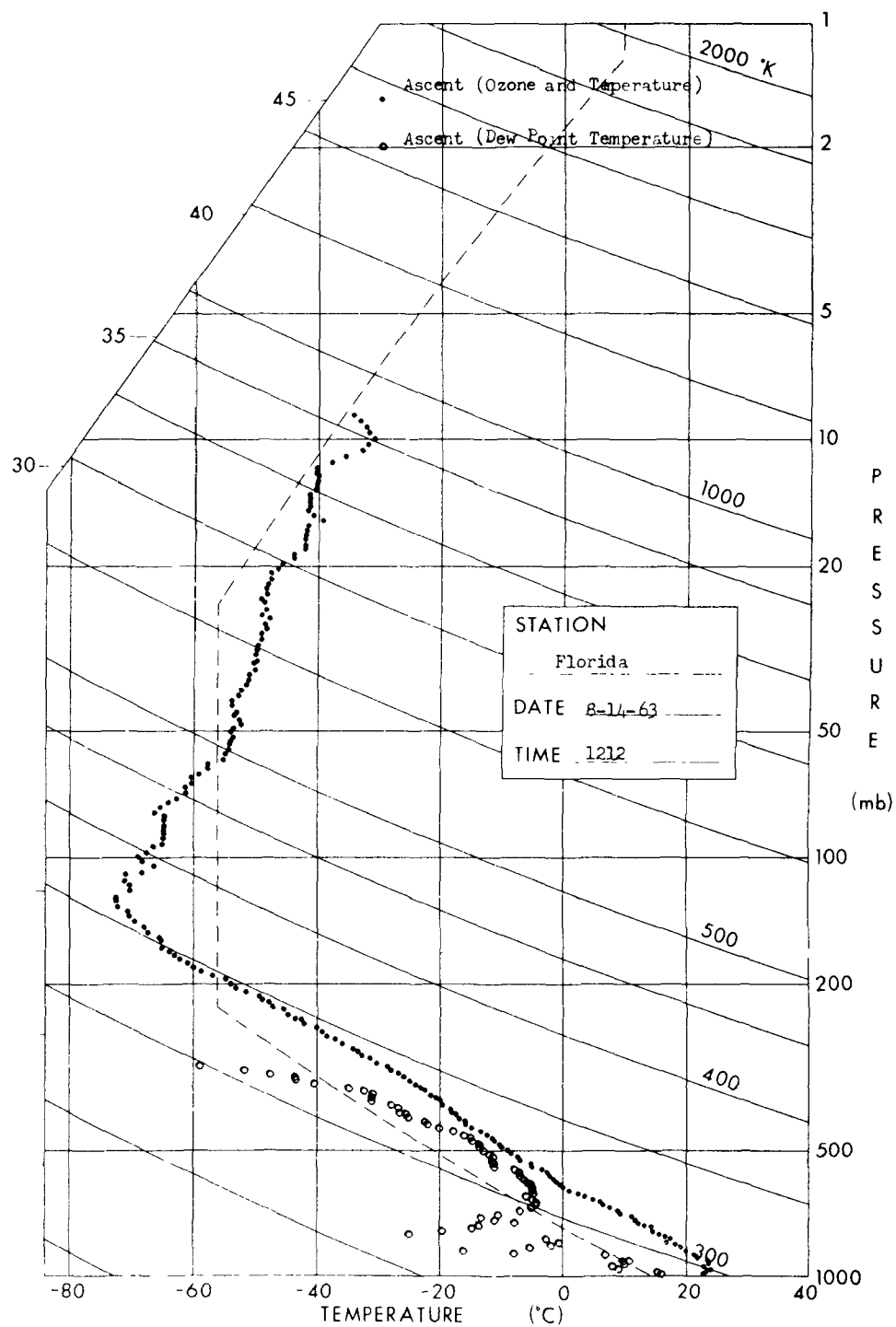


FIGURE 13 TEMPERATURE AND DEWPOINT SOUNDINGS AT
TALLAHASSEE, FLORIDA, 14 AUGUST 1963

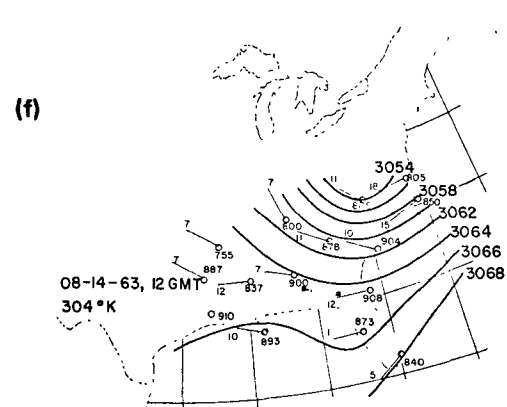
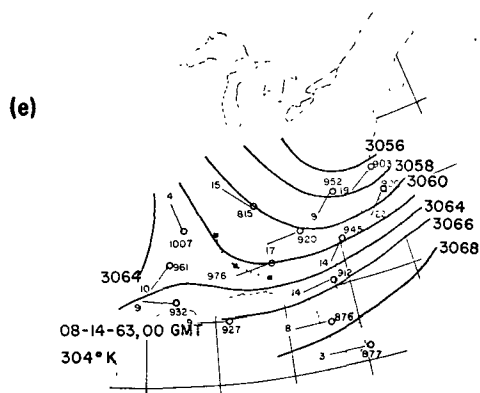
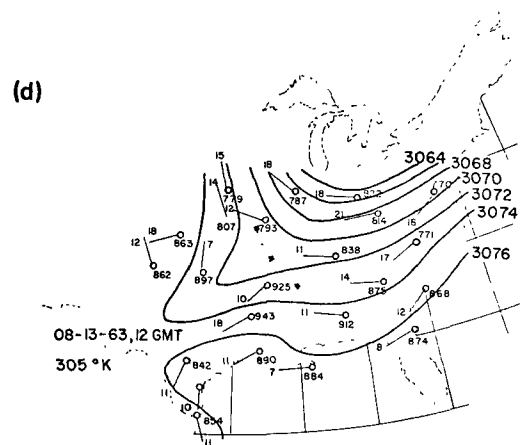
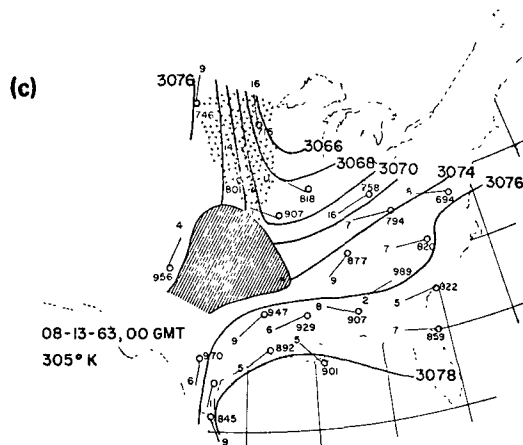
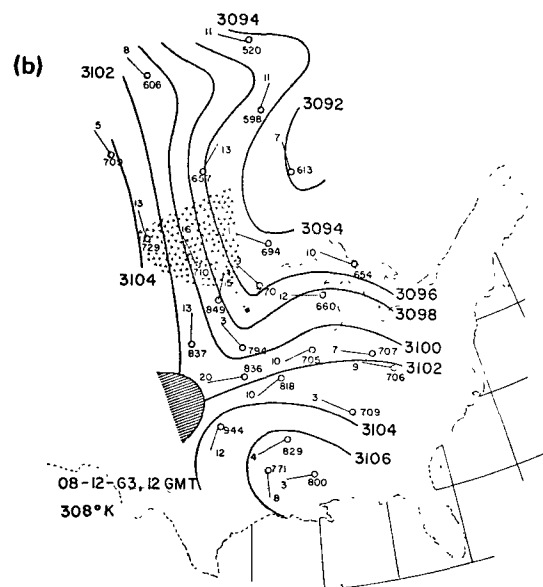
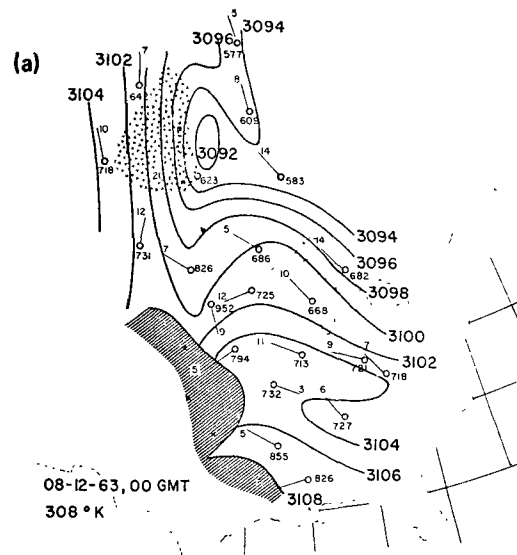


FIGURE 14 MONTGOMERY STREAM FUNCTION ANALYSES ($10^6 \text{cm}^2 \text{s}^{-2}$), 12 AUGUST TO 14 AUGUST 1963 (See Figure 18 for meaning of symbols)

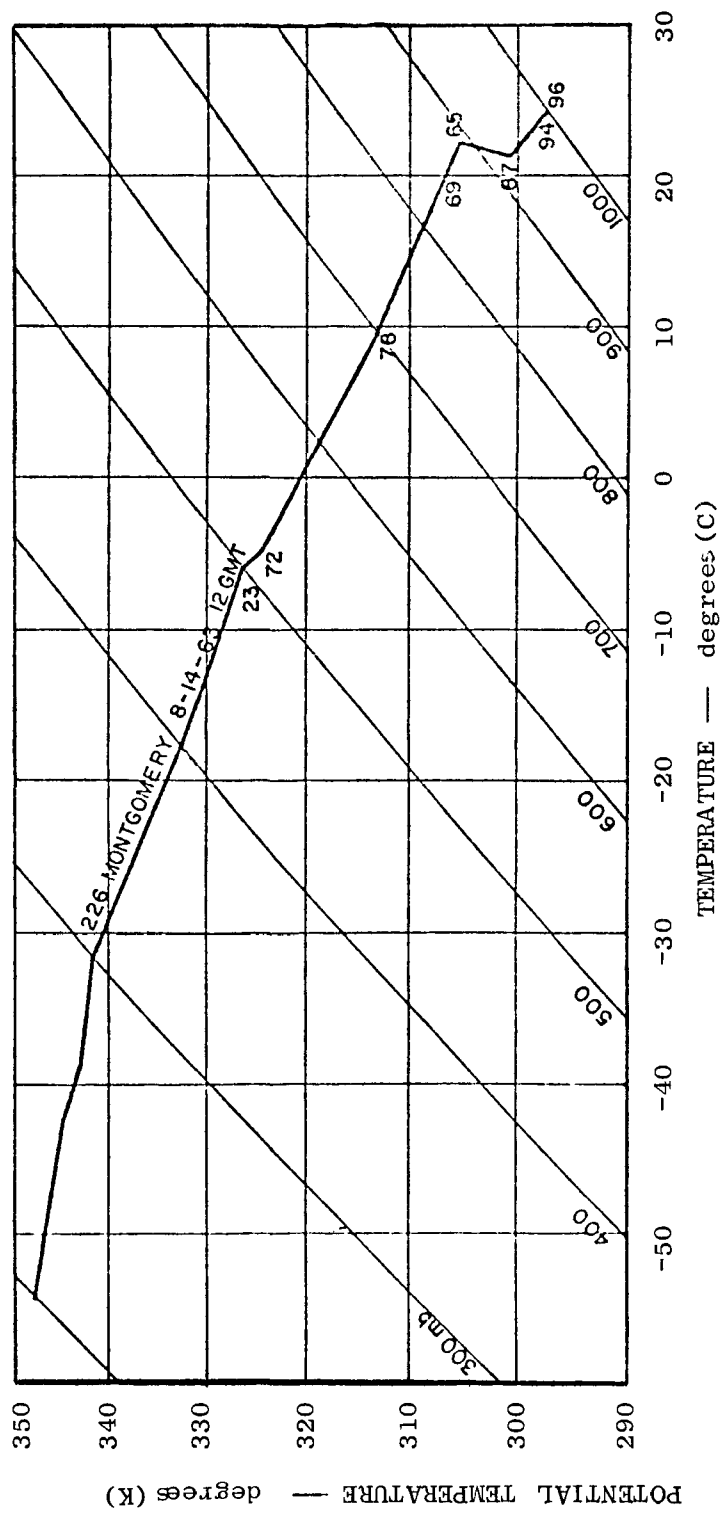


FIGURE 15 SOUNDING AT MONTGOMERY, ALABAMA, 14 AUGUST, 1963, 1200 GMT
(Numbers along the sounding curve indicate relative humidities at significant points.)

The leading edge of the stratospheric air intrusion, according to these analyses, coincides with the edge of a tongue of dry air. The dryness of the air intrusion is documented by the soundings from Omaha, Nebraska, and Columbia, Missouri, on 13 August at 0000 GMT (Figure 16). It appears that the frontal zone at these two stations was located at slightly higher potential temperature than 304°K , as expected with the diabatic processes of radiational cooling and entrainment that occur in a rapidly subsiding air mass. Accordingly, the trajectory segments for 13 August were calculated for the 305°K isentropic surface. On 12 August, 0000 GMT, the sounding at The Pas, Canada, intersected the frontal zone under consideration (Figure 17). Higher potential temperatures (the 308°K isentropic level) were chosen for the trajectory segment calculations for that day.

The sparsity of radiosonde data over northern Canada and the Arctic prevented the construction of reliable trajectories further back in time. Resolute, Canada, had a dry layer above the 600-mb level on 11 August, 0000 GMT (Figure 17), which in all likelihood was connected with the stratospheric air intrusion under consideration.

Figure 18 summarizes the trajectory analysis for this case. Within three days, air presumed to contain relatively high ozone concentrations descended from the vicinity of the 600-mb level to the 900-mb level and traversed Canada and the United States. The high ozone concentrations over Tallahassee on 14 August could therefore have been due to a stratospheric air intrusion.

2.1.1.5. Seattle, Washington, 8 April 1964

The ozone sounding for this case is shown in Figure 19. In this instance, the high ozone concentrations at low altitudes were not found with any of the weather conditions that are usually associated with intrusions of stratospheric air. Figure 20 shows that the Seattle area had had no passages of cold fronts, nor was there evidence of squall line activity associated with an approaching front. Thus, it is unlikely that the observed ozone concentrations at the lower altitudes came from the stratosphere. Tropospheric origins are much more likely. Thus, this case was eliminated from further consideration.

2.1.1.6. Seattle, Washington, 15 and 17 April 1964

The ozone soundings for these two days are shown in Figures 21 and 22. The prolonged period of relatively high concentrations at Seattle was characterized by the passage of a cold front on 15 April and by subsequent northwesterly flow aloft in the rear of a trough, as can be seen in Figure 23. Intrusion of stratospheric air under such conditions is very likely. Unfortunately, detailed trajectory analyses were impossible because of the lack of adequate rawinsonde data over the Pacific. Thus, these cases were not considered further.

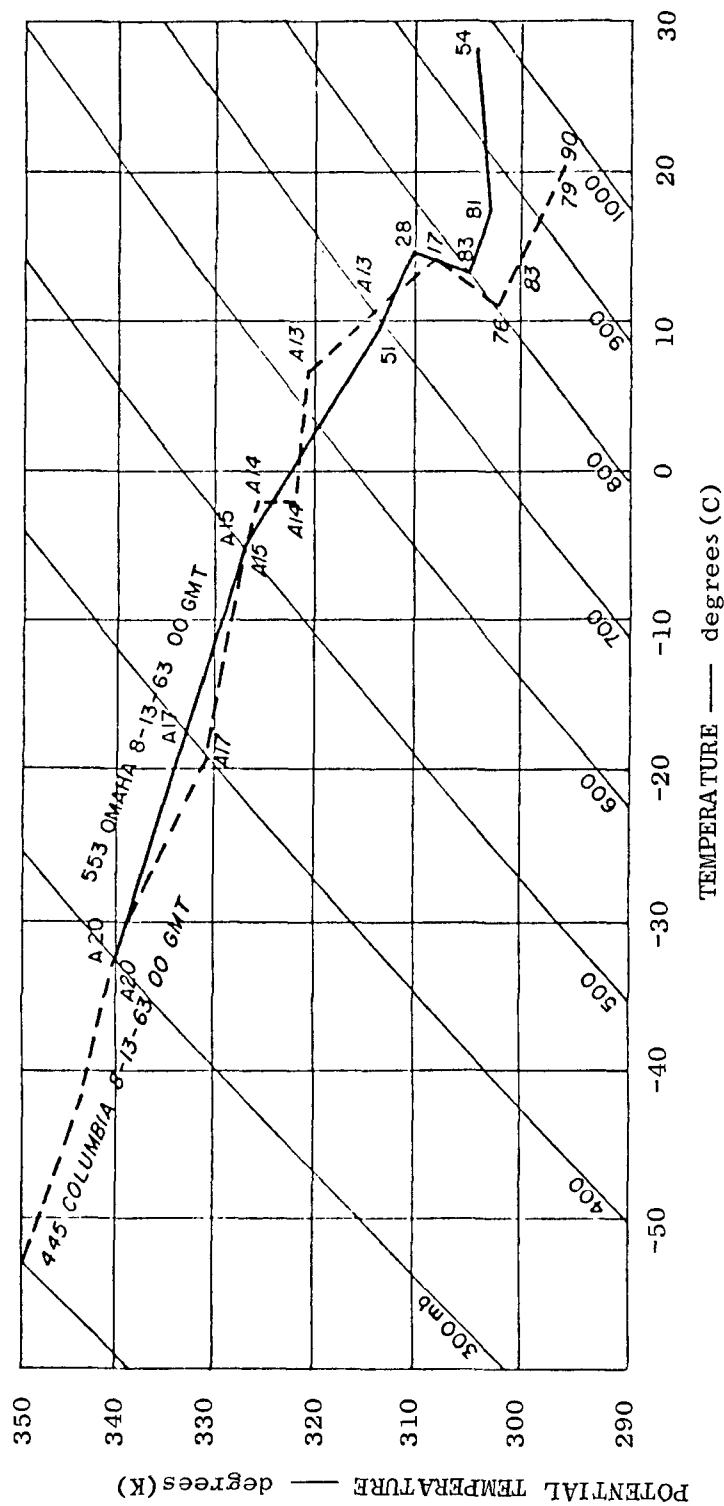


FIGURE 16 SOUNDINGS FOR OMAHA, NEBRASKA AND COLUMBIA, MISSOURI, 13 AUGUST 1963, 0000 GMT
 (Relative humidity values are shown next to sounding. An 'A' indicates that ambient humidity is less than the value shown and had rendered the sensor inoperative.)

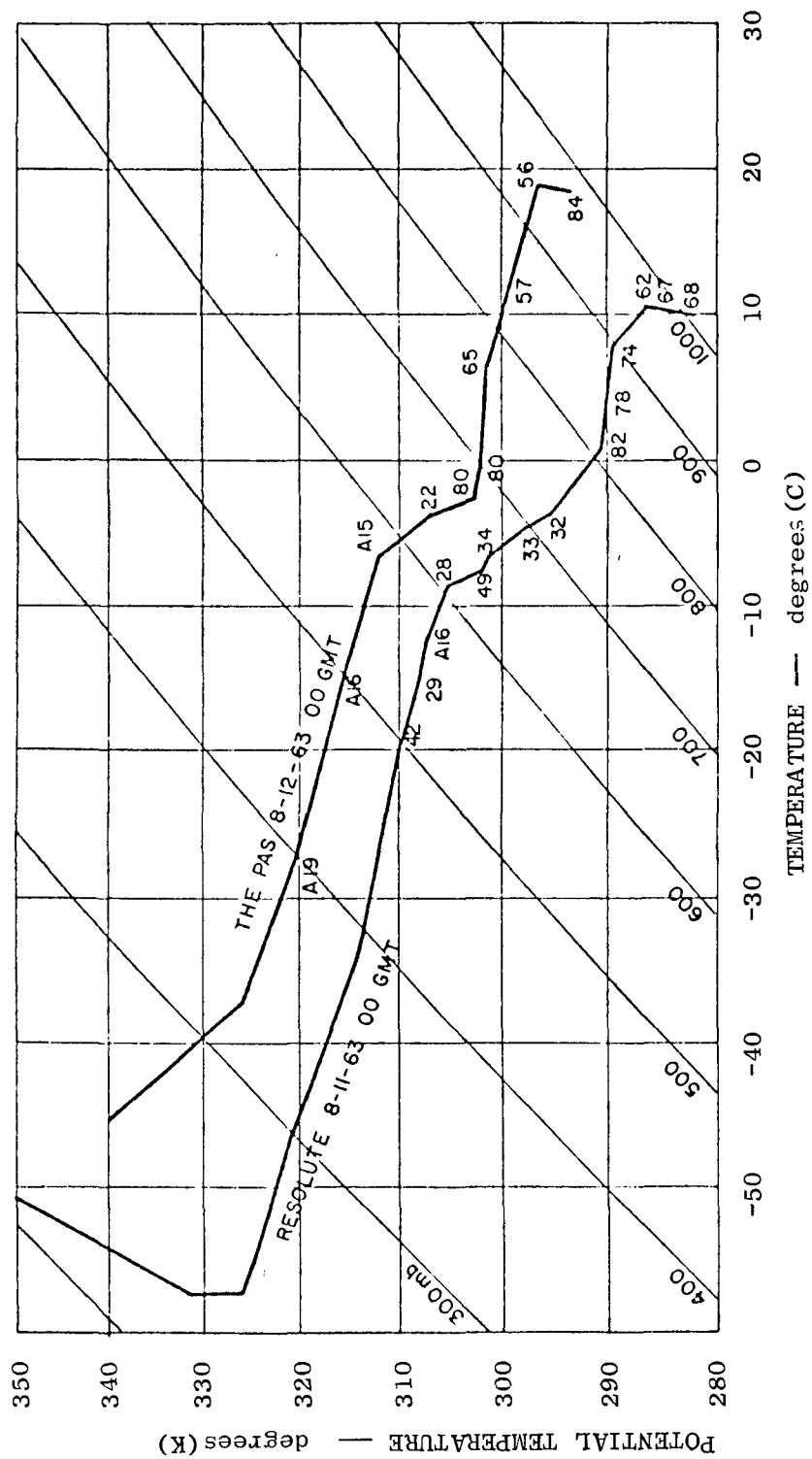


FIGURE 17 SOUNDINGS FOR THE PAS (11 August 1963) AND RESOLUTE, CANADA (12 August 1963) (12 August 1963), 0000 GMT (Humidity values are entered as in previous sounding diagrams.)

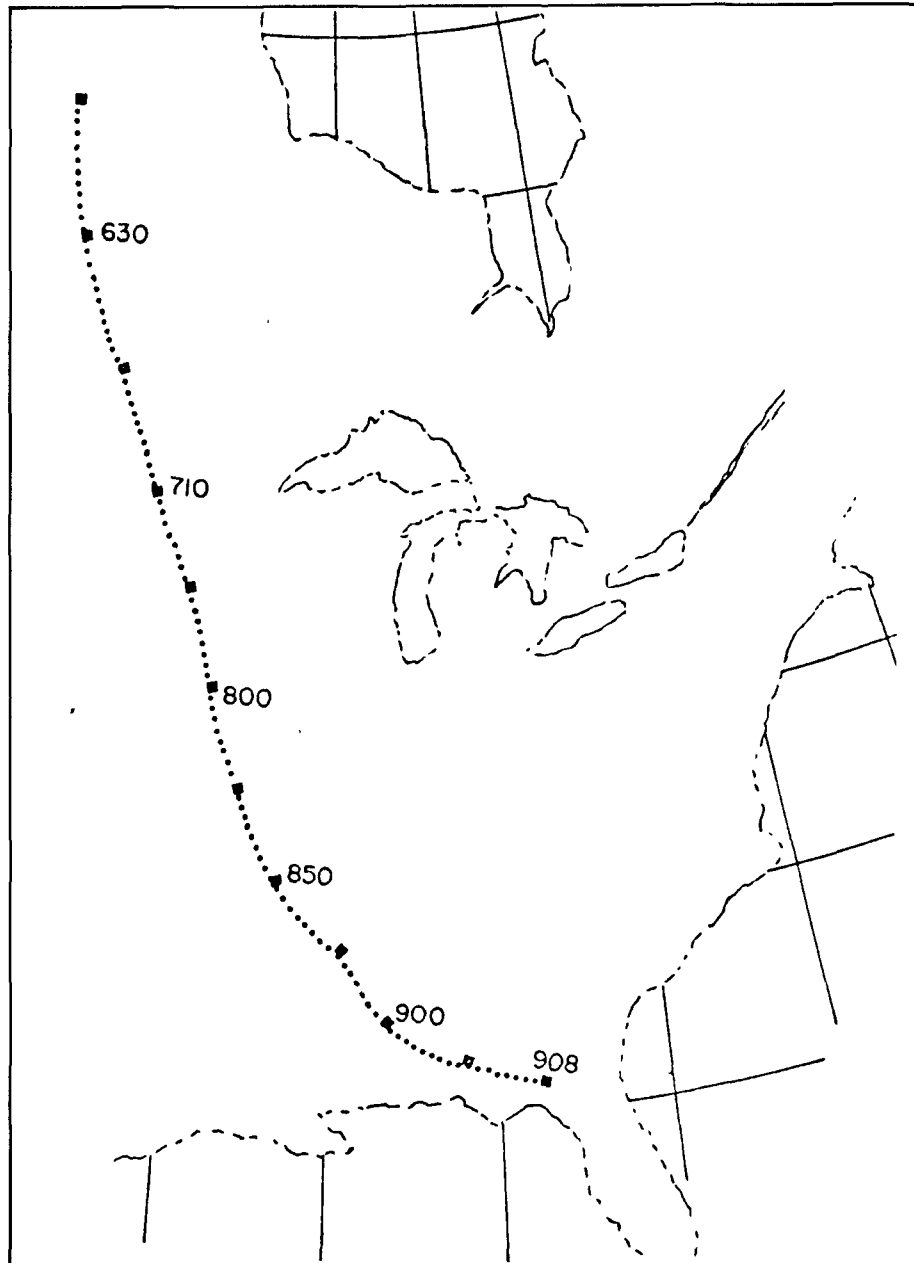


FIGURE 18 COMPOSITE 6-HOUR TRAJECTORY SEGMENTS FROM
11 AUGUST 1963, 1800 GMT TO 14 AUGUST 1963, 1200 GMT
(Pressures in millibars are indicated next to the dots
corresponding to synoptic observation times.)

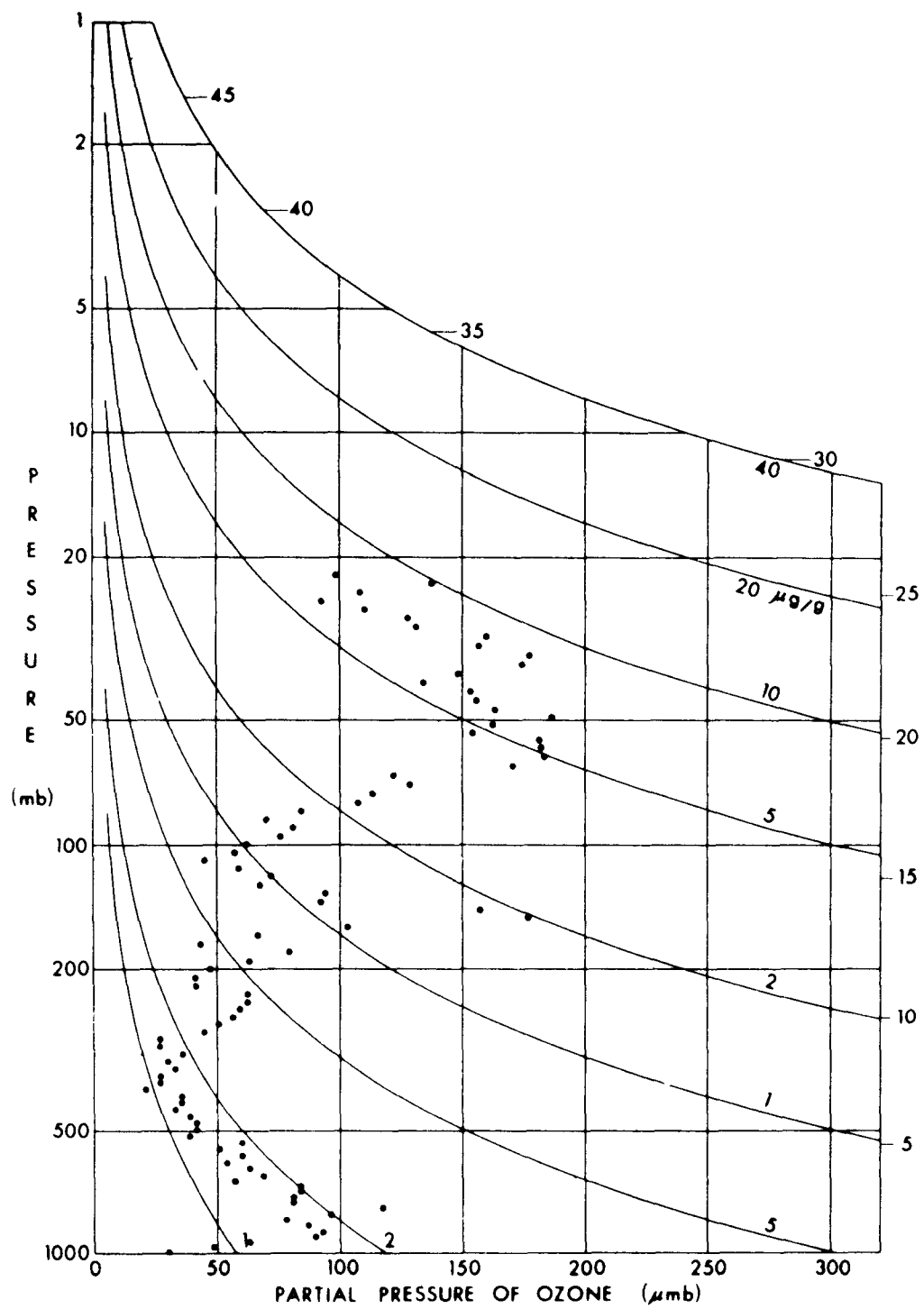
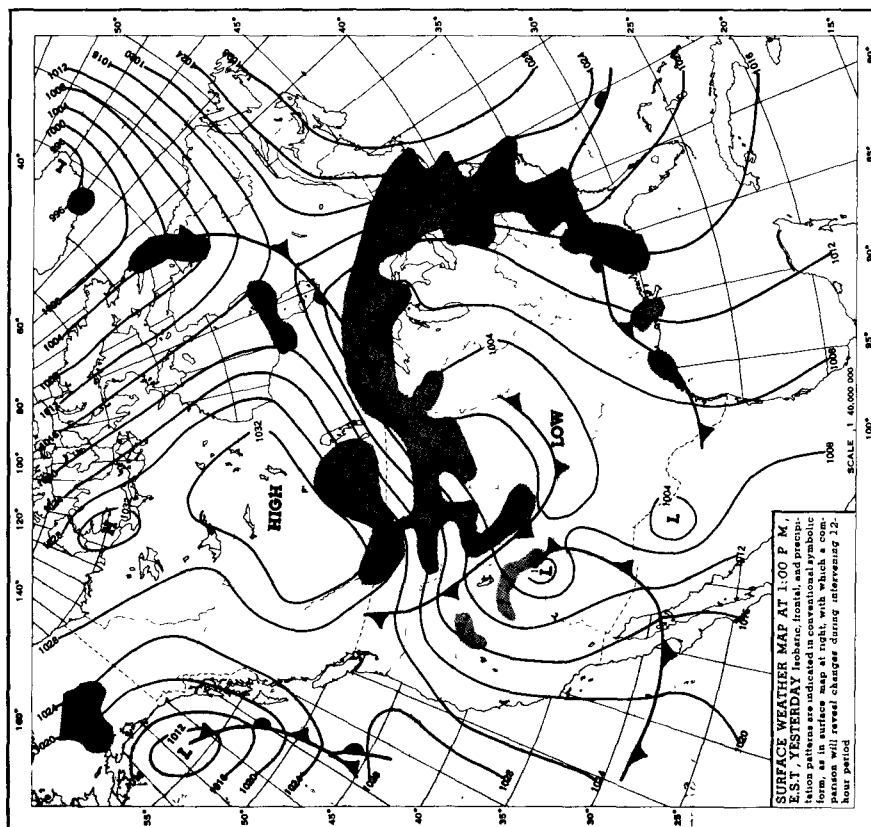
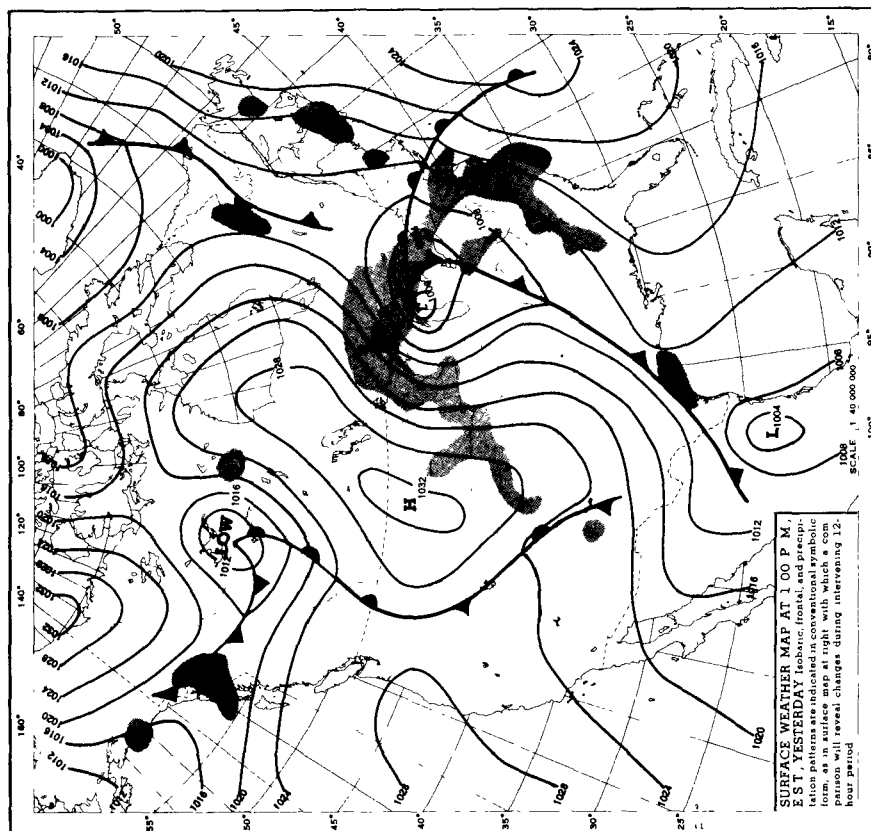


FIGURE 19 OZONE SOUNDING AT SEATTLE,
WASHINGTON, 8 APRIL 1964



SURFACE MAP, 6 APRIL 1964, 1800 GMT



SURFACE MAP, 7 APRIL 1964, 1800 GMT

FIGURE 20 NORTH AMERICAN WEATHER MAPS, 6-7 APRIL 1964

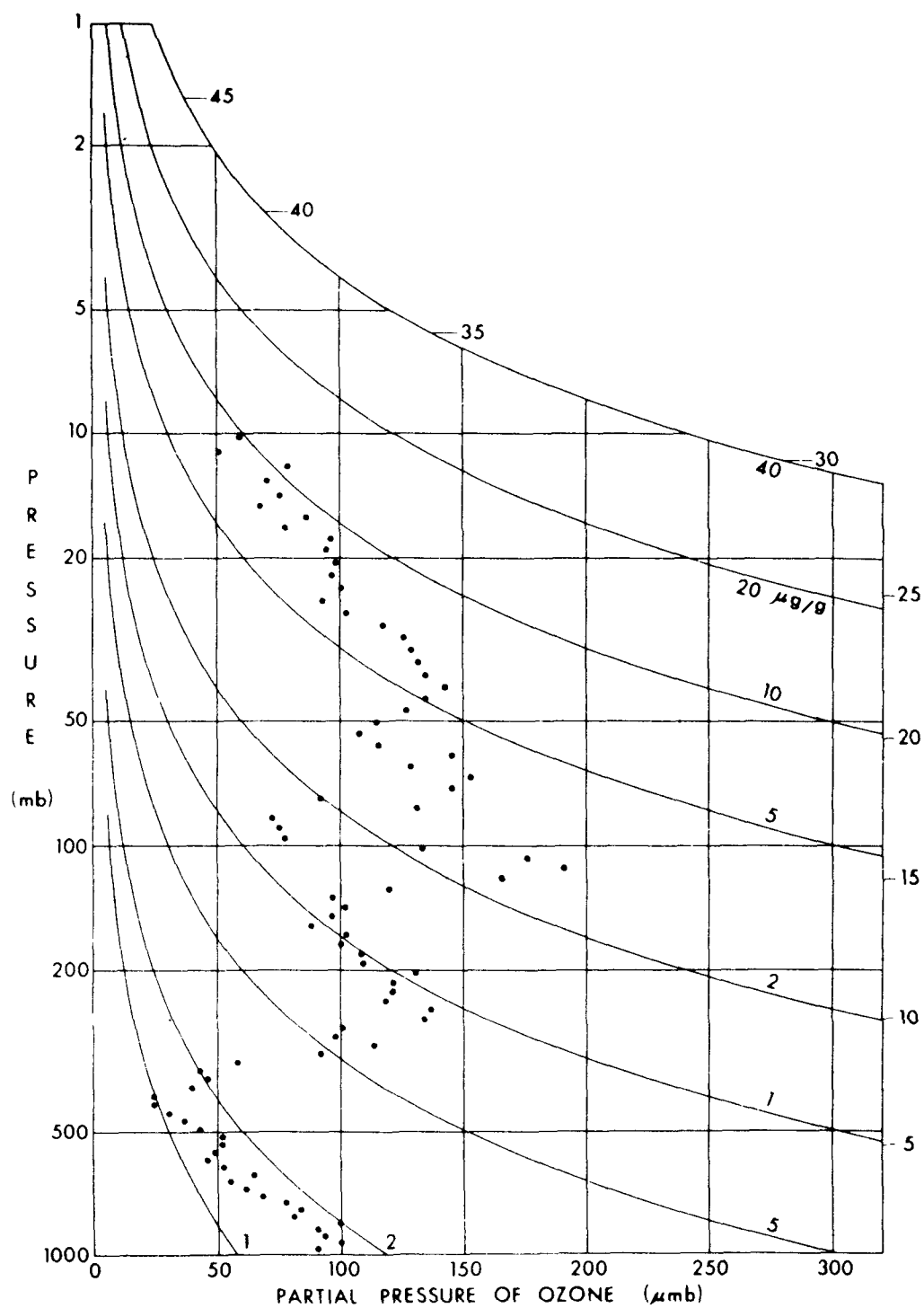


FIGURE 21 OZONE SOUNDING AT SEATTLE,
WASHINGTON, 15 APRIL 1964

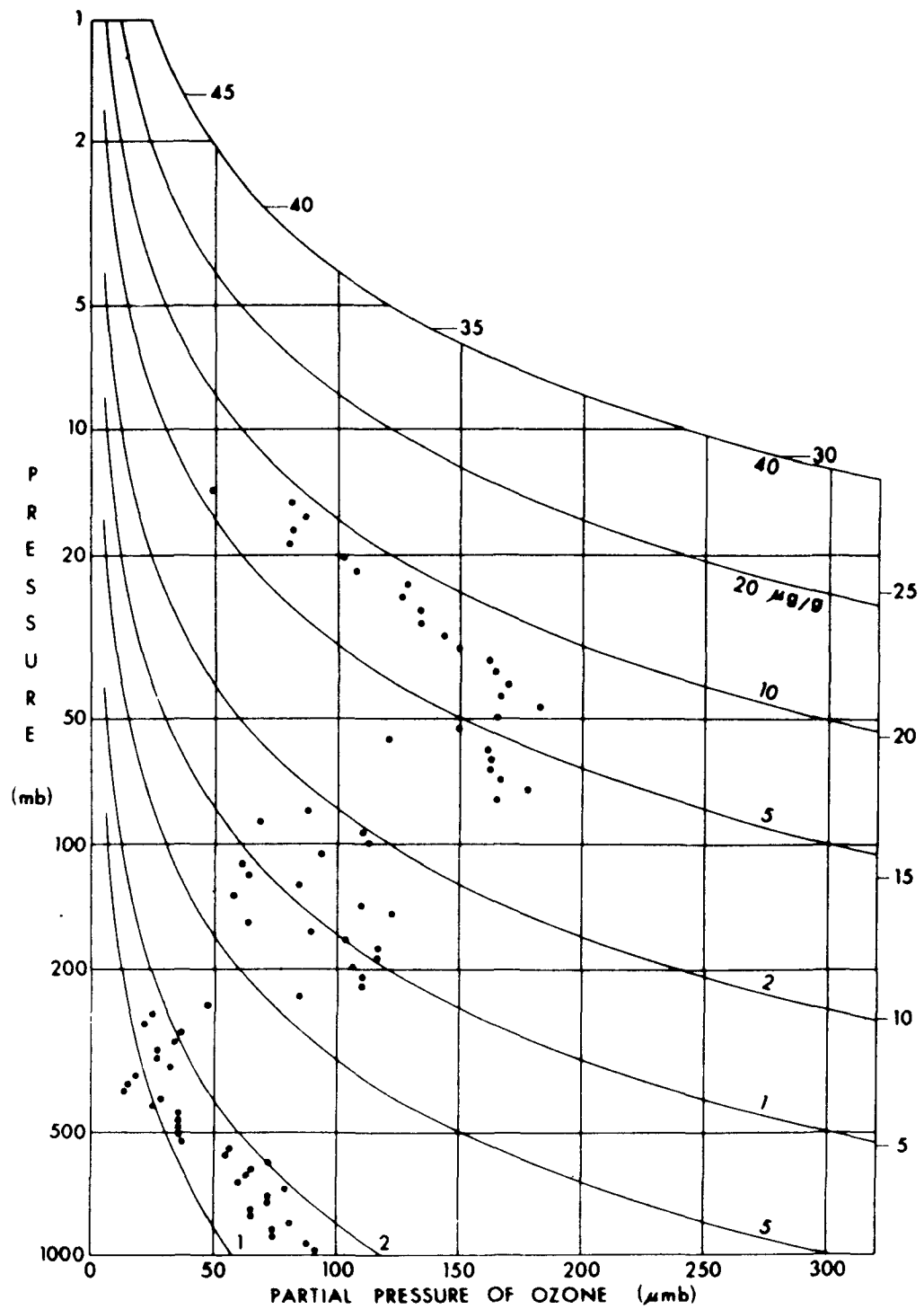
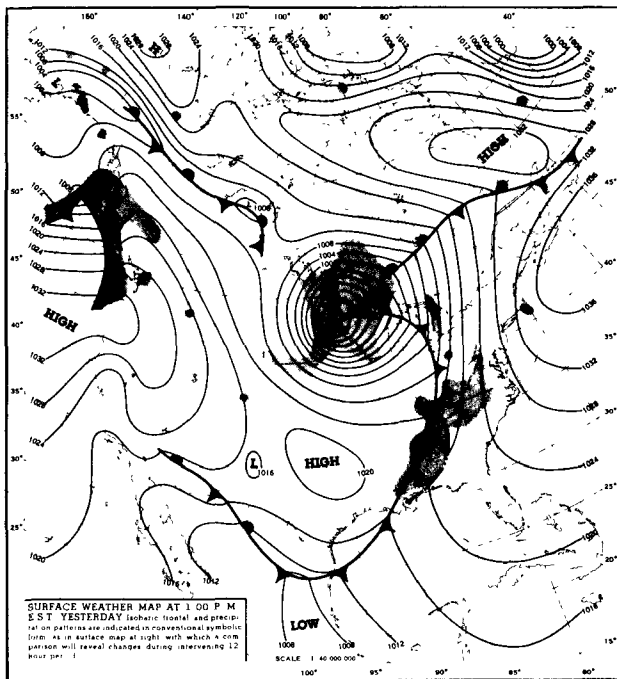
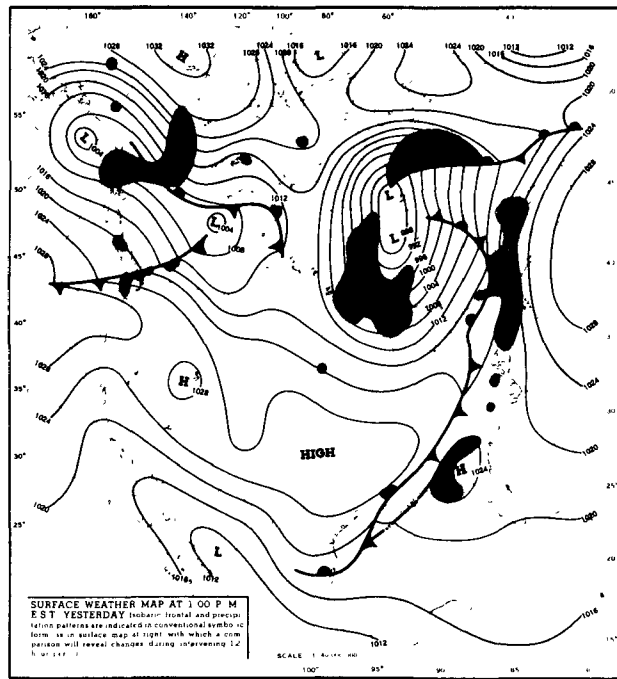


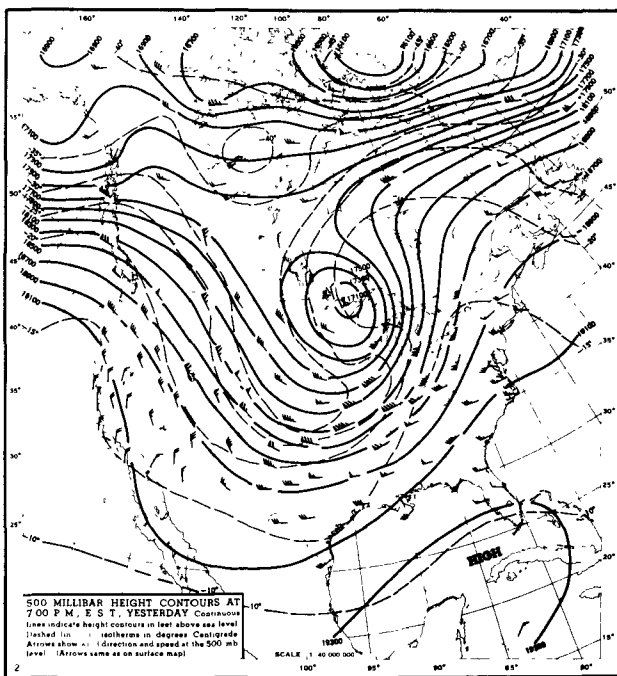
FIGURE 22 OZONE SOUNDING AT SEATTLE,
WASHINGTON, 17 APRIL 1964



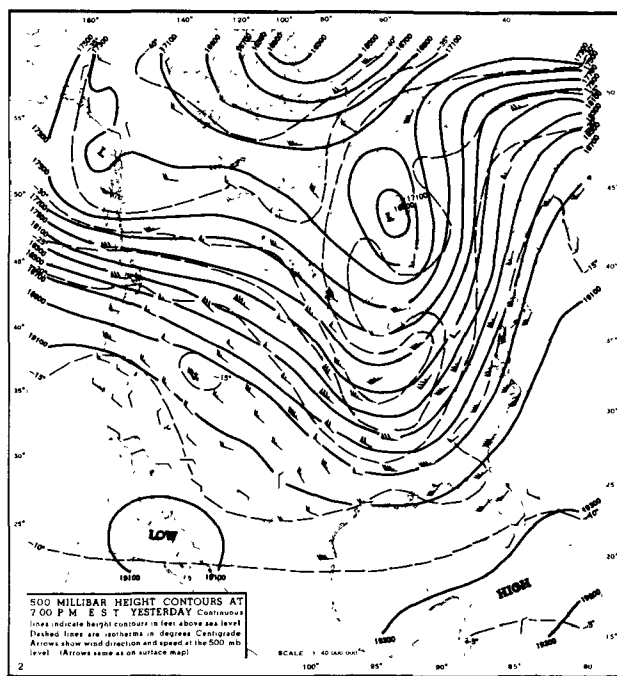
SURFACE MAP, 13 APRIL 1964, 1800 GMT



SURFACE MAP, 14 APRIL 1964, 1800 GMT

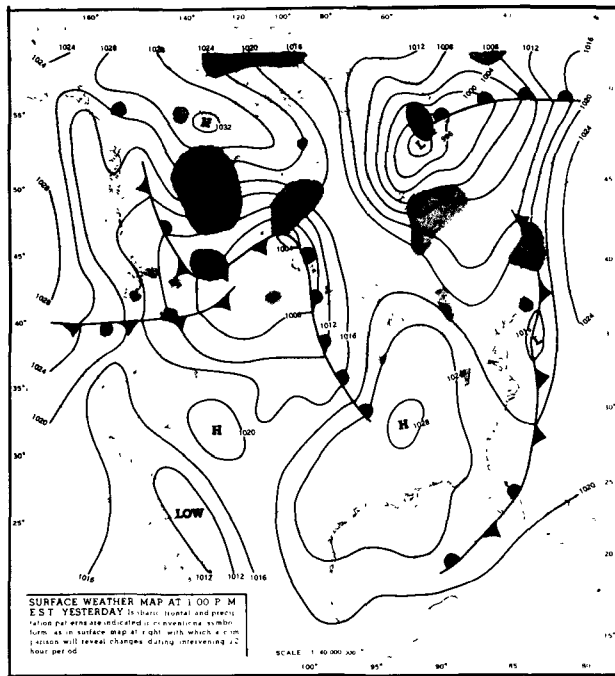


500 MB MAP, 14 APRIL 1964, 0000 GMT

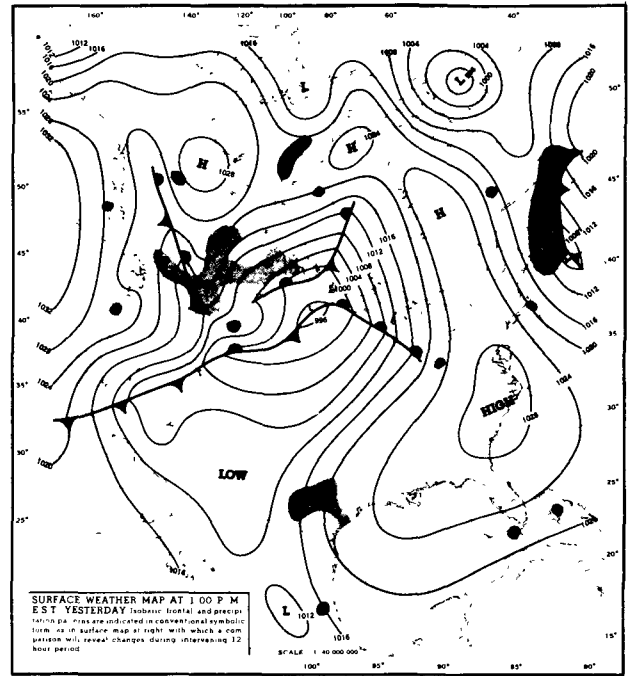


500 MB MAP, 15 APRIL 1964, 0000 GMT

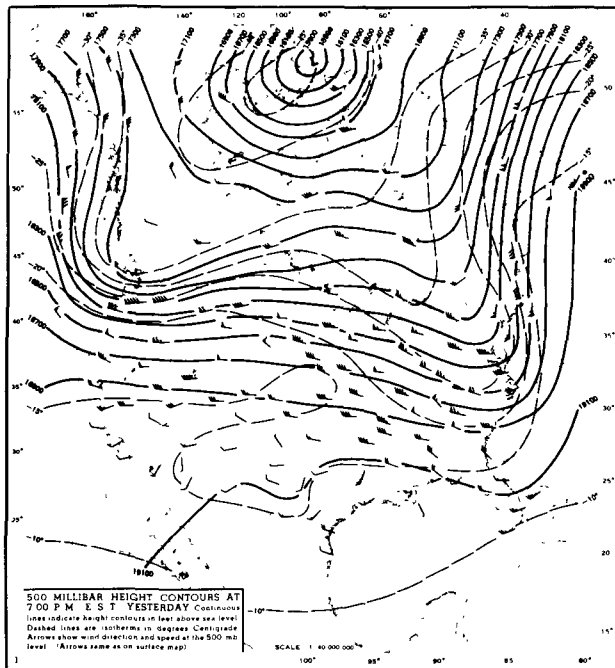
FIGURE 23 NORTH AMERICAN SURFACE AND 500MB CHARTS, 13 APRIL TO 17 APRIL 1964



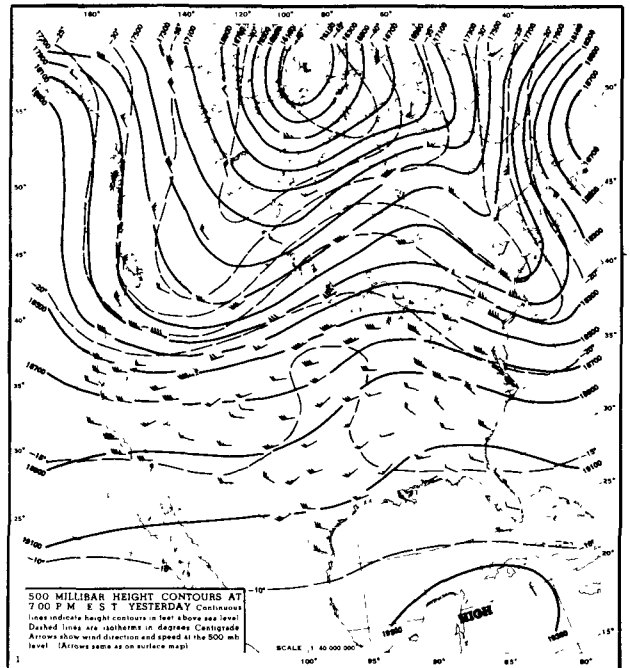
SURFACE MAP, 15 APRIL 1964, 1800 GMT



SURFACE MAP, 16 APRIL 1964, 1800 GMT



500 MB MAP, 16 APRIL 1964, 0000 GMT



500 MB MAP, 17 APRIL 1964, 0000 GMT

FIGURE 23 NORTH AMERICAN SURFACE AND 500MB CHARTS, 13 APRIL TO 17 APRIL 1964 (Concluded)

2.1.2. Evidence of Ozone Transport from the Stratosphere as Deduced from Studies of Radioactive Debris

2.1.2.1. General

Many radioactivity measurements have been made in the troposphere and stratosphere (for references see Reiter, 1976a). Observations of the geographic and seasonal distribution of ozone are also abundant (Reiter, 1972; Reiter et al., 1975). The evidence from radioactivity and ozone observations can be combined to estimate average and maximum ozone concentrations to be expected at ground level as a result of the transport of stratospheric air into the troposphere. Such an analysis relies on a statistical treatment of the data, as opposed to the tracking of individual stratospheric air excursions by trajectory techniques as was done in the preceding discussion. Radioactivity observations and ozone measurements are not usually available at the same places and times, so some license must be taken in comparing these data of different origins.

The premises involved in using ground-level radioactivity measurements to estimate ground-level concentrations of ozone of stratospheric origin are as follows:

1. The ratio of ozone concentration to radioactivity in the stratospheric source area can be determined
2. All the measured radioactivity at ground level is of stratospheric origin
3. The radioactivity and the ozone are transferred from the stratosphere to the ground level by the same processes.

As is true of most methodologies, some difficulties are involved. The ratio of ozone to radioactivity is somewhat uncertain because there is an annual cycle of ozone concentration, in response to the cyclic variations in incoming solar radiation and seasonal changes in stratospheric circulation patterns. Also, the radioactivity levels changed during the period of study in response to the decay times of the various radioactive elements and due to atmospheric diffusion. Nevertheless, with some reasonable assumptions, it is possible to estimate ozone/radioactivity ratios. With regard to ozone concentration, it is assumed that year-to-year variations of ozone are small, especially when compared with season-to-season variations. With regard to radioactivity, the decay and removal rates of the radioactive materials can be used to estimate concentrations at times other than when the measurements were taken.

In essence, dry radioactive fallout is used as a surrogate for stratospheric ozone. The behavior of stratospheric ozone is deduced by analogy from the measured behavior of the radioactive fallout. There are a number of short-comings to the approach and some of these will be identified during subsequent discussions. One of these short-comings arises from the fact that the radioactivity data are in the form of 24-hour averages and hence it is not possible to identify peak hour-

average ozone concentration that can be compared directly with the federal standard. Other shortcomings arise from two sources: 1) uncertainties in the radioactivity and ozone measurements, and 2) the failure of ozone and radioactive matter to behave in a perfectly analogous manner. Uncertainty in the low-stratospheric ozone-to-radioactivity ratio is probably the most serious shortcoming. In spite of these difficulties the technique provides a very useful tool for studying stratospheric/tropospheric interchange.

2.1.2.2. Ratio of Radioactivity to Ozone in the Stratosphere

The mean meridional distributions of ozone (Dutsch, 1971), shown in Figure 24 illustrate the seasonal differences in ozone concentration.* The year-to-year variability may also be appreciable, although perhaps not as great as that exhibited by the Arosa, Switzerland, data in Figure 25 (Wallace and Newell, 1966). The Arosa data may be more indicative of shifts in stratospheric long-wave patterns than of the total mid-latitude stratospheric reservoir of ozone. Lovill (1974) has found that considerable short-term changes in total global ozone take place. Reiter (1975b) suggests that these short-term changes are related to fluctuations in the available potential energy of the atmosphere. Since McGuirk et al. (1975) find a significant year-to-year variability in the atmospheric energy cycle, it appears that the stratospheric ozone reservoir will display a similar variability. For purposes of the present analysis, it is estimated that a 10-15% uncertainty in the assumed stratospheric ozone concentrations will result from this interannual variability.

The production of the isotopes Sr-90 and Cs-137 is representative of peak yields from U-235 and Pu-239. These isotopes are taken as a measure of the total radioactivity production from nuclear devices. Twenty years after the explosion of a nuclear device the combined activity from Cs-137, Sr-90, and Y-90 amount to about 90% of the radioactivity remaining in the environment. For "younger" debris this percentage is considerably smaller.

Figure 26 shows the mean distribution of Sr-90 in the stratosphere during the period May-August 1963, using measurements from Project Stardust (Seitz et al., 1968). The units dpm/1000-scf are "disintegrations per minute per 1000 standard cubic feet". The average ozone values for the March-April period (from Figure 24) are also shown in the figure. The region of interest, the lower stratosphere in the middle latitudes of the northern hemisphere, is denoted by the shaded area in Figure 26. A ratio of Sr-90 to ozone of about 500 units** appears to be appropriate for much of the shaded region.

* It should be noted that the ozone concentrations are given in the mixing-ratio units of ug/g (1 ug/m³ is approximately 0.6 ppm of 25 degrees C and standard pressure).

** The units of this ratio are derived from those of the figure and are (ug/1000 SCF)/(dpm-g). These units are used throughout the discussion.

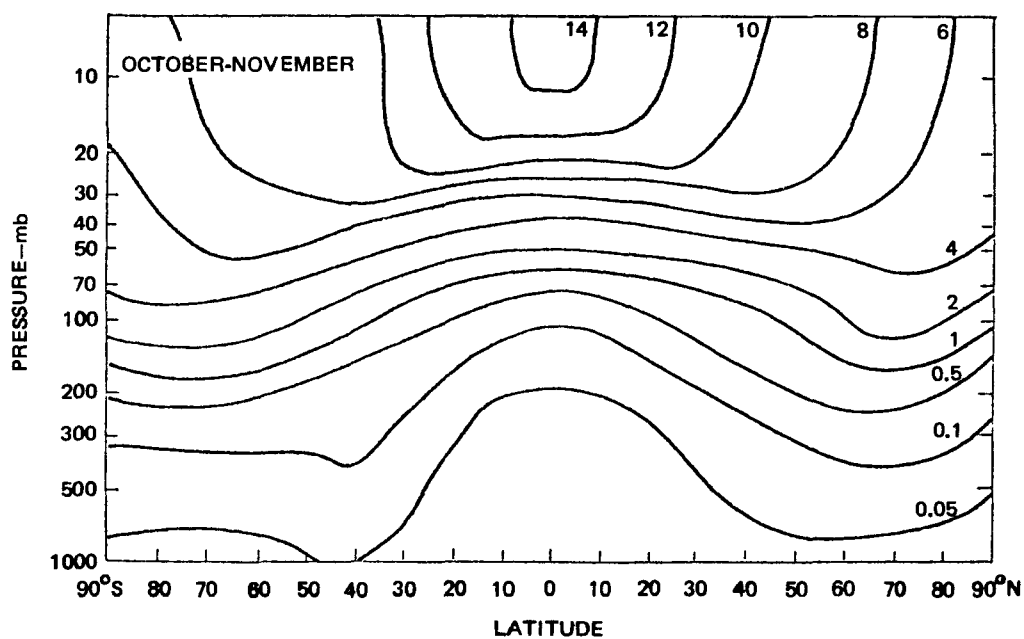
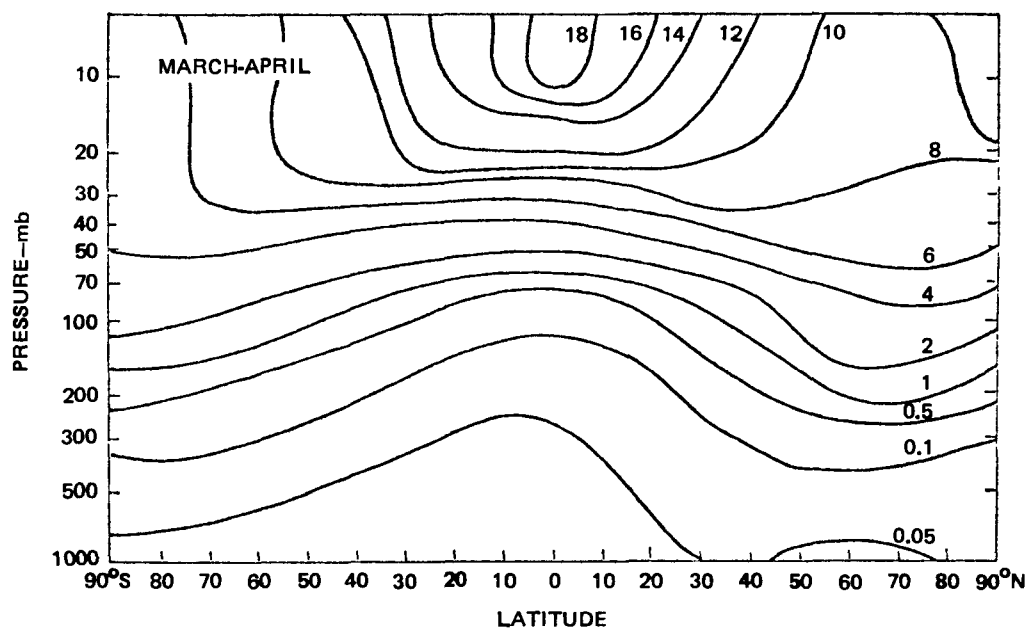
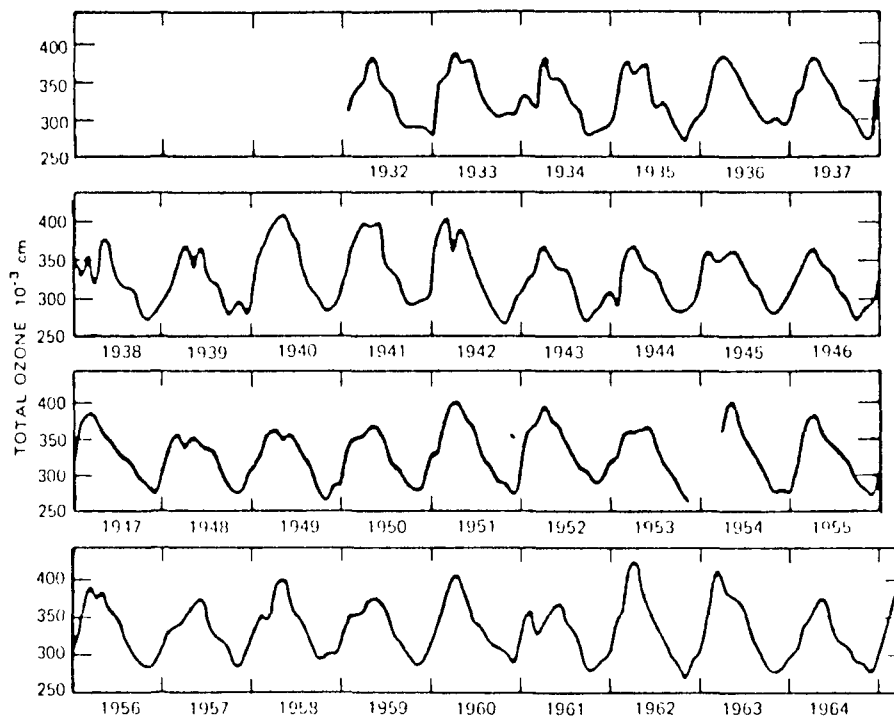


FIGURE 24 MEAN MERIDIONAL DISTRIBUTION OF OZONE
 ($\mu\text{g/g}$; $1 \mu\text{g/g} = 0.6 \text{ ppm}$)



Source: Wallace and Newell, 1966

FIGURE 25 MONTHLY MEAN TOTAL OZONE AMOUNTS AT AROSA, SWITZERLAND

As noted before, the ratio of Sr-90 to ozone will vary with time in response to seasonal variations in ozone and the diffusion, removal, and decay of the fission products. Therefore, corrections must be applied. Figure 27 suggests that in the absence of nuclear tests, the northern hemisphere stratospheric inventory of Sr-90 decreases by a factor of $1/e$ every 14 months (where e is the base of natural logarithms). This depletion of stratospheric strontium is mainly due to transport processes into the troposphere of the northern hemisphere and into the stratosphere of the southern hemisphere. Correcting for the discrepancy of about three months in the time periods to which the ozone data (March-April) and the Sr-90 data (May-August) apply gives a value of 620 (rather than 500) for the ratio of Sr-90 to ozone during the March-April period of 1963. If the 10 to 15% interannual variability in stratospheric ozone is ignored, then the 14-month $1/e$ decay can be assumed to apply to the Sr-90 to ozone ratio from one year to the same season of the next year.

In Figure 28a, an analysis by List and Telegadas (1969) of stratospheric Sr-90 concentrations measured from September to November of 1964 has been plotted on the same graph with the mean ozone concentrations for October through November (from Figure 24). An average Sr-90 to

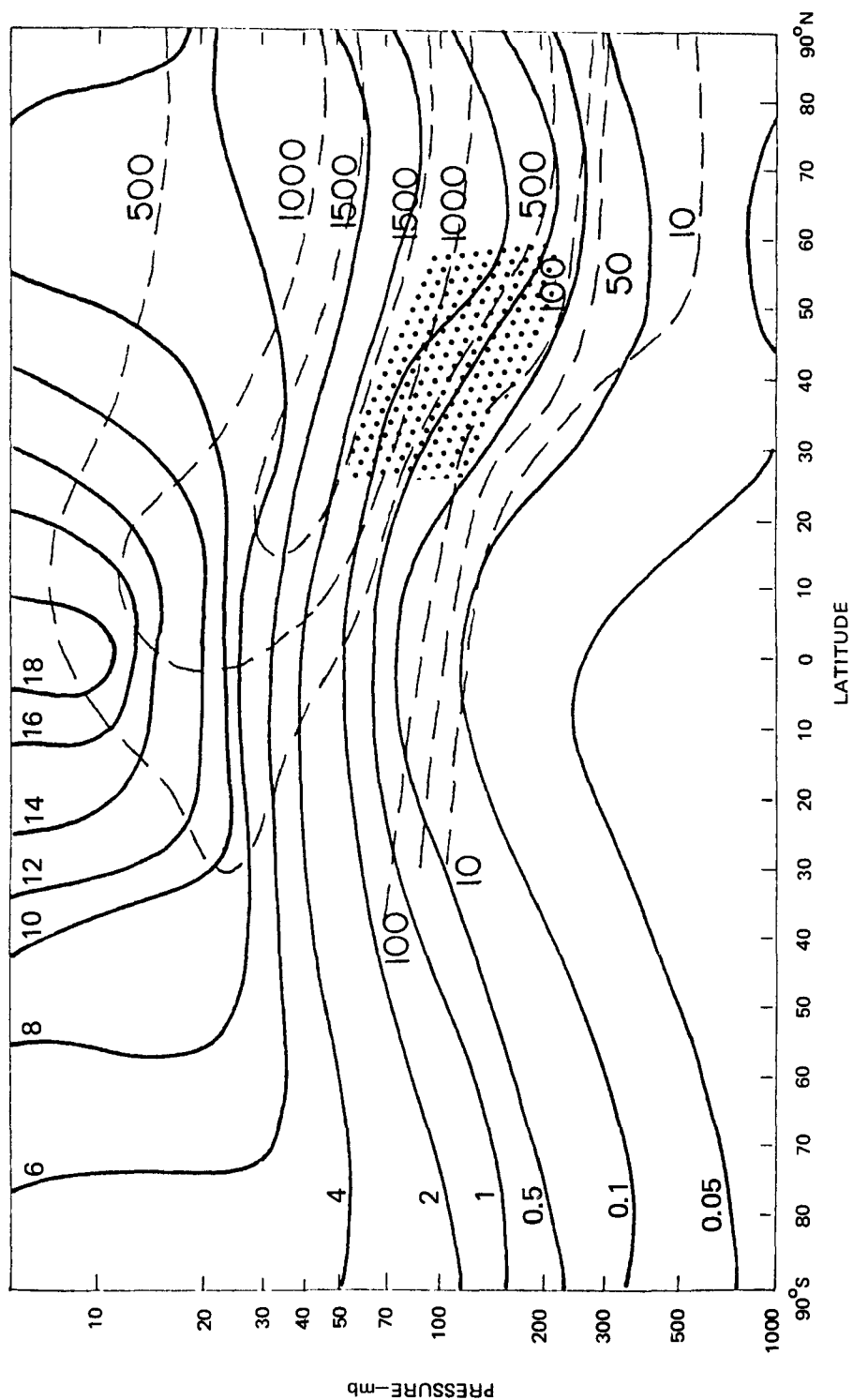


FIGURE 26 MEAN OZONE DISTRIBUTION FOR MARCH-APRIL 1963 (Solid Lines, $1 \mu\text{g/g} = 0.6 \text{ ppm}$)
AND STRONTIUM-90 DISTRIBUTION FOR MAY-AUGUST 1963 (Dashed Lines, Disintegrations
per Minute/1000 SCF)

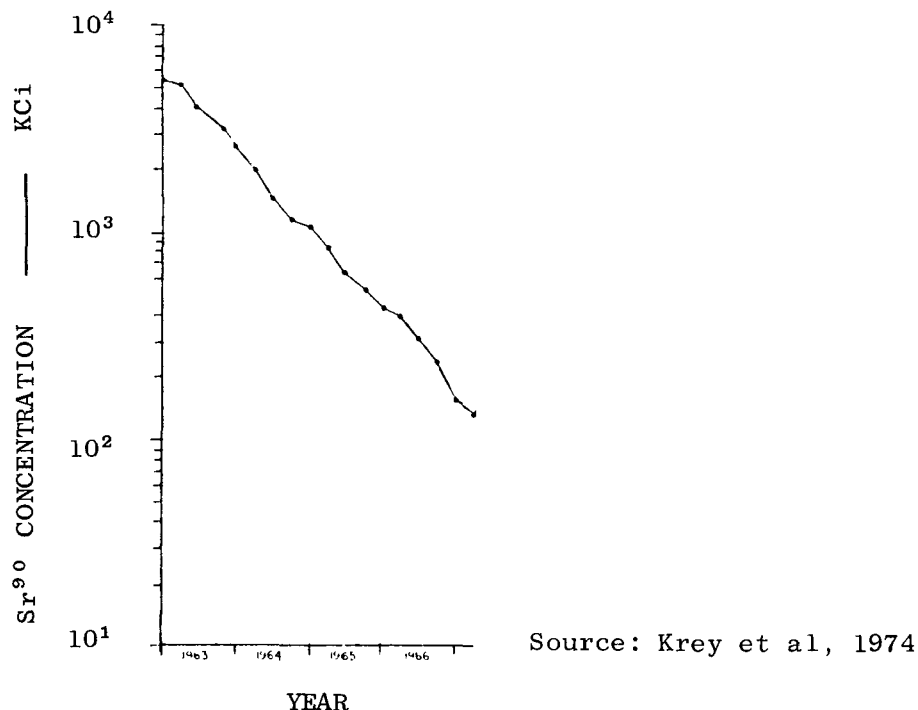
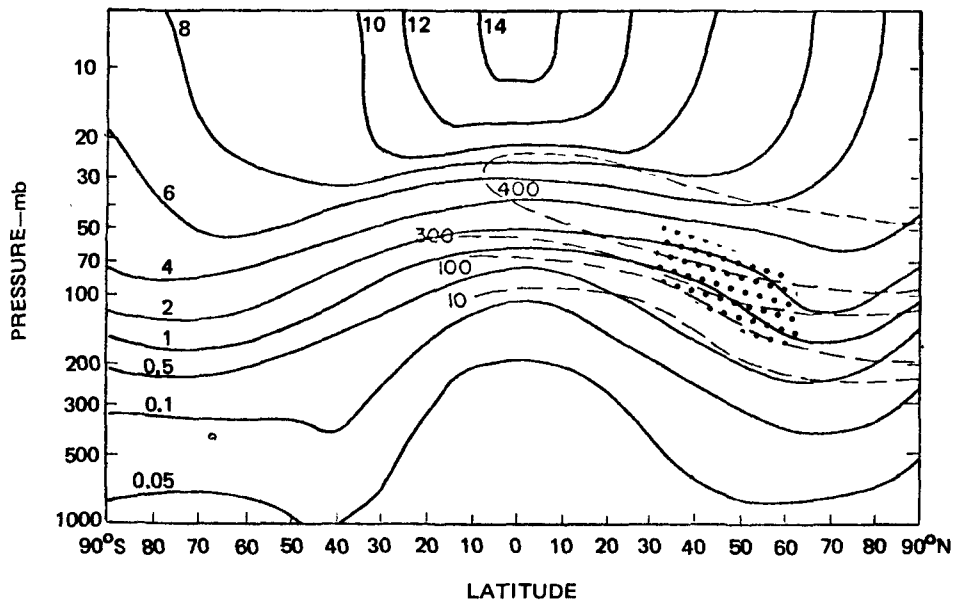


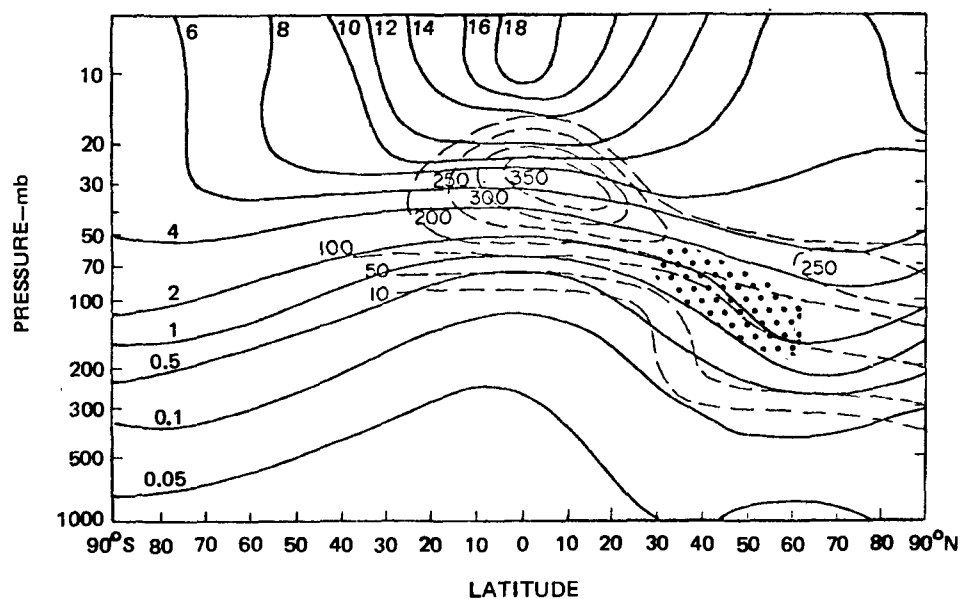
FIGURE 27 STRATOSPHERIC INVENTORY OF Sr^{90} IN THE NORTHERN HEMISPHERE

ozone ratio of 250 to 300 appears to be valid for the shaded area. In Figure 28b, the March-April, 1965, distribution of Sr-90 in the stratosphere (List and Telegadas, 1969) is superimposed on the mean March-April ozone distribution from Figure 24. In this case the ratios range from 70 to 100 in the area of interest, with an average of about 90.

The ratios of Sr-90 to ozone calculated above are plotted as a function of time in Figure 29, along with a line showing the changes expected with at a $1/e$ depletion rate of 14 months. It appears that the $1/e$ curve describes the decrease between (March-April 1963 and March-April 1965) quite well. This says that fluctuations in the ratio due to inter-annual variations in ozone concentrations are quite small. It also appears from this diagram that the ratio computed for October-November 1964 is too high. However, the ratio for autumn was strongly influenced by seasonal changes in the ozone distribution. During autumn, the ozone concentrations in the lower stratosphere of the northern hemisphere tend to be lower than the spring concentration values (see Figure 24) by a factor of about two. Accounting for this in Figure 29 brings the October-November, 1964, ratio approximately in line with the expected ratio for an e-folding Sr-90 residence time of 14 months. This is indicated in Figure 29 by the dashed box, which was based on a seasonal reduction of a factor of two. Thus, the estimated autumn ratio is quite consistent with the assumed 14-month e-folding time for Sr-90 and the known seasonal variations in stratospheric ozone content.



(a) OZONE FOR OCTOBER-NOVEMBER AND STRONTIUM-90
FOR SEPTEMBER-NOVEMBER 1964



(b) OZONE FOR MARCH-APRIL AND STRONTIUM-90 FOR
MARCH-MAY 1965

FIGURE 28 ATMOSPHERIC OZONE (Solid Lines, $\mu\text{g/g}$) AND Sr^{90} (Dashed Lines, $\text{dpm}/1000\text{SCF}$) DISTRIBUTIONS, FALL 1964 AND SPRING 1965

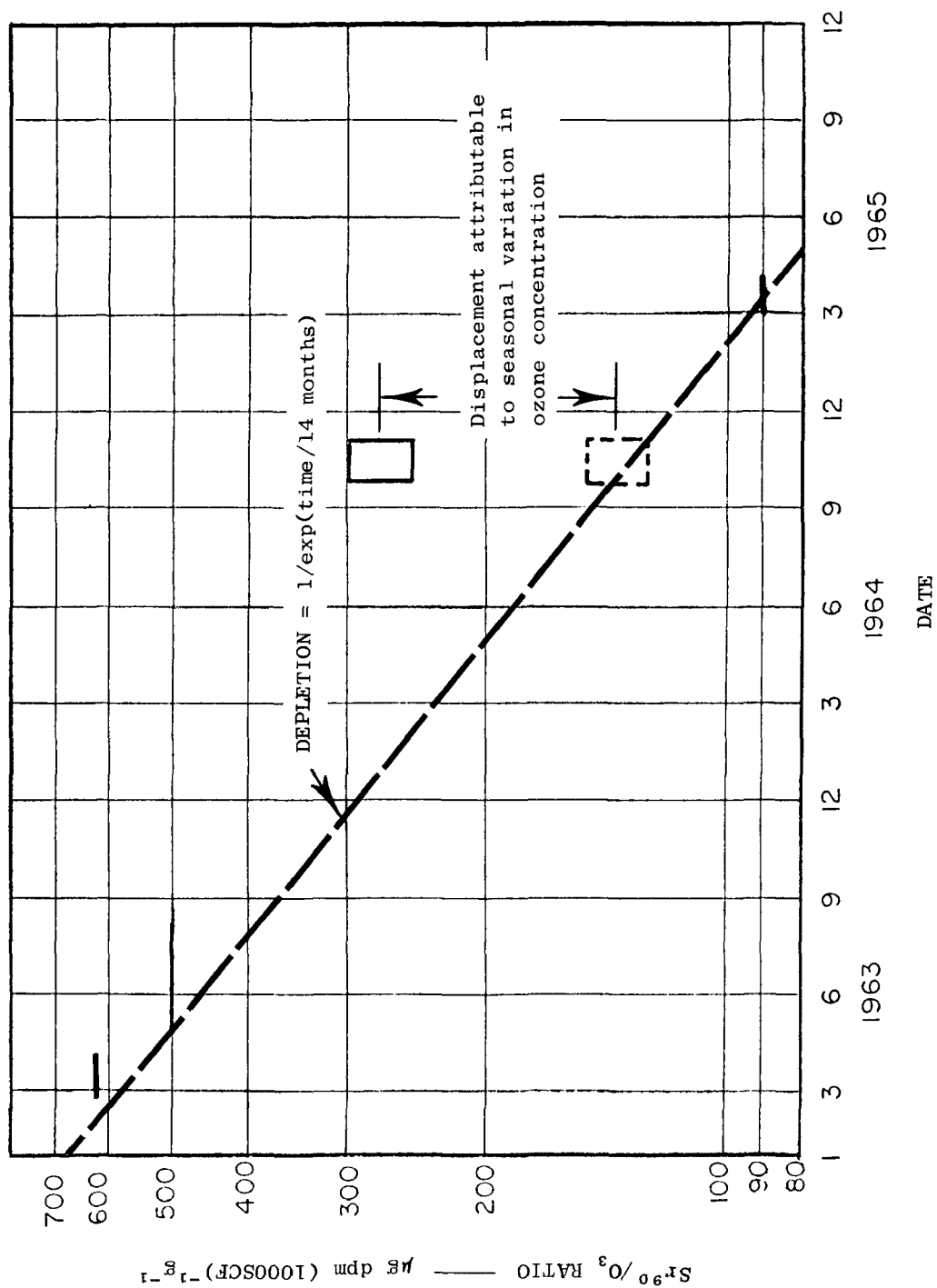


FIGURE 29 Sr^{90}/O_3 RATIOS AS A FUNCTION OF TIME (See text for discussion)

2.1.2.3. Observations of Radioactivity at Ground Level

Surface fallout radioactivity observations conducted by the U.S. Public Health Service Radiation Surveillance Network were used to estimate possible ozone concentrations of stratospheric origin near the ground. The radioactivity data are reported in units of pC m^{-3} (picocurie per cubic meter of air passed through a filter), where $1 \text{ dpm}/1000 \text{ scf} = 0.0159 \text{ pC m}^{-3}$.

It should be recalled here that these measurements are 24-hour averages. The ozone estimates that are derived directly from them are representative of the same averaging period. Such being the case, comparisons with the federal air quality standards for 1-hour average ozone concentration are possible only indirectly.

In the spring and summer of 1963 the bulk of stratospheric radioactive debris was less than 1 year old, stemming from the U.S. and USSR test series of multi-megaton devices conducted during 1962 and ending in December of that year. The relative disintegration rates of the individual fission products (in the case of U-238, fission produced by a thermonuclear reaction spectrum--Freiling et al., 1965) and measurements in rainfall at Westwood, New Jersey (Mahlman, 1965) indicate that radioactivity from Sr-90 and Y-90 amounted to 0.9 to 4.0 percent of the total radioactivity during spring and summer 1963. The following calculations assume that the contribution from Sr-90 + Y-90 to the total stratospheric radioactivity during spring and summer 1963 was 2%, which, from the measurements quoted above, appears to be a reasonable average value, and that the contribution from Y-90 can be neglected because it is a very short-lived daughter product of Sr-90. These figures provide a basis for estimating the stratospheric ozone concentrations that might have been present when the radioactive fallout measurements were made. For instance, 1 pC m^{-3} of total fallout would contain 0.02 pC m^{-3} of Sr-90 (2 percent of the total) which is equivalent to $1.26 \text{ dpm}/1000 \text{ scf}$. According to Figure 29, the spring and summer ratios of Sr-90 to ozone in the stratosphere were about 500-650. During autumn of 1963, the ratio should have been about 300 to 350. An average ratio of about 500 can then be assumed for much of the year 1963. Hence, an average annual fallout of 1 pC m^{-3} would correspond to average ozone concentrations, of stratospheric origin, of about $2.5 \times 10^{-3} \mu\text{g/g}$, or about 1.5 ppb.

The above procedure can be applied to the dry fallout (not including precipitation washout) data as measured by the Public Health Service Radiation Surveillance Network. The average fallout for 1963 is shown in Figure 30. The highest value of 8.94 pC m^{-3} was observed near Las Vegas. One must suspect that radioactive fallout in Nevada and adjacent regions included a significant fraction of tropospheric origin, i.e., coming from the Nevada test site. A secondary region of relatively large fallout values appears along the eastern slopes of the Rocky Mountains. Downdrafts during chinook-wind episodes can carry upper-tropospheric and stratospheric air down into the well-mixed planetary boundary layer. Lovill (1969), for instance, finds relatively high ozone concentrations at Boulder, Colorado, during strong chinook-winds. The downward transport under such wind conditions occurs in conjunction

with strong orographic lee-wave development. The fallout values of about 6 pC m^{-3} in this region correspond to an average annual stratospheric ozone contribution of nearly 9ppb.

According to Figure 30, a relative minimum in the radioactive fallout distribution extends in a meridional direction over the midwestern United States. To the east of this, values approaching 6.0 are seen in several locations. According to the previous calculations the average annual concentration of stratospheric ozone at these locations was about 7.5 ppb.

Most of the radioactive fallout is observed during spring (Reiter 1971; 1972; 1975a). Figure 31a shows the average dry fallout concentration during the first 6 months of 1963. The pattern of this chart is similar to that of the preceding figure, but the values are approximately 50% higher. The equivalent semi-annual average ozone concentrations are generally 15 ppb or less. Again, the anomalous value near Las Vegas is discounted.

Figure 31b shows the number of days during which fallout values of 10 pC m^{-3} or greater (corresponding to about 15 ppb or about 19% of the federal 1-hour standard) were encountered during 1963. A slight bias may exist in these numbers because most stations reported 10 to 15% of the daily data as missing. Again, the Nevada region is probably anomalous because of local tropospheric contamination.

Figure 31c shows the maximum fallout reported during any day of 1963. If the Nevada area data are discounted because of possible local contamination, we find that the maximum values were measured over the eastern United States and in the Pacific Northwest. These maxima of about 26 to 28 pC m^{-3} translate into equivalent ozone concentrations of about 40 ppb, or approximately 50 percent of the federal 1-hour standard. It should be reemphasized that the values based on the radioactivity data are the equivalent of 24-hour averages, and are not strictly comparable to the federal 1-hour standard.

Returning to Figure 29, it can be seen that a Sr-90/ozone ratio of about 220 is appropriate for the spring of 1964. The contribution of Sr-90 to total fission product radioactivity would be about 4 percent by this time (about two years after the major input of radioactive material). Thus, 1 pC m^{-3} of radioactive fallout during the spring of 1964 corresponds to stratospheric ozone contribution of about 6.9 ppb.

This correspondence can be used to interpret the pattern of maximum fallout for 1964 that is shown in Figure 32. Areas of maximum fallout along the eastern slope of the Rocky Mountains and in a band stretching from Texas into the northeastern United States bear some resemblance to the 1963 pattern exhibited in Figure 31c. In drawing the isopleths, a

[illegible]

FIGURE 30 MEAN FALLOUT IN 1963, (pC/m³)

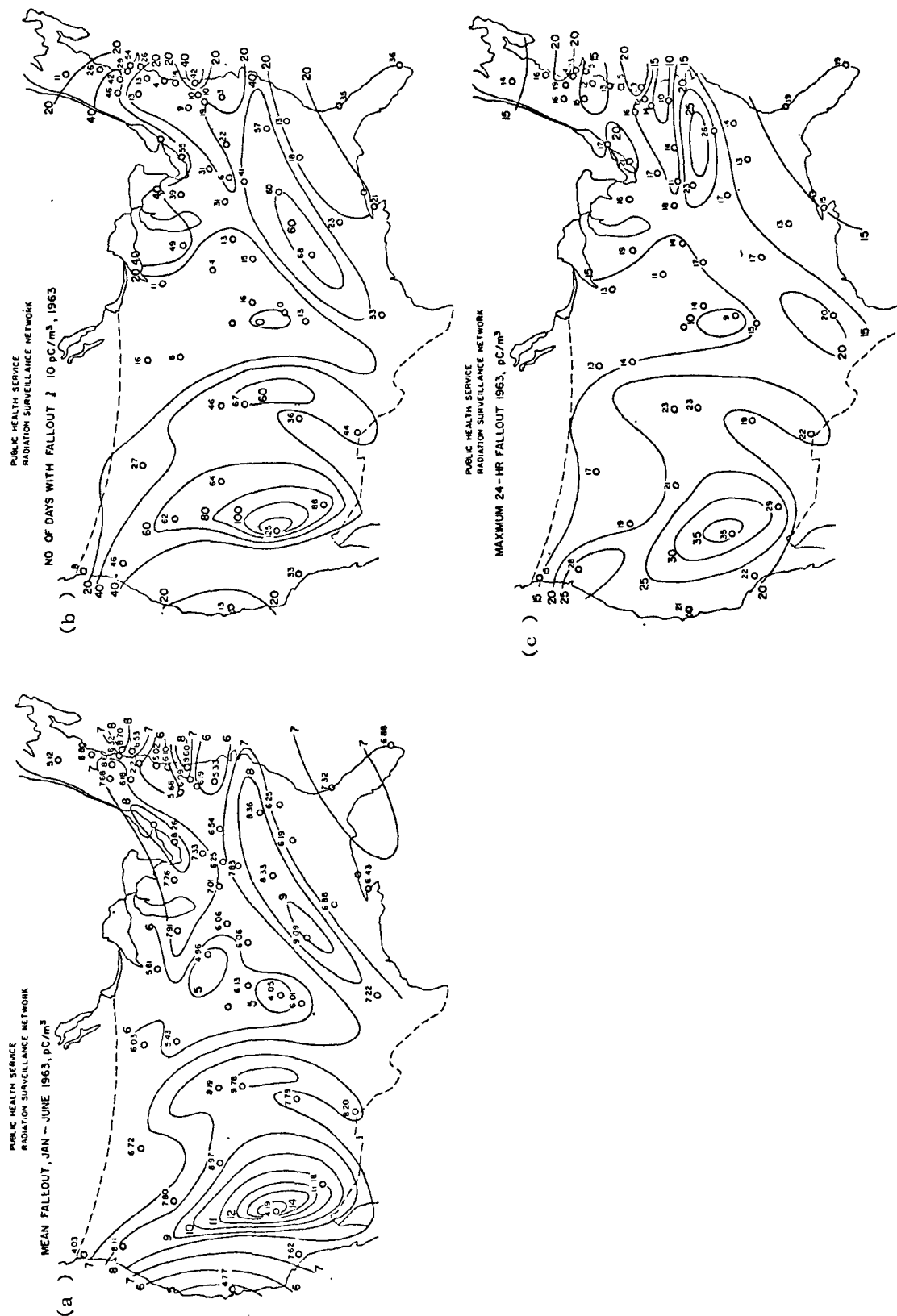


FIGURE 31 SEASONAL, MAXIMUM AND DAILY FALLOUT FREQUENCY MAPS FOR 1963 (pC/m³)

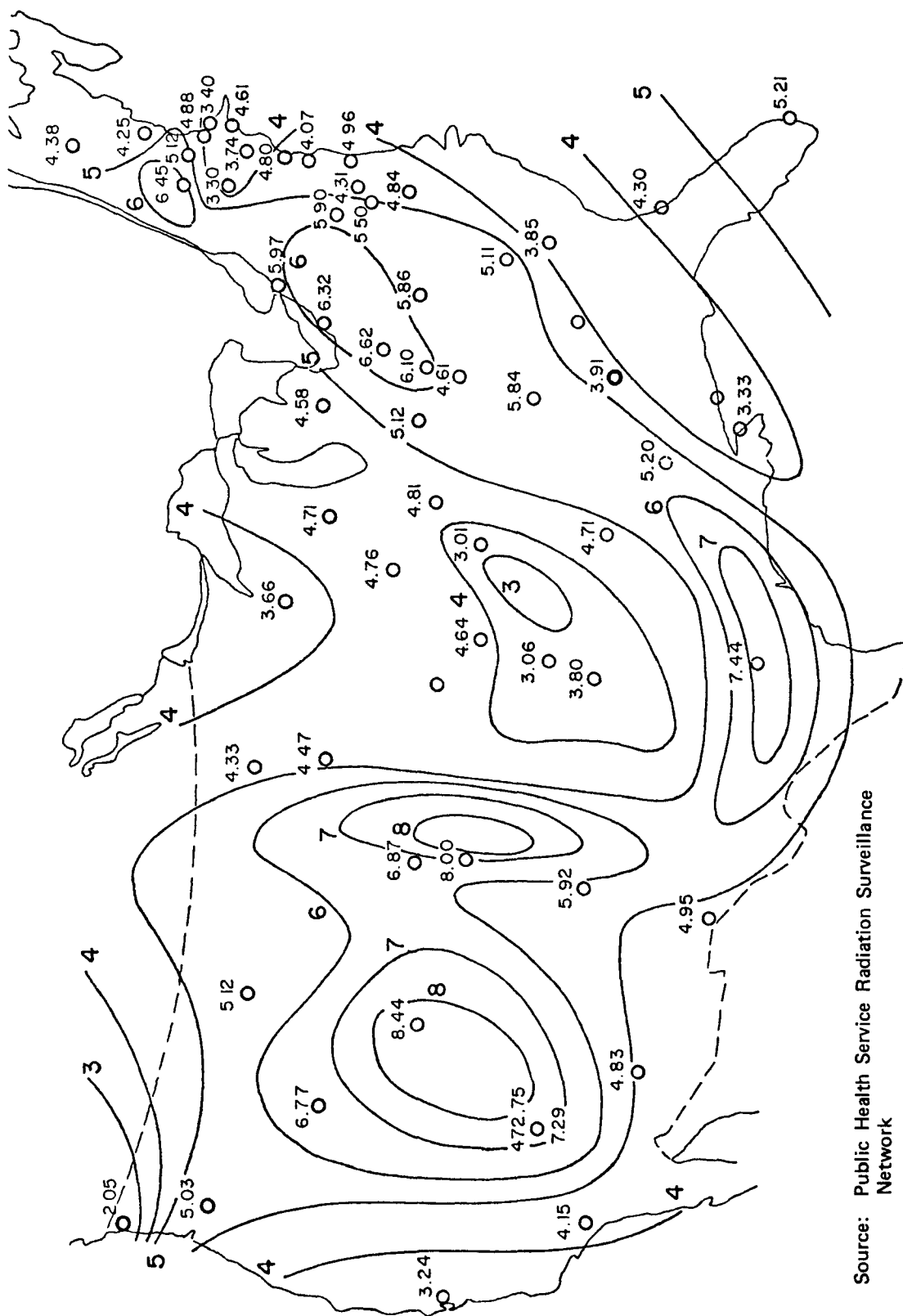


FIGURE 32 MAXIMUM 24-HOUR FALLOUT IN 1964, (pCi/m³)

maximum value of 472.75 pC m^{-3} , reported at Las Vegas on 14 March, and another high value at Las Vegas (16 March) were disregarded as having come from the Pike shot of 13 March at the Nevada test site. The maximum value outside of Nevada is about 8 pC m^{-3} or approximately equivalent to a 55 ppb concentration of stratospheric ozone. This is somewhat greater than the 40 ppb deduced for 1963, and is about two-thirds of the 80 ppb 1-hour standard.

2.1.3. Ozone Observations at Zugspitze

To this point, the analyses of stratospheric influences have not been strictly consistent for comparison to the federal one-hour-average oxidant standard. The ozonesonde data represent near-instantaneous concentrations in the lower troposphere. The concentrations inferred from the radioactivity data are 24-hour averages. In this section, ozone data from Zugspitze Mountain in Germany are examined in order to estimate relationships between 24-hour and 1-hour averages at a ground-level station. The elevation of the station (3000 m above sea level) ensures that the ozone is mostly of stratospheric origin.

One has to assume that hourly ozone concentrations vary about the daily mean value. A relatively high daily-mean concentration, therefore, produces a certain chance that hourly-mean concentrations for one or more hours will exceed 80 ppb, although the daily average is well below that value. The ozonesonde observations over North America revealed that in 0.2% of the available cases, instantaneous ozone concentrations of stratospheric ozone exceeded 80 ppb in the lower troposphere. However, as noted before, ground-level observations were made over one-hour averaging times. It is to be expected that the averaging process, even over one-hour periods, would reduce excessive instantaneous concentrations. Also, it is expected that concentrations are lowered during the mixing processes that bring the ozone to ground level. Destruction processes at ground level lower the concentrations even more.

Hourly ozone observations from Zugspitze Observatory* were used to compare daily one-hour-maximum and daily average ozone concentrations. Figure 33 shows the distribution of daily one-hour maximum ozone concentrations in relation to the daily mean values for a 529-day period. To the right of the slanting shaded line the standard of 80 ppb is exceeded. Figure 33 suggests that it is not exceeded under the "normal" behavior of maximum one-hour concentrations. However, two days, January 8 and 9, 1975, departed significantly from this "normal" behavior. The maximum one-hour ozone concentrations on these days were in excess of 145 ppb. These days are indicated by the two points to the right of the slanting shaded line in Figure 33. The hourly ozone values for these two days are reproduced in Figure 34. All evidence indicates that these data are realistic. The following facts support this conclusion:

* These data were generously provided by Drs. R. Reiter and Kantor of the Institut für Atmosphärische Umweltforschung, Garmisch-Partenkirchen, West Germany.

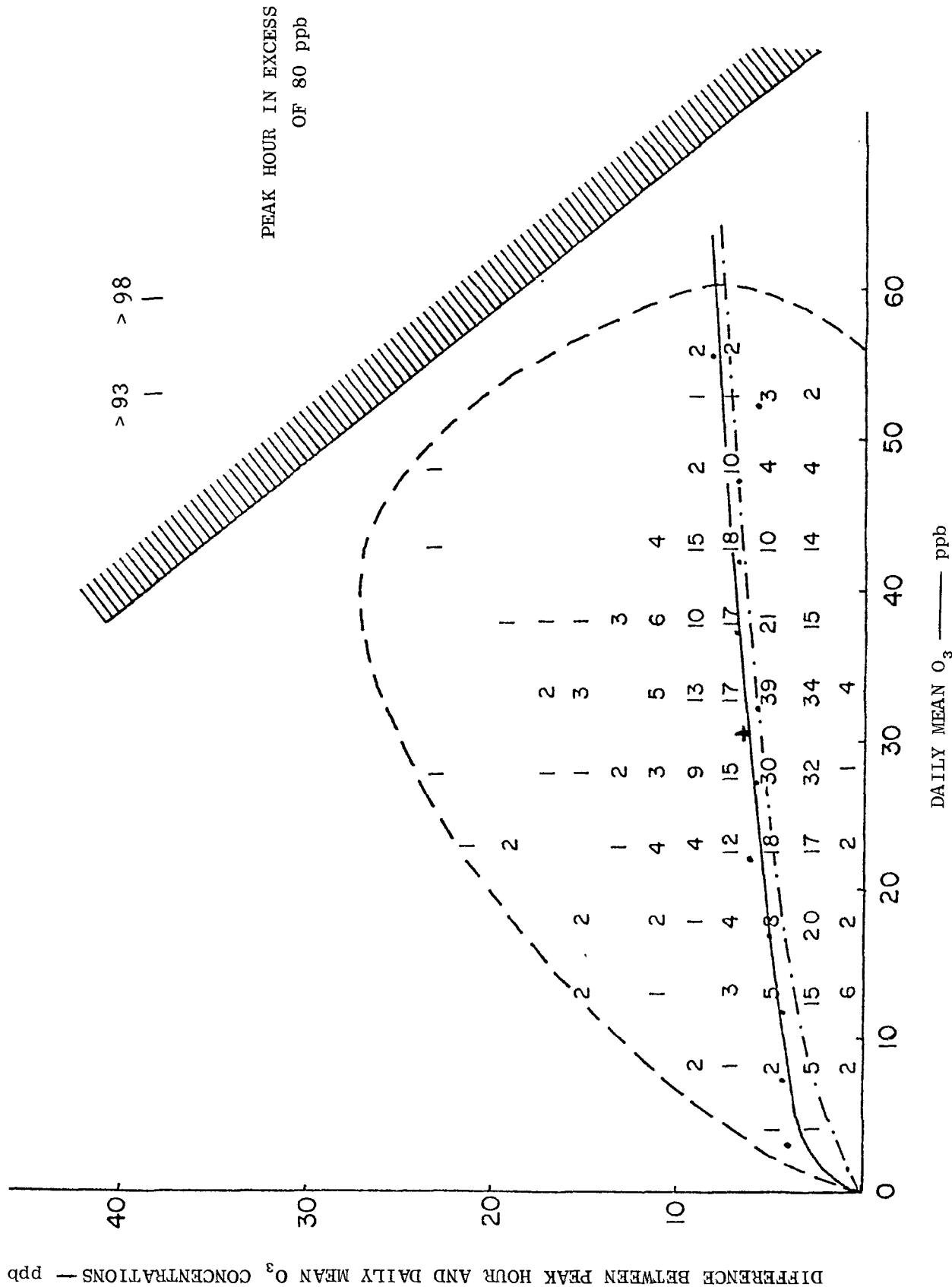


FIGURE 33 JOINT FREQUENCY DIAGRAM OF PEAK-HOUR VERSUS 24-HOUR AVERAGE OZONE CONCENTRATIONS AT ZUGSPITZE

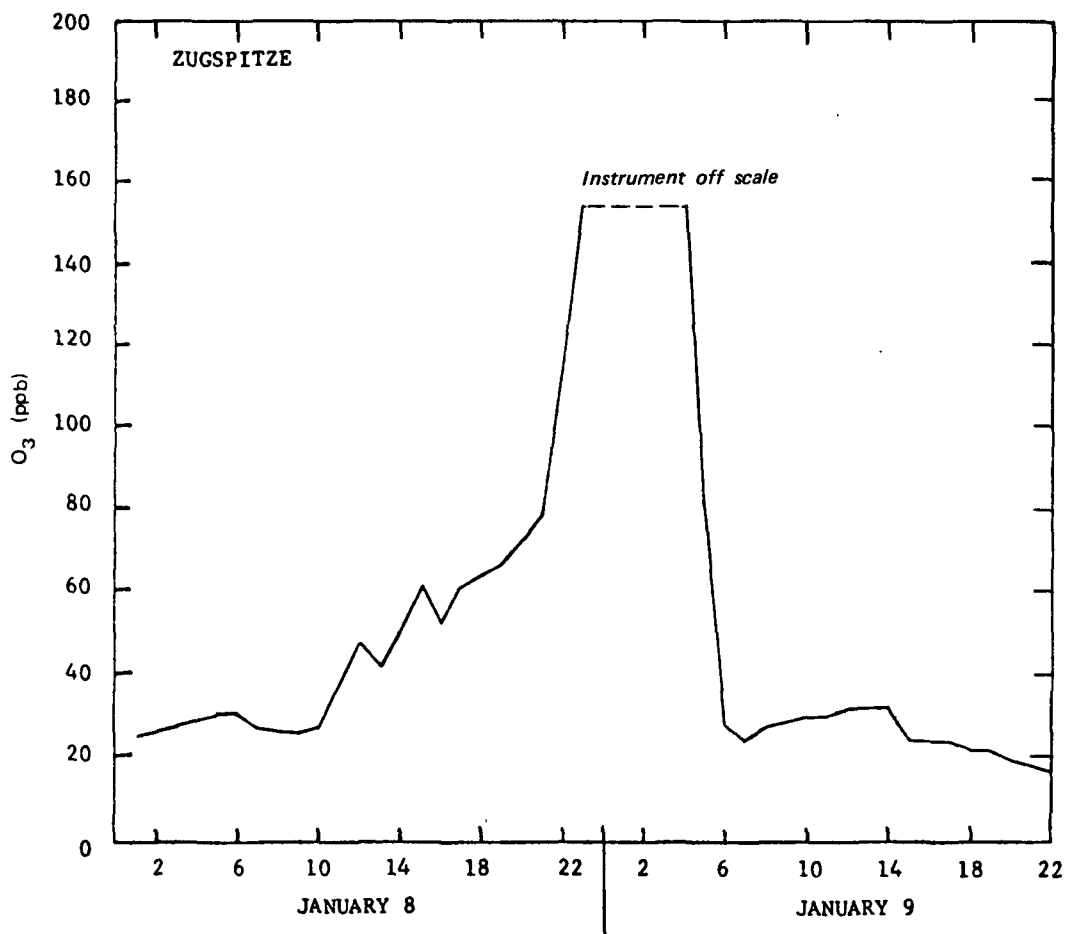


FIGURE 34 OZONE CONCENTRATIONS AT ZUGSPITZE 8-9 JANUARY 1975

- The hourly ozone concentrations on these two dates do not behave spuriously but reveal an orderly increase from, and later an orderly decrease to, the "normal" range of ozone concentrations observed at Zugspitze.
- Two days constitute 0.4 percent of the available sample. Since the excessive concentrations straddled the midnight hour they could be considered a single case, i.e. 0.2 percent of the available sample. Such a frequency of occurrence is in agreement with the data from the North American ozonesonde network.
- Be-7 measurements suggested an influx of stratospheric air.
- Weather maps show the passage of a cold front with precipitation and a strong jet stream, even at the 500 mb surface, early on January 8. A short-wave trough which, on January 7 at 00 GMT, was over the North Sea, passed the Alps by January 8, 00 GMT. Such a weather situation is conducive to the import of stratospheric air into the lower troposphere, as discussed earlier.
- An exceptionally strong trough was located in the stratosphere over Europe, with sinking motions on its rear side capable of moving large amounts of ozone from the middle to the lower stratosphere over this region.

It appears, then, that the ozone reservoir in the lower stratosphere--replenished by downward motions in the stratosphere--was "tapped" by a typical intrusion event associated with the strong jet stream and the advancing cold front. The anomalously high concentrations observed at Zugspitz appear to be due to the unusual stratospheric flow pattern which coincided with a rather typical intrusion event. Such unusual transport processes in the lower stratosphere can easily produce ozone concentrations just above the tropopause which are more than twice as high as seasonally averaged values (see e.g. Reiter, 1971 and Reiter et al., 1975a). Over North America the climatological mean position of the long-wave trough in the winter stratosphere makes these occurrences somewhat more likely than over Germany.

It should be remembered that the Zugspitze observatory is at an elevation of 3000m. Strong dilution to less than half of the concentrations encountered in layers embedded in the middle troposphere (e.g., 3000m) should be expected from mixing processes between there and ground level. Even though short-term "spikes" of ozone concentrations at low elevations can approach the undiluted values in the upper layers, concentrations averaged over one-hour intervals near ground level should be less than half of the corresponding values encountered in the mid-troposphere. If we assume that maximum concentrations of 2 to 3 times the federal standard occur in such elevated layers (e.g., at Zugspitze), it appears that the federal standard might be expected to be violated occasionally at ground-level sites with elevations typical of populated areas. These instances would occur at cyclogenetically active locations of the middle latitudes in regions over which the stratospheric long-wave trough pattern is able to establish a greater-than-normal reservoir of ozone in the layers above the tropopause.

2.2. Tropospheric Sources

Control strategies for ozone are necessarily tropospheric strategies because this is where controllable precursor emissions occur. In this section, the problem of the origins of tropospheric ozone and the meteorological factors that affect its formation are examined using two different (but related) techniques. First, a Lagrangian approach is used to define the history of the air and relate it to the observed ozone concentrations. The second approach examines weather patterns, large-scale ozone distributions, and the locations of major emissions areas, in order to see what relationships there might be among these different patterns at any given time.

Of course, the history of a given air parcel, with regard, to meteorological factors and to anthropogenic emissions, is determined by a succession of weather patterns and a certain distribution of emissions. Thus, the results of the two approaches should be consistent. However, the use of both approaches increases the probability of identifying those factors that are of greatest importance. A dual approach also provides opportunities for cross-verification that would not otherwise be available.

2.2.1. Trajectory Analyses

2.2.1.1. The Trajectories

As noted in the Introduction, 120 air trajectories were constructed and used as a basis for this part of the study. These trajectories are shown in Figures 33 through 42. Positions at 3-hourly intervals are marked. Trajectories that led to ozone concentrations in the upper 20 percentile for a station are plotted separately from the remaining trajectories. The trajectories are identified by the date of their termination.

2.2.1.2. Oxidant Concentrations Related to Precursor Emissions and the Meteorological History of the Air

A logical first step in this phase of the investigation was to examine the correlations between the ozone concentrations and the 12-hour averaged indices of the different meteorological and emissions parameters. The derivation of the meteorological and emission indices is discussed in detail in Volume 3 (Appendices A and B). Table 3 shows the calculated linear correlation coefficients for those cases where the significance is better than 0.05. It is important to note that 175 correlation coefficients were calculated in the preparation of this table, so that many of the "correlations" that appear to be significant at the 0.05 level are not indicative of true physical relationships. It might be argued, that a better criterion for acceptance would probably be the 0.005 significance level. However, the first entry in the table would argue against the physical relevance of even this level of significance. This entry suggests that there is a significant correlation between the oxidant concentration at Queeny and the hydrocarbons released into the air 48 to 60 hours before, whereas no such significant relationship is noted for more recent emissions. This example suggests

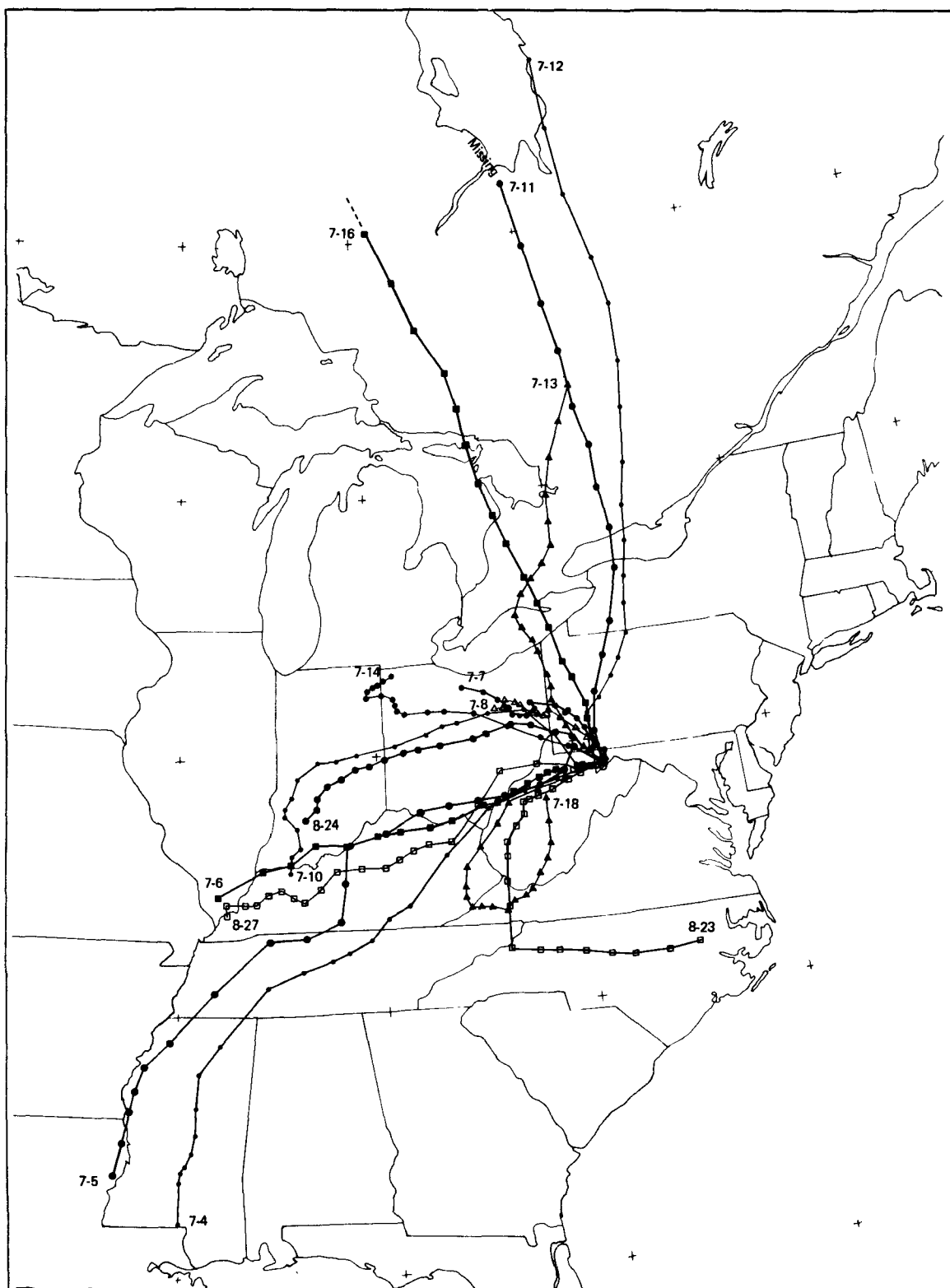


FIGURE 35 McHENRY TRAJECTORIES—OZONE CONCENTRATIONS IN TOP 20 PERCENTILE

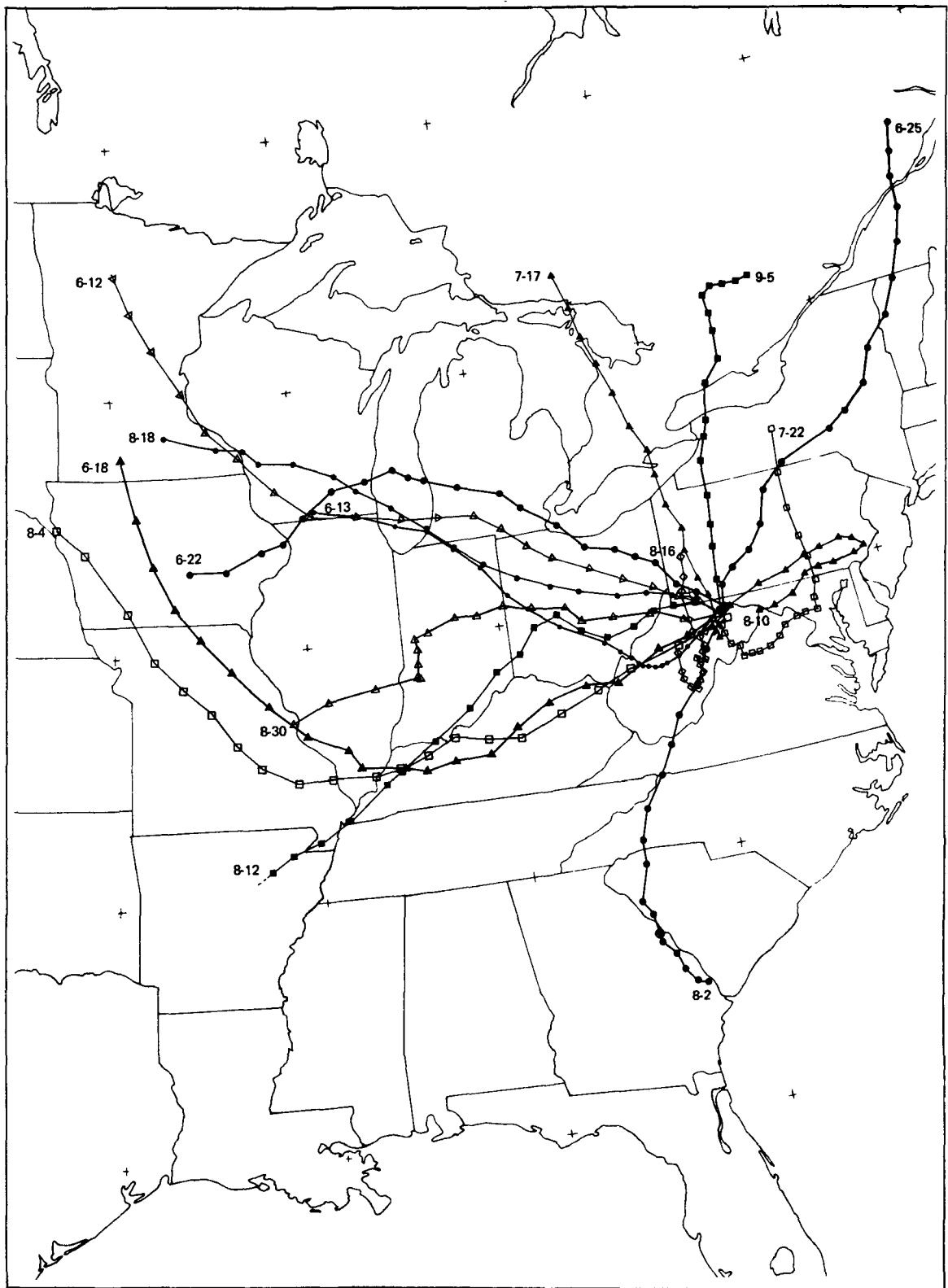


FIGURE 36 McHENRY TRAJECTORIES-OZONE CONCENTRATIONS NOT IN TOP 20 PERCENTILE

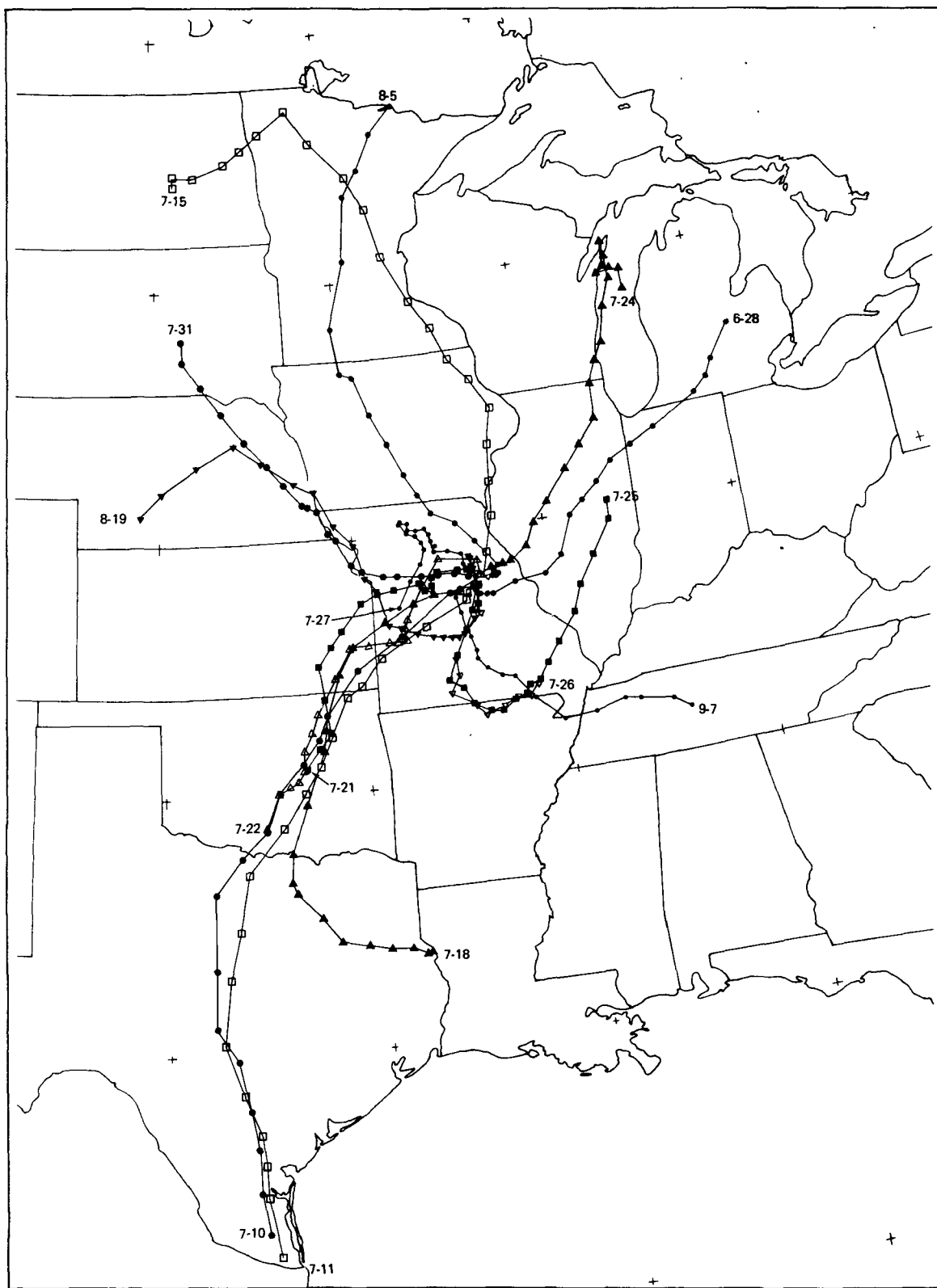


FIGURE 37 QUEENY TRAJECTORIES-OZONE CONCENTRATIONS IN TOP 20 PERCENTILE

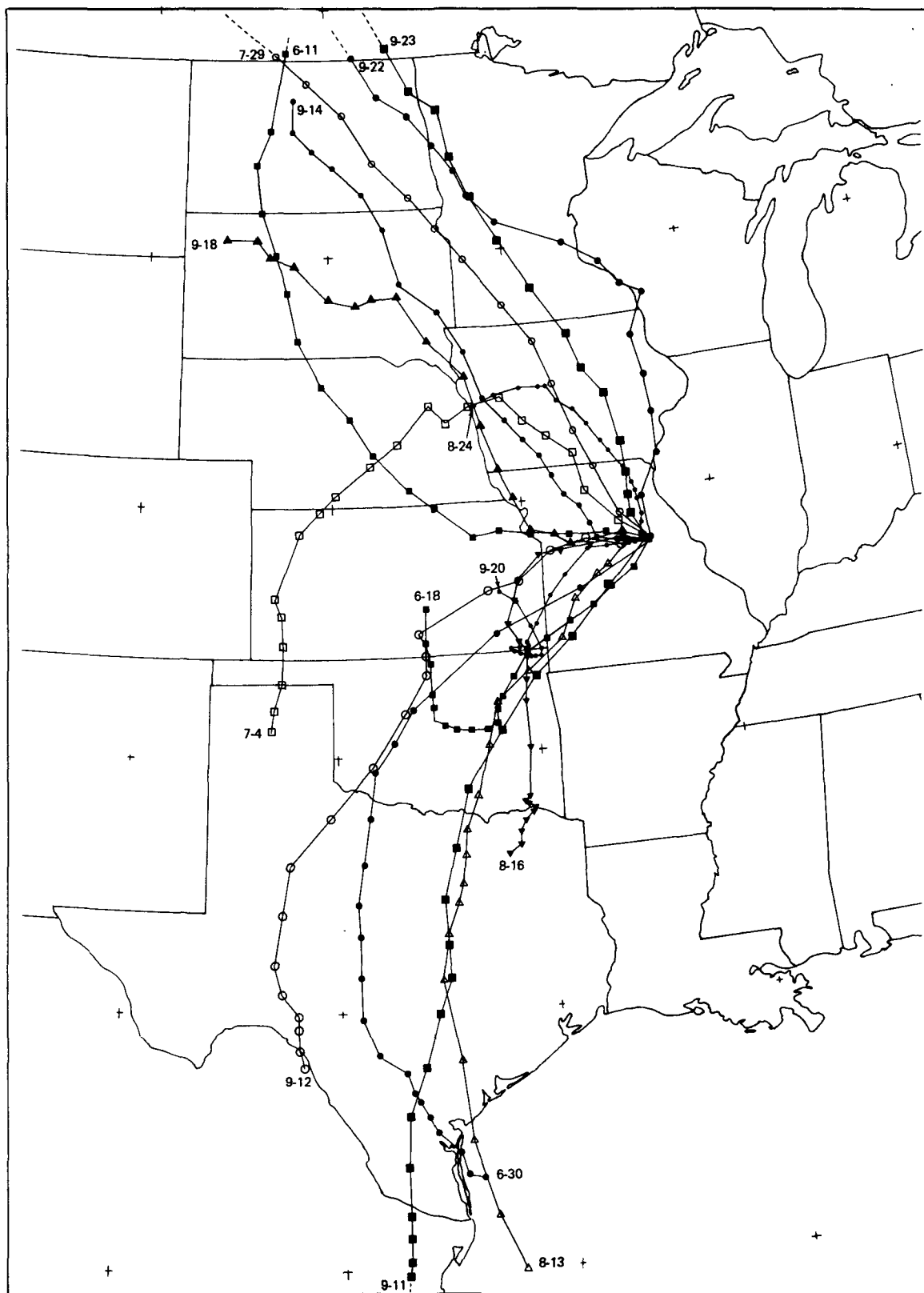


FIGURE 38 QUEENY TRAJECTORIES-OZONE CONCENTRATIONS NOT IN TOP 20 PERCENTILE

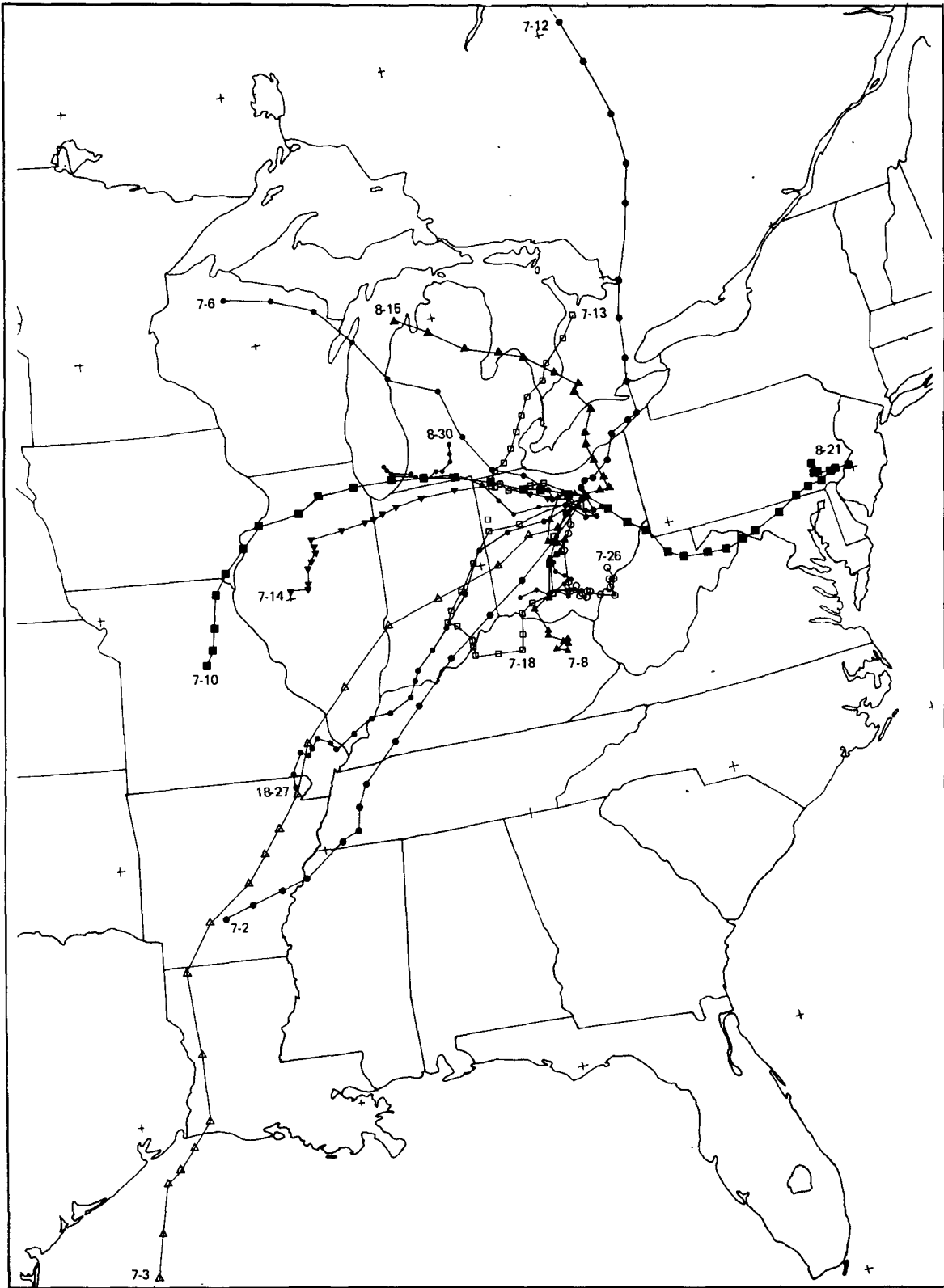


FIGURE 39 WOOSTER TRAJECTORIES-OZONE CONCENTRATIONS IN TOP 20 PERCENTILE

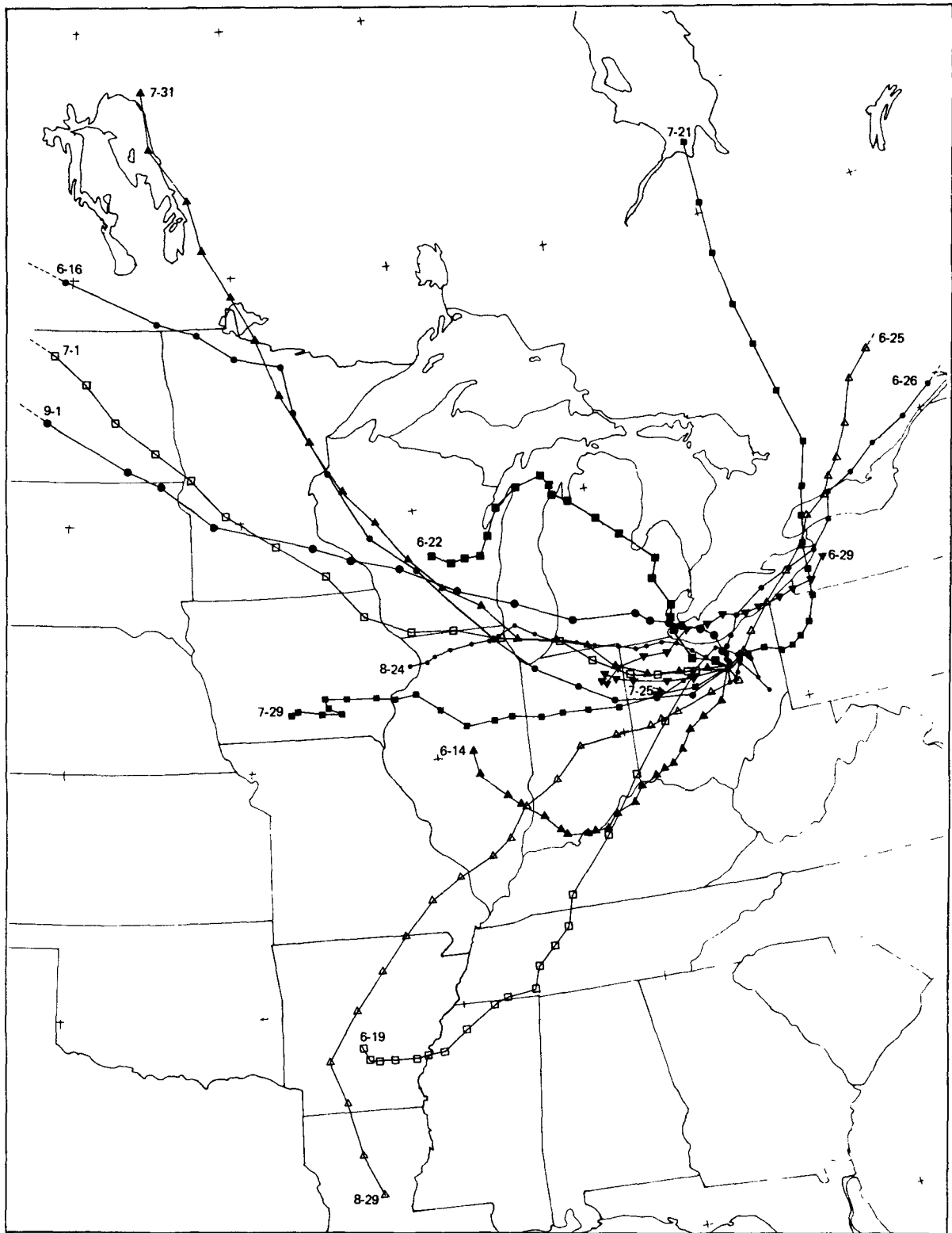


FIGURE 40 WOOSTER TRAJECTORIES—OZONE CONCENTRATIONS NOT IN TOP 20 PERCENTILE

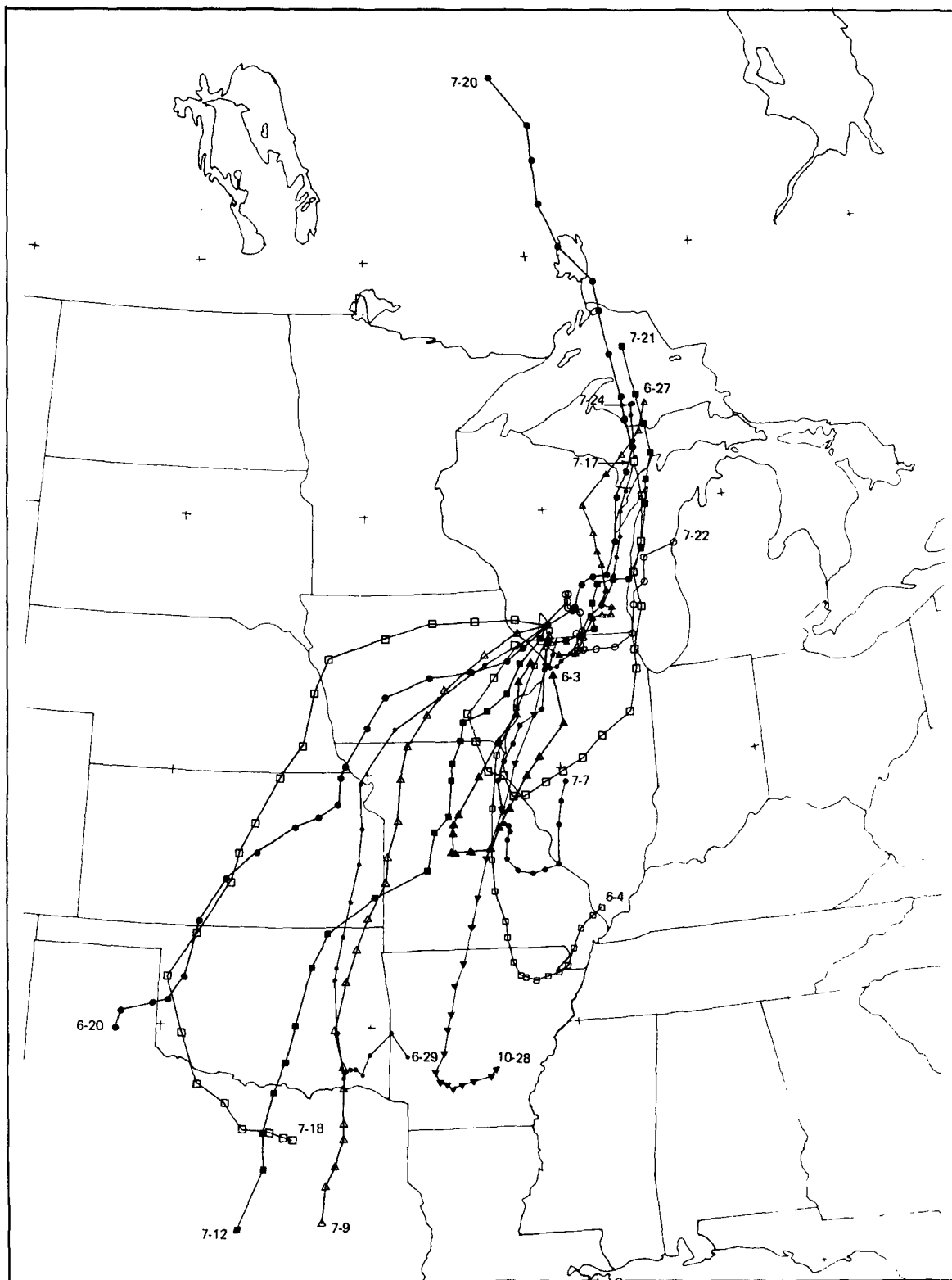


FIGURE 41 YELLOWSTONE LAKE TRAJECTORIES-OZONE
CONCENTRATIONS IN TOP 20 PERCENTILE

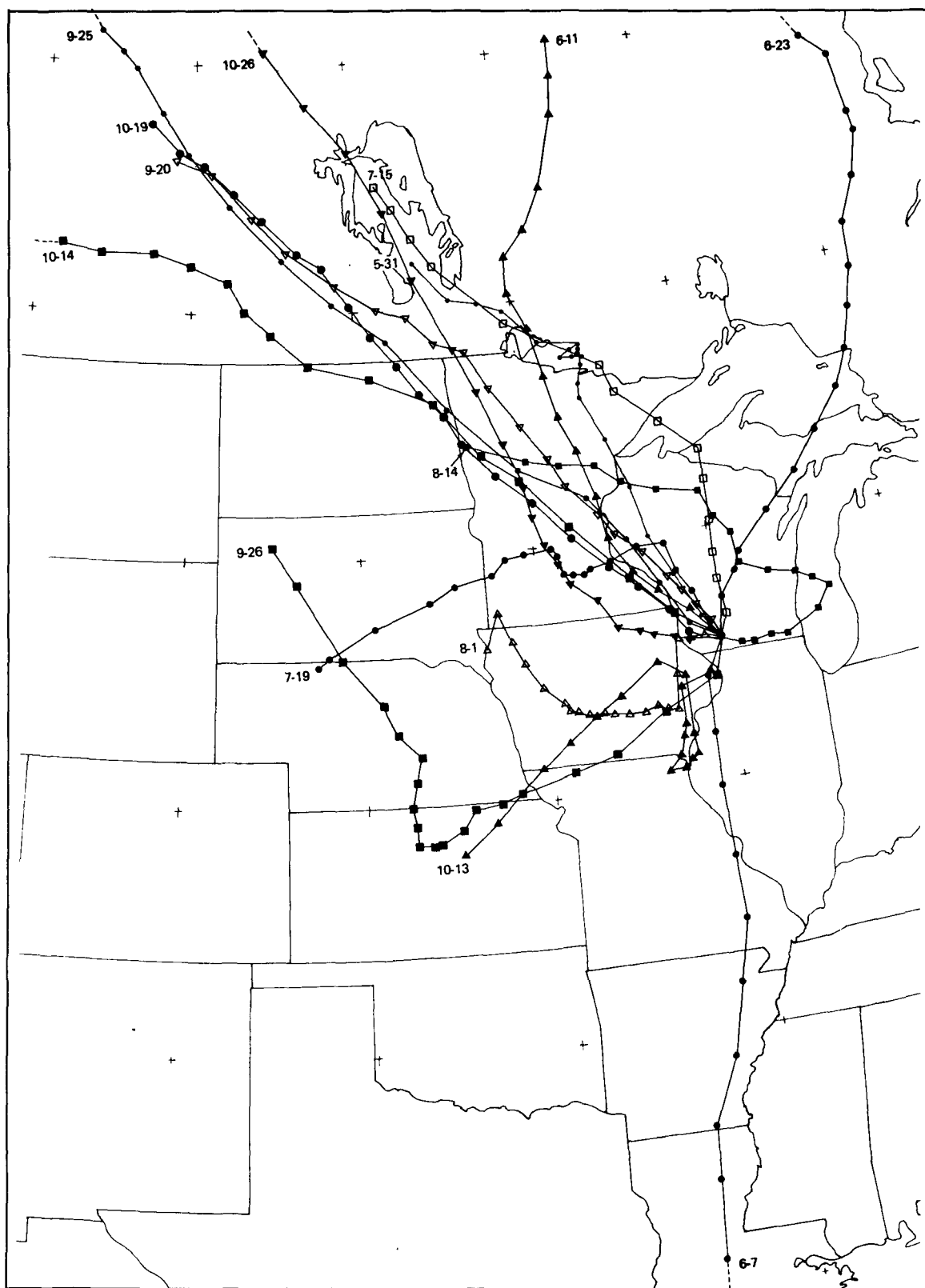


FIGURE 42 YELLOWSTONE LAKE TRAJECTORIES-OZONE CONCENTRATIONS
NOT IN TOP 20 PERCENTILE

Table 3

CORRELATION COEFFICIENTS BETWEEN OBSERVED OZONE CONCENTRATIONS
AND VARIOUS METEOROLOGICAL AND CHEMICAL INDICES

INDEX	TIME PERIOD	McHENRY		QUEENY		WOOSTER		YELLOWSTONE LAKE		COMBINED DATA	
		Hours Before O ₃ Observation	Correlation	Significance	Correlation	Significance	Correlation	Significance	Correlation	Significance	Correlation
Hydrocarbon Emissions	0-12										
	12-24										
	24-36										
	36-48										
NO _x Emissions	0-12										
	12-24	0.64	0.000								
	24-36	0.38	0.02	0.56	0.001					0.27	0.001
	36-48			0.47	0.004					0.32	0.000
Insolation	0-12										
	12-24	0.53	0.001	0.59	0.000	0.53	0.001	0.40	0.01	0.44	0.000
	24-36			-0.32	0.04			0.32	0.04		
	36-48			0.66	0.00	0.62	0.000	0.59	0.000	0.40	0.000
Relative Humidity	0-12										
	12-24	0.37	0.03	0.39	0.02			0.60	0.001	0.31	0.001
	24-36										
	48-60										
Temperature	0-12	-0.38	0.02	-0.48	0.003	-0.60	0.000			-0.31	0.000
	12-24	-0.47	0.004								
	24-36	-0.53	0.001	-0.38	0.02	0.35	0.03	-0.35	0.03	-0.32	0.000
	36-48	-0.33	0.04	0.34	0.03						
Dew Point	0-12										
	12-24	0.57	0.001	0.68	0.000	0.81	0.000	0.70	0.000	0.54	0.000
	24-36	0.40	0.01	0.46	0.005	0.61	0.000	0.64	0.000	0.27	0.001
	36-48							0.61	0.000	0.41	0.000
Precipitation	0-12					0.48	0.005	0.54	0.003	0.20	0.02
	12-24							0.54	0.003	0.26	0.003
	24-36			0.38	0.02	0.33	0.04	0.64	0.001	0.36	0.000
	36-48					0.31	0.05	0.56	0.001	0.26	0.002
	0-12					0.42	0.01	0.50	0.002	0.23	0.007
	12-24			0.32	0.04	0.31	0.05	0.57	0.001	0.25	0.003
	24-36			0.34	0.03	0.38	0.02	0.60	0.001	0.26	0.003
	36-48										
	0-12			-0.41	0.013	-0.60	0.000			0.31	0.000
	12-24	-0.33	0.04			-0.46	0.005			0.25	0.003
	24-36	-0.40	0.02			-0.38	0.02			-0.26	0.002
	36-48	-0.35	0.03					-0.48	0.005	-0.17	0.04
	0-12	-0.35	0.03	0.33	0.04			-0.40	0.03		
	12-24										
	24-36										
	36-48										
	0-12										
	12-24										
	24-36										
	36-48										
	0-12										
	12-24										
	24-36										
	36-48										
	0-12										
	12-24										
	24-36										
	36-48										
	0-12										
	12-24										
	24-36										
	36-48										
	0-12										
	12-24										
	24-36										
	36-48										
	0-12										
	12-24										
	24-36										
	36-48										
	0-12										
	12-24										
	24-36										
	36-48										
	0-12										
	12-24										
	24-36										
	36-48										
	0-12										
	12-24										
	24-36										
	36-48										
	0-12										
	12-24										
	24-36										
	36-48										
	0-12										
	12-24										
	24-36										
	36-48										
	0-12										
	12-24										
	24-36										
	36-48										
	0-12										
	12-24										
	24-36										
	36-48										
	0-12										
	12-24										
	24-36										
	36-48										
	0-12										
	12-24										
	24-36										
	36-48										
	0-12										
	12-24										
	24-36										
	36-48										
	0-12										
	12-24										
	24-36										
	36-48										
	0-12										
	12-24										
	24-36										
	36-48										
	0-12										
	12-24										
	24-36										
	36-48										
	0-12										
	12-24										
	24-36										
	36-48										
	0-12										
	12-24										
	24-36										
	36-48										
	0-12										
	12-24										
	24-36										
	36-48										
	0-12										
	12-24										
	24-36										
	36-48										
	0-12										
	12-24										
	24-36										
	36-48										
	0-12										
	12-24										
	24-36										
	36-48										
	0-12										
	12-24										
	24-36										
	36-48										
	0-12										
	12-24										
	24-36										
	36-48										
	0-12										
	12-24										
	24-36										
	36-48										
	0-12										
	12-24										
	24-36										
	36-48										
	0-12										
	12-24										
	24-36										
	36-48										
	0-12										
	12-24										
	24-36										
	36-48										
	0-12										
	12-24										
	24-36										
	36-48										
	0-12										
	12-24										
	24-36										
	36-48										
	0-12										
	12-24										
	24-36										
	36-48										
	0-12										
	12-24										
	24-36										
	36-48										
	0-12										
	12-24										
	24-36										
	36-48										
	0-12										
	12-24										
	24-36										
	36-48										
	0-12										
	12-24										
	24-36										
	36-48										
	0-12										
	12-24										
	24-36										
	36-48										
	0-12										
	12-24										
	24-36			</							

that statistical tests of significance should be tempered with tests based on logic and physical principles.

2.2.1.2.1. Emissions Indices

With the previously discussed exception of the correlation between Queeny oxidant levels and hydrocarbon emissions 48 to 60 hours upstream, there were no significant linear relationships noted between oxidant concentrations and hydrocarbon emissions during any of the 120 trajectories. The following explanations can be proposed:

1. Hydrocarbons do not affect oxidant formation.
2. Trajectories with high hydrocarbon emissions did not occur when meteorological conditions were conducive to oxidant formation.
3. Emissions and trajectory data are not adequate to detect correlations.
4. Enough hydrocarbons are generally present to allow oxidant formation.

The first of the possible explanations is known from laboratory experiments to be untrue, and the second seems unlikely to be true for all four of the sites. For example, the Wooster site has major urban areas to the west-northwest (Chicago), to the southwest (Columbus and Cincinnati) and to the northeast (Cleveland). Yellowstone Lake is west northwest of Chicago; Queeny is west of St. Louis. McHenry has urbanized areas to the west (Columbus), north-northwest (Cleveland), northeast (New York), east (Philadelphia) and southeast (Baltimore and Washington). The meteorological conditions associated with trajectories arriving from such a multitude of directions must be diverse enough to rule out the possibility that high hydrocarbon emissions are only associated with trajectories that occur during meteorological conditions that are unsuitable for ozone formation. The third argument is refuted by the fact that significant relationships were noted between oxidant levels and NO_x emissions. The fourth explanation suggests that hydrocarbons are generally present in sufficient quantities for the formation of ozone near these nonurban sites and, therefore, that ozone concentrations will be governed by other factors.

Table 3 thus indicates a stronger relation, at these four rural sites, between NO_x emissions and ozone formation than between hydrocarbons and ozone formation. This is somewhat surprising in that it was anticipated that the occurrence of high hydrocarbon emissions and high NO_x emissions would be sufficiently in concert that their relationships to ozone formation would be quite similar. There is some evidence, presented later, to suggest that significant relationships between hydrocarbon emissions and ozone do indeed exist despite the fact that they are not evident in the linear correlation analyses.

It should be noted that two effects of possible importance have not been included in these calculations. The first is the difference between emissions on weekends, and those on weekdays. Also, the diurnal corrections that were used are appropriate to weekday conditions. The introduction of weekend factors might change the results somewhat, but it seems unlikely that they would be seriously altered. Perhaps more serious is the fact that the emissions indices that have been used reflect only the direct anthropogenic emissions. They do not include any natural emissions or indirect anthropogenic emissions such as may occur, for example, in the use of nitrogen compounds in agriculture.

It has not been possible to incorporate all the possible effects in determining the emissions indices. No account has been taken of possible differences between stationary and mobile sources, and how the ratio of emissions from the two types varies through the day or from season to season. Neither has any accounting of temperature effects on evaporative emissions been included. Although such effects might cause the magnitude of the results to change somewhat, it seems unlikely that the results would differ substantively. Furthermore, the increased level of detail in the treatment of the emissions would be inconsistent with the countywide, annual-average nature of the emissions inventory that was available as the basic data source or with the uncertainties in the trajectories.

2.2.1.2.2. Meteorological Indices

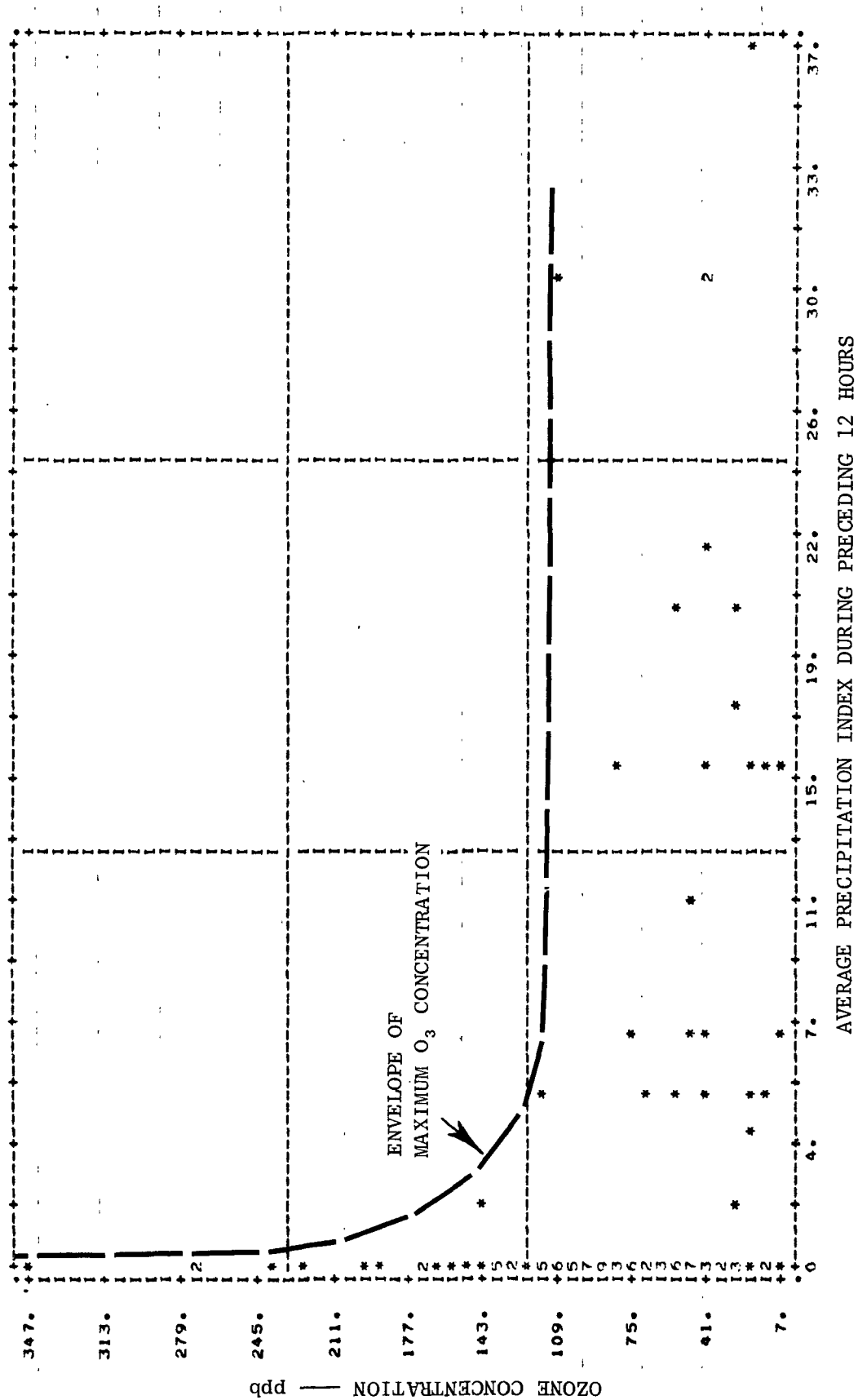
The meteorological indices are very closely related in a physical sense, so that high correlations between ozone concentrations and several of the meteorological indices do not necessarily indicate several independent relationships. For example, relative humidity tends to be inversely related to temperature so that a correlation between ozone and temperature can be expected to be accompanied by one of opposite sign between ozone and relative humidity. Similarly, the relationship between insolation and air temperature would lead to the expectation that the two indices would correlate in the same sense with ozone. Table 3 shows that these expectations are generally met.

Also, the value of an index for one time period will often be closely related to its value for some other time period. In the case of insolation, the values at 24-hour intervals should be similar. Thus, we would expect to see similarities among insolation indices representing alternate 12-hour periods. This is very evident in the combined data results given in Table 3. In the case of dew-point, there should be little diurnal change within an air parcel because dew-point is a measure of absolute humidity and changes only with the addition or removal of water vapor. It is a reasonably conservative property of the air, so that results for one time interval should be similar to those for another; Table 3 supports this.

The interrelationships among the meteorological indices mean that there is considerable redundancy in the information they provide. If one selects the best index and uses it to describe ozone behavior, there is not likely to be much improvement in the description if one of the other indices is incorporated in the regression equation. Furthermore, as one adds variables to the regression expressions, these expressions become more specific to the data from which they are derived and more difficult to generalize to the overall population.

Thus, it is important to try to select the "best" index and use it to represent the others. Table 3 provides a means for doing this. Only two of the indices provide significant correlations at all the stations studied: insolation and temperature during the 12-hours preceding the ozone observations. Of the two, temperature is consistently better correlated with ozone concentration and appears to be the better choice if only one meteorological index is used.

There is no a priori reason why the relationships between oxidant concentrations and the various indices should necessarily be linear. In fact, there is some reason to believe just the opposite. For instance, in the case of precipitation there could be a scrubbing effect on either ozone or its precursors. With no precipitation, oxidant concentrations would be controlled by other factors; but in the presence of precipitation there may be some upper limit to the concentration that can occur. Whether that maximum is achieved will depend on other factors. Figure 43 presents some evidence that such may be the case. This figure is a computer-generated scatter diagram of oxidant concentration versus the composite precipitation index for the last 12-hours of the trajectory. An asterisk is plotted for each case. Plotted numerals indicate the number of cases at the indicated positions. Although there is a significant negative linear correlation between these two variables, the scatter diagram suggests that a more useful representation of the relationship between the two might be a curve describing the envelope of the points. The dashed curve in Figure 43 is an approximation to this curve. The practical significance of such a relationship is that it can be used to define conditions for which high oxidant concentrations are very unlikely, regardless of the emissions history of the air.



Source: Ludwig et al, 1977

FIGURE 43 SCATTER DIAGRAM OF OZONE CONCENTRATION VERSUS PRECIPITATION INDEX DURING
LAST 12 HOURS OF TRAJECTORY-COMBINED DATA

2.2.1.2.3. Rank Correlations

Before leaving the discussion of the relationships between ozone concentrations and each of the individual indices, it is worthwhile to examine the possibility of nonlinear relationships. One way of testing for nonlinear, but monotonic relationships is through rank correlation. In this case, use has been made of Spearman's correlation of ranks (see e.g. Langley, 1970). This test will show if there is a significant monotonic relationship between two variables, even if it cannot be well represented by a linear expression.

Table 4 presents the Spearman correlations between oxidant and each of the individual indices. As in Table 3, the value of the correlation has been entered only when its significance is equal to, or better than, 0.05. The significance is shown in parentheses. The results in the table are based on the combined data from all four sites.

The results presented in Table 4 suggest relationships that are stronger than those evident in the linear correlations given in Table 3. It is particularly interesting that there appears to be a relatively strong relationship between ozone concentrations and emissions of both NO_x and hydrocarbons 24 to 36 hours earlier.

Both Table 3 and Table 4 exhibit evidence of diurnal effects on the relationships. It should be remembered that daily maximum-one-hour concentrations of ozone were chosen for this analysis. Such maxima normally occur in the afternoon or early evening hours. Thus, the first, third, and fifth 12-hour periods before the observation will most often be the periods with the greatest insolation and the largest variability in insolation from case to case. From this, it follows that the possibility of significant correlation is greater for these periods. Similarly, nighttime emissions are lower and have smaller spatial gradients than daytime emissions, so the sample correlations are likely to be less for the even-numbered 12-hour periods than for the others. As is to be expected, diurnal periodicity in correlation is also evident in Table 4 for temperature, relative humidity, and dew-point, but not for precipitation.

2.2.1.3. Ozone Concentration Related to Combinations of Factors

2.2.1.3.1. Unstratified Data

In this subsection the ozone concentrations are related to different combinations of indices through linear regression. As noted before, it is desirable to limit the number of indices used in these expressions to as few as possible, otherwise the results will tend to be specific to this particular data set. Some selection criteria must therefore be used to decide which indices are most appropriate. One approach uses a step-by-step selection process to choose those variables

Table 4

SPEARMAN RANK CORRELATIONS BETWEEN OZONE, METEOROLOGICAL
AND CHEMICAL INDICES FOR THE COMBINED DATA FOR ALL SITES

Index	Time Period Before Measurement (Hours)				
	0-12	12-24	24-36	36-48	48-60
Hydrocarbon Emissions	0.18 (0.03)		0.36 (0.001)	0.17 (0.04)	0.27 (0.003)
NO _x Emissions	0.19 (0.02)		0.40 (0.001)	0.23 (0.007)	0.26 (0.004)
Insolation	0.49 (0.001)		0.48 (0.001)		0.33 (0.001)
Temperature	0.68 (0.001)	0.31 (0.001)	0.47 (0.001)	0.25 (0.004)	0.29 (0.002)
Precipitation	-0.45 (0.001)	-0.37 (0.001)	-0.31 (0.001)	-0.31 (0.001)	
Relative Humidity	-0.34 (0.001)		-0.32 (0.001)		
Dew-Point	0.40 (0.001)	0.28 (0.001)	0.26 (0.003)	0.30 (0.001)	0.30 (0.001)

that explain the greatest part of the variance in oxidant concentration that remains unexplained by the variables selected in earlier steps. This approach is used by the SPSS (Nie et al., 1975) computer program. When this step-by-step selection process was applied to the combined data, the four indices that explained the most variance were the following:

1. Temperature during preceding 12 hours
2. NO_x emissions during preceding 12 hours
3. Temperature 48 to 60 hours earlier
4. Hydrocarbon emissions during preceding 12 hours.

These indices are listed in order of their decreasing ability to describe the resulting ozone concentrations.

Practical considerations relating to the purposes of this project can be invoked to provide a rationale for selection of indices to be included in regression expressions. The purpose of this project is related to ozone control strategies, hence the emphasis should be on those indices that are related to controllable processes, i.e., emissions rather than weather.

Another possible basis for selecting variables for inclusion in the studies is the degree to which one variable can serve as a surrogate for another. To a large extent, this ability is represented by the correlation between the variable and its surrogate. The linear correlation coefficient is a measure of the redundancy of information contained in the data sets containing the two variables. Table 5 shows all the correlations between meteorological indices that are 0.3 or greater. It is evident from this table that the temperature during the last 12 hours of the trajectory is highly correlated with most of the other meteorological indices--except the precipitation index. Temperature during the last 12 hours of the trajectory would thus seem to be a good choice for an "all purpose" indicator of the meteorology along the trajectory.

The emissions indices do not show the same degree of redundancy with each other as temperature does with other meteorological indices. Table 6 indicates that NOx emissions are significantly related to HC emissions for the same time period. This was expected. However, there is virtually no relationship seen between different time periods. Also, (though not shown in Table 6) there was no significant relationship noted between emissions of either pollutant with emissions of the same pollutant during a different period.

For the reasons presented above, most of the following discussions are limited to multivariate relationships between ozone concentrations and combinations of temperature, NOx, and hydrocarbon indices. These relationships take the form:

$$C_e = A + B_T T + B_N N + B_H H$$

where

C_e = estimated ozone concentration

A = constant determined by regression

B_T, B_N, B_H = coefficients of the temperature, NOx, and hydrocarbon indices, respectively, as determined by regression

T, N, H = temperature, NOx, and hydrocarbon indices, respectively *

* Units of temperature are degrees Fahrenheit; units of the emissions indices are $10^{-3} \text{ m}^{-2} \text{ hr}^{-1}$; units of concentration are ppb.

Table 5
CORRELATION BETWEEN PAIRS OF METEOROLOGICAL INDICES
(All Sites Combined)

INSOLATION	INSOLATION				PRECIPITATION				DEW POINT				RELATIVE HUMIDITY				TEMPERATURE			
	0-12	12-24	24-36	36-48	0-12	12-24	24-36	36-48	0-12	12-24	24-36	36-48	0-12	12-24	24-36	36-48	0-12	12-24	24-36	36-48
	0-12	- .50																		
	12-24	.80																		
	24-36	-.52																		
	36-48	.70	-.51	.75	-.50															
PRECIPITATION	0-12	-.33																		
	12-24		-.35																	
	24-36																			
	36-48																			
DEW POINT	0-12		.32	.41																
	12-24			.36																
	24-36																			
	36-48																			
RELATIVE HUMIDITY	0-12	-.56	-.37	-.52	-.33															
	12-24																			
	24-36	55		61	-.44															
	36-48	36	-.33	-.53																
TEMPERATURE	0-12	.60	.63	.56																
	12-24			.35																
	24-36	.44	.54	.55																
	36-48		.31	.46																
	0-12																			
	12-24																			
	24-36																			
	36-48																			
	0-12																			
	12-24																			
	24-36																			
	36-48																			
	0-12																			
	12-24																			
	24-36																			
	36-48																			
	0-12																			
	12-24																			
	24-36																			
	36-48																			
	0-12																			
	12-24																			
	24-36																			
	36-48																			
	0-12																			
	12-24																			
	24-36																			
	36-48																			
	0-12																			
	12-24																			
	24-36																			
	36-48																			
	0-12																			
	12-24																			
	24-36																			
	36-48																			
	0-12																			
	12-24																			
	24-36																			
	36-48																			
	0-12																			
	12-24																			
	24-36																			
	36-48																			
	0-12																			
	12-24																			
	24-36																			
	36-48																			
	0-12																			
	12-24																			
	24-36																			
	36-48																			
	0-12																			
	12-24																			
	24-36																			
	36-48																			
	0-12																			
	12-24																			
	24-36																			
	36-48																			
	0-12																			
	12-24																			
	24-36																			
	36-48																			
	0-12																			
	12-24																			
	24-36																			
	36-48																			
	0-12																			
	12-24																			
	24-36																			
	36-48																			
	0-12																			
	12-24																			
	24-36																			
	36-48																			
	0-12																			
	12-24																			
	24-36																			
	36-48																			
	0-12																			
	12-24																			
	24-36																			
	36-48																			
	0-12																			
	12-24																			
	24-36																			
	36-48																			
	0-12																			
	12-24																			
	24-36																			
	36-48																			
	0-12																			
	12-24																			
	24-36																			
	36-48																			
	0-12																			
	12-24																			
	24-36																			
	36-48																			
	0-12																			
	12-24																			
	24-36																			
	36-48																			
	0-12																			
	12-24																			
	24-36																			
	36-48																			
	0-12																			
	12-24																			
	24-36																			
	36-48																			
	0-12																			
	12-24																			
	24-36																			

Table 6
CORRELATIONS BETWEEN HYDROCARBON AND NO_x EMISSIONS
(COMBINED DATA)
(No values < 0.3 are shown)

Oxides of Nitrogen Emissions	Hydrocarbon Emissions				
	0-12 Hrs.	12-24 Hrs.	24-36 Hrs.	36-48 Hrs.	48-60 Hrs.
0-12 Hrs.	0.39				
12-24 Hrs.		0.41			
24-36 Hrs.			0.38		
36-48 Hrs.				0.66	0.39
48-60 Hrs.					0.77

Linear regression equations of the above type were calculated for each of the sites and for the combined data using both weighted composite indices and indices referring to the last 12-hours of the trajectory. The weighted indices are an attempt to characterize conditions throughout the 60-hour duration of the trajectory. The weighted average indices were computed by giving five times as great a weight to the values in the last 12-hours as to those in the 48 to 60 hour period; while a weighting factor of four was given to values in the 12 to 24 hour period, and so forth. This subjective weighting scheme is meant to reflect the likelihood of greater physical relationships with the more recent events. It also minimizes the weight given to the earlier, more uncertain, parts of trajectory. Table 7 gives the constants for a regression equation that contains the weighted indices of NO_x and hydrocarbon emissions and the temperature index for the last 12 hours of the trajectory. The multiple correlation coefficients are also given. The missing entry for the coefficient of the NO_x index indicates that the addition of this variable did not improve the predictive capabilities of the equation.

It is obvious that a zero coefficient for one of the terms in a regression equation indicates no contribution from the corresponding index. Inasmuch as the values of the coefficients are derived from limited data sets, it is reasonable to wonder what the chances are that the coefficients might have been zero if the total population had been used. To some extent this can be estimated by establishing confidence intervals for the values of the coefficients. Figure 44 shows the 95% confidence intervals for each of coefficients shown in Table 7. The fact that these intervals all span zero for the weighted hydrocarbon index tends to deprecate the importance of this index. The significantly nonzero values of the coefficients of the temperature index support the importance of this index as a predictor of ozone concentration.

Table 7

REGRESSION CONSTANTS RELATING OZONE CONCENTRATIONS TO WEIGHTED
INDICES OF NO_x AND HYDROCARBON EMISSIONS AND TO
TEMPERATURE DURING THE LAST 12 HOURS

Site	Constant Term	Coefficient for Weighted Hydrocarbon Index	Coefficient for Weighted NO _x Index	Coefficient for Temper- ature Index	Multiple Coeffi- cient Index
McHenry	-297.41	-7.8	15.0	5.3	0.67
Queeny	-146.35	3.4	6.7	2.8	0.70
Wooster	-228.25	-1.1	--*	4.4	0.81
Yellowstone Lake	-61.07	-0.8	6.3	1.8	0.73
Combined	-145.72	-1.2	5.1	3.1	0.60

* For this station, weighted NO_x emissions did not significantly contribute to the explanation of any of the variance left unexplained by the temperature and hydrocarbon emissions.

Table 8 summarizes the constants for the regression equations when the indices for the final 12 hours of the trajectory are used instead of the weighted emissions indices. The multiple correlations are also shown. Comparison of these values with the corresponding correlations in Table 7 shows that there is little difference between the predictive capabilities of the weighted emission indices and the final 12-hour emission indices. Figure 45 shows the 95% confidence intervals for the coefficients given in Table 8. Again, the lack of a linear relationship between ozone and hydrocarbon emissions is indicated.

Inasmuch as the various meteorological indices are highly cross-correlated, the possibility of replacing the temperature index with a linear composite of all the meteorological indices was investigated. Factor analysis (Nie et al., 1975) was used to derive two uncorrelated composite indices that explained virtually all of the variance in the original set of 6 meteorological indices. However, when multiple regression analyses were performed using these factors, no significant improvement was found over the results achieved by using temperature alone. It appears that the dependence of temperature on other meteorological conditions is such that the relationship between ozone and temperature is as strong as that which can be established between ozone and any optimized combination of other meteorological parameters.

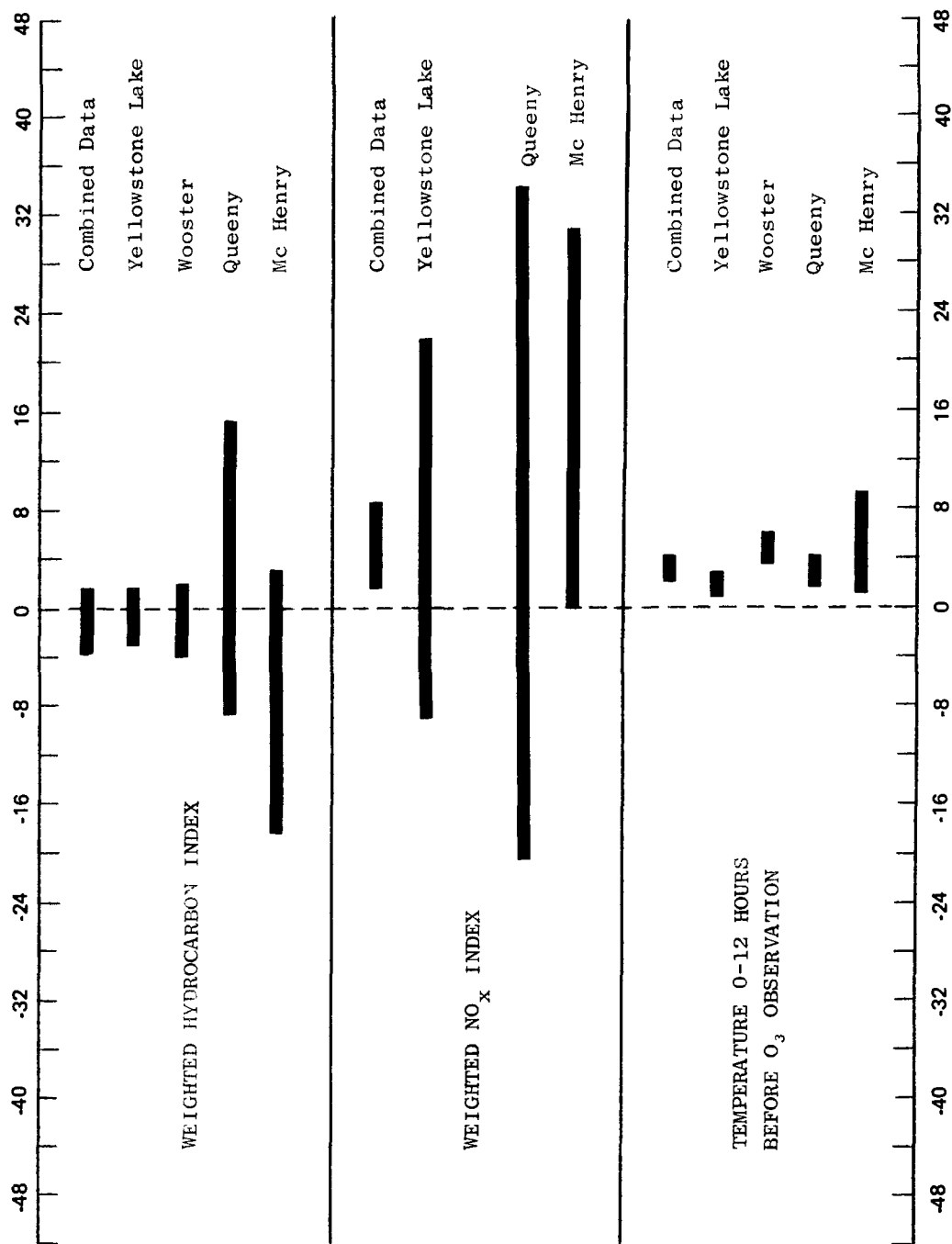


FIGURE 44 95% CONFIDENCE LIMITS FOR COEFFICIENTS IN THE REGRESSION EQUATIONS USING WEIGHTED EMISSIONS INDICES

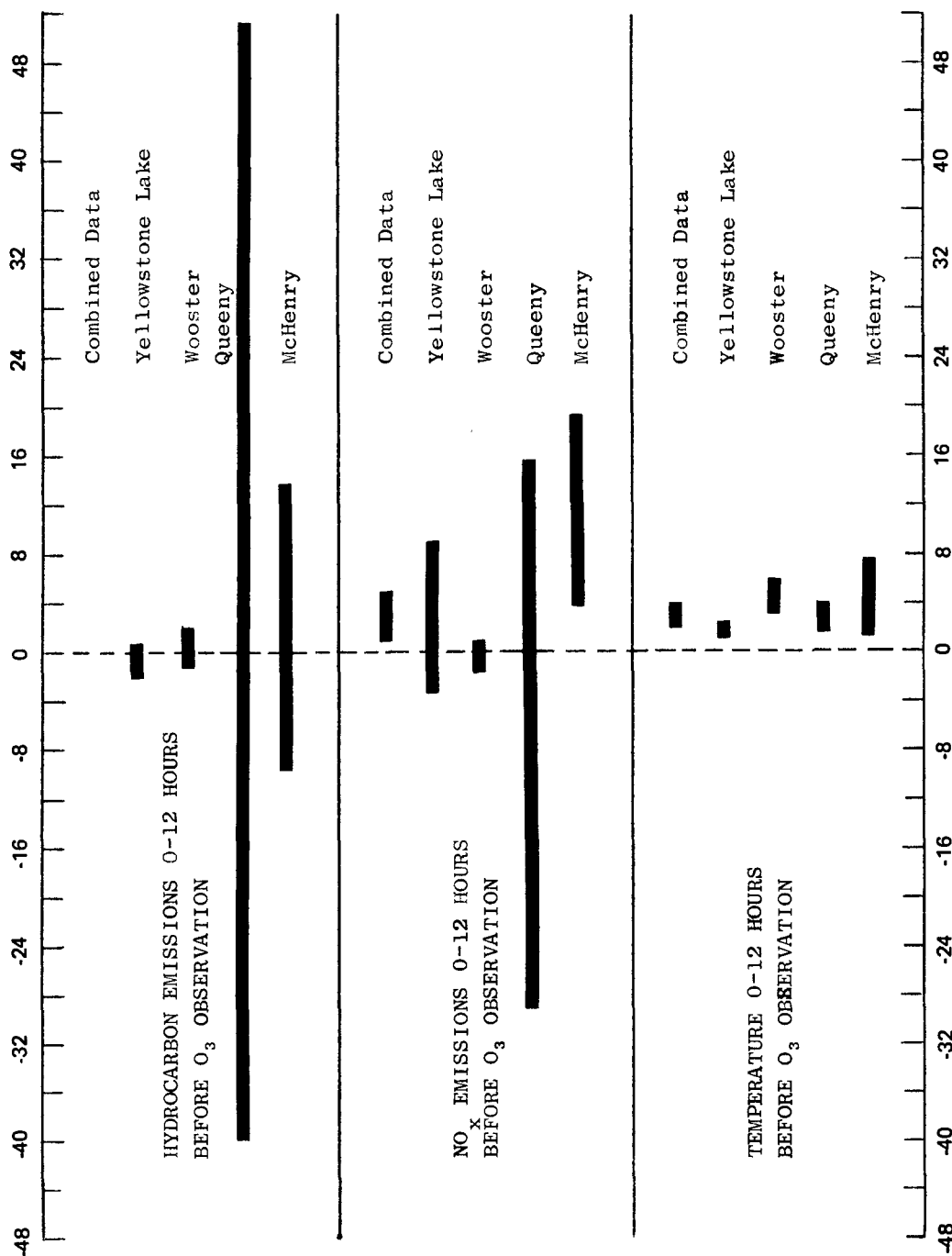


FIGURE 45 95% CONFIDENCE LIMITS FOR COEFFICIENTS IN THE REGRESSION EQUATION USING EMISSIONS FOR LAST 12 HOURS

Table 8

REGRESSION CONSTANTS RELATING OZONE CONCENTRATIONS TO
TEMPERATURE AND EMISSIONS INDICES FOR THE LAST
12 HOURS OF THE TRAJECTORY

Site	Constant Term	Coefficient for Hydro-carbon Index	Coefficient for NO _x Index	Coefficient for Temperature Index	Multiple Correlation
McHenry	-219.01	2.0	11.4	3.9	0.71
Queeny	-138.98	4.9	-7.0	2.9	0.69
Wooster	-237.43	0.3	-0.5	4.5	0.81
Yellowstone Lake	-68.02	-0.7	2.7	1.9	0.72
Combined	-141.38	-0.8	3.0	3.1	0.59

Another measure of the effectiveness of a regression equation, besides the multiple correlation coefficient, is a comparison between the values predicted by the equation and the values observed. Table 9 shows the standard errors for the two classes of equations-- those using the weighted emissions indices and those using the emissions during the last 12 hours of the trajectory. By this measure there is little difference between the two kinds of index. Figures 46 and 47 are scattergrams that illustrate how well the observed concentrations are fit by the regression equations derived from the total data set. There is one anomalous point at the far right of each diagram. The data for that point were reexamined and appear to be correct; but it should be recognized that only slight miscalculations in the trajectory analysis could have caused the assignment of unrealistically high values for the emissions indices. In this case, the air appeared to have passed over a major urban area, when in fact the air may have passed over an area of much lower emissions only a few tens of kilometers away. In general, the points in Figure 46 and 47 form tight, consistent patterns. There appears to be a change of slope at around 80 to 100 ppb.

Table 9

STANDARD ERROR OF ESTIMATE OF THE REGRESSION EQUATIONS

Site	Equation	
	Weighted Emissions	Emissions 0 to 12 hours prior
McHenry	65 ppb	60 ppb
Queeny	35	36
Wooster	22	22
Yellowstone Lake	24	23
Combined Data	47	47

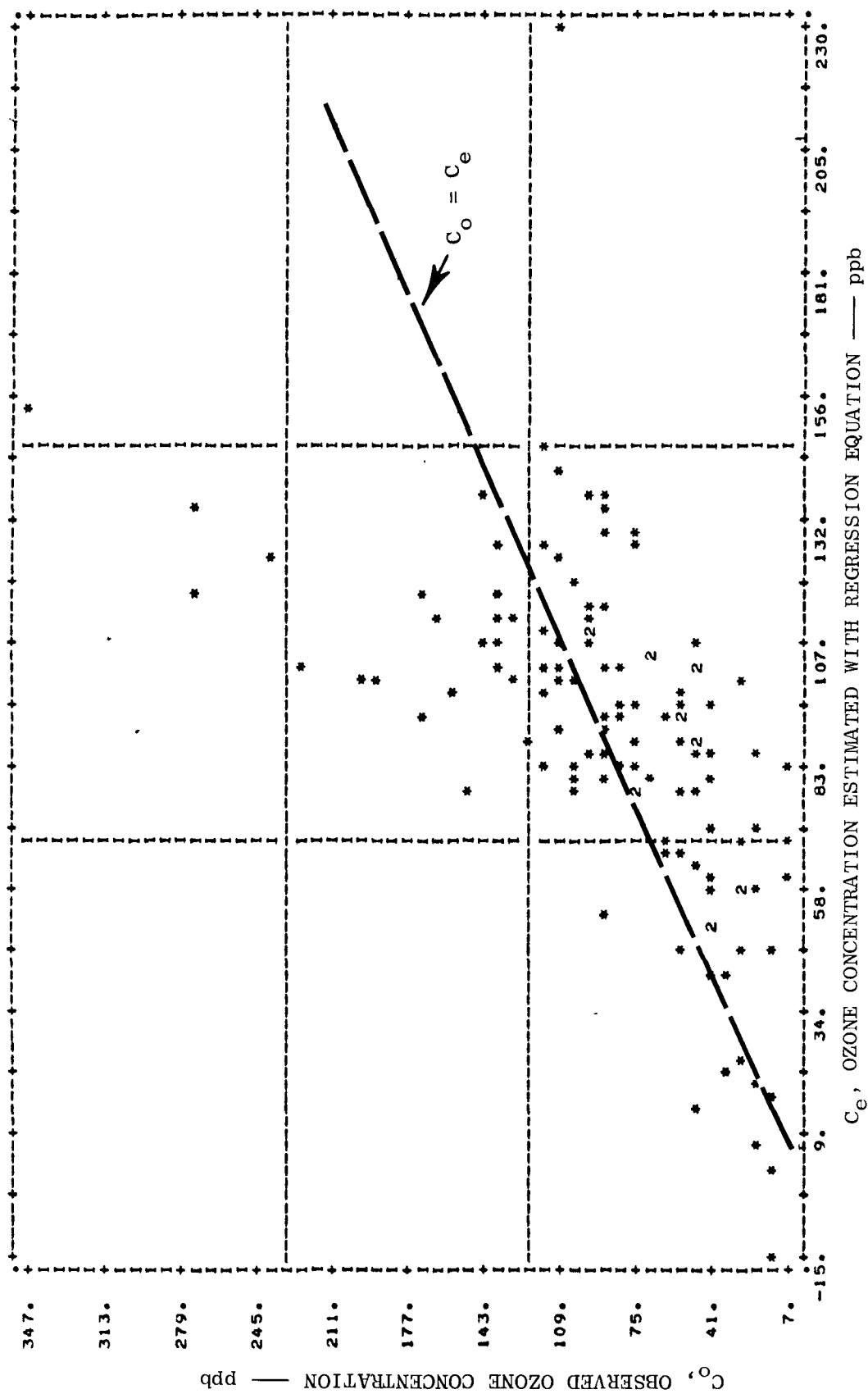


FIGURE 46 SCATTER DIAGRAM OF OBSERVED OZONE CONCENTRATIONS VERSUS THOSE ESTIMATED FROM A REGRESSION EQUATION USING INDICES OF EMISSIONS AND TEMPERATURE DURING THE LAST 12 HOURS (Combined data)

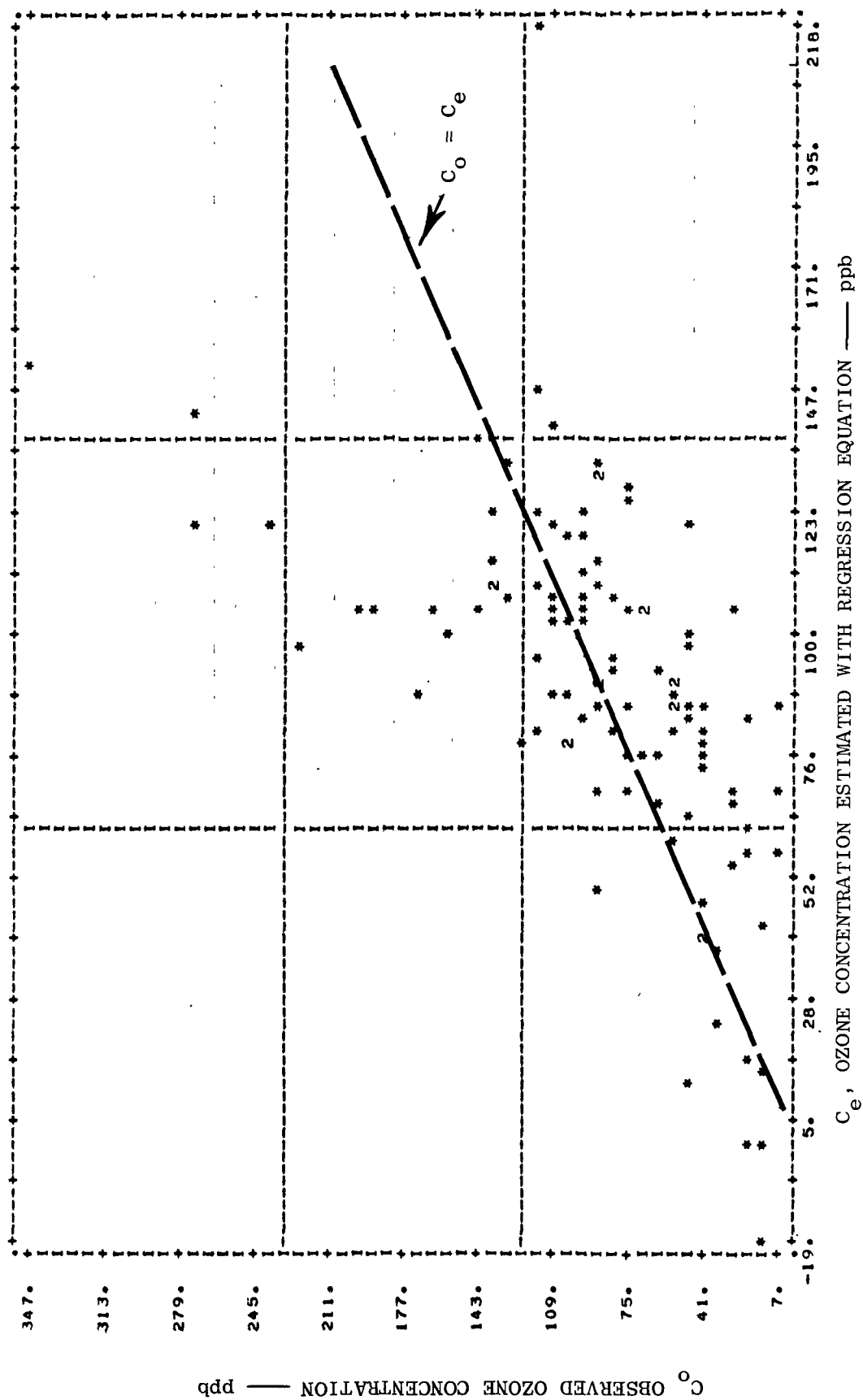


FIGURE 47 SCATTER DIAGRAM OF OBSERVED OZONE CONCENTRATIONS VERSUS THOSE ESTIMATED FROM A REGRESSION EQUATION USING TEMPERATURE AND WEIGHTED EMISSION INDICES

Other measures of the effectiveness of the regression equations are available. The degree to which a regression equation that is based on one set of data fits other data sets provides an assessment of the applicability of the equation. Such a comparison was made using the five data bases (4 sites and the combined data set) and the ten equations (one per site using weighted-average emissions, and one per site using emissions for the last 12 hours). None of the equations based on data from other locations fit the Wooster data very well; correlation coefficients range from 0.35 to 0.37. However, the Wooster equation provides reasonably good estimates for the concentrations, at other stations with correlations ranging from 0.60 to 0.71. The Wooster equation that is based on emissions during the last 12 hours of the trajectory also provides a good fit to data from the other stations, with multiple correlations from 0.55 to 0.70.

When the equations based on the combined data set are applied to the subsets for the different stations, the multiple correlations range from 0.55 to 0.72 for the equation using the emissions during the final 12 hours, and from 0.58 to 0.72 for the equation using the weighted emissions. The standard error of estimate for the weighted-index equation lies between 24 and 67 ppb for the different sites; using the equation based on the final 12-hour indices, the extremes are 23 and 64 ppb.

Multiple-regression equations were also formed using combinations of indices other than those discussed above. For example, the rank correlations suggest that emissions during the 24-36 hour time interval are important. A regression equation was formed using the temperature and NO_x indices for the 0 to 12 hour period and the NO_x index for the 24 to 36 hour period. The resulting equation is as follows:

$$C_e = 2.89 T(0) + 2.45 N(0) + 2.55 N(24) - 133.4$$

where

C_e = estimated ozone concentration

$T(0), N(0)$ = average temperature (°F) and NO_x (10^{-3} ton mi⁻² hr⁻¹) emissions 0 to 12 hours before observation.

$N(24)$ = average NO_x emissions, 24 to 36 hours before observation

The correlation achieved with this combination of indices was 0.62, very slightly better than with the combinations discussed above. Figure 48 shows the fit achieved with this equation.

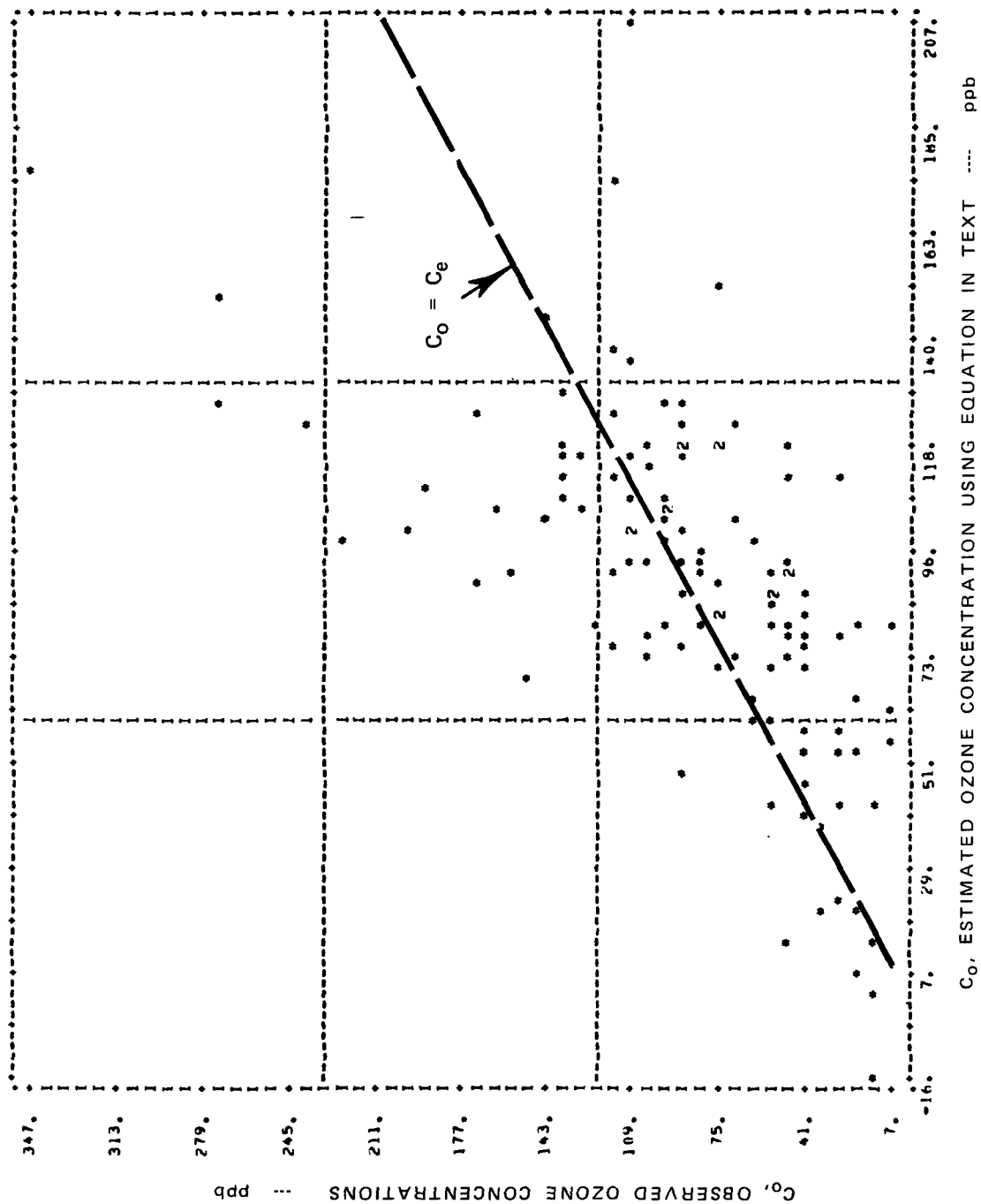


FIGURE 48 SCATTER DIAGRAM OF OBSERVED OZONE CONCENTRATIONS VERSUS THOSE ESTIMATED FROM A REGRESSION EQUATION USING TEMPERATURE FOR THE LAST 12 HOURS AND NO_x EMISSIONS FOR THE PERIOD 24 - 36 HOURS BEFORE THE OBSERVATION

Another equation that was checked used emissions indices for the 24 to 36 hour period for both hydrocarbons and oxides of nitrogen, along with the temperature index for the final 12 hours before observation. It was observed that the addition of the hydrocarbon index did not contribute to the explanation of the ozone concentrations.

2.2.1.3.2. Stratified Data

Figures 46, 47, and 48 suggest that a better fit might be achieved if the data were stratified according to the observed ozone concentration. Two equations were derived using the temperature, NO_x, and hydrocarbon indices for the last 12 hours. One equation was derived to fit the cases where the observed ozone concentration exceeded the federal standard of 80 ppb; the second equation fit those cases with lower ozone concentrations. The resulting equations were as follows:

$$C_e = 1.14 T(0) + 1.52 N(0) + 0.11 HC(0) - 38.8 \quad (O_3 > 80 \text{ ppb})$$

and

$$C_e = 0.93 T(0) + 2.22 N(0) + 0.31 HC(0) + 48.9 \quad (O_3 \leq 80 \text{ ppb})$$

These equations suggest that the dependence of ozone concentrations on temperature is greater for the concentrations above 80 ppb than for concentrations under the standard.

Figure 49a shows the scattergram of observed concentrations versus those calculated from the above equations (all sites combined). It is apparent that the two expressions achieve better agreement than the corresponding single equation illustrated in Figure 46. This piecewise linear regression results in a correlation between observed and estimated ozone concentrations of 0.76, as compared to the 0.59 obtained with the single expression (Table 8). The standard error was reduced from 47 ppb (Table 9) to 38 ppb.

During the derivation of the equations just discussed, it was discovered that the insolation indices for the last two 12-hour periods of the trajectory S(0) and S(12) were better predictors of the higher ozone values than the temperature index. With these parameters substituted for temperature, the equation for the cases where observed ozone concentrations were over 80 ppb is:

$$C_e = 298 S(12) + 133 S(0) + 2.40 N(0) - 1.79 HC(0) + 35.5$$

Using this equation, in combination with the one for low ozone concentrations given earlier, results in a correlation of 0.81 between observed and estimated concentrations. The standard error of the estimate is 34 ppb. The scattergram is shown in Figure 49b. It is thus seen that ozone concentrations can be reasonably well estimated on the basis

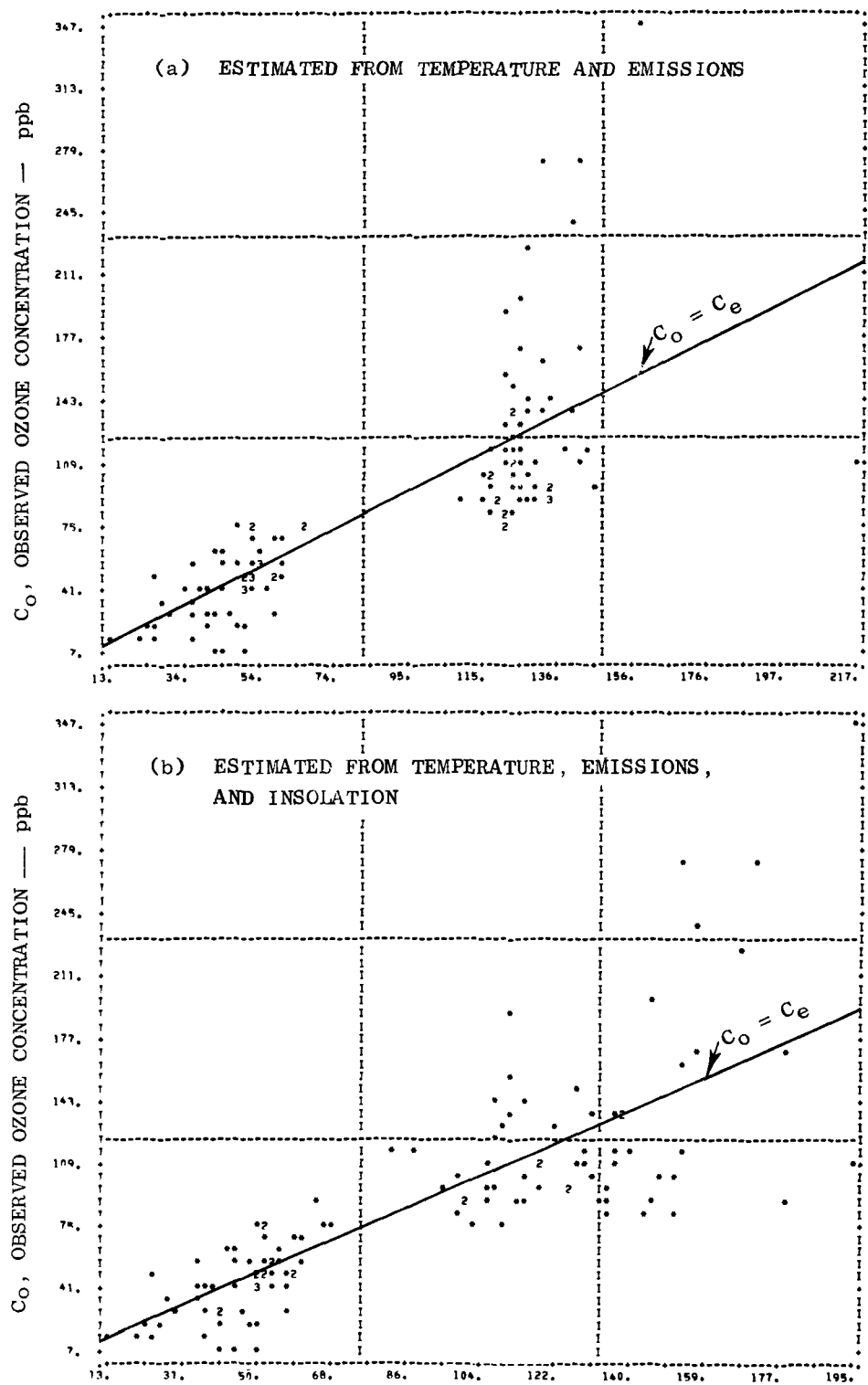


FIGURE 49 SCATTER DIAGRAM OF ESTIMATED VERSUS OBSERVED OZONE FOR TWO PIECEWISE LINEAR REGRESSION EXPRESSIONS

of the recent exposure of the air to sunlight. It is worth inquiring whether the same degree of predictability can be achieved without using any emissions indices as predictors. Piecewise regression was used in the same manner as discussed above, but with only temperature and insolation indices used. The equations are:

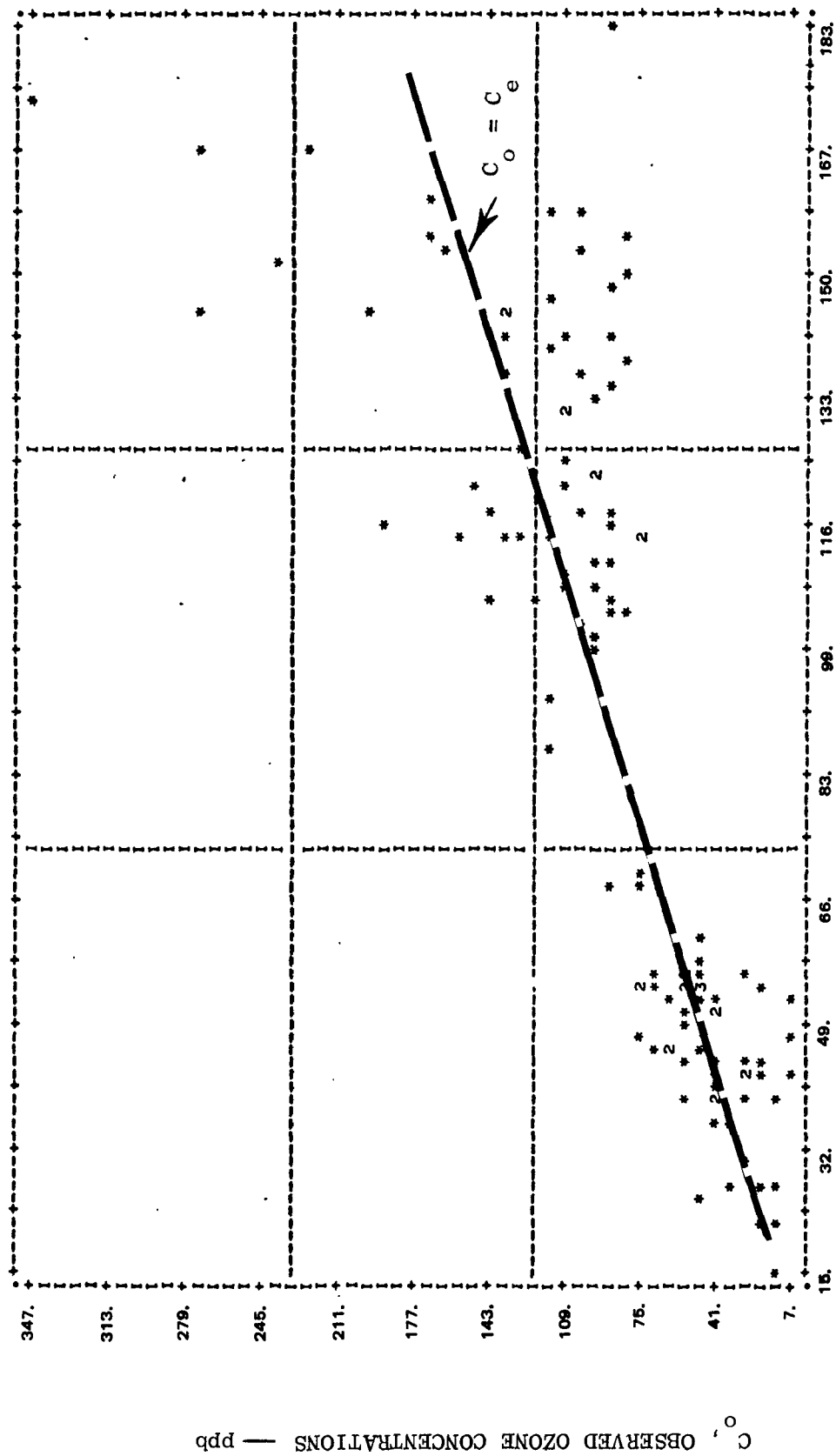
$$Ce = 1.15 T(0) - 31.1 \quad O_3 \leq 80 \text{ppb}$$

$$Ce = 299 S(12) + 136 S(0) + 38.9 \quad O_3 < 80 \text{ppb}$$

The concentrations are estimated with these equations nearly as well as with those that include emissions. The scattergram of observed ozone versus estimated ozone concentration is shown in Figure 50. The correlation is 0.79 and the standard error is 36 ppb. These results show that the addition of the emissions indices to the piecewise regression equations explains only about three or four percent more variance in the ozone data. The errors in the estimates are reduced by only one or two ppb.

The strong dependence of ozone concentration on meteorological conditions suggests that stronger correlations might be seen between ozone and emissions if the data were stratified according to whether meteorological conditions are unfavorable or favorable to ozone formation. Accordingly, correlations between ozone concentration and emission indices were calculated from two subsets, as follows: 1) those for which the average temperature during the last 12 hours was greater than 70°F, and 2) those for which there was no precipitation during the last 12 hours. There was only one case where the temperature index for the last 72 hours was less than 70°F and the federal standard of 80 ppb was exceeded. Data from all stations were used. However, for the subset of data for which the temperature index for the last 12 hours was greater than 70°F, no significant correlation was found between ozone concentration and any of the hydrocarbon emissions indices. In this higher temperature data set, ozone was significantly correlated with NO_x emissions 0 to 12 hours and 24 to 36 hours before the observation. However, the correlations were about the same as those shown in Table 3 for the unstratified data. Because of the reduced sample size, the correlations were slightly less significant.

For those cases where no precipitation occurred along the air trajectory during the last 12 hours, there were no significant correlations between ozone and the HC emissions indices. Significant correlations were found with NO_x emissions during the preceding 12 hours (0.32 correlation) and the 24-36 hour period (0.29). Again, however these values do not differ much from those found for the unstratified data (Table 3).



C_e , OZONE CONCENTRATION ESTIMATED BY REGRESSION — ppb

FIGURE 50 SCATTERGRAM OF ESTIMATED VERSUS OBSERVED O_3 FOR PIECEWISE LINEAR REGRESSION USING TEMPERATURE AND INSOLATION

2.2.1.4. Characteristics of the Trajectories

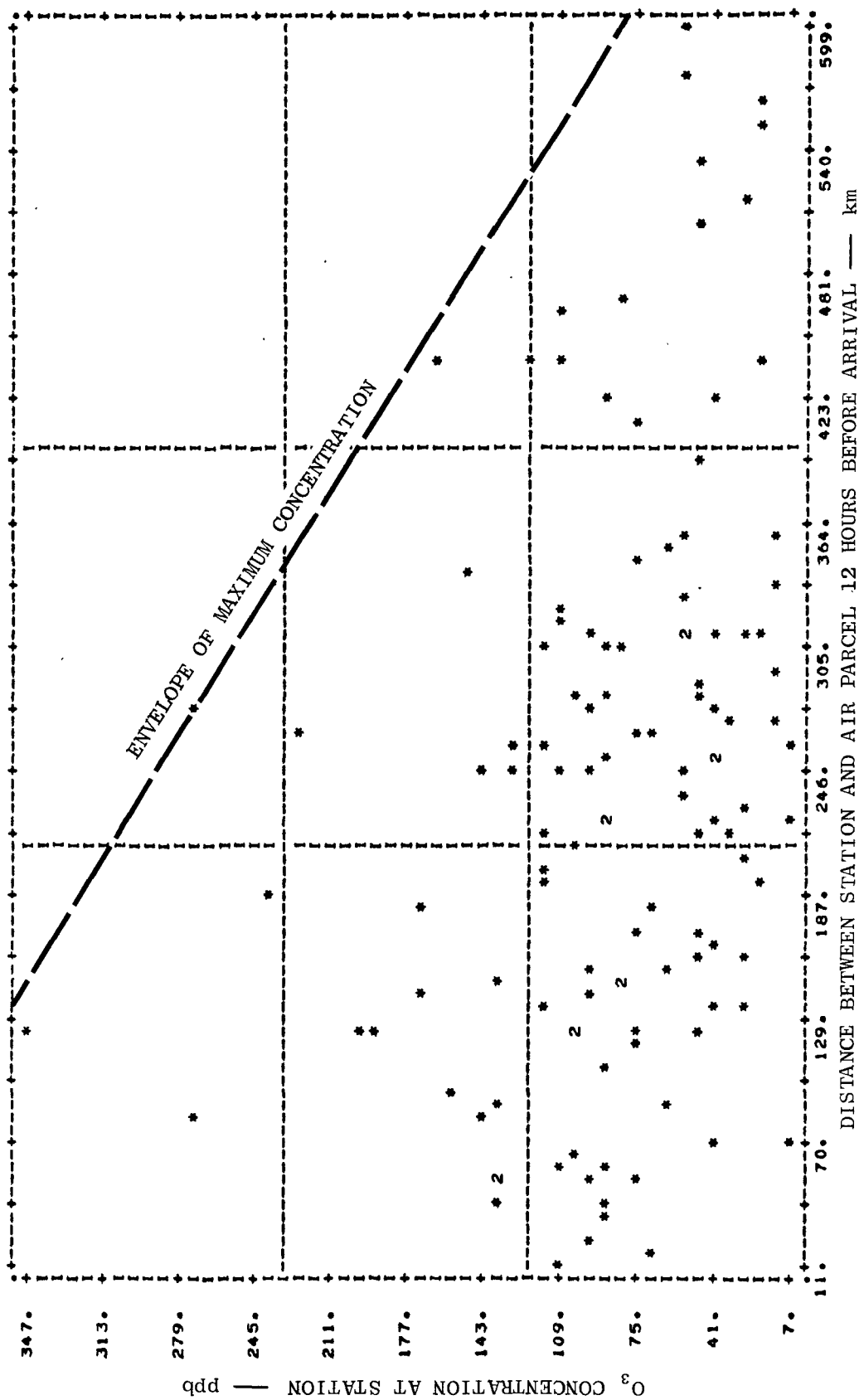
2.2.1.4.1. Background

The practical objective of this project was to determine relationships between ozone concentrations and anthropogenic emissions in the hope that such relationships will be useful for the formulation of control strategies. In the case of a secondary pollutant like ozone, this problem has two aspects. The first is identifying the controllable factors causing high ozone concentrations. The second is identifying the temporal and spatial relationships between the causative factors and the resulting ozone concentrations. Any control strategy will have to deal with the likely spatial relationships between pollutant sources and the areas impacted by the resulting ozone.

Thus far, only the relationships between ozone concentrations and the various indices have been discussed. The strongest ties have been observed to be with solar radiation and with temperature. These obviously are not controllable items. Based on the linear correlations, NO_x emissions during the last 12 hours of the trajectory and those between 24 and 36 hours before the end of the trajectory appear to be the most important factors. This section examines the distances and directions traveled by the air during the last 12 hours and during the last 36 hours of the trajectories. In some instances, the data are stratified into two categories: "high" ozone cases and "not high" ozone cases. As discussed earlier, and in Appendix A (Volume III), half the cases were selected from those days which had maximum-hour ozone concentrations among the highest 20% of the available data sample. These are the "high" cases. The remaining half of the cases, divided about equally between values in the lowest 20% and those within 10 percentile of the median of the maximum-hour concentrations, are the "not high" cases. To some extent the following statistical analyses simply quantify the distance/direction relationships that are qualitatively evident in Figures 33 through 42.

2.2.1.4.2. Travel Distances

Figure 51 is a scatter diagram of ozone concentration at the four rural sites (combined) versus the straight-line distance between the monitoring site and the location of the air 12 hours before the observation. Figure 52 is similar, but uses the 36-hour separation between the air parcel and the site. The figures indicate that the higher ozone concentrations occur more often with lower wind speeds and correspondingly shorter net travel distances. The dashed lines in Figures 51 and 52 are envelopes that might be used to estimate the maximum ozone concentrations at a rural location in an air mass that has come from the distance shown on the abscissa during the preceding 12 hours (Figure 51) or 36 hours (Figure 52). In about one half of the instances where the federal standard of 80 ppb was equaled or exceeded, the air was ap-



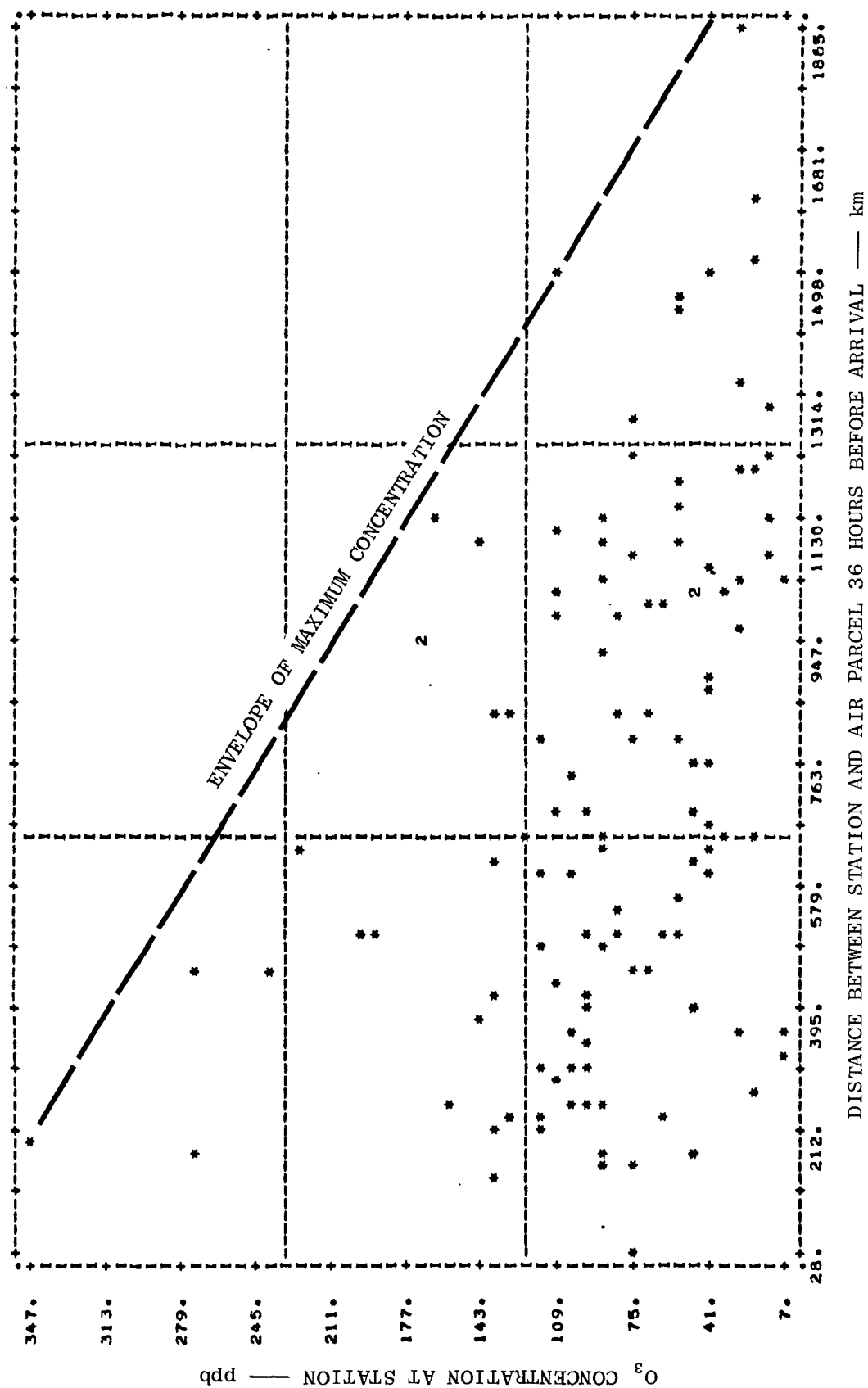


FIGURE 52 OZONE CONCENTRATION VERSUS THE DISTANCE TO THE AIR PARCEL POSITION 36 HOURS BEFORE MEASUREMENT

parently within about 180 km of the receptor, 12 hours earlier. Similarly, one half of the cases where the standard was violated involved air that had been within 500 km of the site 36 hours earlier.

The information shown in Figures 51 and 52 can be displayed in still another way. One can examine the frequency distributions of travel distance for the two different classes of data: "high" and "not high" ozone concentrations. Figure 53 shows the results of such analysis. As expected, the travel distances for the higher concentration cases tend to be less than those for the lower.

Analysis of the travel distances associated with the higher concentration can be useful in guiding the formulation of control strategies. The frequency distributions of travel distance, combined with the time span over which emissions are influential, roughly define the dimensions of the area within which controls should be applied.

2.2.1.4.3. Directional Effects

It is not sufficient to define only the travel distance between the ozone observation and the related emissions; the direction is also important. Figure 54 is a scatter diagram of ozone concentrations versus the direction from the observation site to the position of the air 12 hours before the observation. Figure 55 shows the scatter diagram for the air position 36 hours before the observation. The dashed lines in Figures 54 and 55 are estimated envelopes of the maximum ozone concentration that might be expected at a rural location in an air parcel that has traveled from the direction shown on the abscissa during the preceding 12 hours (Figure 54) or 36 hours (Figure 55). Note that for both time periods the highest ozone concentrations occur when the air arrives from directions southwest through northwest, and the lowest ozone values are brought in by air coming from the east through south.

Although Figures 54 and 55 show the extremely high ozone concentrations to be associated with arrivals from the northwest, more "high" ozone cases arrive from the southwest. When the flow directions are divided into four quadrants-- 0° to 89° , 90° to 179° , and so forth--the largest number of "high" ozone concentrations occurred when the air came from directions between 180° and 269° . For the "not high" cases, the most frequent directions were in the 270° to 359° quadrant. Figure 56 summarizes the findings of this analysis.

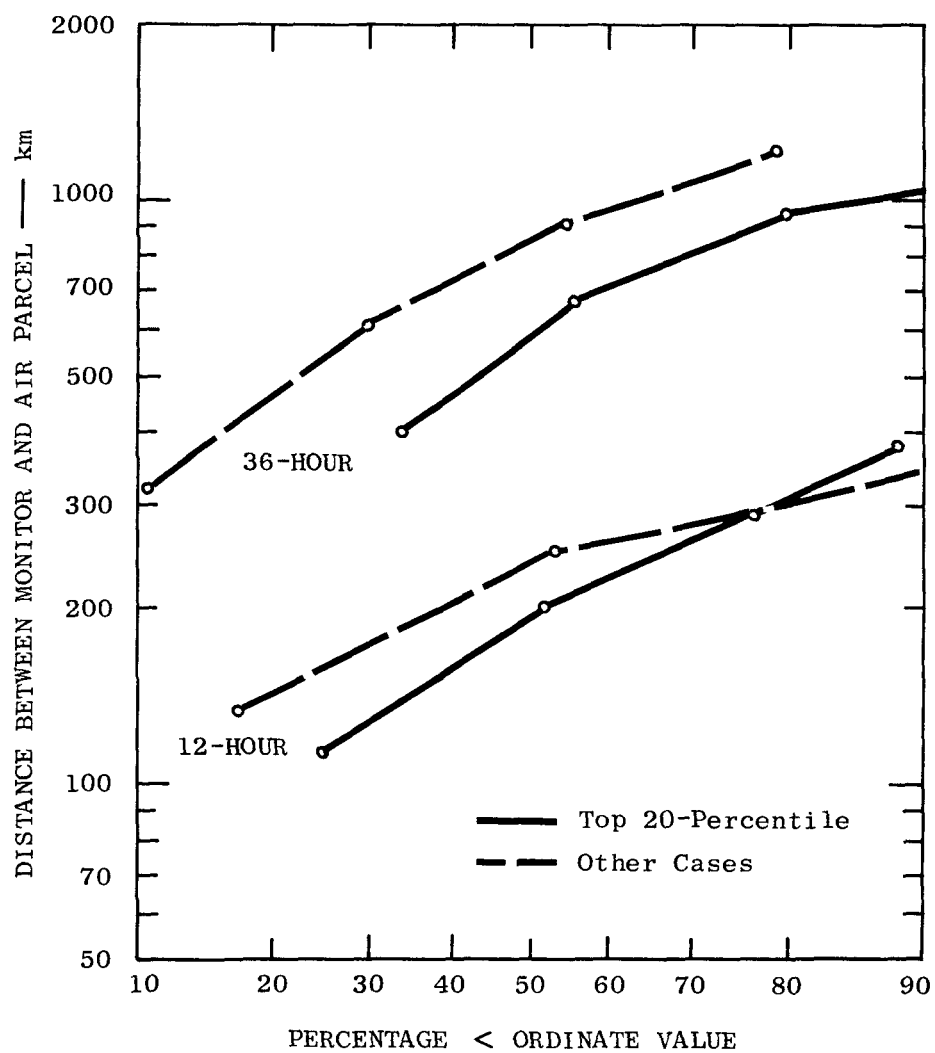


FIGURE 53 FREQUENCY DISTRIBUTIONS OF 12 AND 36 HOUR TRAVEL DISTANCES

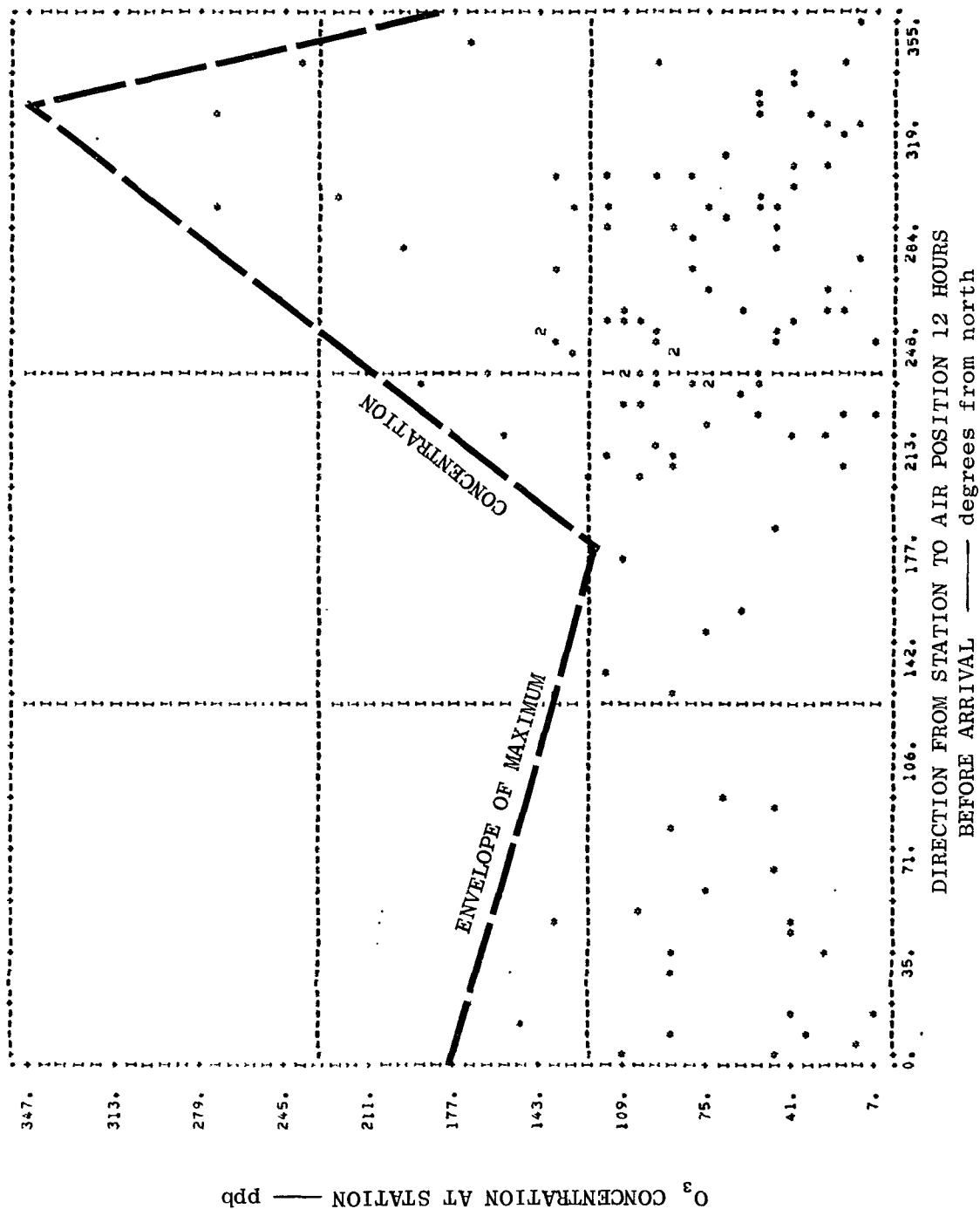


FIGURE 54 SCATTER DIAGRAM OF OZONE CONCENTRATION VERSUS THE DIRECTION
 TO THE AIR PARCEL POSITION 12 HOURS BEFORE MEASUREMENT

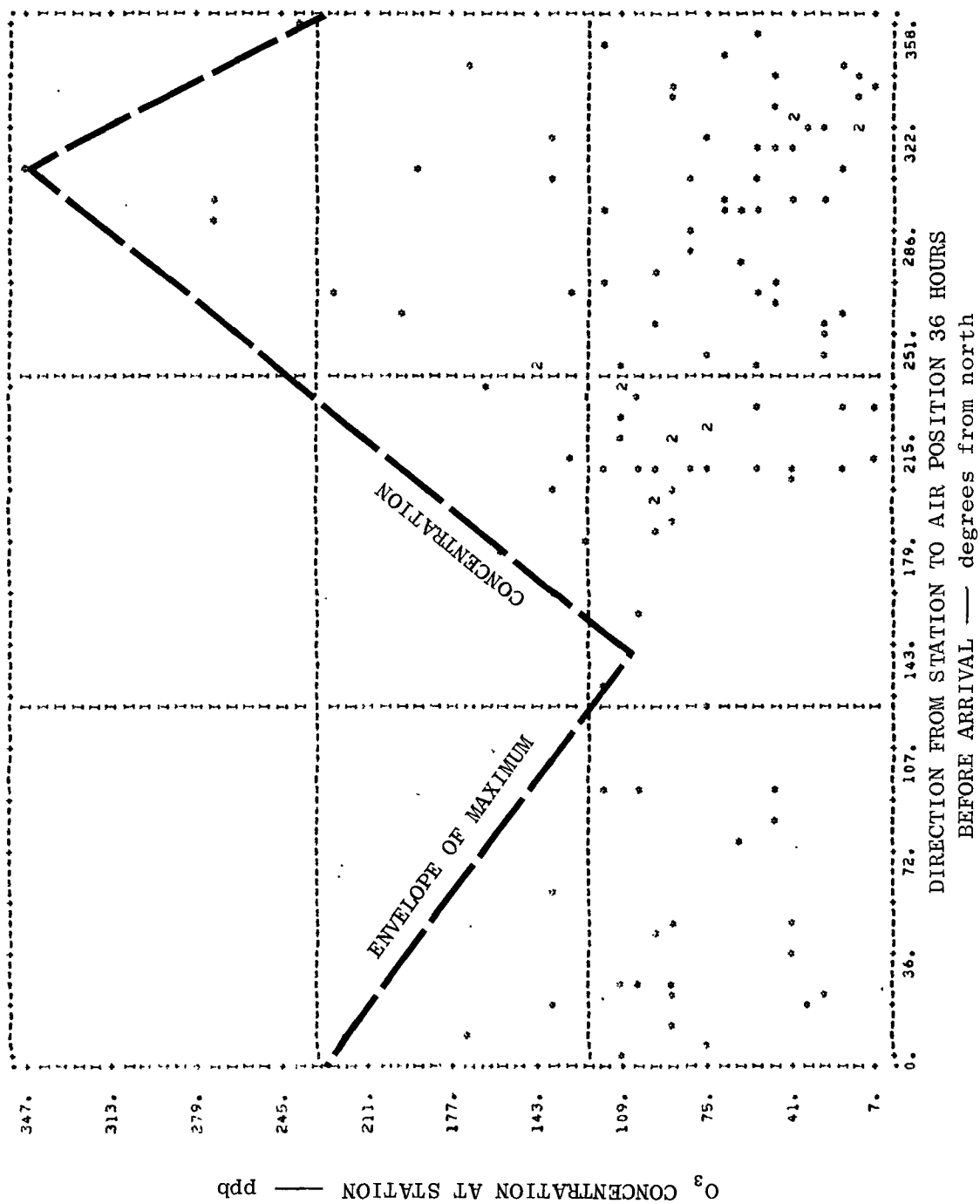


FIGURE 55 SCATTER DIAGRAM OF OZONE CONCENTRATION VERSUS THE DIRECTION TO THE AIR PARCEL POSITION 36 HOURS BEFORE MEASUREMENT

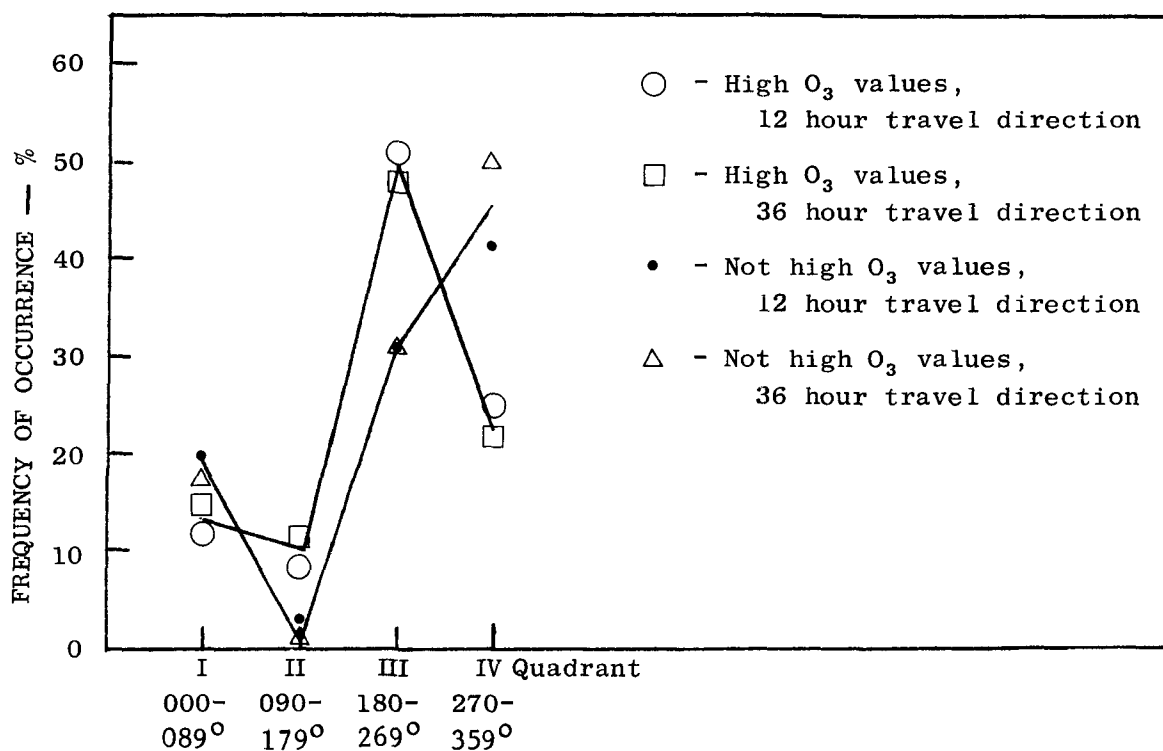


FIGURE 56 FREQUENCY DISTRIBUTION OF 'HIGH' OZONE AND 'NOT HIGH' OZONE TRAVEL DIRECTIONS (Combined data)

2.2.2. Studies of Synoptic-Scale Ozone Distributions and Weather Patterns

2.2.2.1. Large-scale Spatial Distributions of Ozone Concentration

2.2.2.1.1. Background

The daily peak-hour ozone concentration observed at SAROAD stations during 1974 were used as the basis for a set of isopleth maps of the peak-hour ozone concentrations over the eastern* United States for each day of the year. The locations of SAROAD sites measuring ozone during 1974 are shown in Figure 57.

* The states east of, or traversed by, 100 degrees W. meridian.

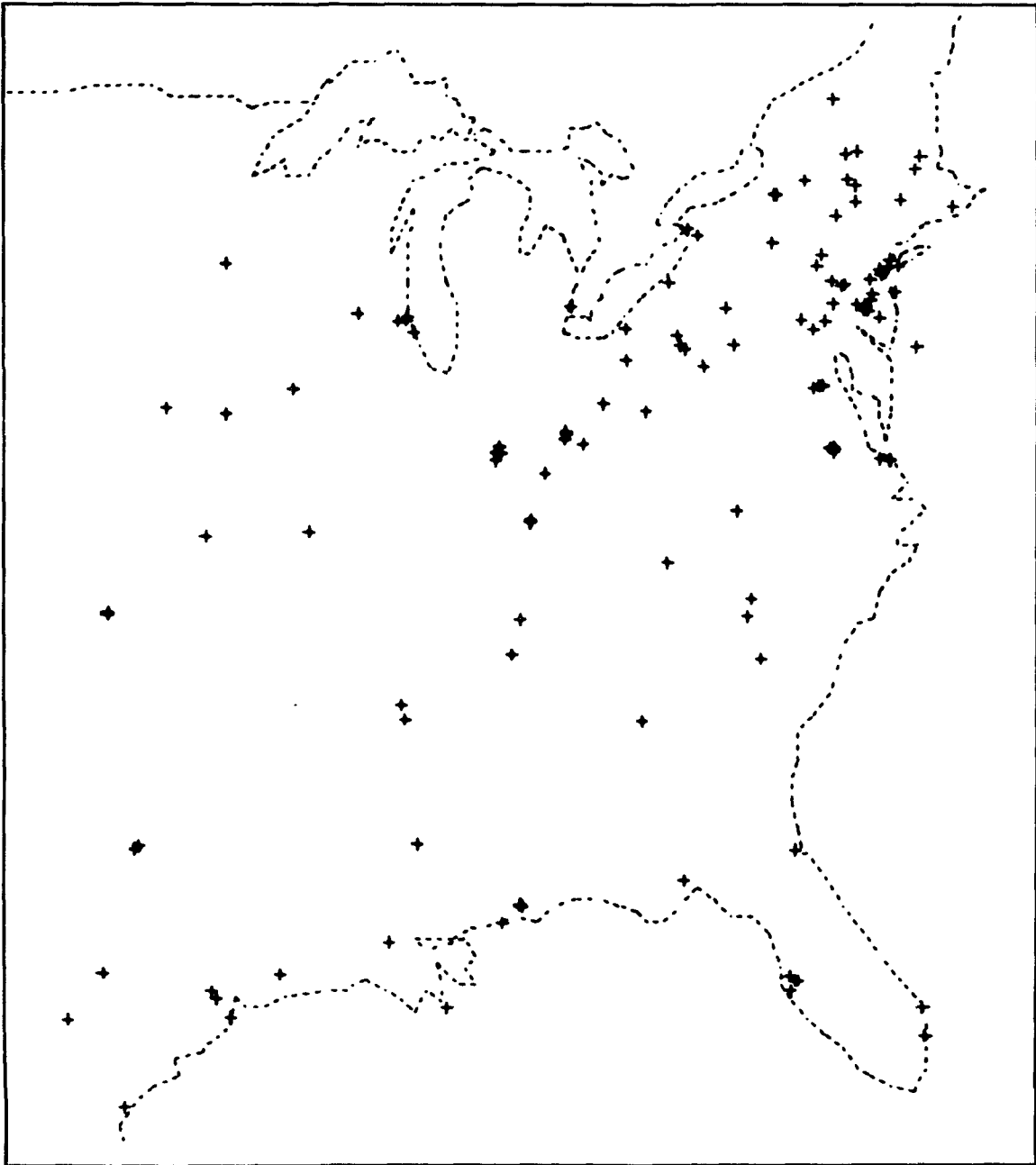


FIGURE 57 LOCATIONS OF SAROAD SITES IN THE EASTERN UNITED STATES
MEASURING OZONE DURING 1974

Some subjectivity was involved in the ozone isopleth analysis. In order to eliminate the worst of those cases where keypunch errors in the data cards had occurred, or where the decimal place indicator or the units were misreported, no values were used which were greater than 500 ppb during the summer or late spring months or greater than 300 ppb at other times. Occasionally some observations still appeared to be anomalously high relative to neighboring observations. In such cases a subjective decision was made whether to retain or discard the data, usually based on the hourly observations at the site before and after the observation in question. In one instance, data from a given site appeared anomalously high for a full 3-month period, and was discarded when the agency confirmed that they had experienced trouble with a newly installed data acquisition system during that time. Other than this instance, very few data were discarded.

Volume III of this report contains the isopleth analysis of maximum-hour ozone for each day of 1974. The ozone analyses are paired with the morning weather maps for each day. The objective in comparing these maps was to investigate geographical relationships between weather patterns and ozone concentration in the context of a defined geographical pattern of precursor emissions (NEDS data, discussed earlier).

Three approaches have been used to establish those relationships. The first of these approaches was the simplest. The ozone maps for each day were examined to see where and when violations of the federal oxidant standard occurred. Eight geographical regions of frequent ozone violations were identified. The number of incidents per month in each of these regions were counted. This provided a picture of seasonal and geographic variability. Those parts of weather systems most subject to ozone violations were also identified. The frequency of occurrence of the higher ozone concentrations in the different parts of the weather systems were determined. As might be expected, some meteorological conditions are much more conducive to widespread ozone violations than others.

The second approach to the analysis of the ozone and weather patterns was more formal (and less successful). Pressure patterns and ozone patterns were classified objectively using the technique proposed by Lund (1963). Briefly, each of 134 days during 1974 on which ozone violations were widespread in the eastern United States was characterized by a set of 20 pressures read from the daily weather map at regularly spaced points in the eastern United States. The correlations between the twenty pressures for each day and those at the same twenty points on each of the other days were calculated. The daily pressure pattern that correlated with the most other daily patterns at the 0.7 significance level or greater was considered to be the prototype for the most important group of pressure patterns. In theory, a second prototype can then be similarly chosen from among those daily pressure patterns that are not in the first group. The classification can continue so long as there are a significant number of cases in a class. The ozone patterns can be similarly classified. The coincidences of weather and ozone patterns was to be studied but, as is discussed later, this was not possible because there were not enough distinct types of ozone or pressure pattern found in the data set.

Table 10

FREQUENCY OF OCCURRENCE OF DAYS WHEN THE FEDERAL OXIDANT
STANDARDS WERE VIOLATED IN THE EASTERN UNITED STATES

Month	No. of Days with $O_3 \geq 80$ ppb in the Eastern U.S. (1974)
January	2
February	4
March	10
April	21
May	30
June	30
July	31
August	31
September	21
October	25
November	7
December	3

In the third approach, some of the trajectory analyses discussed in the preceding section were used in the interpretation of the ozone isopleth analyses. The trajectories were used in a qualitative way to illustrate the recent history of the air in the high ozone areas.

2.2.2.1.2. Frequency of Occurrence of Ozone Concentrations Above the Federal Standard

The first step in the analysis of synoptic ozone patterns was to determine how frequently ozone levels exceeded the federal standards in one of more parts of the eastern United States. The maps were examined and the days with values of 80 ppb or greater were counted. Table 10 shows the results of this analysis. As expected, the table shows that violations of the standard were an everyday occurrence somewhere in the eastern United States during the warm summer months and were quite infrequent during the winter.

2.2.2.1.3. Areas of Most Frequent Ozone Standard Violations During 1974

A preliminary comparison of the daily map series suggested that areas of high ozone concentrations were most frequently found in the following regions:

- Florida peninsula
- Texas-Louisiana Gulf coast
- New York-New England
- Western portions of Oklahoma, Kansas, and Nebraska
- Southeast of Lakes Erie and Ontario
- Washington-Philadelphia
- South or southwest of Lake Michigan
- St. Louis and Ohio River Valley

Figures 58 through 62 show examples of high ozone concentrations occurring in the listed areas. Figure 63 shows the counties with the highest NO_x emissions densities in the United States. The average NO_x emissions in the blackened counties exceeds 75 tons mi⁻² yr⁻¹. There are only 134 such counties in the entire U.S. Of course, many of these same counties are also among the highest in hydrocarbon emissions. Figure 63 shows that, with the exception of the western Oklahoma-Kansas-Nebraska area and perhaps the Florida peninsula, the areas of the most frequent high ozone concentration also contain regions of major emissions. This simple comparison shows that the expected relationship between anthropogenic emissions and high ozone concentrations is subjectively identifiable in the data.

Table 11 summarizes the number of days per month that the federal oxidant standard was violated in each of the listed areas during 1974. In most of the various areas the annual trends parallel those of the country as a whole. As might be expected, the warmer, more southerly locales have occurrences of ozone concentration greater than 80 ppb in the early spring and late fall more often than do most of the more northerly areas. Surprisingly, New England also has rather frequent violations of the standard in these seasons, as do the western parts of Oklahoma, Kansas, and Nebraska. The violations in the remaining areas are limited almost completely to July and August.

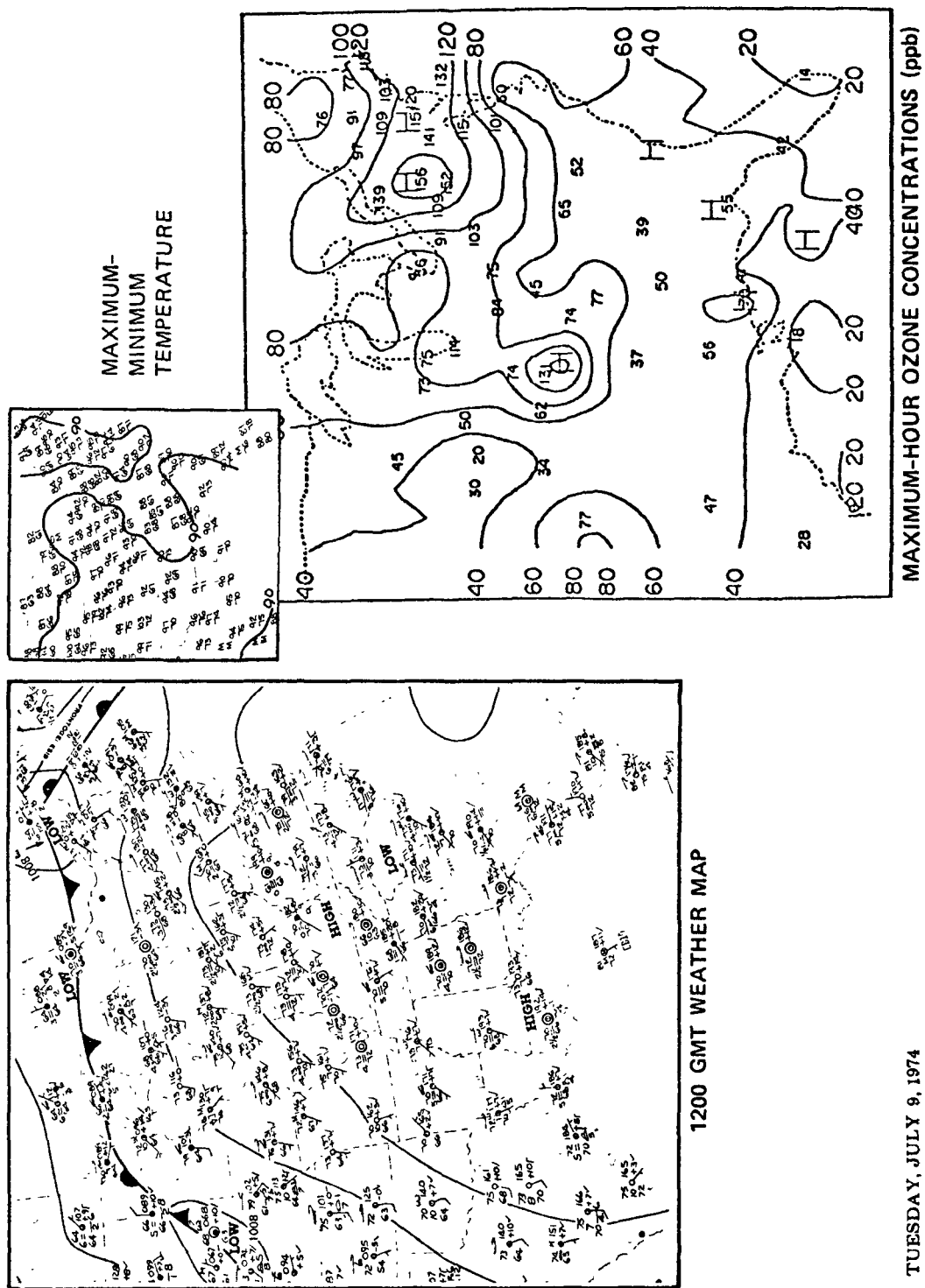


FIGURE 58 EXAMPLE OF HIGH OZONE CONCENTRATIONS SOUTHEAST OF LAKES ERIE AND ONTARIO AND IN THE ST. LOUIS-OHIO RIVER VALLEY

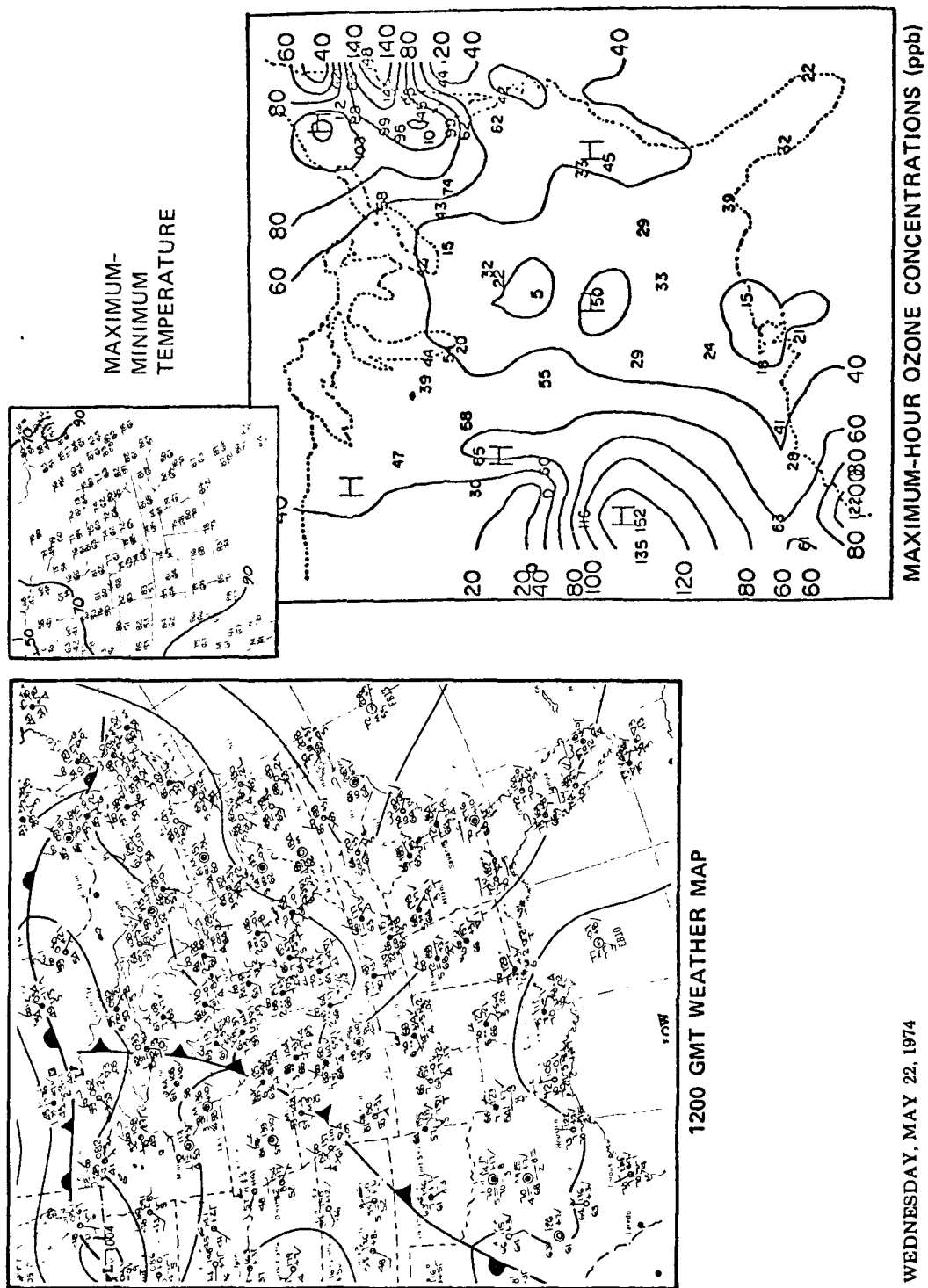
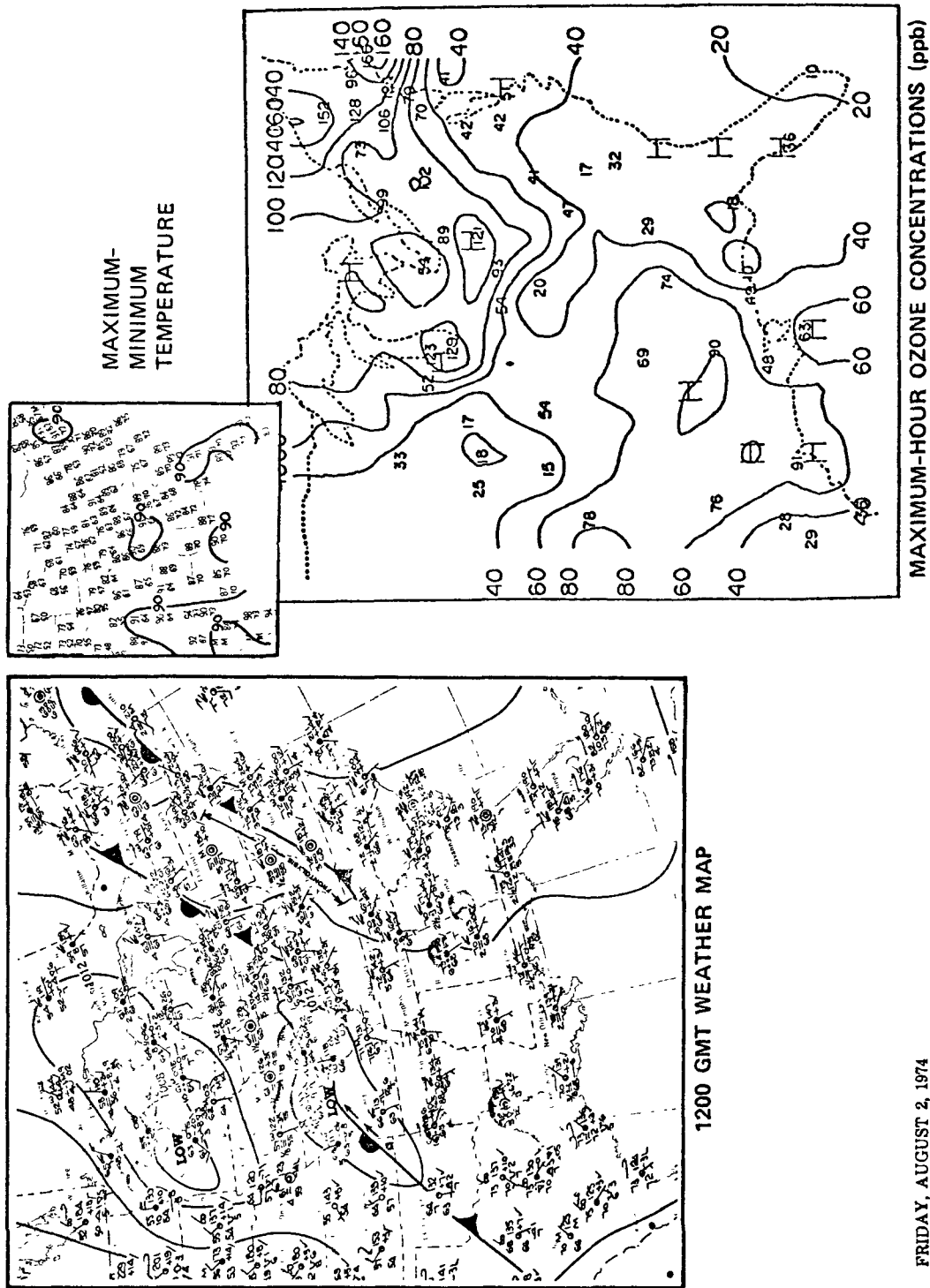
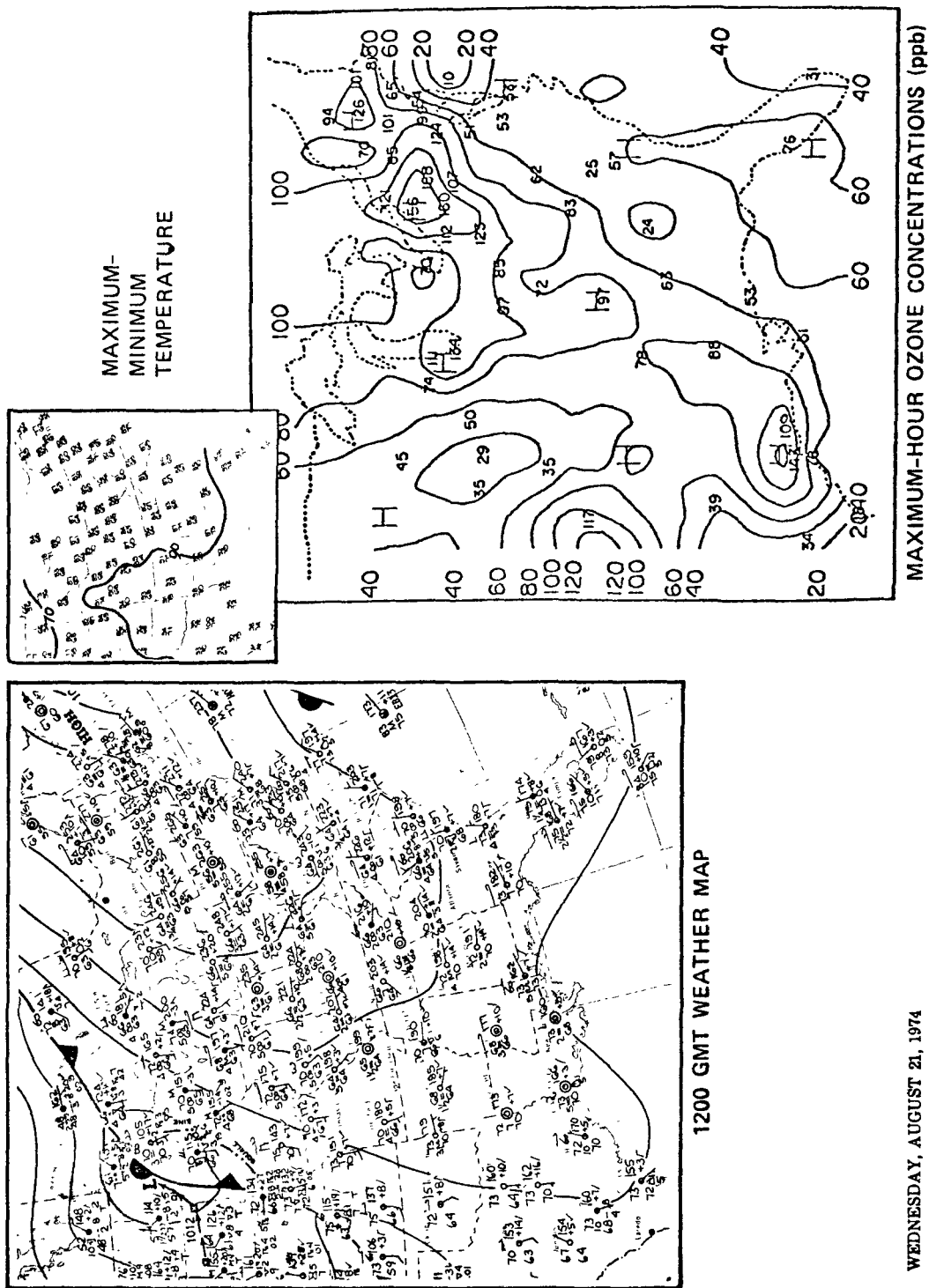


FIGURE 59 EXAMPLE OF HIGH OZONE CONCENTRATIONS IN WESTERN KANSAS AND THE NEW YORK-NEW ENGLAND AREA



FRIDAY, AUGUST 2, 1974

FIGURE 60 EXAMPLE OF HIGH OZONE CONCENTRATIONS SOUTH OF LAKE MICHIGAN AND IN THE NEW ENGLAND AREA



WEDNESDAY, AUGUST 21, 1974

FIGURE 61 EXAMPLE OF HIGH OZONE CONCENTRATIONS SOUTHEAST OF LAKES ERIE AND ONTARIO AND ALONG THE TEXAS-LOUISIANA GULF COAST

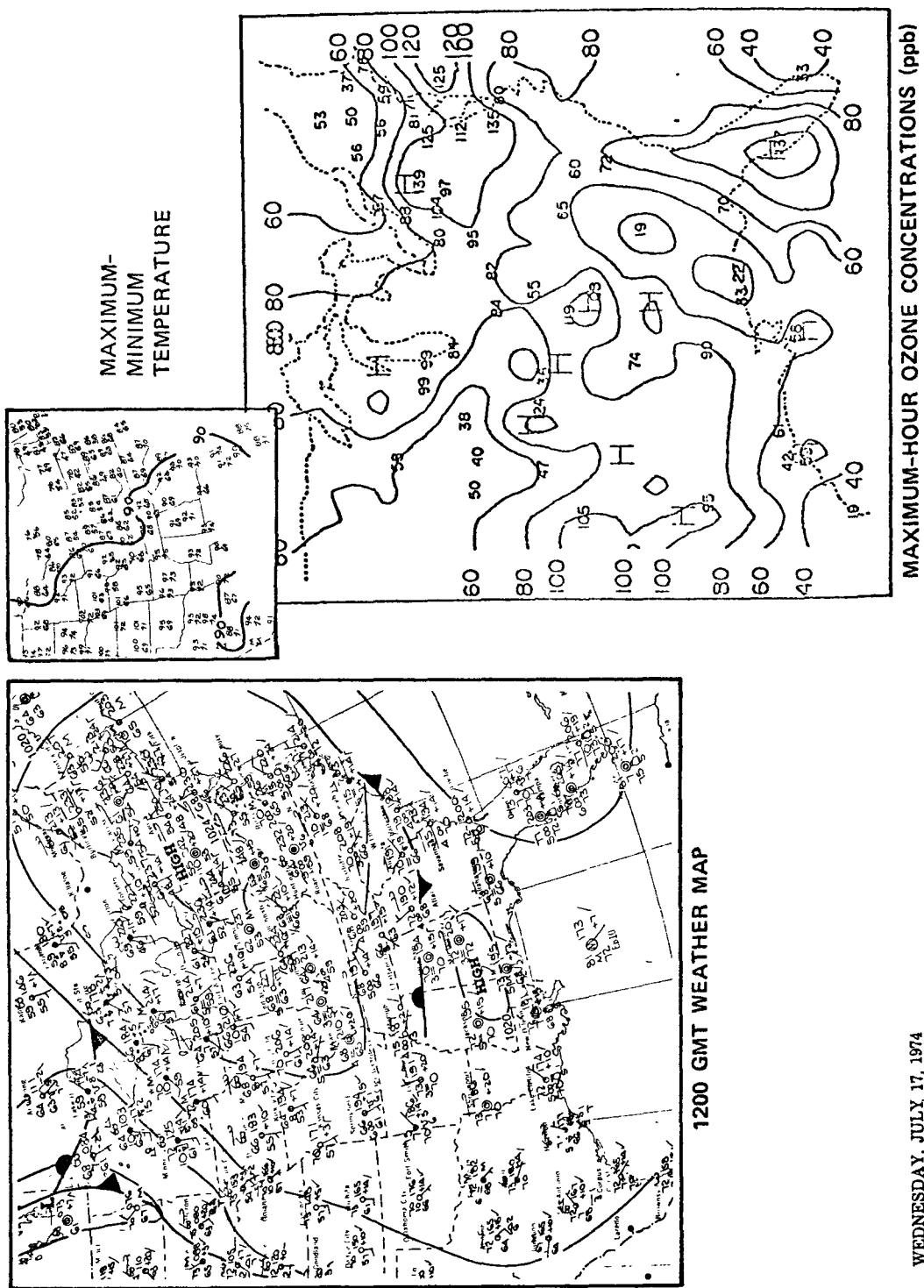


FIGURE 62 EXAMPLE OF HIGH OZONE CONCENTRATIONS IN WESTERN KANSAS, THE FLORIDA PENINSULA, AND THE WASHINGTON-PHILADELPHIA CORRIDOR

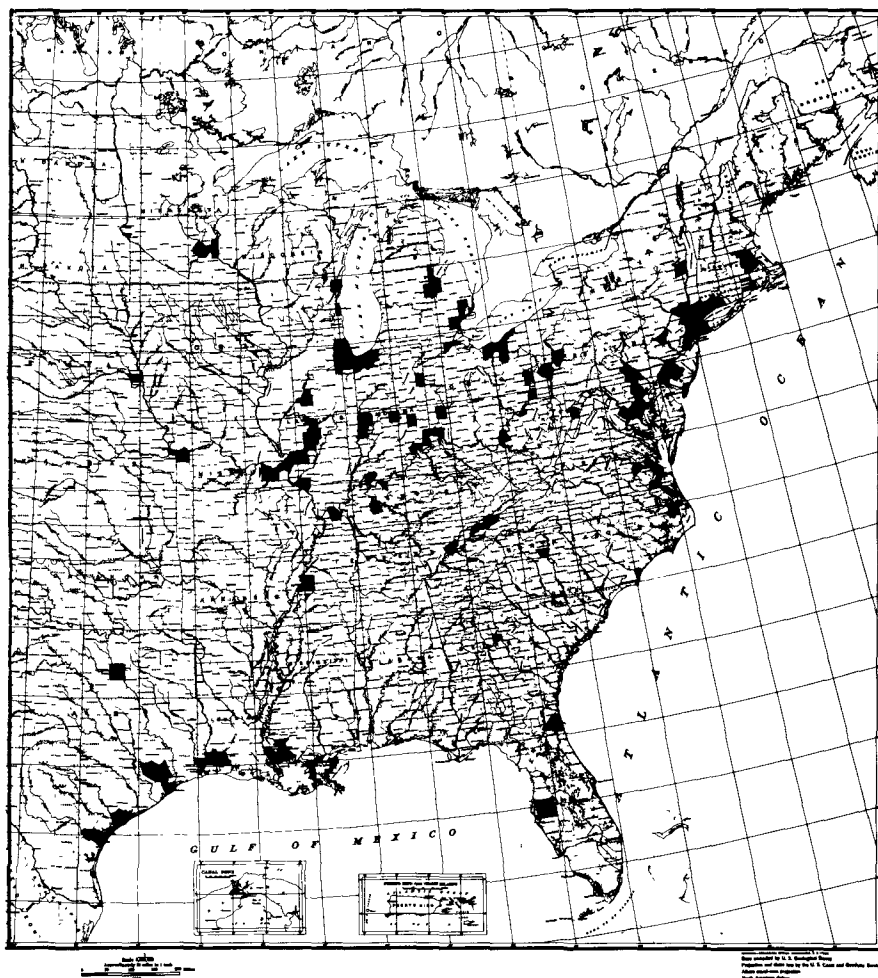


FIGURE 63 COUNTIES WITH AVERAGE ANNUAL NO_x EMISSIONS
GREATER THAN $75 \text{ t mi}^{-2} \text{ yr}^{-1}$

It should be noted that, although the data in the Kansas area sometimes appear out of place, they are not consistently higher or lower than other surrounding values. Discussions with personnel of the Wichita-Sedgwick County Department of Community Health, the agency responsible for the measurements, provided no reason to discard the data. It is interesting that the high concentrations are found rather frequently during seasons other than the photochemically active summer season. Also, the area is relatively free of major anthropogenic sources of precursor emissions. These facts suggest that an important natural source mechanism may be operative. Earlier in the study, this area was seen to have relatively high radioactive fallout, and hence stratospheric ozone at ground level (Figures 30-32). Of course, the concentrations discussed presently are much higher than those to be inferred from the fallout data or to be otherwise derived from the stratospheric portion of this study. Thus, no explanation can be offered at this time for the cause of these high ozone values.

Table 11

NUMBER OF CASES FOR EACH MONTH WITH DAILY MAXIMUM OZONE > 80 ppb
IN SPECIFIED REGIONS OF THE EASTERN UNITED STATES

	January	February	March	April	May	June	July	August	September	October	November	December
Florida Peninsula	0	0	5	3	8	10	9	3	1	2	0	0
Texas-Louisiana Gulf Coast	0	2	5	5	8	13	15	11	4	10	2	1
New England	2	0	0	6	10	18	9	18	13	1	0	0
Western Oklahoma, Kansas, Nebraska	0	0	3	8	22	20	22	20	12	15	1	0
SE of Lakes Erie & Ontario	0	0	0	0	2	2	20	21	2	0	0	0
Washington-Philadelphia Corridor	0	0	0	2	3	1	15	7	3	5	2	0
S or SW Shores of Lake Michigan	0	0	0	0	1	2	10	9	2	0	0	0
St. Louis and Ohio River Valley	0	0	0	0	3	3	22	13	5	0	2	0
Other Areas	0	2	1	5	0	2	6	6	5	5	0	2

2.2.2.2. Relation Between Ozone Distributions and Weather Features

2.2.2.2.1. Winds Associated with High Ozone Concentrations

Table 12 was prepared in order to determine whether there were differences from region to region in the relation of wind speed and wind direction to the frequency of high-ozone events. The table shows that very light winds are important to the occurrence of high ozone concentrations in several regions. This result is consistent with the findings of the trajectory study, which showed shorter travel distances (corresponding to lower wind speeds) to be associated with higher ozone concentrations.

Table 12

WINDS REPORTED ON MORNING WEATHER MAP IN AREAS
WHERE PEAK-HOUR OZONE EXCEEDED 80 ppb DURING THE DAY
(Number of days from June through August)

Region	Surface Winds				
	Calm	≥ 2 m/s			
		N to E	E to S	S to W	W to N
Florida Peninsula	11	5	4	2	0
Texas-Louisiana Gulf Coast	17	10	0	7	1
New York-New England	3	4	7	26	2
Western Oklahoma, Kansas, Nebraska	1	7	13	36	11
SE of Lakes Erie and Ontario	20	1	10	6	1
Washington-Phil- adelphia Corridor	9	5	7	7	4
S or SW shore of Lake Michigan	7	0	5	6	1
Ohio River Valley & Surroundings	21	2	1	7	0

Two regimes are evident from the table, that is, those for which the high ozone appears to have resulted from nearby precursor emissions and those for which the ozone (and/or its precursors) appears to have been transported by the wind. Most of the situations in the New York-New England area and in the western Oklahoma-Kansas-Nebraska area appear to fall into the latter regime. Most of the situations in the St. Louis-Ohio River Valley area fall into the former regime. Both regimes are evident at the other locales. These observations are qualitatively consistent with the geographic distribution of precursor emissions. Also in agreement with the distribution of emissions -- for the transport

cases -- is the relation between the occurrence of high ozone concentrations and the wind direction. This is especially evident (Table 12) for the New York-New England area, where the S-W direction indicates that the air tends to come from a direction along the east coast urban corridor on high ozone days. This deduction has been confirmed by Cleveland et al. (1975) and Ludwig and Shelar (1977) in more detailed studies of this part of the country.

2.2.2.2.2. Weather Patterns Associated with High Ozone Concentrations

Earlier sections addressed the meteorological conditions that might be expected most often in conjunction with high ozone concentrations. According to the trajectory analyses and the stratospheric intrusion studies, the following types of meteorological situations are likely to be significantly associated with the occurrence of ozone concentrations in excess of the federal standard:

1. Warm air ahead of a cold front
2. Warm sector of a frontal wave
3. Western side of an anticyclone (high pressure area)
4. Other parts of an anticyclone
5. Region behind a vigorous cold front, especially during cyclogenesis
6. Squall lines

The first three of these meteorological situations are related to the observed tendency for high ozone concentration to occur with warm temperatures and southwesterly winds. Item 4 is a meteorological situation likely to be characterized by light winds and abundant sunshine. The final two situations are associated with stratospheric intrusion. Table 13 summarizes the number of times per month during 1974 that ozone concentrations in excess of 80 ppb were associated with these meteorological situations. The table shows that the six specified situations account for a substantial majority of the incidents of high ozone. It should be noted that the meteorological situations thought to be associated with ozone transport downward from the stratosphere are involved in many fewer cases than are those associated with the horizontal transport of ozone and/or its precursors.

2.2.2.2.3. Attempts at Objective Comparisons between Weather and Ozone Patterns

A scheme for the objective comparison of ozone patterns and pressure patterns was described earlier (Section 2.2.2.1.1). Unfortunately,

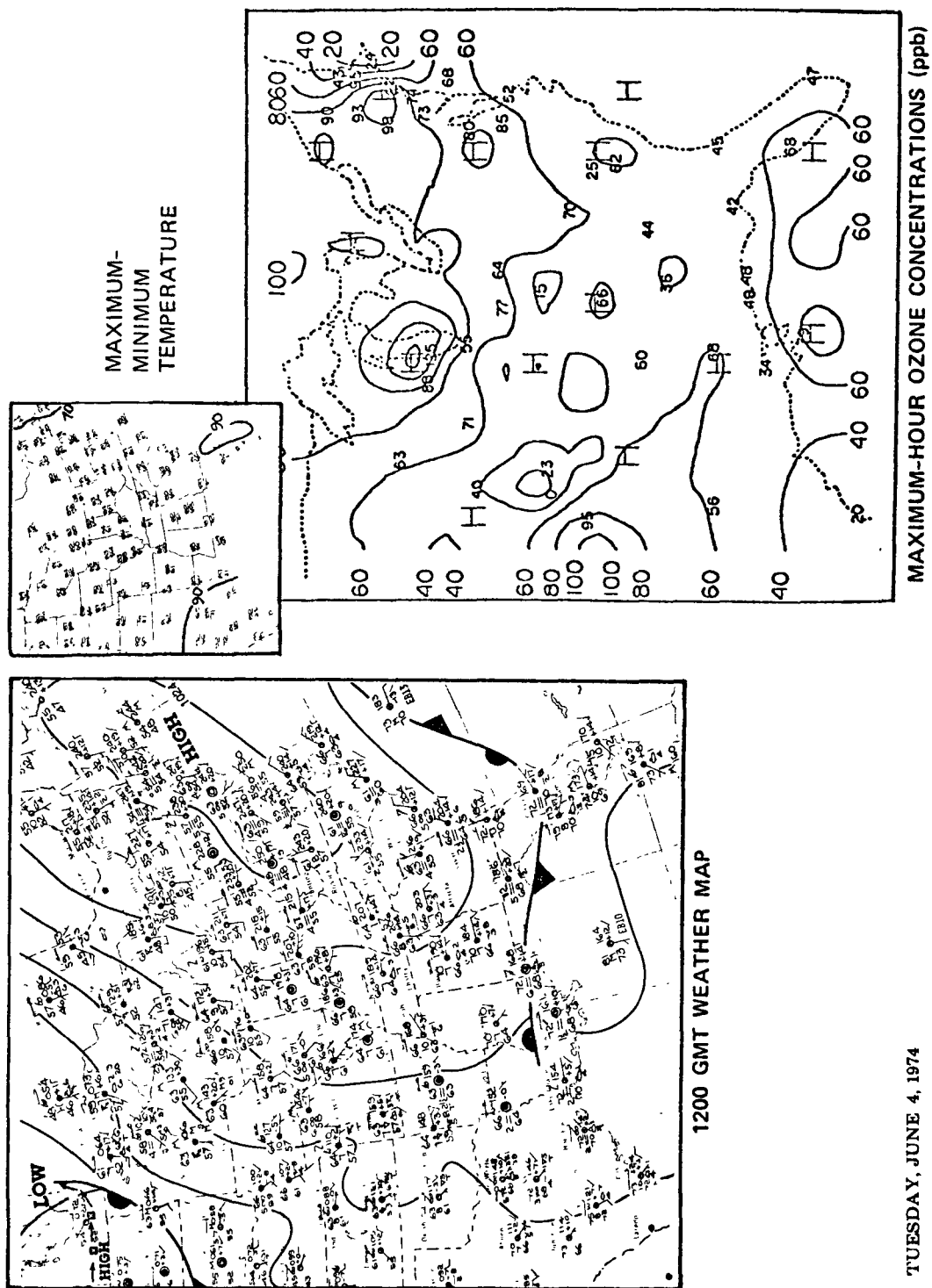
only 42 of the 134 daily pressure patterns could be classified into the same category, and only eighteen of the ozone patterns fell in a single category. There was virtually no correspondence between the two groups. Thus, it was not possible to associate certain ozone patterns with certain pressure patterns.

The prototype day for the one pressure pattern category was June 4, 1974. It is shown in Figure 64 along with the ozone pattern for the same day. The prototype ozone pattern occurred on 2 October 1974. It is shown in Figure 65, with the weather map for the same day. The prototype pressure pattern shows that the frequently recurring weather pattern in this sample involved a high pressure cell near the northeast coast, with air flow from the Gulf of Mexico up into the Midwest. The most frequently recurring ozone pattern (Figure 65) had high concentrations in the southwest and the eastern parts of the Gulf, with flat gradients and lower concentrations prevailing over much of the rest of the eastern United States.

Table 13
METEOROLOGICAL FEATURES ASSOCIATED WITH
HIGH OZONE CONCENTRATIONS

(Number of Cases per Month, 1974)

	January	February	March	April	May	June	July	August	September	October	November	December
Warm Air Mass near Front	1	0	6	5	15	8	19	23	9	8	2	0
Warm Sector of Frontal Wave	0	1	1	0	4	4	8	4	2	2	1	0
West Side of Anticyclone	0	1	2	12	11	22	35	30	18	14	0	2
Center or East of Anticyclone	0	2	2	4	14	15	44	20	11	10	2	1
Squall Line	0	0	0	0	1	1	0	0	0	0	0	0
Behind Strong Cold Front	1	0	2	2	1	6	7	10	0	2	2	0
Other	0	0	1	6	10	15	15	21	7	2	0	0



TUESDAY, JUNE 4, 1974

FIGURE 64 PROTOTYPE PRESSURE PATTERN AND THE OZONE PATTERN FOR THE SAME DAY

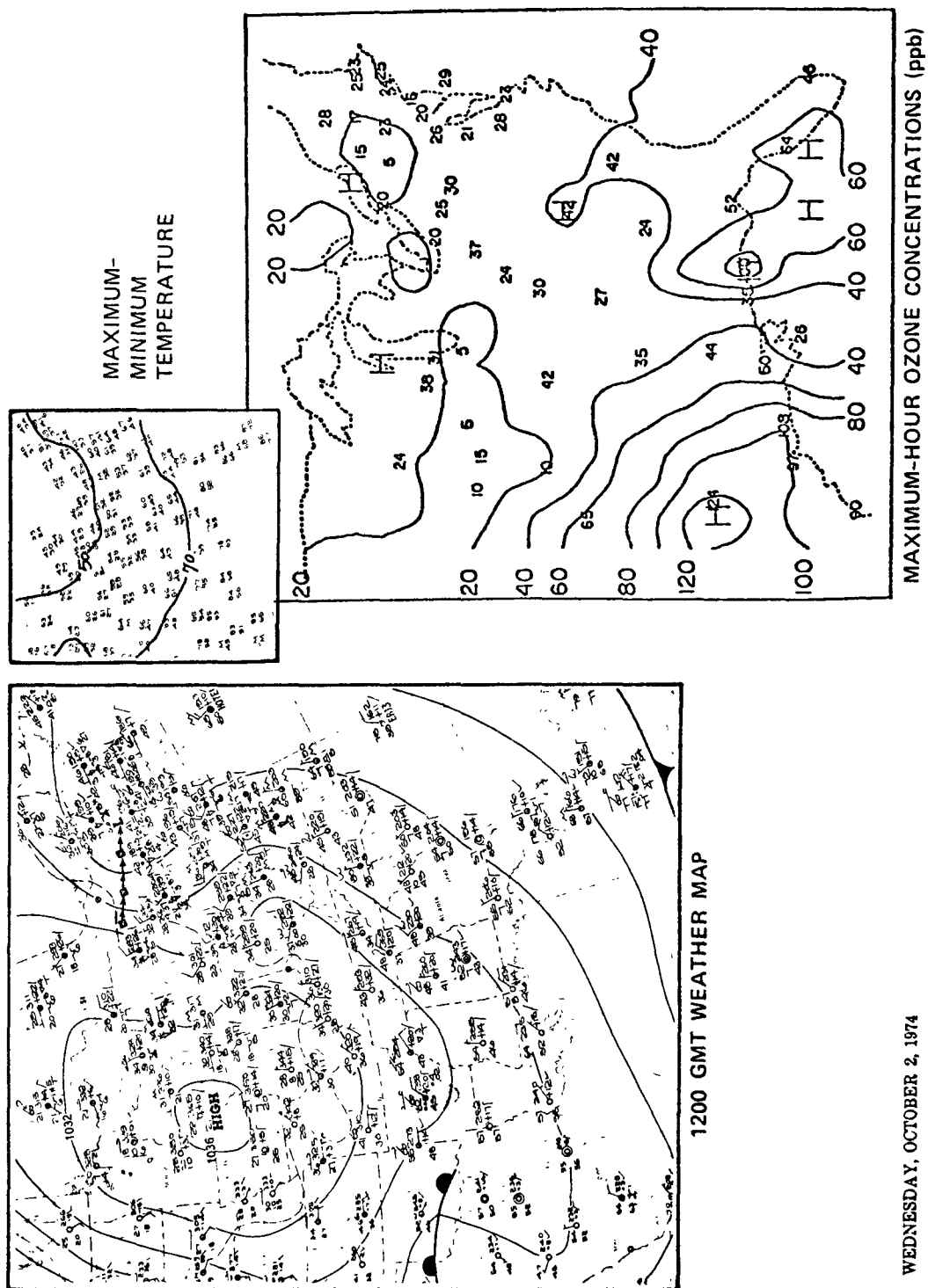


FIGURE 65 PROTOTYPE OZONE PATTERN AND THE WEATHER MAP FOR THE SAME DAY

Table 14 lists the days classified as having pressure and ozone patterns similar to the prototypes. The only day common to both lists is May 28. It should be noted that because of the nature of the correlation coefficient, the features within each group show considerable variation in intensity. The classification system tends to emphasize the relative positions of high and low features rather than their relative intensities.

The lack of repetitious patterns does not necessarily mean that ozone is uncorrelated with atmospheric pressure. The correlations between the 20 pairs of pressure readings and ozone concentrations were determined for each of the 134 days. Table 15 shows the results of this analyses. (The 20 points are shown in Figure 66.)

Table 14
DATES CLASSIFIED AS HAVING PRESSURE
AND OZONE PATTERNS SIMILAR TO THE PROTOTYPES

Dates with Pressure Patterns Similar to that of June 4, 1974		Dates with Ozone Patterns Similar to that of October 2, 1974
April 27	July 17	January 30
April 28	July 18	May 6
May 8	July 24	May 7
May 11	July 25	May 12
May 14	July 26	May 26
May 16	August 7	May 27
May 21	August 12	May 28
May 28	August 15	June 16
June 3	August 16	June 27
June 5	August 19	July 22
June 6	August 20	July 23
June 7	August 21	September 20
June 13	August 25	October 3
June 14	August 26	October 9
June 18	September 10	October 19
June 19	September 11	October 20
June 28	September 26	October 26
June 29	September 27	
July 2	October 11	
July 6		
July 7		
July 13		

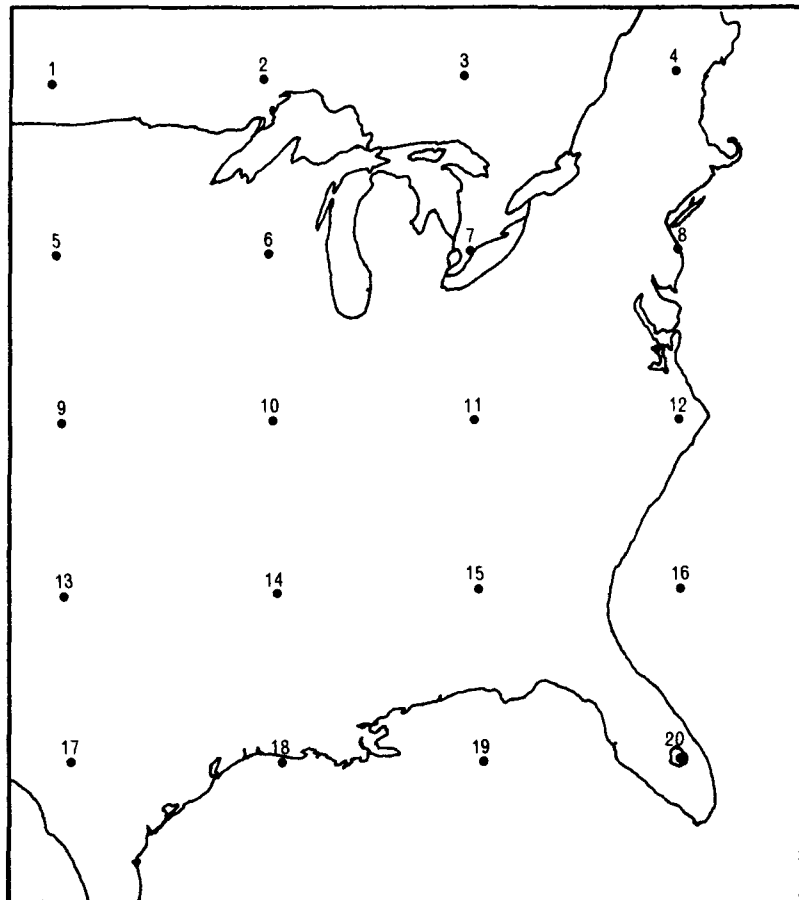


FIGURE 66 LOCATIONS OF GRID POINTS USED FOR CLASSIFYING OZONE AND PRESSURE PATTERNS AND FOR PRESSURE-OZONE CORRELATIONS

Table 15

FREQUENCY OF CORRELATION VALUES BETWEEN PRESSURE AND OZONE
AT 20 POINTS IN THE EASTERN UNITED STATES

Correlation	-0.999 to -0.3	-0.299 to -0.1	-0.099 to 0.099	0.01 to 0.299	0.3 to 0.599	≤0.6
No. of Cases	16	31	44	26	16	1

At first it may seem surprising that the correlations are not greater since it is generally noted that high ozone concentrations are frequently associated with high pressure cells. Indeed, if high-pressure cells were the only favorable location for high ozone concentrations, then the correlations should generally be high. However, as has been noted already, there are several other types of weather situation that are also associated with high ozone concentrations. One of these is the warm air just ahead of a front or in a frontal wave. In general, these are regions of relatively low pressures, clearly such instances contribute to negative correlations between pressure and ozone concentration. There are even frequent instances when high ozone concentrations are found in association with both high and low pressure areas on the same day. Figure 67 shows an example of this that occurred on 21 July. One area of high ozone is in the warm sector of the frontal wave, near the low pressure center that is situated over the Minnesota-South Dakota border. Another high ozone area is in the high-pressure ridge over the Texas Gulf coast. It is not surprising that the correlation between pressures and ozone concentrations at the twenty grid points was -0.2 on this day.

The highest correlation in the set of 134 cases occurred on 28 April (Figure 68). Surprisingly, this is a case dominated by a high ozone area ahead of a cold front. The high correlation of 0.64 is the result of the fact that over the area, (eastern U.S. as whole, both pressure and ozone generally increase as one moves from the northwest toward the southeast (except over the southeastern United States itself, where both gradients are rather flat).

The highest negative correlation in the sample, -0.5, was for 20 September. The ozone and weather maps for this date are shown in Figure 69. A front is seen stretching diagonally from southwest to northeast across the eastern United States. This front is situated in a low-pressure trough between two high pressure cells. A ridge of high ozone concentrations is seen to be just ahead of the frontal trough. This coincidence of high ozone values and lower pressures accounts for much of the negative correlation.

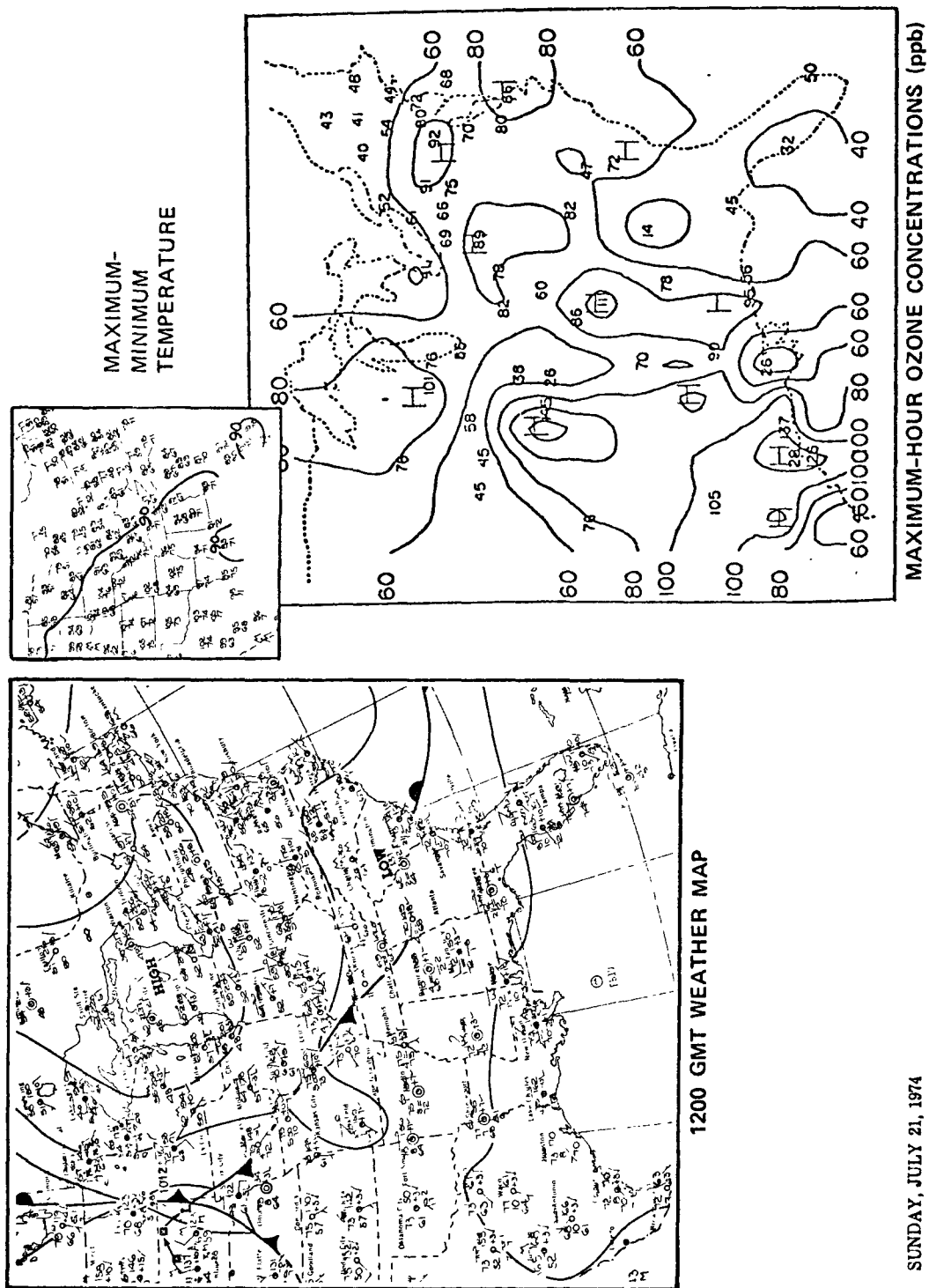
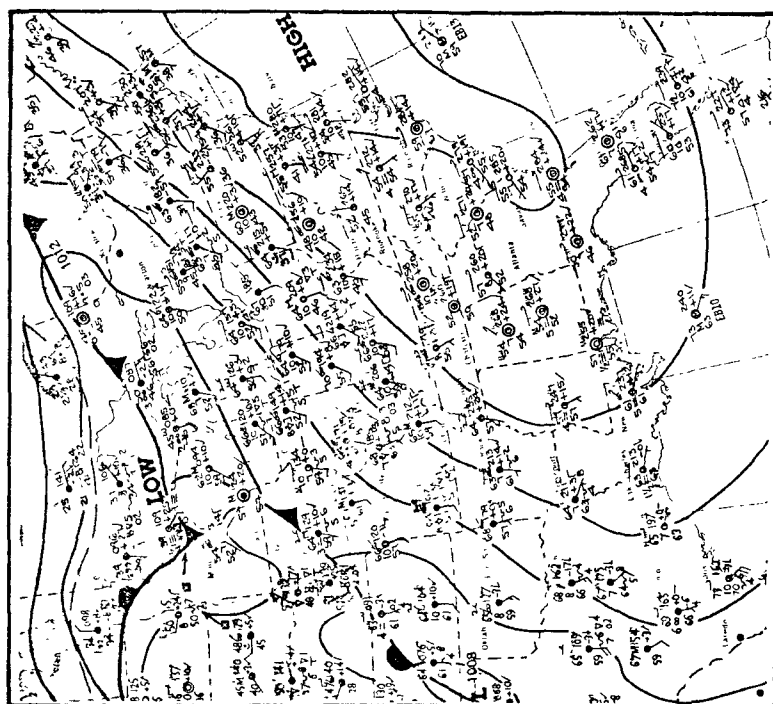
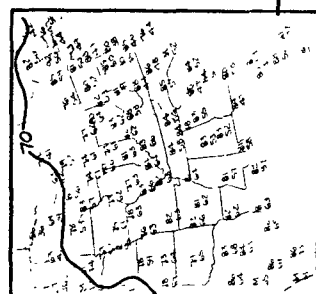


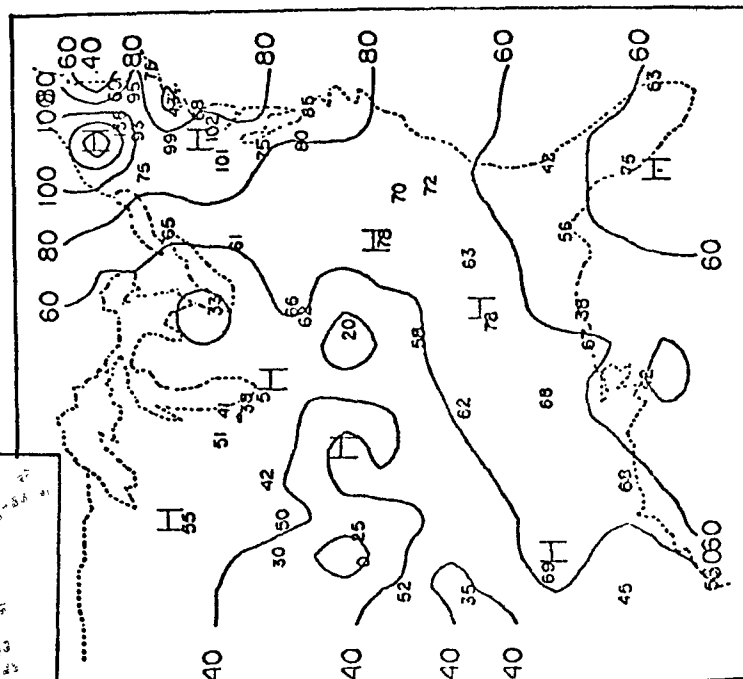
FIGURE 67 WEATHER MAP AND OZONE DISTRIBUTION FOR SUNDAY, 21 JULY 1974



1200 GMT WEATHER MAP



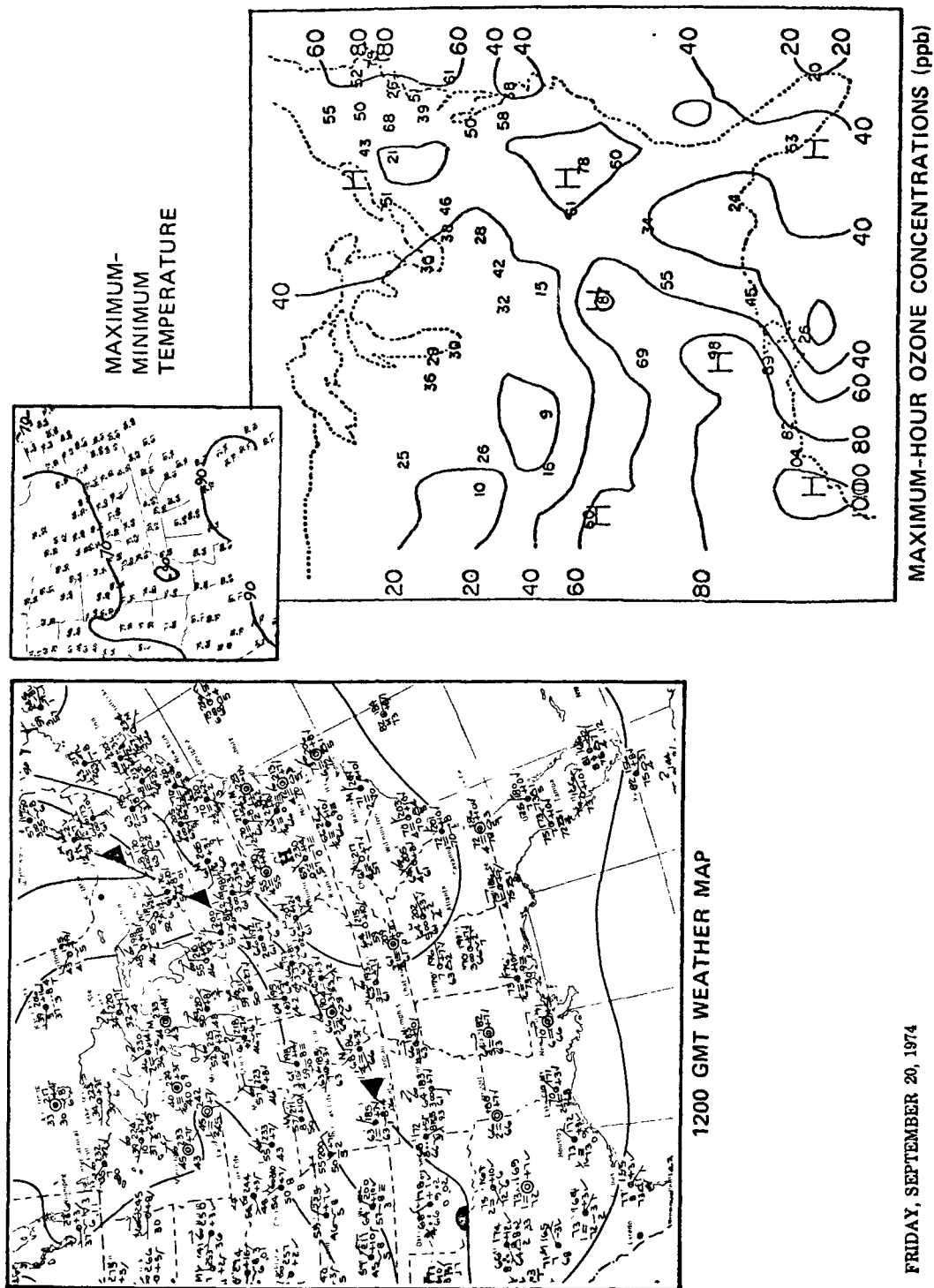
MAXIMUM-
MINIMUM
TEMPERATURE



MAXIMUM-HOUR OZONE CONCENTRATIONS (ppb)

SUNDAY, APRIL 28, 1974

FIGURE 68 WEATHER MAP AND OZONE DISTRIBUTION FOR SUNDAY, 28 APRIL, 1974



FRIDAY, SEPTEMBER 20, 1974

FIGURE 69 WEATHER MAP AND OZONE DISTRIBUTION FOR FRIDAY, 20 SEPTEMBER, 1974

Singh, Ludwig and Johnson (1977) have examined the day-to-day variations in pressure and ozone concentration at several remote monitoring sites in the west. They found that the temporal variations (at fixed sites) of these two parameters, like their spatial variations discussed above, are not closely related. Figure 70 shows an example of this for the site at McCrae, Montana. In this figure, daily pressure values, obtained by interpolation from the daily weather maps are plotted on the same graphs as peak-hour and daily average ozone values. As can be seen, the fluctuations in ozone values from day-to-day do not follow the pressure changes with any consistency.

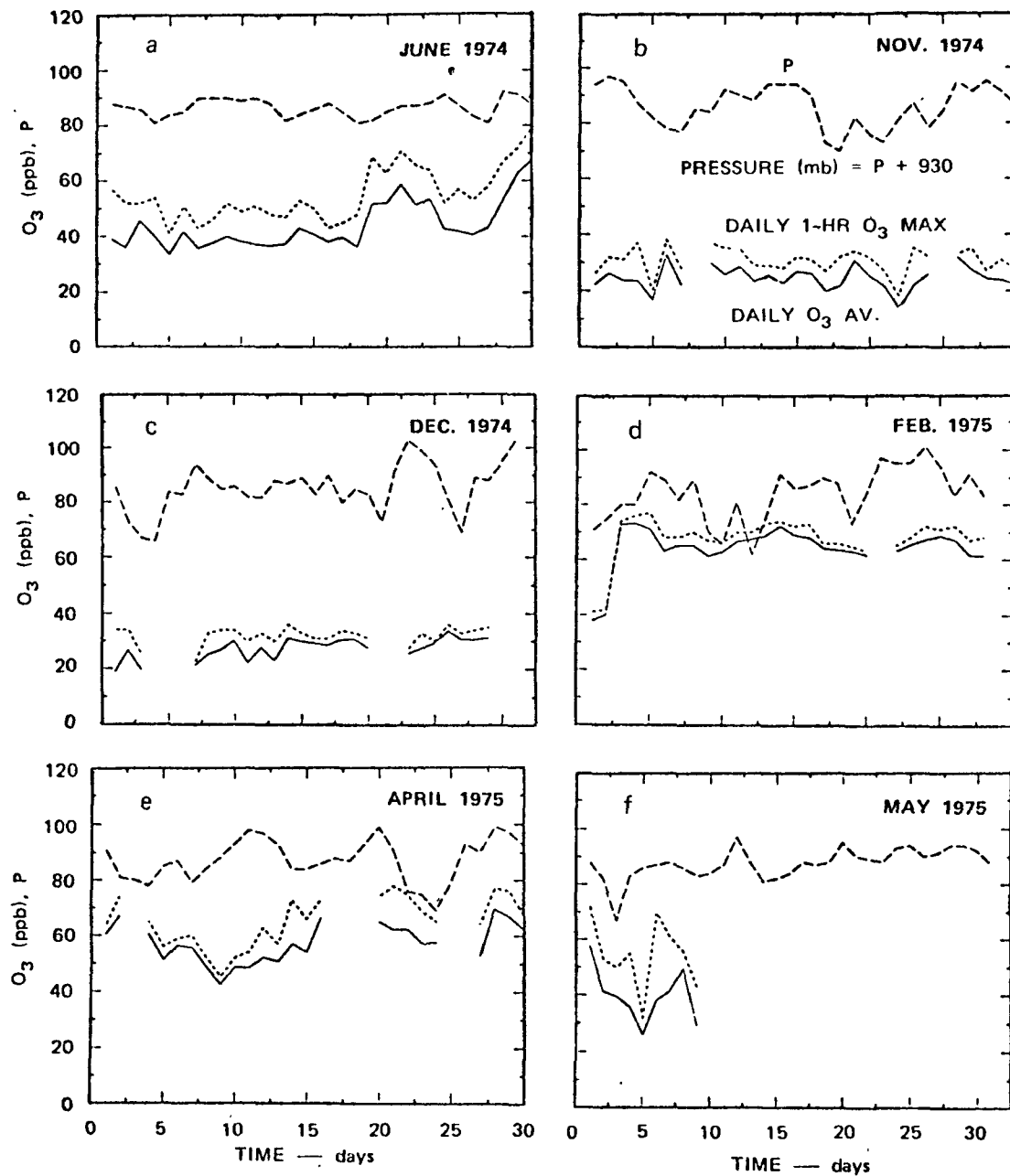
2.2.3. Combining the Trajectory Approach with Synoptic-Scale Comparison

The trajectory studies indicated that there are preferred air motions associated with ozone concentrations in the highest 20 percentile at the various stations. While some directions may be favored over others, it is obvious from the trajectories (Figures 35 through 42) that there is virtually no uniformity. However, some general observations about the air motions can be made from an examination of the figures. Probably the most generally applicable of these is that the higher ozone concentrations are almost always associated with trajectories of clockwise curvature. Such motions are often associated with air flow in the vicinity of high pressure centers. Subsidence and clear skies (hence, abundant sunshine) are generally associated with such flow.

Cases were chosen for study from among those days for which high ozone (top 20 percentile) trajectories were constructed for two or more of the four sites. The trajectories were superimposed on the weather and ozone maps so that their relationships with both the weather patterns and the ozone distributions could be seen more clearly (Figures 71 through 81). The trajectories represent 60 hours of travel, except where they extend outside the area covered by the map.

Such depictions for 7 and 8 July, 1974 are shown in Figures 71 and 72. A large high pressure cell dominates the eastern U.S. on both of these days. The trajectories ending at Wooster, Ohio, and McHenry, Maryland, show that the winds in this anticyclone had been quite light. On 7 July, the air arriving at Wooster had spent 2 1/2 days meandering across central Ohio from Cincinnati, accumulating emissions along the way. The air arriving at McHenry traveled somewhat farther. On this same day (7 July), the air arriving at Yellowstone Lake, Wisconsin, had traveled a clockwise loop from central Illinois. A center of high ozone is seen northeast of Yellowstone Lake. If the air arriving at this center had traveled a path parallel to the Yellowstone Lake trajectory. It would have left the Chicago area 2-1/2 days before.

On 8 July the trajectories ending at McHenry and Wooster were similar to those for the day before, indicating continued stagnation in the region. The results of this stagnation, and the concomitant accumulation of pollutants, is evident in the widespread high ozone concentrations. In general, the additional day of accumulation caused even higher ozone concentrations throughout most of the midwest.



Source: Singh, Ludwig and Johnson, 1977

FIGURE 70 OZONE-PRESSURE RELATIONSHIPS AT McRAE, MONTANA

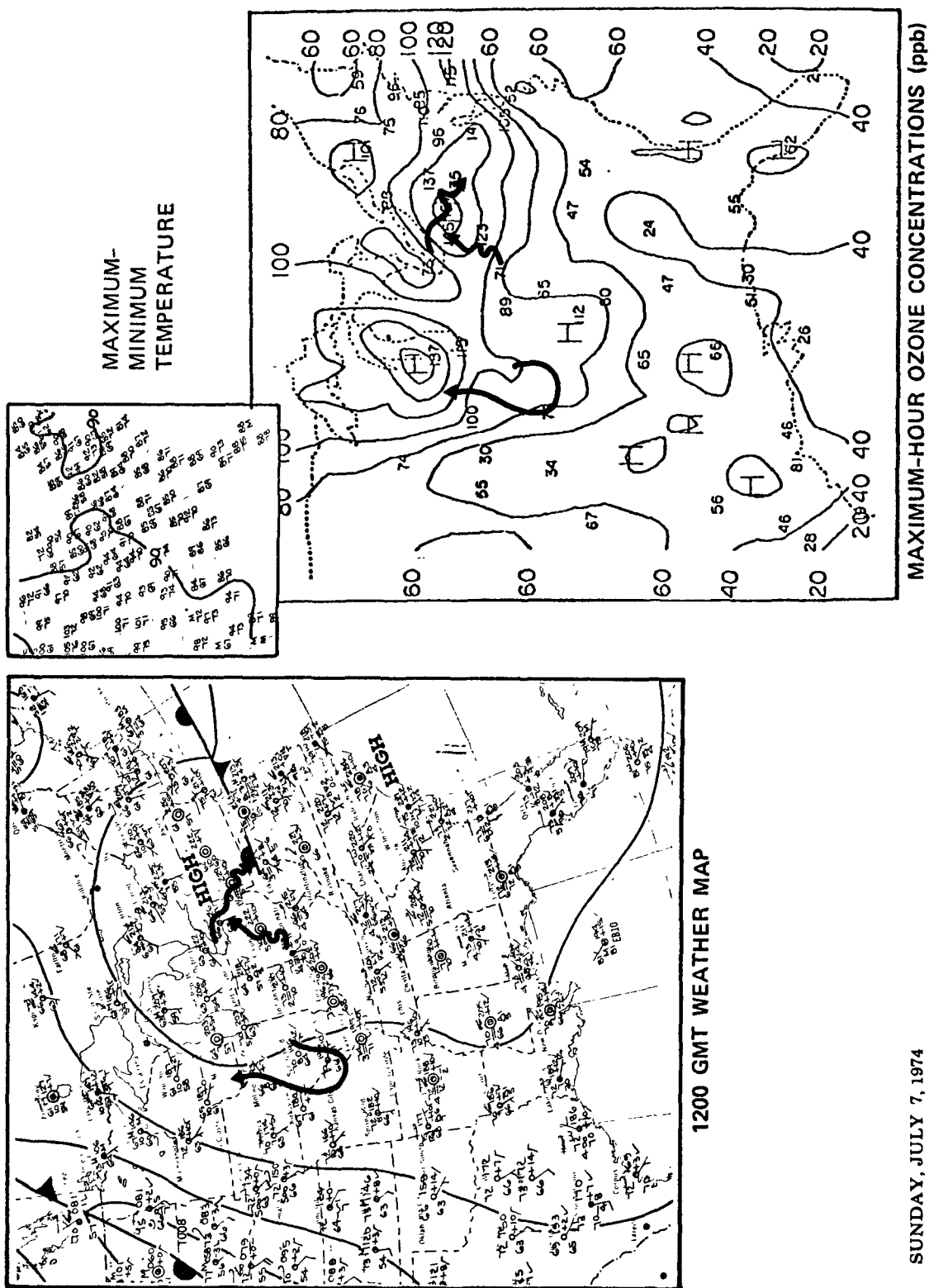
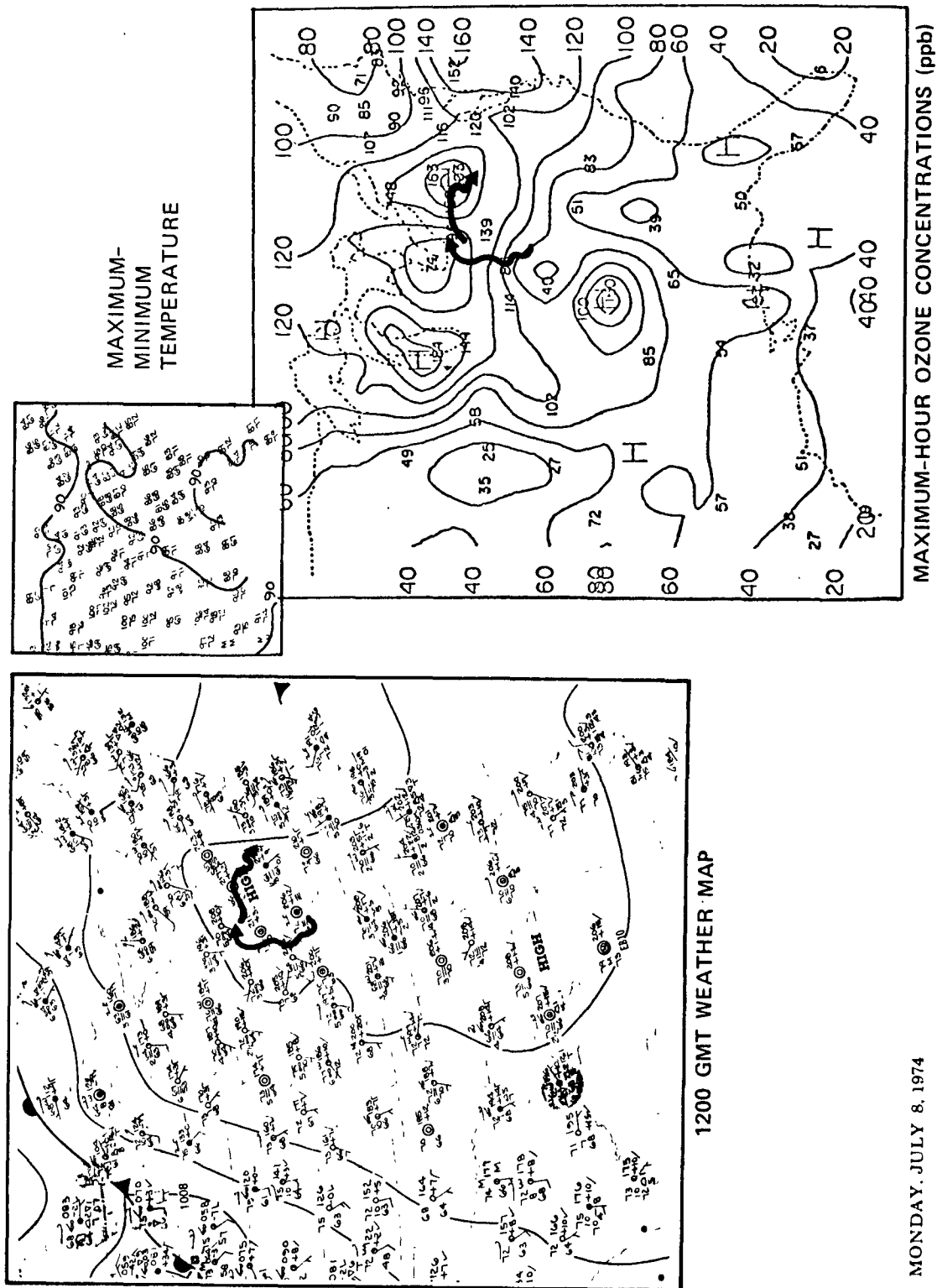


FIGURE 71 WEATHER MAP, OZONE DISTRIBUTION AND TRAJECTORIES FOR 7 JULY 1974.



MONDAY, JULY 8, 1974

FIGURE 72 WEATHER MAP, OZONE DISTRIBUTION AND TRAJECTORIES FOR 8 JULY 1974.

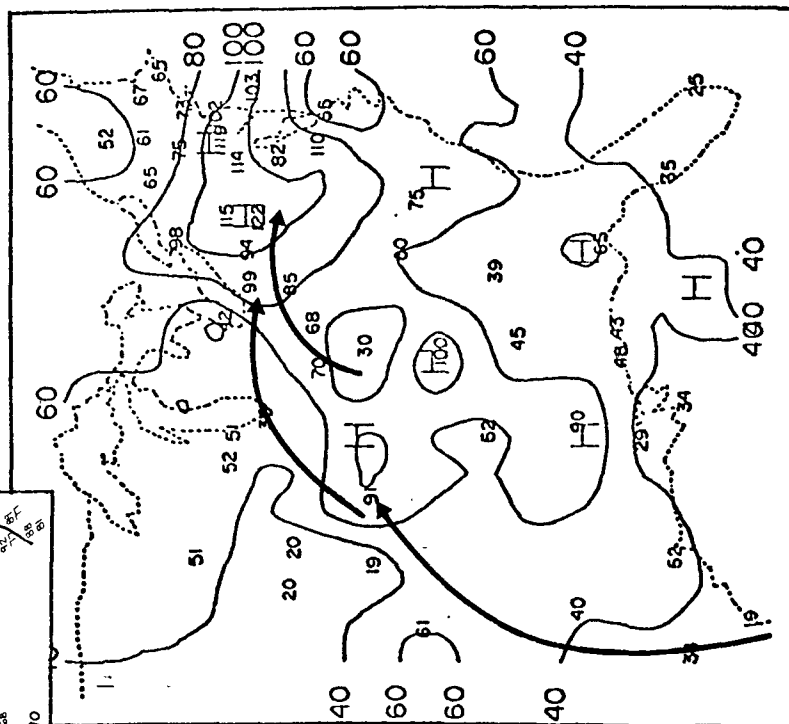
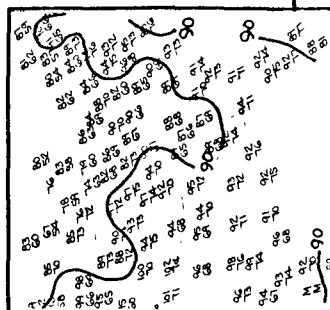
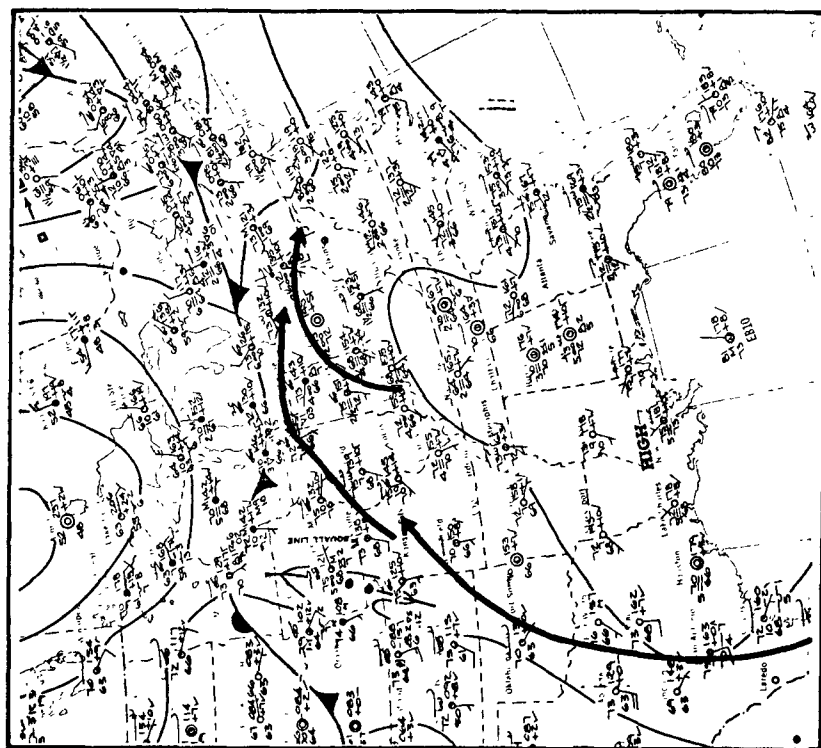
Figures 73 through 77 depict the period 10 July through 14 July 1974. The high pressure area that led to the stagnation seen in the July 7-8 cases was no longer present and the three trajectories shown arriving at Queeny, Wooster, and McHenry on 10 July (Figure 73) show much longer travel, generally arriving from the southwest ahead of an advancing cold front. Although ozone levels exceeded the federal standard in many areas, they were well below those observed during the stagnation episode two days earlier. The air arriving at McHenry on July 10 had moved generally up the Ohio River Valley and had apparently accumulated enough precursor emissions to cause ozone concentrations in excess of 100 ppb. The other two locations, Wooster and Queeny, did not have concentrations quite so high.

By 11 July (Figure 74), the cold front had passed McHenry. The cleaner air moving in from the north caused concentrations in the Maryland-West Virginia-Pennsylvania area to be lower. Queeny was still under the influence of warm air arriving from the south and appears on Figure 74 to have been near a center of quite high ozone concentrations. However, the 173 ppb observation at this center seems to be unrepresentative; other values nearby are nearer 75 ppb.

By 12 July, a new high pressure area had been established in the upper midwest, as shown in Figure 75. The air arriving at Wooster and McHenry had come from Canada. The trajectory arriving at Yellowstone Lake had come from far to the south during the preceding 2-1/2 days. It would have been interesting to investigate the source of the air with the high ozone concentrations around St. Louis, but no trajectory had been constructed for that area for this day.

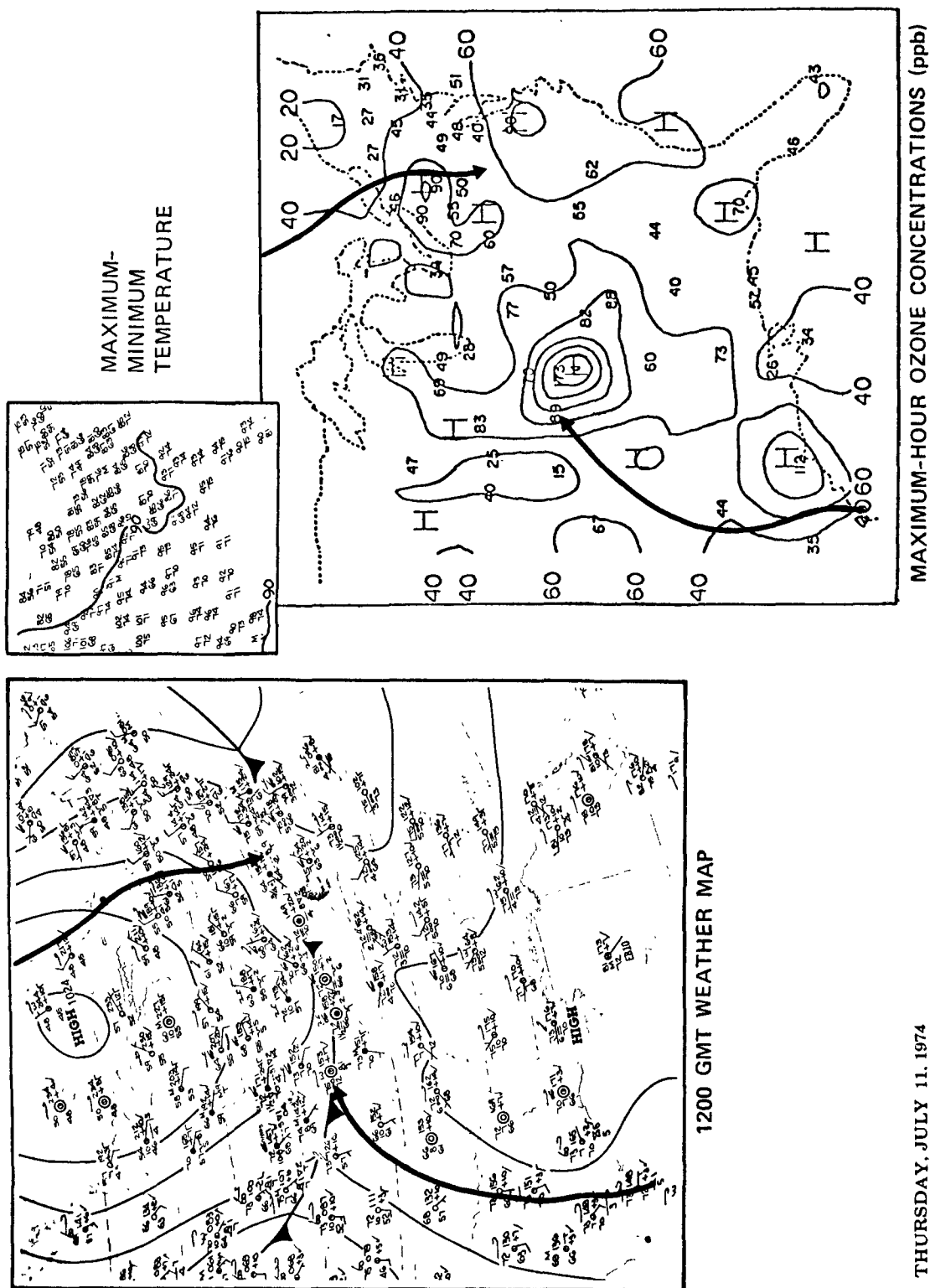
The air arriving at Wooster and McHenry on 13 July (Figure 76) had covered much shorter distances during the preceding 60 hours than had the air that arrived at the same locations a day earlier. As might be expected, the ozone concentrations increased. Concentrations exceeded 140 ppb just south of Toronto. On 14 July, the high pressure area persisted and thus the air movement remained quite slow. As the trajectories in Figure 77 show the air at Wooster and McHenry had come from the west rather than from the north as on the preceding day. Judging from the Wooster and McHenry trajectories, the air in the region of very high ozone concentrations (around 200 ppb) probably had come from Detroit and southern Michigan.

As shown in Figure 78, 18 July was a day on which the eastern United States was dominated by a large high pressure center off the east coast. The air arriving at McHenry had spent the preceding 2-1/2 days traveling in an almost complete circle over West Virginia. The air in Wooster had traversed a path of similar shape over Ohio. The air at the high ozone area north of McHenry had probably circled over Pennsylvania. By contrast, the air that arrived at Queeny and Yellowstone Lake had moved much greater distances, traveling northward ahead of an approaching cold front.



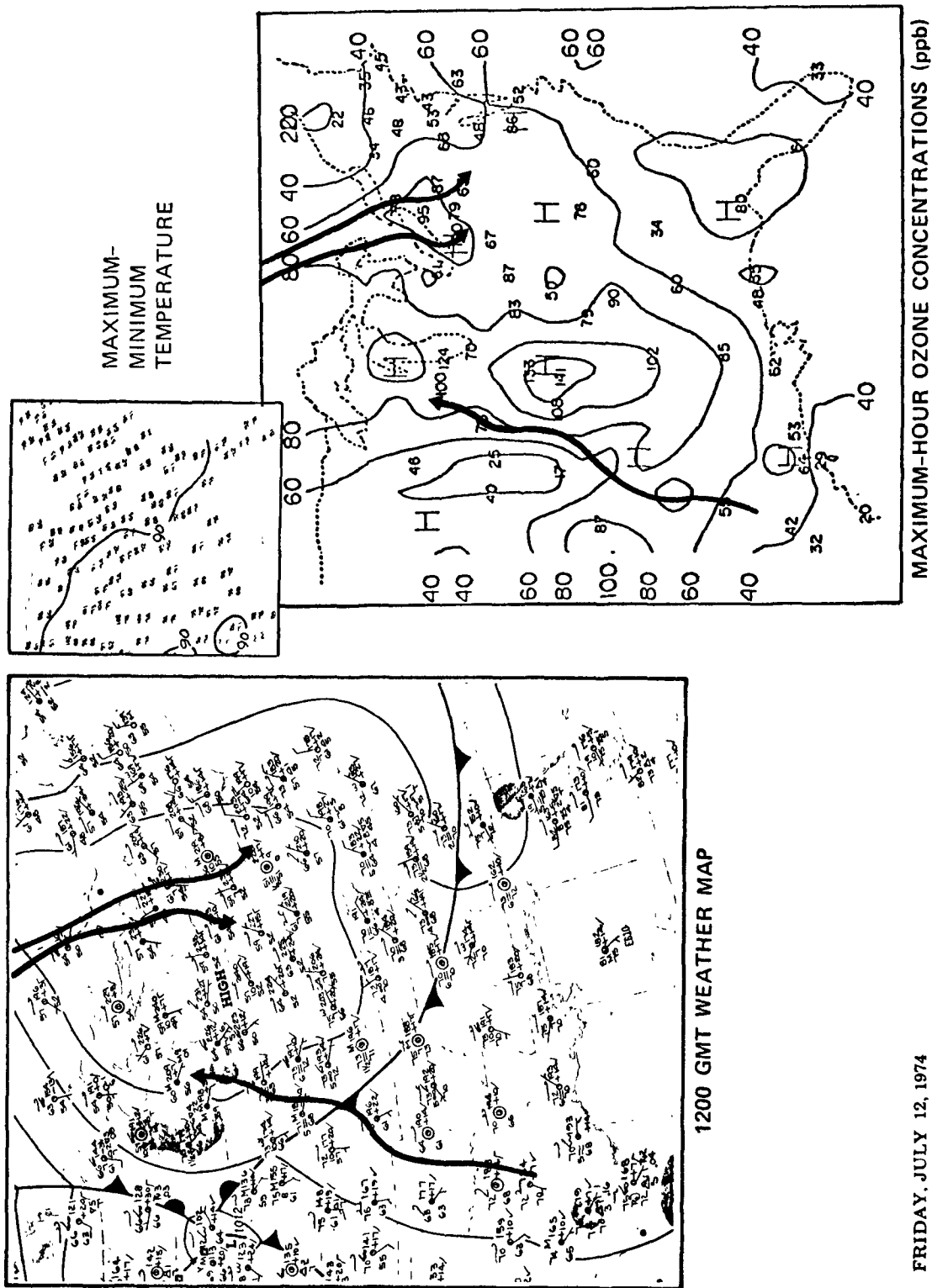
WEDNESDAY, JULY 10, 1974

FIGURE 73 WEATHER MAP, OZONE DISTRIBUTION AND TRAJECTORIES FOR 10 JULY 1974.



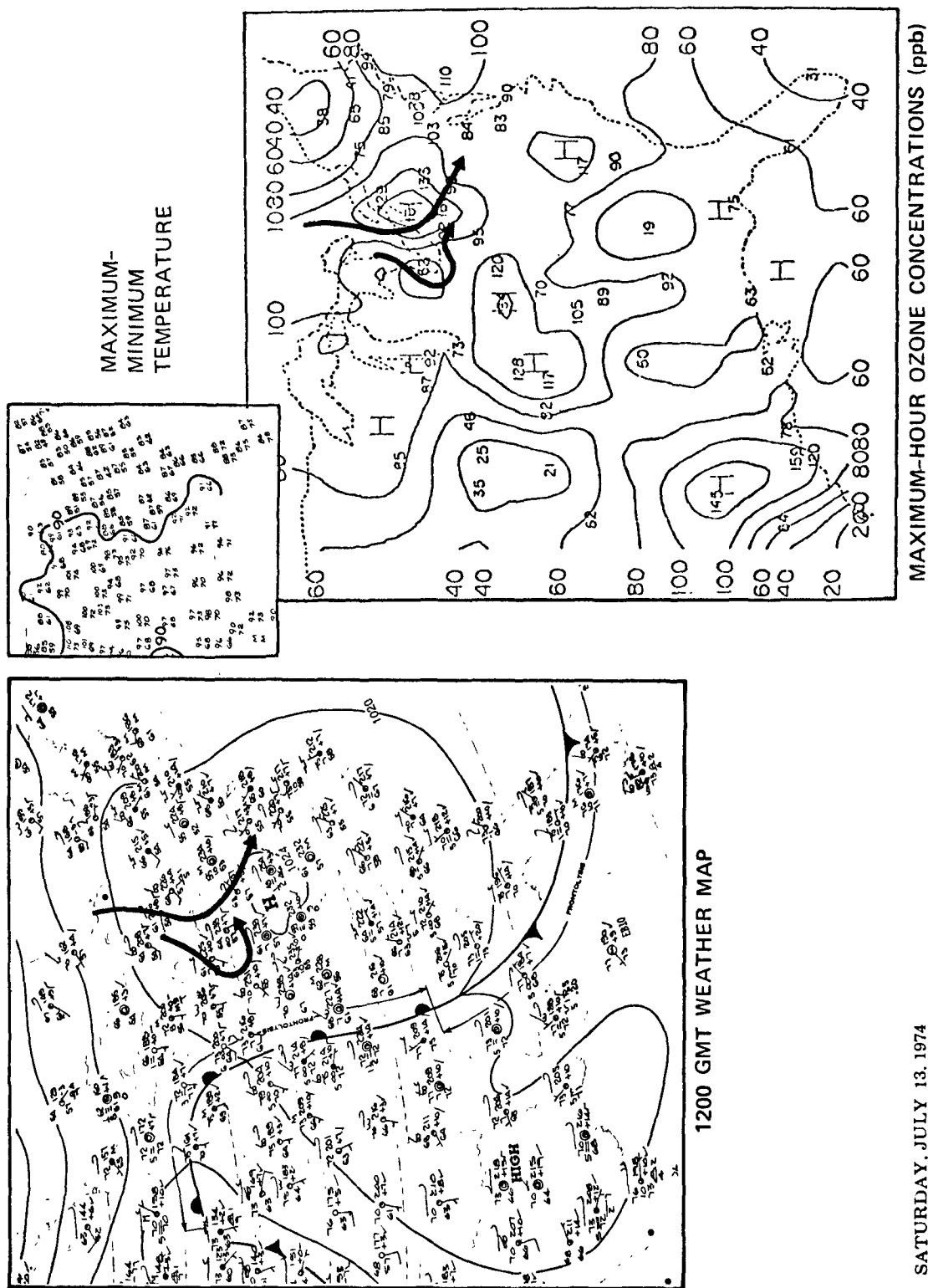
THURSDAY, JULY 11, 1974

FIGURE 74 WEATHER MAP, OZONE DISTRIBUTION AND TRAJECTORIES FOR 11 JULY 1974.



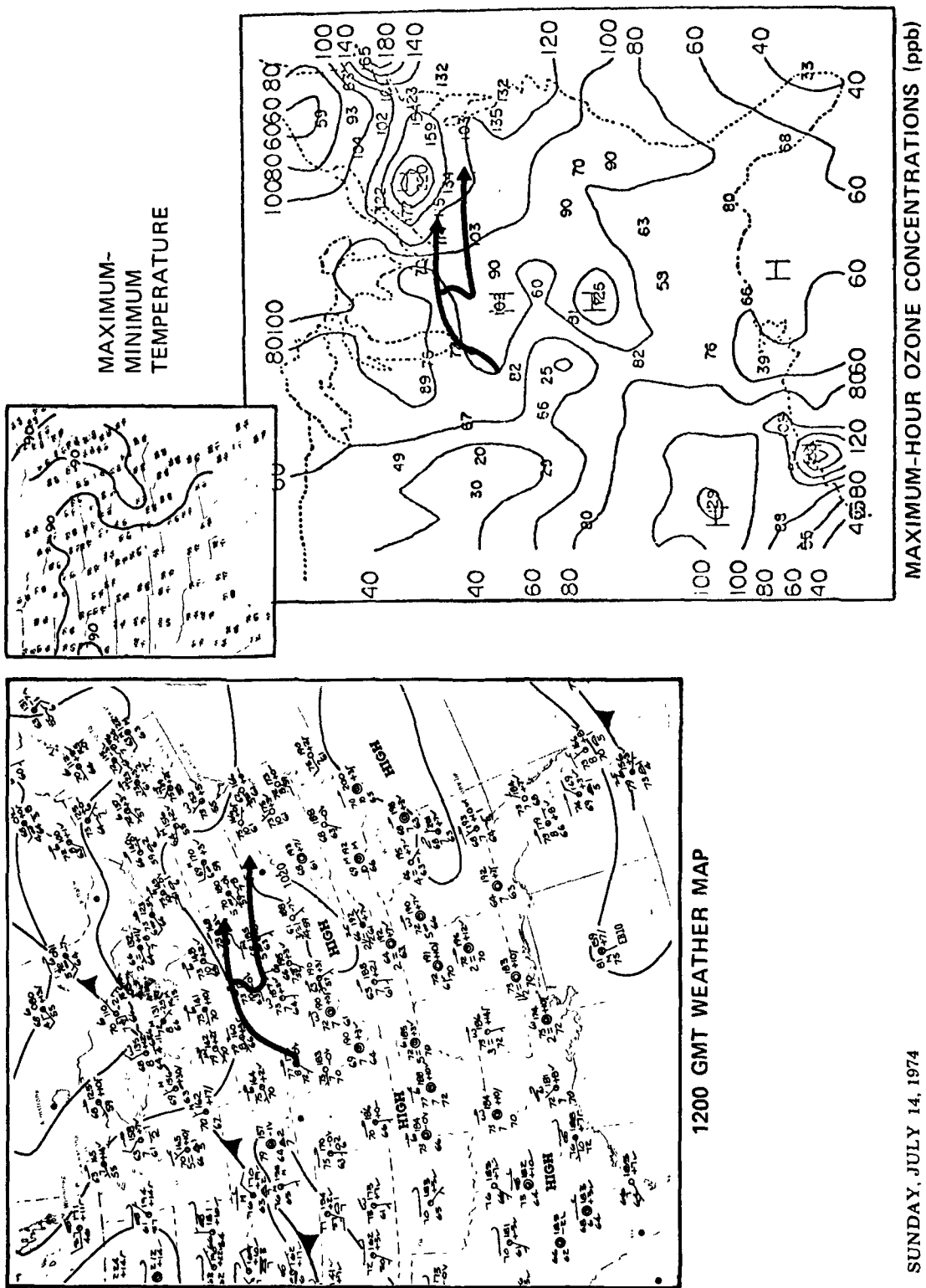
FRIDAY, JULY 12, 1974

FIGURE 75 WEATHER MAP, OZONE DISTRIBUTION AND TRAJECTORIES FOR JULY 12 1974.



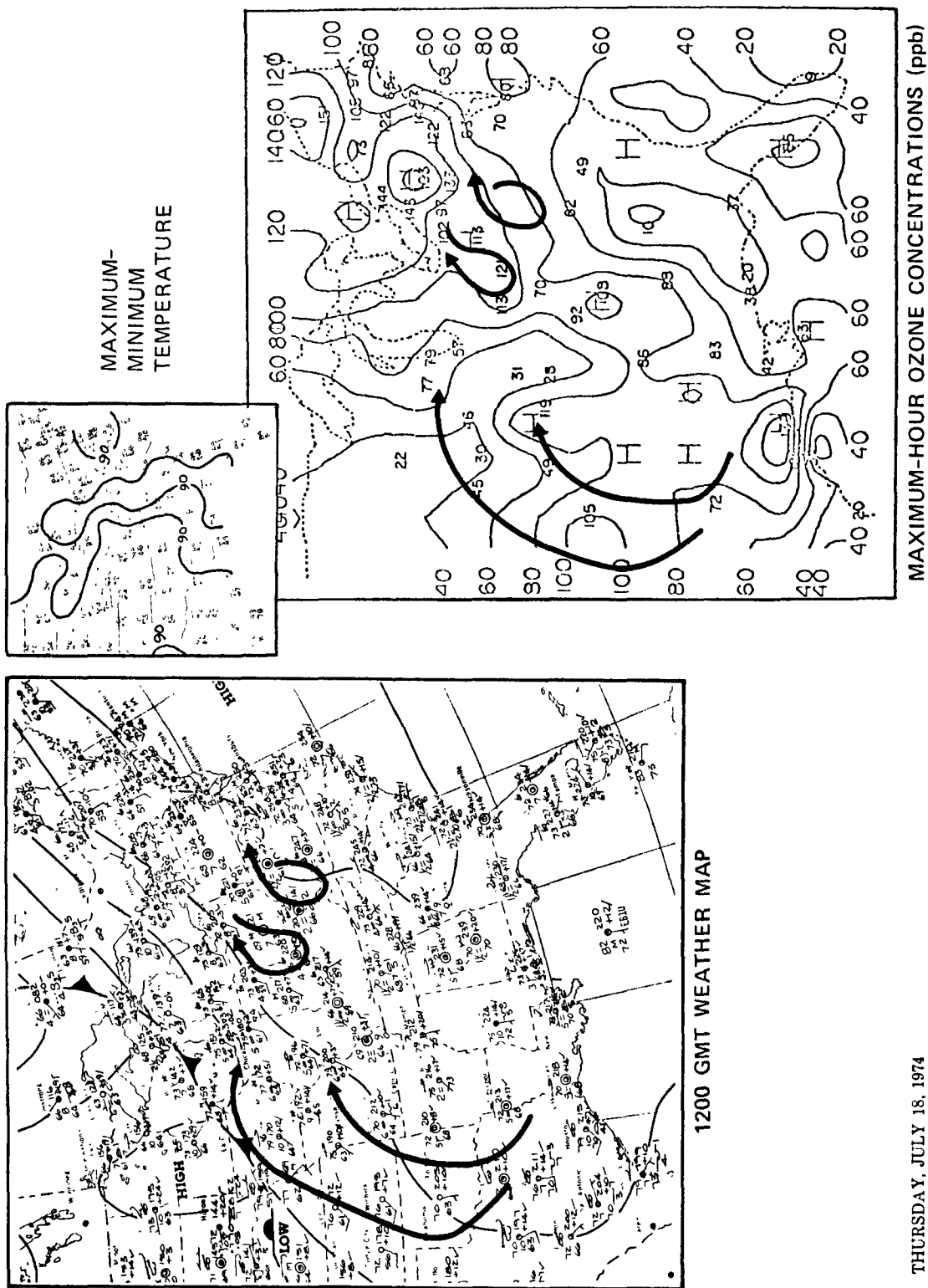
SATURDAY, JULY 13, 1974

FIGURE 76 WEATHER MAP, OZONE DISTRIBUTION AND TRAJECTORIES FOR 13 JULY 1974.



SUNDAY, JULY 14, 1974

FIGURE 77 WEATHER MAP, OZONE DISTRIBUTION AND TRAJECTORIES FOR 14 JULY 1974.



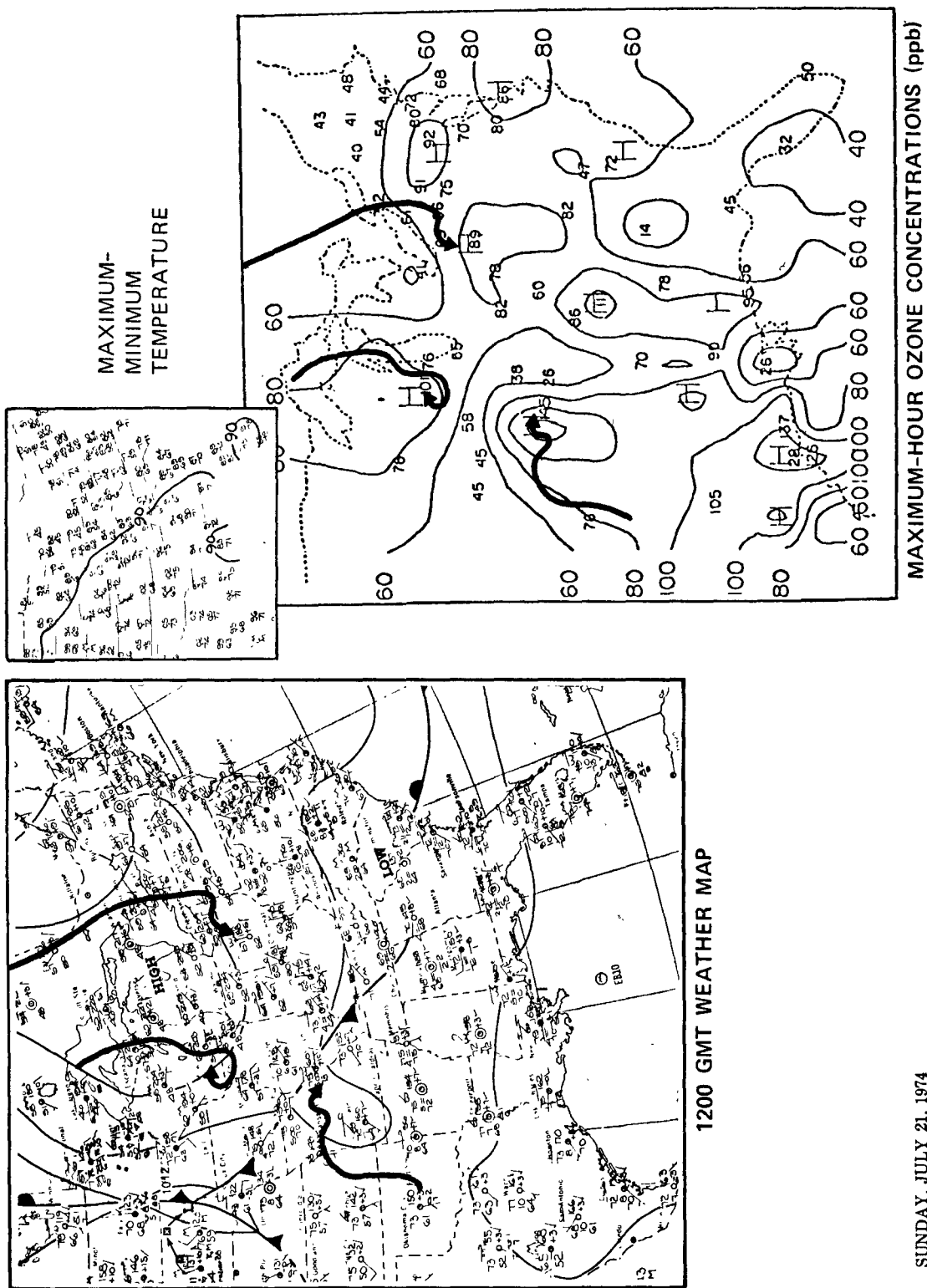
THURSDAY, JULY 18, 1974

FIGURE 78 WEATHER MAP, OZONE DISTRIBUTION AND TRAJECTORIES FOR 18 JULY 1974.

A high pressure area was over the Great Lakes on 21 July 1974 (Figure 79). This day was discussed earlier (Section 2.2.2.2.3) in connection with Figure 67 and the correlation between ozone concentration and pressure. Weak pressure gradients and light winds prevailed over Missouri, Kansas, Arkansas, and Oklahoma. The air arriving at Queeny had meandered from the southwest rather slowly with these light winds. The air at Wooster and Yellowstone Lake had traveled greater distances from the north; ozone concentrations at these locations were somewhat higher than the federal standard.

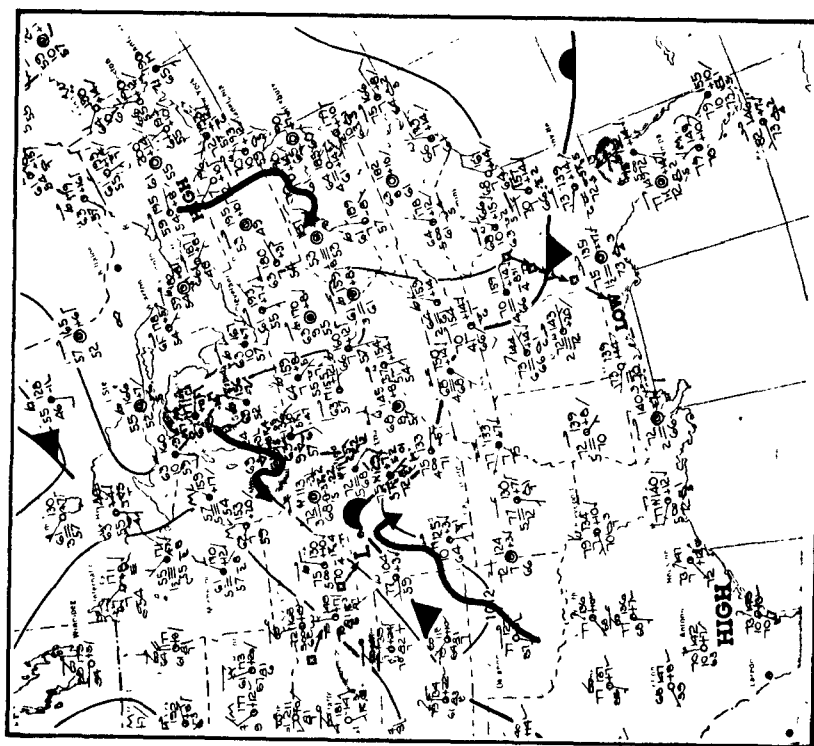
The weather pattern for 22 July, 1974 (Figure 80) shows weak pressure gradients and light winds over much of the eastern United States. Ozone concentrations had increased in much of the area in response to the accumulations of pollutants in this slowly moving air. Figure 80 shows the trajectories of the air arriving at Yellowstone Lake, McHenry and Queeny. Judging from the trajectory arriving at McHenry, the air in the high ozone area south of Lake Erie had passed near Toronto, Buffalo, Cleveland and other Ohio cities, before arriving in southern Ohio.

The maps for 26 July 1974 are shown in Figure 81. This was another day of weak pressure gradients and light winds. The Wooster and Queeny trajectories both exhibit the rather short circular character seen in the other weak gradient cases. The Wooster trajectory spent 2-1/2 days over Ohio, terminating near the center of a high ozone area with concentrations in excess of 140 ppb.

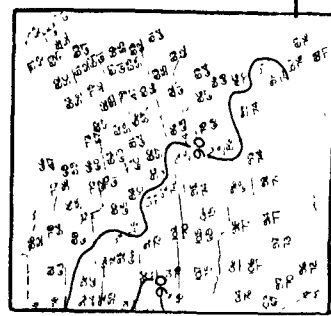


SUNDAY, JULY 21, 1974

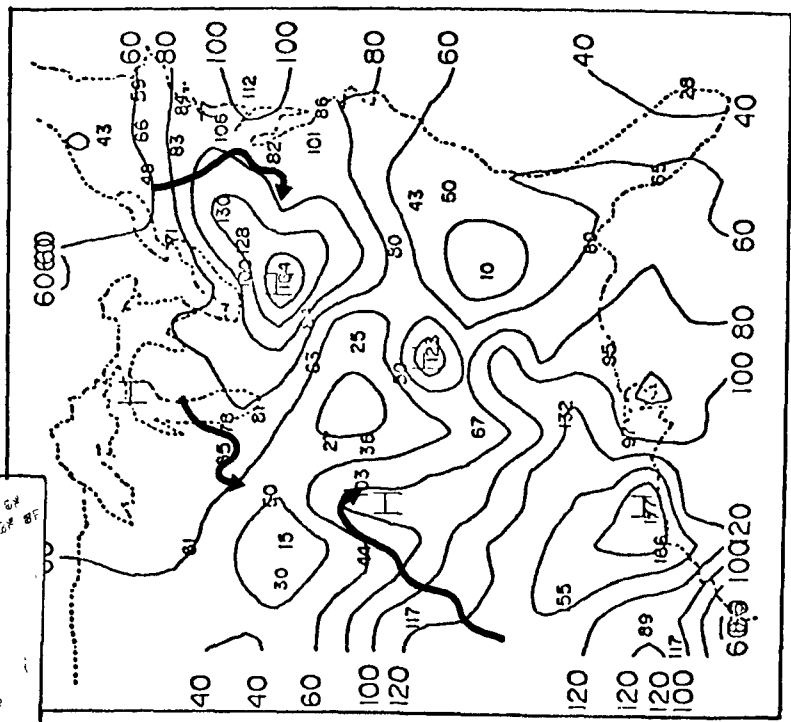
FIGURE 79 WEATHER MAP, OZONE DISTRIBUTION AND TRAJECTORIES FOR 21 JULY 1974.



1200 GMT WEATHER MAP



MAXIMUM-
MINIMUM
TEMPERATURE



MAXIMUM-HOUR OZONE CONCENTRATIONS (ppb)

MONDAY, JULY 22, 1974

FIGURE 80 WEATHER MAP, OZONE DISTRIBUTION AND TRAJECTORIES FOR 22 JULY 1974.

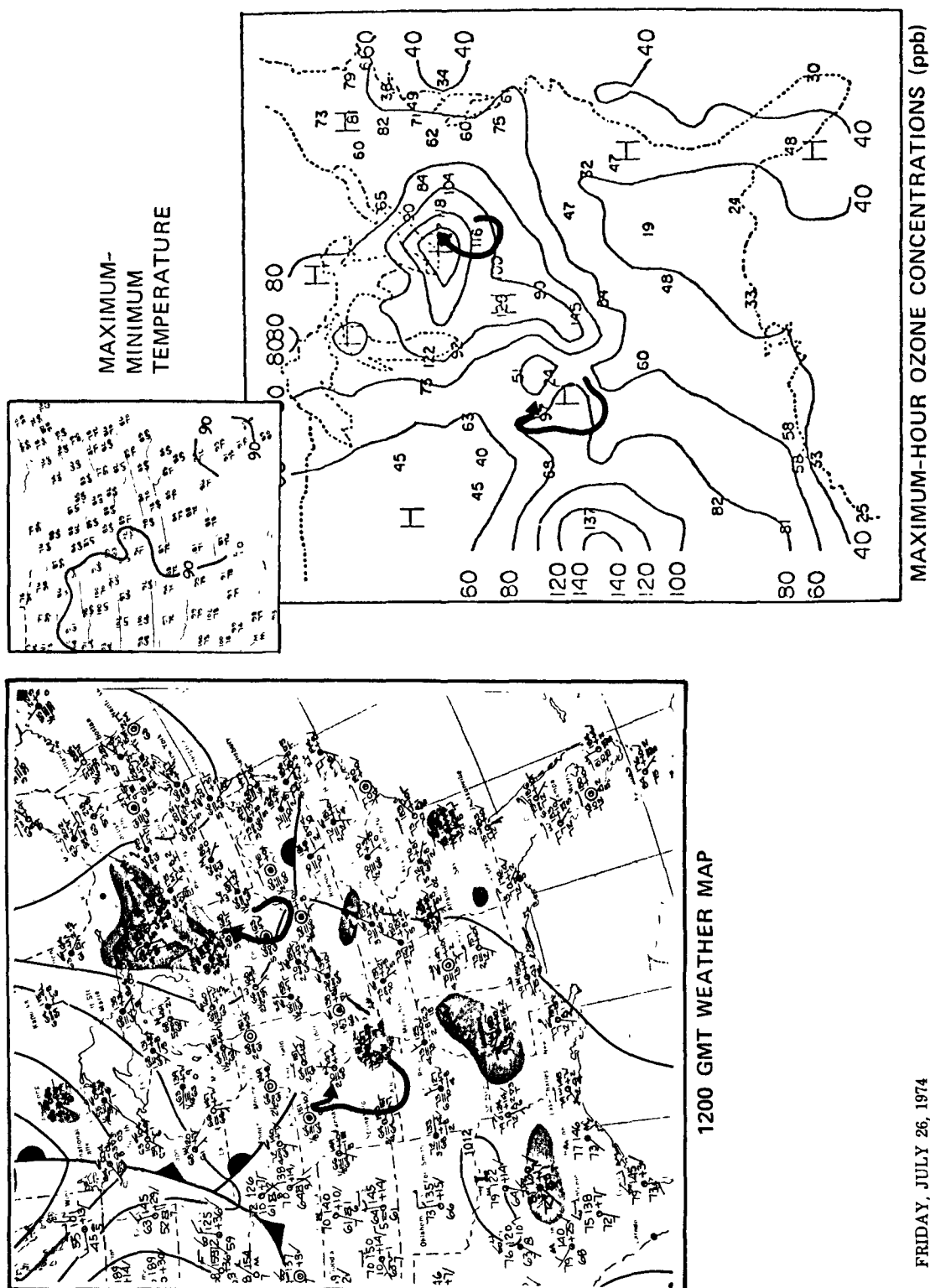


FIGURE 81 WEATHER MAP, OZONE DISTRIBUTION AND TRAJECTORIES FOR 26 JULY 1974.

3. DISCUSSION

This section is an attempt to draw together the results presented in the preceding section and to compare them with the results of other studies. Many of the more important studies of tropospheric ozone have been reviewed in Volume II of this report. That review was prepared and published during the early phases of this project. In the meantime, several other important studies have been completed and will be referred to here. An important feature of much of the recently published information is its consistency. There is considerable agreement concerning the importance of the stratospheric contribution to tropospheric ozone, the extent of long range transport within the troposphere, and the meteorological factors that have the greatest influence on ozone production and accumulation.

Any review of results requires a vantage point. In this case the vantage point is that of the control strategist assessing the difficulty of his task. That strategist is attempting to answer the same questions that this study has attempted to answer. Those questions are:

1. How much does ozone of stratospheric origin contribute to ground-level oxidant concentrations?
2. What are the anthropogenic causes of high oxidant values; that is, how do HC and NO_x emissions interact with weather features to cause high oxidant concentrations?
3. What are the implications of these answers to control strategies -- is it possible to define geographic regions where unified oxidant control strategies are feasible? If so, how can these regions be defined?
4. What new research is needed?

Another question, that of the possible role of geological and biological precursor emissions, was not addressed in this study. The analysis described in the preceding section have provided partial answers to the other questions. The results of other recent studies serve to make some of these answers more nearly complete.

3.1. How Much Does Stratospheric Ozone Contribute to Ground-Level Ozone Concentrations?

3.1.1. General

There are two answers to the question of stratospheric impact and both are of importance to the strategist. First, there is the question of the long-term average contribution of stratospheric ozone to ground-level concentrations. This is the baseline, the foundation that tells the strategist what would be left if all anthropogenic, geologic, and biological sources of precursors were removed. It is a generally irreducible reservoir that the strategist must recognize.

The other answer to the stratospheric question is the one that addresses short-term effects. Does ozone ever travel from the stratosphere to ground-level while undergoing so little dilution that it arrives at concentrations greater than the federal standard? The answer to this question will determine whether there are some "violations" of the standard that are completely beyond the control of the strategist.

3.1.2. Long-Term Average Stratospheric Contributions

The analyses of radioactive fallout data suggest that the seasonally average stratospheric contribution to ozone near ground level is on the order of 15 ppb during springtime. This is in qualitative agreement with the values presented by Fabian and Pruchniewicz (1976). They found seasonally averaged concentrations in the free troposphere of about 20 ppb in mid-latitudes during the spring and early summer. They attribute most of this to stratospheric origins, but concede the possibility of other contributions. Singh, Ludwig and Johnson (1977) indicate even greater natural, probably stratospheric, contributions. Thus, the evidence points to a significant stratospheric contribution to seasonally averaged, ground-level ozone concentrations in the middle latitudes of the northern hemisphere. This contribution may be 20 ppb or more in the springtime. The evidence provided by radioactive fallout suggests that the effects are most pronounced near the typical locations of the polar and arctic jet streams. Fabian and Pruchniewicz (1976) reached the same conclusion from observations of ozone in the eastern hemisphere. They also suggested that the subtropical subsidence areas were also regions of important stratospheric ozone contributions to tropospheric ozone concentrations.

3.1.3. Short-term Stratospheric Contributions

One thing is certain about short-term stratospheric contributions to ground-level ozone concentrations--they do not cause the federal oxidant standard to be exceeded frequently. The analyses presented here suggest that stratospheric contributions exceeded the federal standard only 0.2 percent of the time in the lowest few hundred meters of the troposphere.

Nevertheless, there have been incidents in which stratospheric ozone reached ground-level very directly and with much less than the usual dilution. The Zugspitze results show clear evidence of such an event at a high altitude (3000 m) ground-level site. Lamb (1976) makes a very strong case for stratospheric intrusion as the cause of hour-average ozone concentrations as high as 230 ppb in Santa Rosa, California, during the predawn hours of 19 November, 1972. The incident reported by Lamb lasted less than 5 hours and was restricted to an area with dimensions of only a few tens of kilometers.

As with the Zugspitze case, the Santa Rosa incident was associated with a rather special set of meteorological circumstances. In Santa Rosa, a classical stratospheric intrusion event brought ozone in high concentrations to the middle and upper troposphere where it was then "tapped" by the downdrafts associated with a convective shower. This is similar to the mechanism hypothesized in Section 2.1.1.4 for the

high ozone concentrations observed over Tallahassee, Florida on 14 August, 1963.

Danielsen and Mohnen's (1976) analyses of stratospheric penetration behind the jet stream over the United States during April 1975 show concentrations of 200-300 ppb at altitudes of about 6-8 km. While these data confirm the importance of stratospheric intrusions in transferring ozone from the stratosphere to the troposphere, they are not examples of ground-level effects. Such intrusions can seriously affect ground-level concentrations only in special circumstances when convective circulations bring these high concentrations to the ground via a rather direct route.

It must be concluded that direct penetrations of stratospheric air to ground-level and the consequent high ozone concentrations are rare events. As is true of all rare events, it is difficult to accumulate reliable statistics concerning their frequency. Nevertheless, the reality of such incidents must be considered in the interpretation of ozone records and in the formulation of control strategies.

3.2. What are the Tropospheric Causes of High Ozone Concentrations?

3.2.1. Meteorological Factors

It is clear from the tropospheric analyses that meteorological factors play a very important role in determining the ozone concentrations at locations that are removed from urban areas. The results show that those atmospheric conditions that are associated with warm temperatures are also conducive to the formation of ozone. Meyer et al. (1976) have obtained very similar results from studies that used techniques very much like those used here. They found that recent air temperature was the parameter most highly correlated with ozone concentrations.

The correlation between ozone concentrations and the temperature of the air parcel has been shown to be a reflection of a complete set of meteorological factors that combine to provide the conditions conducive to the photochemical production of ozone from its precursors. As a result, it is possible to identify those meteorological patterns where ozone buildups are likely.

The results presented here are in good agreement with the findings of others. It is generally agreed that high pressure areas are favored locations for the accumulation of high ozone concentrations in the eastern United States (e.g. EPA, 1975; Bach, King and Vukovich, 1976; Wolff et al., 1976). The low wind speeds and the vertical mixing in the vicinity of high-pressure centers allow precursors to accumulate while the prevailing fair skies and abundant sunshine promote photochemical activity. If temperatures are also high, this appears to further enhance the formation of ozone.

Under some circumstances, the same combination of conditions is found in areas other than high-pressure areas. For instance, fair skies and warm temperatures are found in prefrontal warm air, but light winds and stable stratifications (which limit the vertical mixing) are not as common as in the high pressure areas. It appears that a build-up of

ozone can nevertheless take place in those instances in which the air spends considerable time over high-emissions areas. This is exemplified by prefrontal air flow from the southwest along the east coast urban corridor. Ludwig and Shelar (1977) have presented some rather dramatic examples of ozone buildups in prefrontal warm air over New England with subsequent abrupt drops in concentration as cleaner, cooler air moves in with the windshift behind the front.

3.2.2. Emissions Factors

If one carefully reviews the meteorological factors found to be important to the photochemical formation of ozone in the troposphere, it becomes apparent that these same conditions are conducive to the accumulation of high concentrations once it is formed. This set of conditions is optimized near high pressure centers. Furthermore, the high pressure centers with their light and variable winds are areas in which the calculated trajectories are least reliable. Thus, the path of the air is most difficult to trace during precisely those situations when any precursors that are introduced are most likely to produce high ozone concentrations. This may explain why the contributions of precursors were not better defined by the statistical analyses of conditions along the trajectories.

Meyer et al. (1976) found in their trajectory analyses that for those stations that were near major emissions areas, ozone concentrations were significantly correlated with the hydrocarbons introduced into the air during the last several hours of the trajectory. They conclude that local hydrocarbon emissions are important to ozone formation near cities.

Other studies have established the influence of urban sources on ozone concentrations at fairly great distances from the cities. Cleveland et al (1976) suggested that the influence of the New York area emissions may extend for as much as 300 km downwind. Analyses by Ludwig and Shelar (1977) identify ozone "plumes" from the New York area 100 km downwind. The Boston ozone plume was observed by Zeller et al. (1976) at distances of 50 or more kilometers from the city. These are by no means isolated observations. It can be assumed that identifiable urban effects may extend for distances of 100 km or more beyond major source areas. However, under optimum ozone formation/accumulation conditions, these distances are probably reduced by the low speed of the winds. Furthermore, the more erratic air motions during the optimum meteorological conditions reduce the likelihood of definitively following the path of the pollutants.

Before leaving the subject of emissions, it should be noted that the methods by which the emissions were estimated suffers some shortcomings that the measures of meteorological conditions do not. The first of these is the use of total hydrocarbon (THC) emissions data from the NEDS countywide inventories. Total hydrocarbon emissions may be poor representatives of those hydrocarbons which serve as precursors in ozone formation processes. Also, the NEDS inventories do not include natural sources. Although control strategies must treat anthropogenic emissions, better understanding of the mechanisms operating to form ozone would be achieved if estimates of natural emissions were available.

A definite drawback in the statistical analysis of the trajectories was the poor spatial resolution of the emissions data (county-wide averages) coupled with the uncertainty as to the actual paths that the air had taken. A change in the calculated position of an air trajectory of a few tens of kilometers could cause the emissions from a major source county to be included or excluded depending on where the trajectory is placed. Regression and correlation analyses are quite sensitive to such changes. By contrast, the meteorological observations tend to be representative of much larger areas and are therefore much less sensitive to uncertainties in the trajectory.

3.3. Implications for Control Strategies

3.3.1. Interactions Between Ozone of Stratospheric and Tropospheric Origin

The analyses show that stratospheric effects are not negligible. There are long-term tropospheric levels of stratospherically originated ozone of 25 to 30 percent of the federal standard. Ozone concentrations in the lowest two kilometers of the atmosphere may be in excess of federal standards perhaps 0.2 percent of the time because of individual intrusion events. But concentrations above the standard at ground-level are apt to be less frequent, except on mountain peaks, because of mixing and surface destruction processes. Undoubtedly, rare circumstances do result in concentrations of stratospheric ozone in excess of the federal standard for short periods at elevations more typical of populated areas.

All the evidence indicates that spring is the period for the most pronounced stratospheric interaction with the troposphere over most of the United States. From the strategic standpoint, this is fortunate because it means that the periods of maximum stratospheric effect and maximum tropospheric photochemical ozone production do not coincide. Analyses of ozone data from remote locations in the western United States (Singh, Ludwig and Johnson, 1977) indicate that background ozone concentrations reach their highest levels (40 to 80 ppb) in late winter and spring at the most remote sites. Stratospheric effects are postulated as an important factor in this behavior. At some of the less remote stations the high concentrations continue into summer and early fall. It is presumed that local photochemical ozone production at these sites more than offsets the declining stratospheric contribution. Observed increases in NO_x concentrations (of unknown origin) in late spring and summer at these same sites tend to support this view.

The likely locations for stratospheric intrusions generally fall outside the areas where low altitude accumulations of photochemical oxidant are most likely. The tropospheric analyses have shown that the warm, clear conditions associated with high pressure cells or the warm conditions just ahead of cold fronts are most conducive to tropospheric ozone formation. On the other hand, stratospheric studies suggest that the area just behind a fast moving cold front, accompanying an outbreak of polar or arctic air, is a more likely area for a significant intrusion of stratospheric ozone. The meteorological conditions suitable for the tropospheric buildup of ozone are quite different than those accom-

panying stratospheric intrusions, so the two processes are unlikely to be operative at the same place and time.

Overall, it does not appear that stratospheric ozone and tropospheric ozone are apt to occur at high concentrations in combination. Nevertheless, the possibility of high ozone concentrations from the stratosphere does have important consequences for the formulation of control strategies. Strategies are often formulated so that if they had been in effect the standards would not have been violated during some specific historical incident, e.g. for the day of the second highest concentration for some past year. If the specific incident for which an oxidant strategy is designed involved important ozone contributions from the stratosphere, then the strategy would be faulty in assuming that controls on anthropogenic emissions are suitable for attaining standard. Obviously, strategy formulation should involve the examination of individual cases to assess the importance of stratospheric contributions.

3.3.2. Strategies for Control of Ozone of Anthropogenic Origin

The studies reported here have emphasized regions that are well removed from urban areas. The rationale has been that such locations could be used to determine the longer-term processes that govern the larger scale features of ozone patterns. These larger-scale features, while important, cannot be considered to the exclusion of the smaller scale processes that affect ozone concentrations near urban areas. As noted before, urban emissions are known to influence concentrations for distances of a hundred kilometers or more from their centers (see e.g. Martinez and Meyer, 1976).

EPA (1977) has pointed out that the present strategy of controlling hydrocarbon emissions in order to reduce ozone concentration is effective only where the ratio of the concentration of non-methane hydrocarbons (NMHC) to that of oxides of nitrogen (NO_x) is less than about 30:1. Low ratios are found in and near cities or large NO_x point-sources. As a general rule the ratios are quite high in rural areas, primarily because, as Meyer (1977) points out, the concentrations of NO_x are very low.

The above facts could explain why Meyer et al. (1976) found close relationships between ozone and hydrocarbon emissions for stations near cities, but not at more remote sites. Similarly, the results of the present study can be explained on this basis. Using the fact that ozone concentrations are closely related to hydrocarbon emissions where the NMHC/NO_x ratios are high, Meyer (1977) proceeded to delimit the distances from urban regions where such controls might be effective. Using average per capita emissions data, he proposed that the effectiveness of controlling hydrocarbon emissions would extend about 20 miles outward from the center of a city of 200,000 people and about 85 miles out from a city of 4 million.

Figure 82, taken from Meyer's paper (1977), shows the areas that are within specified distances (related to population) of major urban

centers. According to Meyer's proposal, these are the areas in which oxidant concentrations are largely controllable by controlling hydrocarbon emissions. It is interesting to note the close correspondence of the shaded areas in Figure 82 to many of those areas where widespread violations of ozone standards are found to occur. Another important feature of Figure 82 is the generally southwest to northeast alignment of the overlapping areas along the east coast, in the Ohio River Valley and along the shores of the Great Lakes. This alignment almost certainly affects the frequency with which southwest winds and high ozone concentrations are seen to be concurrent in these regions.

Dodge (1976) has shown that NO_x concentrations control ozone concentrations when NMHC/NO_x ratios are high. As already mentioned, Meyer (1977) showed that high ratios prevail in rural areas. Thus, the finding of the present study--that rural ozone correlates better with NO_x emissions than with hydrocarbon emissions--and the similar results obtained by Meyer et al (1976), is not surprising. Singh, Ludwig, and Johnson (1977) observed that, in the summer months, concentrations of ozone in remote locations appear to be controlled by the presence of oxides of nitrogen. All these results suggest that the control of oxidant in rural areas may require a quite different strategy than is applicable to urban areas and their environs.

For the rural areas, control of the contributing NO_x emissions is clearly the strategy of choice. The correlations of ozone with NO_x emissions are significant over long periods of time that correspond to travel distances of four or five hundred kilometers for the very high ozone concentrations. So it appears that the control of rural ozone will require that much larger geographic regions be considered than for the urban situation. The implications are that the regions where control of NO_x could be required might extend hundreds of kilometers upwind of the areas where the violations occur.

Great care would have to be taken in the design of such strategies however, because the reduction of NO emissions over areas with dimensions of several hundred kilometers might well lead to higher ozone concentrations within the urban environs. Probably, greater emphasis should be given at present to hydrocarbon control in urban areas than to NO_x control in rural areas because of population-exposure considerations. However, it does seem clear that the continued siting of large NO_x sources in rural areas would tend to aggravate the present oxidant problem in those areas. Meyer (1977) has pointed out that large portions of the eastern U.S. are subject to prolonged summertime periods of stagnation during which large concentrations of hydrocarbons can accumulate from the multitude of sources in the area. Introduction of large amounts of NO_x into such an air mass would probably be undesirable in the rural areas.

3.4. Recommendations for Future Research

It is important that better statistics be developed to define the importance of stratospheric intrusion. Initially, such investigations should use existing data from the SAROAD system and from past special studies. Those geographic areas that have been identified as undergoing the highest impact should be emphasized. For instance, cases of anomalously high concentrations in the western portions of Kansas, Nebraska and Oklahoma should be studied individually, using isentropic trajectory analyses to identify instances of stratospheric influence. Other regions having episodes with high probability of stratospheric influence should be treated similarly.

Since stratospheric ozone penetrates to within a few kilometers of the surface much more often than it does to near-ground-level, the mixing and ozone destruction processes in the lowest layers are quite influential in determining stratospheric influence at ground-level. Past aircraft studies of ozone aloft could be used to investigate these important processes. In such investigations, the ozone need not be of stratospheric origin. Often there are layers of ozone aloft that originated at the surface (see e.g., Miller and Ahrens, 1970; Ludwig and Shelar, 1977). The behavior of these layers may, by analogy, provide information on the extent to which ozone concentrations in elevated layers introduced by stratospheric intrusion are reduced during mixing to ground-level.

Meyer's radii (Figure 82) can be refined by a consideration of weather effects. That is, the circular areas might be better defined as asymmetric areas, where the asymmetry is governed by the nature of those weather conditions known to be most likely to accompany high ozone concentrations. The 1976 data from the Regional Air Pollution Study (RAPS) in St. Louis is now available and could be used to test this hypothesis. Data from other relatively dense monitoring networks like those in Los Angeles, San Francisco, Chicago and Southern New England might also be used in such a study.

Where possible, ozone records from rural areas should be examined in combination with NO_x records at the same locations. If ozone concentrations in nonurban areas are in reality related to NO_x emissions, then there may be evidence of this in the monitoring data. Unfortunately routine NO_x measurements generally lack the threshold sensitivity necessary for such a determination. Data from past special studies may be found to be better in this respect than routine monitoring data.

There are theoretical investigations that would be useful to the formulation of control strategies for reducing ozone levels in nonurban areas. Existing computer simulation models might be used to evaluate the effect of adding nitric oxide to the well aged remnants of urban emissions. This would help to define the impact (both initial and net) of some major NO_x sources such as power plants in rural areas. Data from field studies, in combination with the model results, would also be useful to the evaluation of such impacts.

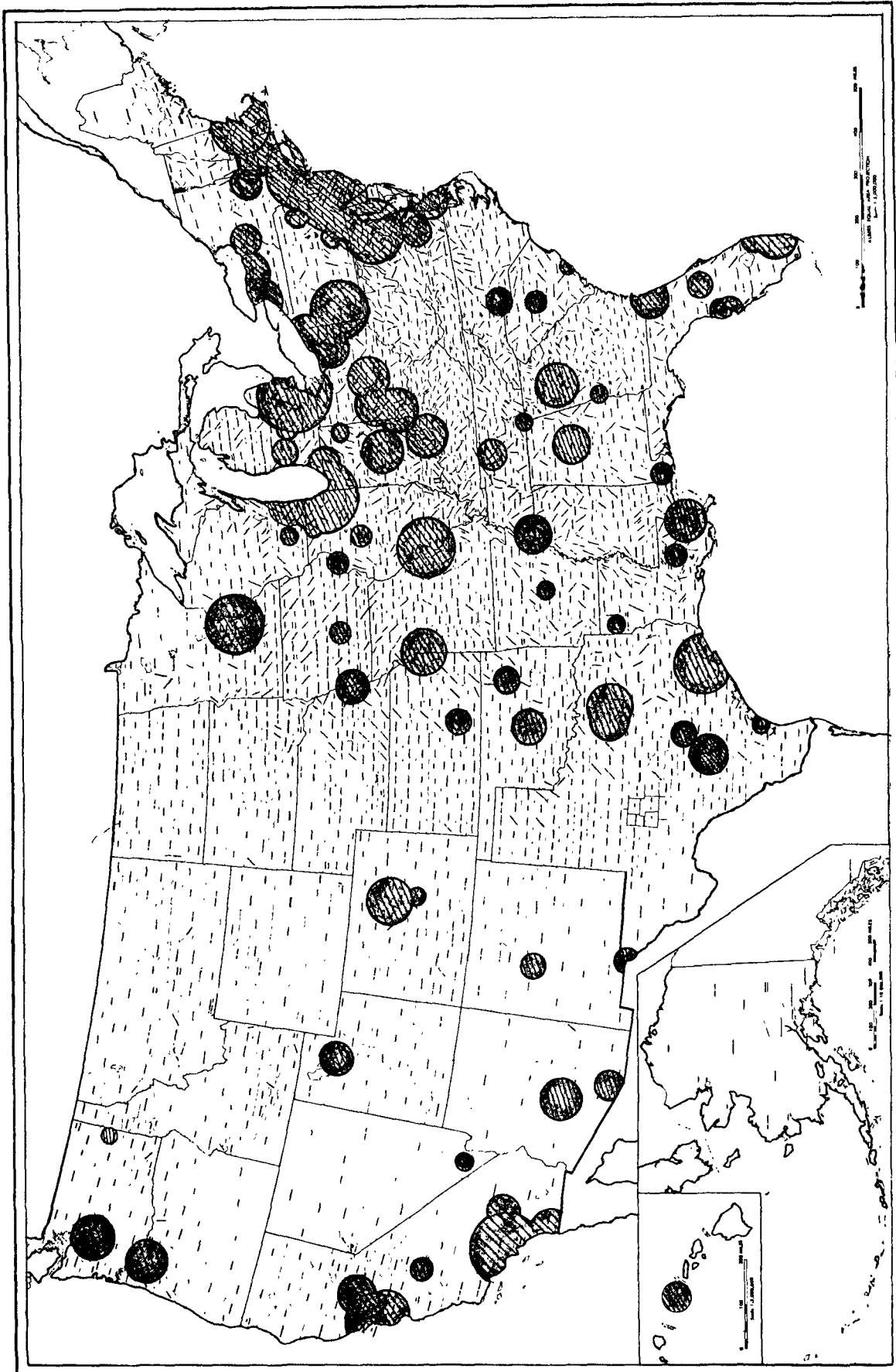


FIGURE 82 AREAS APPROPRIATE FOR HYDROCARBON EMISSION CONTROLS ACCORDING TO MEYER (1977)

In summary, it is recommended that existing routine data and data from past special studies be used to 1) investigate the importance of stratospheric intrusions, 2) determine the extent of the direct urban influence on ozone concentrations in the urban environs, and 3) investigate the more widespread nonurban ozone problem. It is expected that considerable information can be extracted from existing data. Furthermore, any studies using existing data will provide a strong basis for the design of future data collection projects so that they will fill the gaps in the existing data base most effectively.

Finally, in the present study, the selection of cases for the construction of trajectories was made before the daily ozone maps were drawn. In retrospect, it would have been better to have performed the studies (i.e., the trajectories and the map-comparisons) in the reverse order. This would have made possible a more judicious selection of the cases so that trajectories could have been constructed for those cases that appeared from the map comparison to have the greatest likelihood of yielding useful results. The cases, discussed earlier, for which it was possible to compare trajectories, weather maps, and ozone patterns, suggested that more such analyses would be quite productive. This is therefore recommended.

REFERENCES

- Bach, W.D., W.J. King and F.M. Vukovich, 1976: Nonurban ozone concentrations in transient high pressure systems. Presented at the Nonurban Troposphere Symposium, Sponsored by Amer. Geophys. Un. and Amer. Met. Soc., Hollywood, Fla., 10-12 November.
- Cleveland, W.S., B. Kleiner, J.E. McRae, and J.L. Warner, 1975: The analysis of ground-level ozone data from New Jersey, New York, Connecticut, and Massachusetts; Transport from the New York City Metropolitan Area, Mimeo Report, Bell Laboratories, Murray Hill, New Jersey, 65 pp.
- Cleveland, W.S., B. Kleiner, J.E. McRae, and J.L. Warner, 1976: Photochemical air pollution: transport from the New York City area into Connecticut and Massachusetts. *Science*, 191, 179-181.
- Danielsen, E.F. and V.A. Mohnen, 1976: Project Dustorm Report: Ozone measurements and meteorological analyses of tropopause folding. Proceedings Joint Symposium on Nonurban Tropospheric Composition. Amer. Geophys. Un. and Amer. Met. Soc., Hollywood, Fla., 10-12 November 1976, pp. 17-1 to 17-13.
- Dodge, M.C., 1976: Combined use of modeling techniques and smog chamber data to derive ozone precursor relationships. Presented at International Conference on Photochemical Oxidant Pollution and Its Control; Raleigh, N.C., Sept. 13-17.
- Dutsch, H.U., 1971: Photochemistry of atmospheric ozone. *Adv. Geophys.*, 15, 219-322.
- Environmental Protection Agency, 1975: Control of photochemical oxidants--technical basis and implications of recent findings. Report No. 450/2-75-005, 35 pp.
- Fabian, P. and P.G. Pruchniewicz, 1976: Final Report on Project "Tropospharische Ozon", Max-Planck-Institut für Aeronomie, Report MPAE-W-100-76-21, Kutlenburg-Lindau, Germany, 28 pp.
- Freiling, E.C., G.R. Crocker and C.E. Adams, 1965: Nuclear-debris formation. In: *Radioactive Fallout from Nuclear Weapons Tests* (A.W. Clement, Jr., Ed.), U.S. Atomic Energy Commission, CONF-765, pp. 1-43.
- Heffter, J.L. and A.D. Taylor, 1975: A regional-continental scale transport, diffusion and deposition model, Part I: Trajectory model., National Oceanic and Atmospheric Administration Technical Memorandum, ERC ARL-50, pp. 1-16.
- Hering, W.S., 1964: Ozonesonde observations over North America, Vol. 1, Research Report, Report AFCRL-64-30(1), pp. 1-512, Air Force Cambridge Research Laboratories.

- Hering, W.S. and T.R. Borden, Jr., 1964: Ozonesonde observations over North America, Vol. 2, Report AFCRL-64-30(II), Air Force Cambridge Research Laboratories.
- Hering, W.S., and T.R. Borden, Jr., 1965a: Ozonesonde observations over North America, Vol. 3, Report AFCRL-64-30(III), Air Force Cambridge Research Laboratories.
- Hering, W.S., and T.R. Borden, Jr., 1965b: Mean distribution of ozone density over North America, 1963-1964. Report AFCRL-65-913, Air Force Cambridge Research Laboratory.
- Hering, W.S., and T.R. Borden, Jr., 1967: Ozonesonde observations over North America, Vol. 4, Report AFCRL-64-30(IV), Air Force Cambridge Research Laboratories.
- Holzworth, G.C., 1972: Mixing Heights, Wind Speeds, and Potential for urban air pollution throughout the contiguous United States. Environmental Protection Agency, Office of Air Programs, Pub. No. AP-101, 118 pp.
- Lamb, R.G., 1976: A Case Study of Stratospheric Ozone Affecting Ground-Level Oxidant Concentrations. Systems Applications, Inc., San Rafael, California, 18 pp.
- Langley, R., 1970: Practical Statistics Simply Explained. Dover Publications, Inc., New York. 399 pp.
- List, R.J. and K. Telegadas, 1969: Using radioactive tracers to develop a model of the circulation of the stratosphere. J. Atmos. Sci., 26, 1128-1136.
- Lovill, J.E., 1969: Transport processes in orographically induced gravity waves as indicated by atmospheric ozone. Colorado State University Atmospheric Sciences Paper No. 135, 78 pp.
- Lovill, J.E., 1974: Contribution to Chapter 2, in Reiter et al., 1975.
- Ludwig, F.L. and E. Shelar, 1977: Ozone in the Northeastern United States. Final Report, EPA Contract 68-02-2352, prepared by Stanford Research Institute, Menlo Park, California. EPA Report No. 90/9-76-005, 286 pp.
- Lund, I., 1963: Map classification by statistical methods. J. Appl. Meteorol., 2, 56-65.
- Mahlman, J. D., 1965: Relation of Tropopause-level Index Changes to Radioactive Fallout Fluctuations. Colorado State University, Atmospheric Science Technical Paper No. 70, pp. 84-109.
- Martinez, E.L. and E.L. Meyer, 1976: Urban-nonurban ozone gradients and their significance. Presented at Air Pollution Control Association Technical specialty Conference on Ozone/Oxidants: Interactions with

the Total Environment; Dallas, Texas, March 12.

McQuirk, J.P., E.R. Reiter and A.M. Barbieri, 1975: On the variability of hemispheric scale energy parameters. Colorado State University Environmental Research Papers, No. 1, 15 pp.

Meyer, E.L., W.P. Freas, J.E. Summerhays and P.L. Youngblood, 1976: The use of trajectory analysis for determining empirical relationships among ambient ozone levels and meteorological and emissions variables. Paper presented at International Conference on Photochemical Oxidant Pollution and Its Control, Raleigh, N.C., 12-17 September.

Meyer, E.L., 1977: Establishing organic emission control strategies as a function of geographic location. EPA Office of Air Quality Planning and Standards, 36 pp.

Reiter, E.R., 1971: Atmospheric transport processes; Part 2: Chemical tracers. U.S. Atomic Energy Commission, Critical Review Series, TID-25314, 382 pp.

Reiter, E.R., 1972: Atmospheric transport processes; Part 3: Hydrodynamic tracers. U.S. Atomic Energy Commission, Critical Review Series, TID-25731, 212 pp.

Reiter, E.R., 1975a: Atmospheric transport processes; Part 4: Radioactive tracers. U.S. Energy Research and Development Administration, in press.

Reiter, E.R., 1975b: The transport of tracers by global circulation systems of the atmosphere. U.S. Energy Research and Development Administration Report C00-1340-46, 12 pp.

Reiter, E.R., 1975c: Stratospheric-tropospheric transport processes and their relation to the influx of ozone into the troposphere. Report to Stanford Research Institute, 12 pp.

Reiter, E.R., 1975d: Stratospheric-Tropospheric exchange processes. Rev. Geophys. Space Phys., 13, 459-474.

Reiter, E.R., 1976a: Atmospheric transport processes, Part 4: Radioactive Tracers. U.S. Energy Research and Development Administration, in preparation.

Reiter, E.R., 1976b: Ozone concentrations in the lower troposphere as revealed by ozonesonde observations. Report to Stanford Research Institute, 26 March, 1976, 106 pp.

Reiter, E.R., E. Bauer and S. Coroniti, 1975: The natural stratospheric 1974. CIAP Monograph No. 1, U.S. Department of Transportation.

Seitz, H., B. Davidson, J.P. Friend and H.W. Feely, 1968: Final Report on Project Streak. Numerical models of transport diffusion and fallout of stratospheric radioactive material. Isotopes, Inc.,

Westwood, N.J., Report No. NYO-3654-4, 97 pp.

Singh, H.B., F.L. Ludwig and W.B. Johnson, 1977: Ozone in remote locations. Final Report, prepared for Coordinating Research Council, Stanford Research Institute, Menlo Park, California, 157 pp.

Volchok, H.L., and L. Toonkel, 1974: Worldwide deposition of Sr90 through 1973, U.S. Atomic Energy Commission, Report HASL-286, pp. I-17 to I-36.

Wallace, J.M., R.E. Newell, 1966: Eddy fluxes and the biennial stratospheric oscillation. Quart. J. Roy. Meteorol. Soc., 92,(394): 481-489.

Wolff, G.T., P.J. Lioy, G.D. Wight, R.E. Meyers and R.T. Cederwall, 1976: An investigation of long-range transport of ozone across the midwestern and eastern United States. Presented at International Conference on Photochemical Oxidant Pollution and Its Control; Raleigh, N.C., 13-17 September.

Zeller, K., R.B. Evans, C.K. Fitzsimmons and G.W. Siple, 1976: Mesoscale analysis of ozone measurements in the Boston environs. Presented at Symposium of Nonurban Tropospheric Components, Hollywood, Fla., 10-12 November.

TECHNICAL REPORT DATA <i>(Please read Instructions on the reverse before completing)</i>		
1. REPORT NO. EPA-450/3-77-022a	2.	3. RECIPIENT'S ACCESSION NO.
4. TITLE AND SUBTITLE The Relation of Oxidant Levels to Precursor Emissions and Meteorological Features. Volume I: Analysis and Findings	5. REPORT DATE September 1977	
	6. PERFORMING ORGANIZATION CODE	
7. AUTHOR(S) F.L. Ludwig, E. Reiter, E. Shelar and W.B. Johnson	8. PERFORMING ORGANIZATION REPORT NO.	
9. PERFORMING ORGANIZATION NAME AND ADDRESS SRI International Menlo Park, CA 94025	10. PROGRAM ELEMENT NO.	
	11. CONTRACT/GRANT NO. 68-02-2084	
12. SPONSORING AGENCY NAME AND ADDRESS Environmental Protection Agency Office of Air Quality Planning and Standards Research Triangle Park, N.C. 27711	13. TYPE OF REPORT AND PERIOD COVERED Final	
	14. SPONSORING AGENCY CODE	
15. SUPPLEMENTARY NOTES		
16. ABSTRACT <p>Published ozonesonde data, radioactive fallout measurements and alpine ozone observations have been used to estimate the stratospheric contribution to observed ozone concentrations at ground level. Long term average effects from the stratosphere over the U.S. are on the order of 10 ppb, with a springtime maximum around 20 to 25 ppb. Short term stratospheric intrusion events resulting in one-hour-average concentrations of stratospheric ozone in excess of 80 ppb in the lower troposphere have a frequency of only about 0.2 per-cent. Still fewer (but some) of these events lead to ground-level impacts of such a magnitude.</p> <p>Tropospheric causes of high ozone concentrations away from cities have been investigated by statistical analysis of meteorological conditions and the precursor emissions occurring along air trajectories and by comparisons of weather maps and large-scale O₃ distributions. Meteorological factors are statistically more strongly correlated with ozone concentration than are emissions, with air temperature being the most highly correlated. At sites well removed from cities, the upwind emissions of oxides of nitrogen are more strongly related to ozone concentrations than are the emissions of hydrocarbons. Widespread violations of the federal oxidant standard are most likely to be found in association with a stagnant high-pressure system or in the warm southwesterly flow in the western portion of a high pressure area, often ahead of an approaching cold front.</p> <p>The results of this and other studies suggest that not all violations of the federal oxidant standard are controllable and this fact must be considered in the design of control strategies. Also, for areas within about 125 km of large cities, control might be achieved through the reduction of HC emissions. In more remote areas, control strategies involving NO_x control throughout large regions must be considered.</p>		
17. KEY WORDS AND DOCUMENT ANALYSIS		
a. DESCRIPTORS	b. IDENTIFIERS/OPEN ENDED TERMS	c. COSATI Field/Group
Tropospheric Ozone Stratospheric Intrusion Oxidant Control Strategies Meteorological Factors Affecting Ozone		
18. DISTRIBUTION STATEMENT Unlimited	19. SECURITY CLASS (This Report) Unclassified	21. NO. OF PAGES 170
	20. SECURITY CLASS (This page) Unclassified	22. PRICE

ENVIRONMENTAL PROTECTION AGENCY

Technical Publications Branch
Office of Administration
Research Triangle Park, North Carolina 27711

OFFICIAL BUSINESS

AN EQUAL OPPORTUNITY EMPLOYER

POSTAGE AND FEES PAID
ENVIRONMENTAL PROTECTION AGENCY
EPA - 335

SPECIAL FOURTH-CLASS RATE
BOOK



Return this sheet if you do NOT wish to receive this material ☐
or if change of address is needed ☐. (Indicate change, including
ZIP code.)

PUBLICATION NO. EPA-450/3-77-022a